

**OPTIMIZATION OF MICROWAVE-ALKALINE PRE-TREATMENTS
CONDITIONS AND CO-IMMOBILIZATION OF XYLANASE, CELLULASE AND
FUNGI SPECIES FOR THE PRODUCTION OF BIOETHANOL FROM SOME
AGROWASTES**

BY

**OMONIJE, Omotayo Oluyemisi
PhD/SLS/2018/7642**

**A THESIS SUBMITTED TO THE POSTGRADUATE SCHOOL, FEDERAL
UNIVERSITY OF TECHNOLOGY, MINNA, NIGERIA, IN PARTIAL
FULFILMENT OF THE REQUIREMENTS FOR THE AWARD OF DEGREE OF
DOCTOR OF PHILOSOPHY (PhD) IN BIOCHEMISTRY**

DECEMBER, 2023

ABSTRACT

The need for bioethanol production arises from drawbacks of fossil fuel such as non-renewable feedstock and emission of dangerous gases during combustion. However, the recalcitrant nature of bioethanol feedstock as well as high cost of hydrolytic enzyme and incomplete fermentation of sugars have been major challenges. The research was aimed at optimizing microwave-alkaline (MA) pre-treatment conditions for the effective delignification of some selected locally available agrowastes and co-immobilization of cellulase, xylanase, and as well co-immobilize yeast and fungi for optimal production of bioethanol. Microwave-alkaline pretreatment conditions, generated using Box-Behnken of design expert software version 11, were optimized for the pretreatment of sugarcane bagasse (SB), plantain pseudostem biomass (PS), and corncob (CC). The pre-treated agrowastes were characterized using Fourier Transform infrared spectroscopy (FTIR), X-Ray crystallography (XRD), and Scanning electron microscopy (SEM). Microorganisms were isolated from different soil sources, palm wine and fermented food to produce enzymes and for fermentation process. Biochar made from sugarcane bagasse was mixed with chitosan to co-immobilize xylanase, cellulase, and fermentation organisms for simultaneous saccharification and co-fermentation (SScF). The functional properties of co-immobilized enzymes and co-immobilized fermentation organisms were characterized. Results showed the optimal MA pre-treatment conditions for plantain pseudostem biomass (1.97% NaOH, 70W, 5 min), sugarcane bagasse (3% NaOH, 96W, 5 min), and corncob biomass (2.8% NaOH, 86W, 4.4 min). Characteristics of pre-treated agrowastes differed from unpre-treated ones. *Aspergillus flavus* (OP107821) and *Aspergillus niger* (OP107822) produced cellulase and xylanase, respectively, while *Saccharomyces cerevisiae* (OP107824) and *Mucor indicus* (OP107823) fermented glucose and xylose respectively. Free cellulase, free xylanase, and co-immobilized enzymes had optimal temperatures of 50, 60, and 70 °C respectively and pH values of 5, 6, and 5-7 respectively. Free cellulase, free xylanase, and co-immobilized enzymes had K_m values of 0.008 mg/mL, 0.028 mg/mL, and 0.022 mg/mL respectively and V_{max} values of 129.87, 119.05, and 114.94 μMmin^{-1} respectively for plantain pseudostem biomass substrate. Likewise, the K_m values for free cellulase, free xylanase, and co-immobilized enzymes were 0.017, 0.006, and 0.018 mg/mL, respectively, and the V_{max} values were 333.33, 555.47, and 227.25 μMmin^{-1} for sugarcane bagasse substrate. Free cellulase, free xylanase, and co-immobilized enzymes had activation energies of 15.899, 29.218 and 3.450 kJ/mol, respectively, and deactivation energies of 48.235, 39.596, and 52.145 kJ/mol respectively. After 10 usages, the co-immobilized enzymes retained 55.13% of its activity. Co-immobilized enzymes released 32.47 ± 0.89 mg/mL, 36.62 ± 1.90 , and 17.42 ± 0.41 mg/mL from PS, SB, and CC, respectively. Co-immobilized enzymes and co-immobilized fermentation organisms yielded the most bioethanol, 68.93 ± 0.33 g/L from PS and 76.09 ± 0.15 g/L from SB. GC-MS profile of distillate showed other valuable products, but SB and PS had 80.84 and 71.15 percent ethanol, respectively. This study showed that microwave-alkaline pre-treatment reduces recalcitrance of lignin, releasing more cellulose and hemicellulose for hydrolysis. The study also found that locally-sourced enzymes and organisms co-immobilized on locally produced matrix can produce high-yield of bioethanol, which may make relatively cheap and eco-friendly fuel for domestic and industrial uses. Considering the seasonal availability of different agrowastes based on harvesting times, it is recommended that in a future study, a mixture of different agrowastes that are available at the same time be optimized for bioethanol production.

TABLE OF CONTENTS

Cover Page	
TITLE PAGE	i
DECLARATION	ii
CERTIFICATION	iii
DEDICATION	iv
ACKNOWLEDGEMENTS	v
ABSTRACT	vii
TABLE OF CONTENTS	viii
LIST OF TABLES	xv
LIST OF FIGURES	xviii
LIST OF PLATES	xxi
LIST OF APPENDICES	xxii
ABBREVIATIONS, GLOSSARIES AND SYMBOLS	xxiii
CHAPTER ONE	
1.0 INTRODUCTION	
1.1 Background to the Study	1
1.2 Statement of the Research Problem	6
1.3 Aim and Objectives of the Study	7
1.4 Justification for the Study	8

CHAPTER TWO

2.0	LITERATURE REVIEW	10
2.1	Definition of Bioethanol	10
2.1.1	Bioethanol generation	10
2.1.1.1	<i>Bioethanol of the first generation</i>	10
2.1.1.2	<i>Bioethanol of the second generation</i>	11
2.1.1.3	<i>Bioethanol of the third generation</i>	11
2.1.1.4	<i>Bioethanol of the fourth generation</i>	12
2.1.2	Lignocellulose as a bioethanol feedstock	12
2.1.3	The advantages of lignocellulosic bioethanol	12
2.2	Composition of Natural Lignocellulosic Feedstocks	13
2.2.1	Cellulose	14
2.2.2	Hemicellulose	14
2.2.3	Lignin	15
2.3	Ethanol Production from Lignocellulosic Biomass	15
2.3.1	Pre-treatment	16
2.3.1.1	<i>Physical pre-treatment</i>	18
2.3.1.2	<i>Pre-treatment with chemicals</i>	20
2.3.1.3	<i>Pre-treatment with biological agents</i>	22
2.3.2	Hydrolysis	22
2.3.2.1	<i>Acidic hydrolysis</i>	22
2.3.2.2	<i>Enzymatic hydrolysis</i>	23
2.3.3	Immobilization of enzymes and cells	26
2.3.3.1	<i>Co-immobilization of enzymes and cells</i>	27

2.3.3.2	<i>Immobilization techniques</i>	27
2.3.3.3	<i>Matrix or support for immobilization of enzymes</i>	28
2.3.3.4	<i>Porous biochar as support for enzyme immobilization</i>	29
2.3.3.5	<i>Activation of biochar for enzyme immobilization</i>	30
2.3.3.6	<i>Biochar-chitosan composite preparations for enzyme immobilization</i>	31
2.3.4	Ethanol production	32
2.3.4.1	<i>Principles of ethanol production through fermentation</i>	32
2.3.4.2	<i>Microbes for fermentation</i>	33
2.3.4.3	<i>Fermentation of hexose and pentose sugars</i>	34
2.4	Strategies for Bioethanol Production	35
2.4.1	Separate hydrolysis and fermentation (SHF)	38
2.4.2	Simultaneous saccharification and fermentation (SSF)	39
2.4.3	Simultaneous saccharification and co-fermentation (SSCF)	49
2.4.4	Consolidated bioprocessing (CBP) or direct microbial conversion (DMC)	40
2.5	Alcohol Recovery	41
2.6	Selected Agricultural Wastes	42
2.6.1	Maize plant (<i>Zea mays</i>)	42
2.6.1.1	<i>Description</i>	42
2.6.1.2	<i>Corncoobs</i>	43
2.6.2	Plantain (<i>Musa paradisciaea</i>)	44
2.6.2.1	<i>Description</i>	44
2.6.2.2	<i>Plantain pseudostem</i>	45
2.6.3	Sugarcane (<i>Saccharum officinarum</i>)	46
2.6.3.1	<i>Description</i>	47

2.6.3.2 <i>Sugarcane bagasse</i>	47
----------------------------------	----

CHAPTER THREE

3.0 MATERIALS AND METHOD	50
3.1 Materials	50
3.1.1 Agrowaste samples	50
3.1.2 Equipments	50
3.1.3 Reagents and chemicals	50
3.2 Methods	51
3.2.1 Overall process description	51
3.2.2 Preparation of agrowaste samples	52
3.2.3 Microwave-alkaline (MA) pre-treatment of biomass	53
3.2.4 Compositional analysis	54
3.2.4.1 <i>Determination of total lignin content</i>	54
3.2.4.2 <i>Determination of cellulose and hemicellulose content</i>	55
3.3 Analysis of Data Generated by Design Expert for Pre-treatment of Agrowastes	56
3.4 Characterization of Pre-treated Agrowastes	56
3.4.1 X-ray diffraction analysis (XRD)	56
3.4.2 High resolution scanning electron microscopy (HERSM)	58
3.4.3 FT-IR (Fourier Transform Infrared) spectroscopic analysis of pre-treated and untreated samples	58
3.5 Screening of Fungi for Enzyme Production and Fermentation Process	59
3.5.1 Screening of fungi for enzyme production	59
3.5.1.1 <i>Qualitative screening of the isolated microorganisms for cellulase and</i>	

<i>xylanase production using agrowastes of interest as a carbon source</i>	59
3.5.1.2 <i>Quantitative screening of the selected organisms for cellulase and xylanase production using agrowastes as carbon source</i>	60
3.5.2 <i>Screening of fungi for fermentation process</i>	62
3.5.2.1 <i>Qualitative screening of the isolated microorganisms for fermentation (sugar fermentation test)</i>	62
3.5.2.2 <i>Quantitative screening of the isolated microorganisms for fermentation</i>	63
3.5.2.3 <i>Determination of ethanol tolerance of the fermentation organisms</i>	64
3.5.3 <i>Molecular characterization of organisms used for enzyme production and fermentation process</i>	64
3.5.3.1 <i>Molecular identification and characterization of organisms</i>	65
3.5.3.2 <i>Molecular identification of enzyme gene extracted from characterized organisms</i>	68
3.5.4 <i>Production of support for enzyme immobilization</i>	69
3.5.4.1 <i>Preparation of porous biochar as support for immobilization</i>	69
3.5.4.2 <i>Preparation of biochar-chitosan composite for enzyme immobilization</i>	71
3.5.5 <i>Characterization of biochar-chitosan beads for enzyme immobilization</i>	72
3.5.5.1 <i>Determination of the sizes of biochar-chitosan bead prepared at different drying temperatures</i>	72
3.5.5.2 <i>Determination of the swelling behaviours of biochar-chitosan beads prepared at different drying temperatures</i>	73
3.5.5.3 <i>Thermogravimetric analysis (TGA) and derivative thermogravimetry (DTG) of biochar-chitosan beads</i>	73
3.5.5.4 <i>Determination of pore size, pore volume, and surface area of the biochar-chitosan beads prepared at different drying temperatures</i>	74
3.6 <i>Co-immobilization of Enzyme</i>	74
3.6.1 <i>Determination of activities of free and enzyme co-immobilized on beads prepared at different drying conditions</i>	74
3.6.2 <i>Determination of total protein concentration, specific activity and</i>	

immobilization efficiency of the co-immobilized crude enzyme	75
3.6.3 Effect of reaction temperature on the activity of free and co-immobilized enzymes	76
3.6.4 Effect of pH on the activity of free and co-immobilized enzymes	77
3.6.5 Effect of substrate concentration on the activity of free and co-immobilized enzymes	77
3.6.6 Determination of half-life for free enzyme and enzyme co-immobilized on freeze-dried biochar-chitosan bead	77
3.6.7 Re-usability test for co-immobilized enzymes	77
3.6.8 Determination of thermal stability of free and co-immobilized enzymes	78
3.6.9 Determination of storage stability of co-immobilized enzymes	78
3.7 Enzymatic Hydrolysis of Agrowaste using Free and Co-Immobilized Enzymes	78
3.8 Immobilization of Fungi	79
3.9 Production of Bioethanol	80
3.9.1 Experimental design for simultaneous saccharification and co-fermentation (SScF)	80
3.9.2 Re-usability of co-immobilized fungi and mucor	81
3.10 Distillation of Fermented Broth	81
3.11 Estimation of Ethanol Concentration	81
3.12 Ethanol Characterization	82
3.13 Cost Estimation for the Production of 1.5 L of Bioethanol	82
3.14 Statistical Analysis	85
CHAPTER FOUR	
4.0 RESULTS AND DISCUSSION	86
4.1 Results	86

4.1.1	Composition of dried native (unpre-treated) agrowaste	86
4.1.2	Solid yield and composition of microwave-alkaline pre-treated Agrowastes	87
4.1.3	Process variables and responses for microwave-alkaline pre-treatment of agrowaste	90
4.1.4	Optimal parameters for microwave-alkaline pre-treatment of agrowaste	94
4.1.5	Three-Dimensional Response surface plots for percentage delignification, cellulose and hemicellulose content of microwave-alkaline pre-treated plantain pseudostem biomass	96
4.1.6	Three-Dimensional Response surface plots for percentage delignification, cellulose and hemicellulose content of microwave-alkaline pre-treated sugarcane bagasse	100
4.1.7	Three-Dimensional Response surface plots for percentage delignification, cellulose and hemicellulose content of microwave-alkaline pre-treated corncob biomass	104
4.1.8	X-Ray Diffraction Pattern of the untreated and treated agrowastes	108
4.1.9	Infrared Spectra of the untreated and treated agrowaste samples	110
4.1.10	Scanning Electron Microscopy of pre-treated and untreated agrowastes	112
4.1.11	Organisms and substrate for enzyme production and fermentation process	116
4.1.12	The hydrolytic zone of clearance observed on agar plates prepared with different agrowaste substrates	120
4.1.13	Activity of cellulase produced by different microorganism isolated from soil using three agrowaste as carbon source	123
4.1.14	Activity of xylanase produced by different microorganism isolated from soil using three agrowaste as carbon source for five days	124
4.1.15	Qualitative profile of isolates for fermentative ability using sugar fermentation test	125
4.1.16	Quantitative profile of isolates for fermenting ability using Dichromate test	126
4.1.17	Ethanol tolerance test	128
4.1.18	Molecular identification of screened organisms for enzyme	

	production and fermentation process	129
4.1.19	Average diameter of biochar-chitosan beads prepared at different drying conditions	132
4.1.20	The swelling behaviours of biochar-chitosan beads	133
4.1.21	Thermogravimetric curves (TGA) and the derivative Thermogravimetric analysis (D TGA) curves of biochar-chitosan beads	134
4.1.22	Specific surface area, pore size and pore volume of biochar-chitosan Composite	136
4.1.23	Enzyme Loading and Activity assay	137
4.1.24	Effect of reaction Temperature and pH on the activity of free and co-immobilized enzymes	138
4.1.25	Effect of different agrowaste substrate concentrations on the kinetic parameters of free and co-immobilized cellulase and xylanase	140
4.1.26	Kinetic Parameters (K_m and V_{max}) of free and co-immobilized enzymes using different agrowaste as substrate	142
4.1.27	Effects of incubation time and conditions on the storage stability of free and co-immobilized enzymes	143
4.1.28	Thermal stability of free and co-immobilized enzymes	145
4.1.29	The effect of number of usages on the relative efficiency of the co-immobilized enzymes	148
4.1.30	Enzymatic Hydrolysis of agrowaste using free and immobilized enzymes	149
4.1.31	Amount of bioethanol produced determined by potassium dichromate Method	151
4.1.32	Characterization of bioethanol by GC-MS	152
4.1.33	Infrared Spectra of free biochar-chitosan and biochar-chitosan loaded with	

co-immobilized enzymes and co-immobilized yeast and fungi	153
4.1.34 Scanning Electron Micrograph of free biochar-chitosan bead	155
4.1.35 Re-usability test of co-immobilized mucor and yeast	157
4.1.36 Estimated cost for the production of 1.5 L of lignocellulosic bioethanol	158
4.2 Discussion	160
4.2.1a Optimal conditions for the pre-treatment of agrowaste using microwave-assisted-alkaline pre-treatment methods	160
4.2.1b Characteristics of agrowaste pre-treated at optimal conditions	172
4.2.2a Qualitative and quantitative potentials of microorganisms for enzyme production and fermentation process	177
4.2.2b Molecular identification of screened organisms for enzyme production and fermentation process	182
4.2.3a Immobilization techniques developed for the co-immobilization of xylanase, cellulase, and suitable pentose and hexose sugar fermenters	183
4.2.3b Characteristics of biochar-chitosan support prepared for co-immobilization	185
4.2.3c Loading strategy for co-immobilized enzymes	190
4.2.5 Enzymatic properties, storage stability and re-usability of free and immobilized moieties	192
4.2.5a Fermentable sugar produced from agrowaste using free, immobilized and co-immobilized enzymes	200
4.2.5b Quantity and Quality of bioethanol produced using immobilized moieties	201
4.2.5c Characteristics of free biochar-chitosan and biochar-chitosan loaded with co-immobilized enzymes and co-immobilized yeast and mucor	203
4.2.5d Estimated cost for the production of lignocellulosic bioethanol	205

CHAPTER FIVE	
5.0 CONCLUSION AND RECOMMENDATIONS	206
5.1 Conclusion	206
5.2 Recommendations	207
5.3 Contributions to Knowledge	208
REFERENCES	210
APPENDICES	241

LIST OF TABLES

Table	Page
3.1 Variable Factors and Runs Generated by Design Expert Software For the Optimization of Microwave-alkaline Pre-treatments of Agrowaste	53
3.2 Bruker D8 Advance XRD Operating Parameters	57
3.3 Experimental Parameters for High Resolution Scanning Electron Microscopy	58
3.4 Molecular Characteristics of Organisms that are Related to the Sample Organisms	67
3.5 Constituents of each Reaction Vessel for Bioethanol Production	81
3.6 Operating Parameter and Conditions for GC-MS Analysis	82
4.1 Cellulose, Hemicellulose and Lignin Content of Dried Unpre-treated Agrowastes	86
4.2a Effect of Microwave-alkaline Pre-treatment on the Weight and Percentage of Lignin in Plantain Pseudostem Biomass	88
4.2b Effect of Microwave-alkaline Pre-treatment on the Weight and Percentage of Lignin in Sugarcane Bagasse	89
4.2c Effect of Microwave-alkaline Pre-treatment on the Weight and Percentage of Lignin in Corncob Biomass	89
4.3a Process Variables and Responses for Microwave-alkaline Pre-treatment of Plantain Pseudostem Biomass	91
4.3b Process Variables and Responses for Microwave-alkaline Pre-treatment of Sugarcane Bagasse	92
4.3c Process Variables and Responses for Microwave-alkaline Pre-treatment of Corncob	93
4.4a Some Criteria Considered for Process Optimization of Microwave-alkaline Pre-treatment of Plantain Pseudostem Biomass	94
4.4b Some Criteria Considered for Process Optimization of Microwave-alkaline Pre-treatment of Sugarcane Bagasse Biomass	94

4.4c	Some Criteria Considered for Process Optimization of Microwave-alkaline Pre-treatment of Corncob Biomass	95
4.5	Macroscopic and Microscopic Features of Microorganisms Isolated for Enzyme Production	117
4.6	Macroscopic and Microscopic Features of Microorganisms Isolated for Fermentation Process	119
4.7	Dimensions (millimeters) of Hydrolytic Zones Formed by Four Organisms Cultivated on Different Substrates in Congo Red Agar Plate	122
4.8	Activity of Cellulase Produced by Different microorganisms isolated from soil using three agrowastes as carbon sources for five days	123
4.9	Activity of Xylanase Produced by Different Microorganisms Isolated from Soil using Three Agrowastes as Carbon Sources	124
4.10	Qualitative Profile of Isolates for Fermentative Ability Using Sugar Fermentation Test	125
4.11	Molecular Identification and Classification of Screened Organisms for Enzyme Production and Fermentation Process by Percentage Similarity Index and Accession Numbers	129
4.12	Average Diameter of Biochar-chitosan Beads Dried at Different Drying Conditions	132
4.13	Cellulase and Xylanase Activity of Free and Co-immobilized Enzymes Loaded in Different Categories on Various Biochar-chitosan Bead as Support	137
4.14	Optimum pH and Temperature for Free Cellulase, Free Xylanase and Co-immobilized enzymes	139
4.15	Km and Vmax Values for Free and Co-immobilized Enzymes	142
4.16	Half-life of Free and Co-immobilized Enzymes (CIE) Stored at 4 °C and 25 °C	144
4.17	Half-life of Free and Immobilized Enzymes at Different Thermal Conditions	147
4.18	Activation and Deactivation Energy of free and co-immobilized enzymes	147
4.19	Reducing Sugar Produced from the Hydrolysis of Different Agrowaste Using Free Cellulase, Free Xylanase and Co-immobilized Enzymes	150

4.20	Concentration of Ethanol (g/L) Produced with Different Combination of Enzyme and Fungi	151
4.21	The Percentages of Compound Identified by GC-MS in the Distillate of Bioethanol Produced by Co-immobilized Enzymes and Co-immobilized Fungi Using Sugarcane Bagasse as Substrate	152
4.22	The Percentages of Compound Identified by GC-MS in the Distillate of Bioethanol Produced Co-Immobilized Enzymes and Co-immobilized Fungi Using Plantain Pseudostem Biomass as Substrate	153
4.23	Functional Group Identified in Infrared Spectra of Free Biochar-chitosan Bead and Biochar-chitosan Loaded with Co-immobilized Enzymes and Co-immobilized fungi	154
4.24	Estimated Cost for the Production of 1.5 L of Lignocellulosic Bioethanol	159

LIST OF FIGURES

Figure		Page
2.1	Major Lignocellulose Constituents	13
2.2	Bioethanol Production from Lignocellulosic Biomass	16
2.3	Effect of Pre-treatment on Lignocellulosic Materials	17
2.4	An Overview of Various Pre-treatment Processes	18
2.5	Mechanism of Action by Cellulase	24
2.6	Mechanism of Action of Xylanase	26
2.7	A Schematic Representation of the Various Methods of Immobilizing Enzymes or Cells	28
2.8	The Main Characteristics of Enzyme Immobilization Support Materials	29
2.9	Methods of Activating Biochar for Enzyme Immobilization	31
2.10	Processes of Ethanol Fermentation	33
2.11	Bioethanol Production Strategies	35
2.12	Flow Diagram for Separate Enzymatic Hydrolysis and Fermentation	37
2.13	Process Flow Diagrams for Simultaneous Saccharification and Fermentation	39
2.14	Flow Diagram for Simultaneous Saccharification and Co-fermentation (SSCF)	40
2.15	Flow Diagram for Simple Consolidated Bioprocessing (CBP)	41
2.16	Maize Production in Nigeria (million tonnes) Between 1994 and 2013	42
2.17	Corncoobs Obtained from Shelled Corn	43
2.18	Plantain Production (tons) in Nigeria from 1961 to 2017	44

2.19	Plantain Pseudostem Biomass Obtained from Plantain Farmland Following Harvesting of the Edible Plantain Bunch	46
2.20	Sugarcane Bagasse Obtained from Sugarcane Stem after Extracting the Juice	48
2.21	Production of Sugarcane Bagasse in Nigeria	49
3.1	Flowchart of Methodology for the Production of Cellulosic Bioethanol by Simultaneous Saccharification and Co-fermentation	52
3.2	Preparation of Porous Biochar from Sugarcane Bagasse	70
3.3	Biochar-chitosan Beads Prepared at Different Drying Conditions	72
3.4	Flowchart for the Production of 1.5 L of Cellulosic Bioethanol	84
4.1a	Three-Dimensional Response Surface Plots of Plantain Pseudostem Biomass for Percentage Cellulose Removed	97
4.1b	Three-Dimensional Response Surface Plots of Plantain Pseudostem Biomass for Percentage Cellulose Removed	98
4.1c	Three-Dimensional Response Surface Plots of Plantain Pseudostem Biomass for Percentage Hemicellulose Retained	99
4.2a	Three-Dimensional Response Surface Plots of Sugarcane Bagasse for Percentage Delignification	101
4.2b	Three-Dimensional Response Surface Plots of Sugarcane Bagasse for Percentage Cellulose Removed	102
4.2c	Three-Dimensional Response Surface Plots of Sugarcane Bagasse for Percentage Hemicellulose Retained	103
4.3a	Three-Dimensional Response Surface Plots of Corncob Biomass for Percentage Delignification	105
4.3b	Three-Dimensional Response Surface Plots of Corncob Biomass for Percentage Cellulose Retained	106
4.3c	Three-Dimensional Response Surface Plots of Corncob Biomass for Percentage Cellulose Retained	107
4.4	X-Ray Diffraction Pattern of the Untreated and Pre-treated Plantain	108
4.5	X-Ray Diffraction Pattern of the Untreated and Pre-treated Sugarcane Bagasse	109

4.6	X-Ray Diffraction Pattern of the Untreated and Pre-treated Corncob Biomass	109
4.7	Infrared Spectra of the Untreated and Treated Plantain Pseudostem Biomass	110
4.8	Infrared Spectra of the Untreated and Treated Sugarcane Bagasse	111
4.9	Infrared Spectra of the Untreated and Treated Corncob Biomass	111
4.10	Quantitative Profile of Isolates for Fermentative Ability Using Dichromate Test	127
4.11	Effect of Different Concentrations of Ethanol on the Viability of Screened Organisms	128
4.12	Phylogenetic Tree Showing the Relationship Between Screened Organisms for Enzyme Production and Fermentation with other Organisms on the Basis of ITS Sequence	130
4.13	Effect of Soaking Time on the Swelling Capacity of Biochar-chitosan Beads Dried at Different Temperature Conditions	133
4.14a	Thermogravimetric (TG) Curves Showing the Effect of Temperature on weight loss of biochar-chitosan beads prepared at various drying conditions	134
4.14b	Derivative Thermogravimetric (DT) curves showing the effect of Temperature on weight Loss of Biochar-chitosan Beads Prepared at Various Drying Conditions	135
4.15	Effect of Different Drying Temperature Conditions on the Pore Size, Pore Volume and Surface Area of Biochar-chitosan Composites	136
4.16	Effect of Temperature on the Activity of Co-immobilized Enzymes, Free Cellulase, and Free Xylanase	138
4.17	Effect of pH on the Activity of Co- Immobilized Enzymes (CIE), Free Cellulase and Free Xylanase	139
4.18	Effect of Substrate Concentration on the Kinetic Parameters for Free and Co-Immobilized Cellulase and Xylanase	141
4.19	Effect of Incubation Time on the Stability of Free and Co- Immobilized Enzyme Stored in the Refrigerator (4 °C) for 45 days	143
4.20	Effect of Incubation Time on the Stability of Free and Co- Immobilized	

	Enzyme Stored at Room Temperature (25 °C) for 10 days	144
4.21	Effect of Different Storage Temperature on the Stability of Free and Co-Immobilized Enzymes	146
4.22	Effect of Number of Usages on the Relative Efficiency of the Co-immobilized Enzymes on Freeze-Dried Biochar-chitosan Beads	148
4.23	Scanning Electron Micrograph of Free Biochar-Chitosan Bead; Biochar-chitosan Beads Loaded with Co-Immobilized Enzymes; and Co-immobilized <i>Mucor indicus</i> and <i>Saccharomyces cerevisiae</i>	156
4.24	The Effect of Number of Usages on the Relative Efficiency of the Co-immobilized <i>Saccharomyces cerevisiae</i> and <i>Mucor indicus</i>	157

LIST OF PLATES

Plate		Page
4.1	Scanning Electron Micrograph of Plantain Pseudostem Biomass	113
4.2	Scanning Electron Micrograph of Sugarcane Bagasse	114
4.3	Scanning Electron Micrograph of Corncob Biomass	115
4.4	Hydrolytic Zone of Clearance of Organisms on Agar Plate	121
4.5	Agarose Gel Showing the Positive Amplification of the Endo-beta-1,4-glucanase Cellulase Precursor (celE) Gene Amplified from <i>Aspergillus flavus</i> Strain RBL	131
4.6	Agarose Gel Showing the Positive Amplification of the Endo-1,4-beta-Xylanase Precursor (xyn11B) Gene Amplified from <i>Aspergillus niger</i> Strain RDS	131

LIST OF APPENDICES

Appendices	Page
A Standard curves	241
B Confirmation Test for microwave-alkaline pretreated agrowastes	244
C Statistical results and model equations for microwave-alkaline pre-treated agrowaste biomasses	245
D Characteristics of treated and untreated Agrowastes	249
E Organisms isolated for the production of enzyme and for fermentation process	251
F Production and characterization of Enzyme support	254
G Production and characterization of bioethanol	255
H Molecular identification and characterization of organisms	257
I Arrhenius plot for the determination of activation and deactivation energy of free and co-immobilized enzymes	263
J Infrared spectra of free biochar chitosan bead (F) and biochar chitosan beads and biochar-chitosan beads loaded with co-immobilized enzyme (CIE) and co-immobilized mucor and yeast (CMY)	264
K Statistical result for the comparison of plantain pseudostem biomass (PS) and sugarcane bagasse (SB) using R statistical package.	265

ABBREVIATIONS, GLOSSARIES AND SYMBOLS

2FI	Two Factor Interactions
ADP	Adenosine Diphosphate
AEI	Amount of Enzyme Introduced
AER	Amount of Enzyme Remaining
ATP	Adenosine Triphosphate
BET	Brunauer Emmett-Teller
BGL	β -glucosidase
BJH	Barrett-Joyner-Halenda
BSA	Bovine Serum Albumin
Ca(OH) ₂	Calcium Hydroxide
CBH	Cellobiohydrolase
CBM	Cellulose-Binding Module
CBP	Consolidated Bioprocessing
CC	Corncob
CIE	Co-immobilized Enzyme
CMC	Carboxyl Methyl Cellulase
CO ₂	Carbon (IV) oxide
DMRT	Duncan Multiple Range Test
DNA	Deoxyribonucleic acid
DNS	3, 5- Dinitrosalicylic Acid
DNTP	Deoxynucleotide triphosphate
DTG	Derivative Thermogravimetry
EDTA	Ethylenediamine Tetra-acetic Acid
EG	Exoglucanase
EMP	Emden-Meyerhoff-Parnas Pathway
FTIR	Fourier Transform Infrared
GC-MS	Gas Chromatography- Mass Spectrometry

H ₂ O ₂	Hydrogen Peroxide
HRSEM	High Resolution Scanning Electron Microscopy
ITS	Internally Transcribed Sequence
KOH	Potassium Hydroxide
MA	Microwave-Alkaline
NaOH	Sodium Hydroxide
NAD	Nicotinamide Adenine Dinucleotide
NJ	Neighbour joining
OD	Optical Density
PCR	Polymerase Chain Reaction
PS	Plantain Pseudostem
SB	Sugarcane Bagasse
SDA	Sabouraud Dextrose Agar
SDB	Sabouraud Dextrose Broth
SDS	Sodium Dodecyl Sulphate
SHCF	Separate Hydrolysis and Co-Fermentation
SHF	Separate Hydrolysis and Fermentation
SSA	Specific surface areas
SSCF	Simultaneous Saccharification and Co-Fermentation
SSF	Simultaneous Saccharification and Fermentation
SPSS	Statistical Package for Social Science
TGA	Thermogravimetric Analysis
XRD	X-ray Diffraction
YPD	Yeast Peptone Dextrose
W	Watts

CHAPTER ONE

1.0

INTRODUCTION

1.1 Background to the Study

Energy is an essential commodity for human development, modernization and industrialization has elevated the need for energy (Singh *et al.*, 2012a). Most rural community in developing countries have shortage of good sources of energy therefore they mostly rely on traditional means of cooking such as wood and charcoal burning (Simonyan and Fasina, 2013). Modern energy are being supplied by non-renewable sources such as fossil fuel (Lei *et al.*, 2020) which releases dangerous compounds of sulfur, Nitrogen and carbon to the environment (Bergthorson and Thomson, 2015).

The large consumption of non-renewable fossil fuel may likely lead to its depletion in the nearest future (Abas *et al.*, 2015). As a result of this and its disastrous effect on the environment at combustion, there is a search for an ideal substitute (Abas *et al.*, 2015). Although some other energy supplies such as nuclear, solar and wave energy are also available, but they have a high initial cost of creation, a complex maintenance process, the possibility of contamination, and inconsistent feedstock supplies.

Biofuels such as bioethanol, biodiesel, biomethane, biohydrogen, and bio-butanol reduce the total reliance on petroleum-based fuels as they supplement energy demand (Rasool and Hemalatha, 2016). The consciousness to have a clean energy has made biofuel appealing to many people thereby reducing reliance on non-renewable petroleum (Gao *et al.*, 2021). The entire process involved in biomass to produce fuel has immense benefit in both rural and urban development as well as enhancing international policy positively (Tock *et al.*, 2010; Santa-Maria *et al.*, 2013). The use of bioethanol as replacement or enhancement for fossil

fuel has been going on in Brazil and USA for a very long time (Nikas *et al.*, 2022; Bilgili *et al.*, 2022), with United States leading the global production with 59.5 million m³ out of the total 117.5 million m³ and Brazil producing 27.8 million m³.

Aside from increasing the availability of fuel, the mixture of bioethanol with liquid fossil fuel gives a better octane rating to the fuel, it also enhances complete combustion especially in vehicles that are too old (Farkade *et al.*, 2012). The ease with which bioethanol can be integrated into the existing road transportation fuel system is a plus. For example, 5% bioethanol can be blended with conventional fuel without requiring engine modifications (Najafi *et al.*, 2015). Since 1970, ethanol has been used as an alternative energy source, but this anciently produced ethanol is mostly from starch and sugar-based feedstock such as corn, cassava, potato, and sugarcane (Wyman, 2001).

This bioethanol that is produced from starch and sugar products is called first generation bioethanol. Although the techniques for the production of bioethanol is well understood and tend to be economically viable, the use of food-based feedstock is a major challenge coupled with the fact that it cannot meet up with the over 12 billion tons of oil required globally each year (Abas *et al.*, 2015). Many of these issues can be addressed by producing second-generation biofuels from Lignocellulose, which is abundant.

The countries which are known to produce and use the first kind of bioethanol most are United States and Brazil. The United States produces 47% of global bioethanol with approximately 385.94 metric tons of corn, while Brazil produces 43% of global bioethanol with approximately 659 megatons of sugarcane. One ton of sugarcane yields 65 litres of bioethanol, while one ton of corn yields 135.4 gallons of bioethanol (Behera *et al.*, 2019; Gatlula *et al.*, 2021).

Obtaining bioethanol from lignocellulose establishes a clear link between energy access and poverty reduction and development. Apart from helping to alleviate poverty, it also promotes social and economic development while ensuring energy security. Because of its superior counterbalance capacity, bioethanol solves the problem of energy supply with little or no release of dangerous gases in the process of re-synthesizing biomass (Sims *et al.*, 2010).

Despite the promising window of lignocellulosic bioethanol production, it is characterized by several challenges. Such challenges include recalcitrance of lignocellulose materials to activities of enzyme, exorbitant means of producing enzymes as well as inability of native *Saccharomyces cerevisiae* to ferment all the available sugar to ethanol (Mu *et al.*, 2010). Bioethanol could be produced biochemically or thermochemically. Biochemical approach is most promising because it has high selectivity and conversion efficiency (Mu *et al.*, 2010). In the biochemical method, recalcitrant lignin will be reduced or removed to give access to enzyme which will act on the exposed polysaccharides to release fermentable sugars which will be eventually converted to bioethanol during fermentation (Wyman, 2007).

Pre-treatment is the most important and likely the most difficult step in lignocellulose bioethanol production because it affects virtually all other operations and is costly on its own (Wyman, 2007). During pre-treatment, the feedstock is split into its individual constituents which are cellulose, hemicellulose and lignin. There are many treatment methods with their consequent advantages and disadvantages (Ezeoha *et al.*, 2017).

Following pre-treatment, cellulose and hemicellulose (collectively known as holocellulose) components of the biomass are saccharified by different enzymes (either produced or purchased externally), which typically convert them into fermentable sugars. Enzyme costs have accounted for a very good proportion (30%) of the total cost required to produce

bioethanol (Kadhun *et al.*, 2019). Furthermore, free enzyme tends to be lost with the product, necessitating the use of fresh enzyme for each production. However, when enzymes are produced locally and immobilized to ensure re-use, the cost of bioethanol production is drastically reduced. The formed sugars are then used to produce bioethanol by microorganisms through the fermentation process. In this scenario, various methods of hydrolysis-fermentation combinations are used. This method includes separate hydrolysis and fermentation (SHF) and simultaneous saccharification and fermentation (SSF), have been proposed (Vohra *et al.*, 2014; Jambo *et al.*, 2016; Olofsson *et al.*, 2017). simultaneous saccharification and co-Fermentation (SSCF) and consolidated bioprocessing are two other strategies (CBP) for fermentation. The downstream fermentation of the reducing sugar produced after hydrolysis is also difficult because the wild *Saccharomyces cerevisiae* strain, which has traditionally and industrially been used to produce ethanol from sugar, cannot ferment the pentose sugar (Subtil and Boles, 2012).

Some native microorganisms capable of fermenting pentose sugar, such as *Pichia stipitis*, *Zymomonas mobilis*, and *Candida tropicalis*, have low ethanol yields and cannot withstand the fermentation conditions. Recently, the ability of zygomycetes to produce ethanol was investigated. *Mucor indicus* (formerly *M. rouxii*), a zygomycete which thrive with or without oxygen on so many kinds of carbon sources, including simple sugars has been shown to produce bioethanol and is also able to tolerate ethanol as much as *Saccharomyces cerevisiae* (Karimi and Zamani 2013; Lennartsson *et al.*, 2014). It's very high tolerance to fermentable sugar, ethanol, as well as various potential inhibitors suggests that it has industrial potential (Abtahi *et al.*, 2011). Therefore, its industrial potential has been explored for bioethanol production.

The total dimension of land owned by Nigeria is 923, 768 km² with close to 200 million occupants and a growth rate of 2.7% (Adegoke *et al.*, 2017). This land can be divided into arable (33%), permanent crop (3.1%) permanent pasture (44%), forest and woodland (12%), and 0.3% is under irrigation. The resources available in Nigeria makes it possible to sufficiently produce biofuels and as well supply feedstock such as plantain biomass, corn residues as well as sugarcane bagasse to other countries (Agbro and Ogie, 2012).

Nigeria is among the leading producers of plantain, with an annual output of over 3 million metric tons (Olumba and Onunka, 2020). However, most of the plantain produced are being consumed within the country due to increasing crave for fast food especially in the urban centres (Udomkun *et al.*, 2021). Out of the three million metric tons generated annually in Nigeria, one hundred metric tons of plantain produced can be generated per hectare (Saraiva *et al.*, 2012). Plantain pseudostem contains 47%, 23%, and 13% of cellulose, hemicellulose and lignin respectively which makes it a good candidate for bioethanol production (Olumba and Onunka, 2020).

Sugarcane (*Saccharum officinarum*) is a perennial, tall grass that resembles a bamboo cane and thrives in tropical climates. Sugarcane can be grown in almost every state in some West African countries, including Nigeria, but it is commercially produced in Katsina, Taraba, Adamawa, Kebbi, and Sokoto (Issa *et al.*, 2020). Sugarcane bagasse is the remnant or leftover shaft remaining after the liquid part of sugarcane stem has been removed. It contains approximately 40% cellulose, 25% hemicellulose, and 21% lignin which made it a good candidate for bioethanol production.

Nigeria is among the ten largest producers of corn, also known as maize, and the second highest producer in Africa after South Africa (Abdoulaye *et al.*, 2018). Nigeria produced 11.6

million metric tons of corn in 2021. However, local demand continues to outstrip supply. In 2020, the Central Bank of Nigeria encouraged increased local corn production by prohibiting the issuance of forex for corn importation. Maize cobs are leftovers of maize crops after the grains are removed. It contains approximately 35% cellulose and 25-40% hemicellulose, making it an excellent candidate for bioethanol production (Raja, 2018). Each ton of maize shelled yields approximately 180 kg of cobs (Atoyebi *et al.*, 2019).

1.2 Statement of the Research Problem

Fossil liquid fuel, which is mostly utilized for modern energy supplies releases dangerous gases at combustion thereby causing environmental pollution. Secondly, Fossil liquid fuel is produced from non-renewable sources like petroleum which is fast depleting due to constant use. Also, the commercially available bioethanol is being produced from food-based feedstock and this is posing a challenge to food security. For instance, United States produces about 385.94 metric tons of corn out of which 40% is used to produce bioethanol (Saini and Sharma, 2021). Nigeria produced about 11.6 metric tons of corn as at 2021, yet its local demand continues to surpass supply by about 4 million metric tons annually (Alabi and Safugha, 2022). Also, the present sugarcane (1.5 million metric tons) and plantain (3 million metric tons) produced in the country are not enough to meet the country local demand. Aside from the fact that these crops are not enough for local consumption talk less of converting them to bioethanol, the waste generated from these crops are being underutilized and mostly constitutes nuisance to the environment. Therefore, there is need to produce bioethanol from non-food lignocellulosic feedstock such as corncob, plantain pseudostem biomass, and sugarcane bagasse. However, production of lignocellulosic bioethanol from non-food-based feedstock at a commercial level is still challenging due to the recalcitrant nature of lignin and

the high cost of hydrolytic processes. Alkaline such as sodium hydroxide has been shown to be very effective in lignin removal while still preserving the cellulose and hemicellulose contents (Sun *et al.*, 2016), However, using alkaline pre-treatment alone takes hours or even days to effectively remove lignin. Studies have shown that combination of alkaline with microwave power reduces the process time and at the same time remove lignin effectively. Therefore, there is need to optimize the conditions at which microwave-alkaline pre-treatment method is being carried out for effective delignification of some selected locally abundant agrowaste. The incomplete fermentation of hexose sugars (C₆) and pentose sugars (C₅) has limited the ethanol yield from lignocellulosic materials due to inability of the industrially preferred *Saccharomyces cerevisiae* to ferment pentose sugars. Therefore, the inclusion of organism which is capable of fermenting pentose sugar in the fermentation process will enhance higher bioethanol yield. The use of cellulase, xylanase and fermenters differently and in free form increases industrial process and consequently increase the cost of bioethanol production. Therefore, there is need to co-immobilize these moieties for an easier and cheaper fermentation process.

1.3 Aim and Objectives of the Study

The aim of this research was to optimize microwave-alkaline (MA) pre-treatment conditions for the effective delignification of some selected locally available agrowaste and co-immobilization of cellulase, xylanase, and as well co-immobilize yeast and mucor for optimal production of bioethanol.

The objectives of this research are to:

- i. determine optimal conditions for agrowaste pre-treatment using microwave – assisted-alkaline pre-treatment methods;

- ii. screen microorganisms from suitable sources for the production of xylanase and cellulase;
- iii. develop suitable immobilization technique for co-immobilization of xylanase, cellulase, and suitable pentose and hexose sugar fermenters;
- iv. evaluate enzymatic properties, storage stability and re-usability of free and immobilized moieties developed from objective iii; and
- v. evaluate production of ethanol using immobilized moieties from objective iii and its quality

1.4 Justification for the Study

Production of cheap and environmentally friendly bioethanol will break the monopoly of fossil fuel and also address its environmental threat. Out of 11.6 million metric tons of corn produced in Nigeria annually as reported by Alabi and Safugha (2022), 2.088 million metric tons of corncob biomass is generated. Also, out of about 1.5 million metric tons of sugarcane produced annually in Nigeria, 30% (454.2 metric tons) of bagasse is generated. Likewise, about 100 metric tons of plantain pseudostem is being generated per hectare in Nigeria. Therefore, the abundant availability of renewable waste biomass in Nigeria for the production of bioethanol justifies its sustainability. Microwave-assisted-alkaline pre-treatment conditions has been widely studied for its effective delignification potential (Arpia *et al.*, 2021), however its optimization for the pre-treatment of locally abundant agrowaste is a step towards cheap bioethanol production. The use of microorganism which can ferment pentose sugars and as well have the same industrial properties like *S. cerevisiae* will enhance high ethanol yield from lignocellulosic. The immobilization of cellulase, xylanase and fungi on suitable supports will enhance stability and re-usability of enzyme and fermenter in a simultaneous saccharification and fermentation process, which will save time and cost of

production. Therefore, this study focused on alkaline delignification of selected agrowaste and the co-immobilization of cellulase, xylanase and fermenters on suitable supports to produce bioethanol. This will enhance maximum lignin removal and ensure efficient hydrolysis of cellulose and hemicellulose. It will also reduce time and cost of production due to stability and re-usability of enzyme and fungi in simultaneous saccharification and fermentation thereby making bioethanol available and affordable for a cleaner and safer environment.

CHAPTER TWO

2.0 LITERATURE REVIEW

2.1 Definition of Bioethanol

Bioethanol is an alcohol containing two carbon atoms which is also called ethyl alcohol. It can be produced biochemically by microbial fermentation unlike some ethanol that is being produced chemically. It is produced by distilling an ethanolic product derived from the fermentation of biomass-derived sugars (Gavahian *et al.*, 2019). Bioethanol being the most widely used liquid biofuel can be used alone or combined with fossil fuel in combustion engine. Currently, ethanol accounts for about 85% of the total fuel produced in the world (Kim and Kim, 2014). The bulk of the total production (about 90%) is done in Brazil and United States of America while other countries like Canada, China, India, and France take the rest proportion (Gavahian *et al.*, 2019).

2.1.1 Bioethanol generation

Depending on the source, bioethanol produced has been classified into various generations. This includes first, second, third and fourth generations.

2.1.1.1 *Bioethanol of the first generation*

First-generation bioethanol is made directly from food-based crops via fermentation. Corn and sugar are the most commonly used feedstock for first generation bioethanol production. However, there are a number of issues with first generation bioethanol. Some of the contentions on the first-generation bioethanol is negative net energy such that the amount of carbon released during its production tend to be higher than the amount released during the growth of the feedstock, thus making their benefits in reducing greenhouse gas doubtful (Dutta *et al.*, 2014). However, the most important concern is the use of food-based feedstock

which has resulted into the scarcity of food due to higher demand for bioethanol in recent years (Chiaramonti *et al.*, 2012).

2.1.1.2 Bioethanol of the second generation

Second-generation bioethanol, otherwise called lignocellulosic bioethanol, was created to address the shortcomings of first-generation bioethanol. This is because they are produced from non-food based feedstock such as wood, waste from food crop as well as some crops like switchgrass grown specifically for energy (Aditiya *et al.*, 2016). Lignocellulosic bioethanol has other added advantages, such as emission of little or no greenhouse gases, positive energy gains as well as no threat to food security (Chiaramonti *et al.*, 2012). It is challenging to effectively produce bioethanol from lignocellulosic biomass because of the need to pre-treat the biomass to release the inherent holocellulose (cellulose and hemicellulose), which also has to be converted to simple sugars before fermentation to ethanol can take place (Singla *et al.*, 2012).

2.1.1.3 Bioethanol of third generation

The third generation of bioethanol is intended on improving on second generation bioethanol in the sense that it is produced using specially engineered crops such as algae which is specifically grown for energy (Chisti, 2007). Algae are grown to be cheap and always available sources. According to predictions, algae is able to produce more fuel per acre than any other crop and it can be grown on land and in water that would otherwise not support food-base crops. Another advantage of using algae for fuel production is that it can be used to produce any kind of fuel including diesel, gasoline, and jet fuel (Jambo *et al.*, 2016). However, third generation biofuel production has disadvantages such as reliance on sunlight in addition to the fact that many microalgal species cannot fit into industrial process (Siaut

et al., 2011). Furthermore, the costs of photobioreactor or open pond cultivation, biomass harvesting, and the means of extracting oil from algal biomass are still very high (Grima *et al.*, 2013).

2.1.1.4 Bioethanol of the fourth generation

This generation of bioethanol is not intended to make energy sustainable but to capture and store CO₂. Although, the processes involved is similar to that of second-generation bioethanol but the main difference is to target the capturing of carbon dioxide at every stage of production (Niphadkar *et al.*, 2018). Carbon dioxide can then be stored in old oil and gas fields or saline aquifers to be preserved. It is a carbon negative process since it actually prevents carbon dioxide from getting to the environment (Lu *et al.*, 2011; Shokravi *et al.*, 2019). Meanwhile, fourth generation is still in its infancy.

2.1.2 Lignocellulose as a bioethanol feedstock

Lignocellulose is generally given to plant-based biomass because they contain cellulose, hemicellulose and lignin. These set of biomasses are in three categories: virgin biomass, waste biomass and energy crops (Nanda *et al.*, 2018). Virgin biomass includes all naturally occurring plants grown on land while waste biomass is low-value by-product from industries, farms and even houses whereas some special crops grown specifically for energy production are called energy crops (Saini *et al.*, 2015).

2.1.3 The advantages of lignocellulosic bioethanol

The production of ethanol from lignocellulosic biomass has many advantages over production from other sources, the most notable of which is the little or no greenhouse gas emissions during its production and use (Ozdingis and Kocar, 2018). Bioethanol production is also important for boosting economic growth, particularly in developing countries where

more energy is required to improve living standards of people (Steckel *et al.*, 2013). It is a way to discourage rural-urban migration because it creates jobs in all areas and provides an appealing way to dispose of agricultural waste. It also increases income for the farmers, ensuring long-term agricultural sustainability. Aside from increasing fuel supply, adding ethanol to gasoline raises octane and adds oxygen to aid complete combustion in the engine, especially in older vehicles (Nwangi *et al.*, 2015).

2.2 Composition of Natural Lignocellulosic Feedstocks

Lignocellulose is a complex matrix made up of numerous polysaccharides, phenolic polymers, and proteins (Jönsson and Martín, 2016). It is made up of 40-50%, 25-30% and 15-20% of cellulose, hemicellulose and lignin respectively, as shown in Figure 2.1.

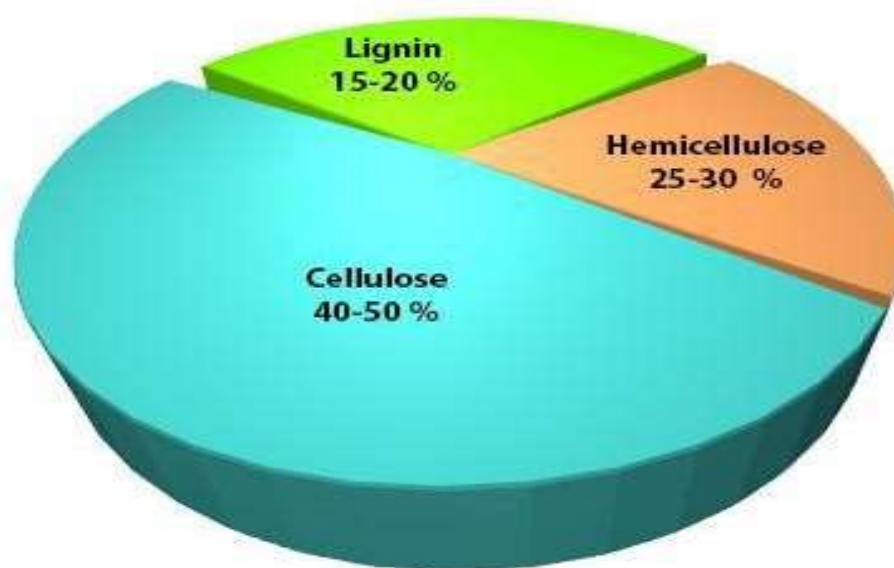


Figure 2.1: Major Lignocellulose Constituents
Source: Jönsson and Martín (2016)

2.2.1 Cellulose

Cellulose is the most abundant part of lignocellulose biomass and one of the most extensively researched chemical compounds on the planet (Xu *et al.*, 2016a). Cellulose is a structural constituent of plant cell wall and it is made up of linear -1,4-linked D-glucopyranose residues with a polymerization degree of at least 15000. The hydrogen bonds which are located within the cellulose molecules enables nearby parallel or anti-parallel linear chains to condense so as to form very long and thin structure resulting into major microfibrillar phase (Limayem and Ricke, 2012). The crystalline network structure of the cellulose chain results in high tensile strength, making it water soluble and less flexible, it is also relatively resistant to biological attack which is a major setback for cell wall hydrolysis (Zhang *et al.*, 2015).

2.2.2 Hemicellulose

The second most abundant polysaccharide in plant cell walls is hemicellulose, accounting for approximately 20-35% of plant materials (Pauly *et al.*, 2013). Unlike cellulose, which has a relatively uniform composition, hemicellulose varies greatly from cell to cell. Furthermore, the level of branching and the properties of the sugars within hemicellulose in different plants vary. However, for a given plant, one type of hemicellulose is usually dominant. The most abundant hemicellulose in agricultural residue is xylan (Limayem and Ricke, 2012). Xylan has a backbone made up of β -1, 4-linked xylose residues. α -linked 4-O-methylglucuronic acid on C2, α -linked arabinose, or acetyl esters on C2 or C3 of some xylose residues can occasionally substitute for this structure (Pauly *et al.*, 2013). Hemicellulose non-covalently bonds to cellulose via hydrogen bonds and its asymmetric C-5 sugar ring aid celluloses in the formation of liquid crystalloid. However, xylan lacks crystalline structure due to its inability to link with its neighboring polysaccharide chains by hydrogen bonds. Few plant

cell walls contain nearly equal amounts of cellulose and xylan; however, because xylan can form hydrogen bonds only on one side, only one half of xylan could be found to directly interact with cellulose, assisting in the construction of the structural backbone of plant cell wall (Rennie and Scheller, 2014). This type of intersection is sometimes referred to as cellulose sheathing by hemicellulose, which is also considered an impediment to cellulose digestion.

2.2.3 Lignin

Lignin is naturally most abundant aromatic polymer that form the foundation during cell elongation and typically accounts for 10-25% of plant material (Vanholme *et al.*, 2010). Hydroxyphenyl alcohol, guaiacyl alcohol, and syringyl alcohol are the major alcohol linked together to form the final phenolic network in lignin (Moreno *et al.*, 2015). Furthermore, as long as the precursors are available, the lignin network expands, filling in the gaps left by other components and significantly taking the place of water. The presence of lignin gives strength to the hydrogen bonds within the complex meshwork of polysaccharides making cellulose-hemicellulose complex more stable and stronger (Mood *et al.*, 2013), while also limiting enzyme access to the internal polysaccharides.

2.3 Ethanol Production from Lignocellulosic Biomass

Although different bioconversion processes have been employed to make bioethanol from lignocellulose, four general processes mostly practiced are: pre-treatment, hydrolysis, fermentation, and distillation (Nanda *et al.*, 2018). The benefit of pre-treatment is that it makes cellulose and hemicellulose available for enzymatic action by removing the lignin seal. The enzyme in turn breaks down the cellulose and hemicellulose to sugars which are then fermented to bioethanol. Finally, purification through distillation and dehydration is

required to meet fuel market demands. Basically, the most important steps in the conversion of lignocellulosic materials to ethanol is shown in Figure 2.2.

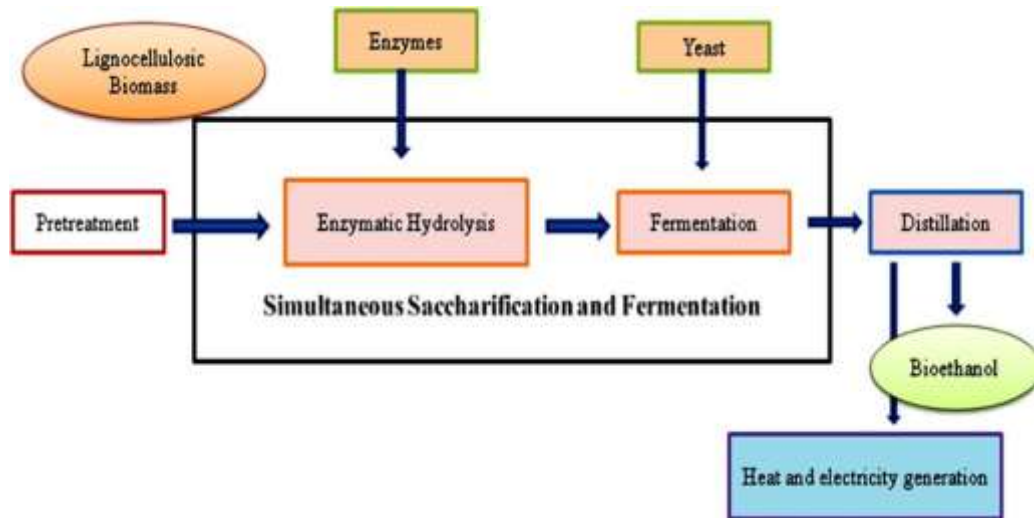


Figure 2.2: Bioethanol Production from Lignocellulosic Materials
Source: Maurya *et al.* (2015)

The primary components of interest during pre-treatment are cellulose and hemicellulose on which chemicals or enzymes can act to produce fermentable sugars

2.3.1 Pre-treatment

The first step involved in bioethanol production is pre-treatment. At this stage, major components (hemicellulose, cellulose, lignin) of biomass are dissolved and separated for easy accessibility (Rezania *et al.*, 2020). It also modifies or removes any impediments to hydrolysis for effective accessibility, improves enzyme hydrolysis rate, and enhance yields of intended products (Moreno *et al.*, 2015). As a result, pre-treatment exposes cell wall materials to enzymatic attack, increases substrate surface area and porosity, increases cellulose crystallinity index, and disrupts the heterogeneous structure of cellulosic materials

(Breig *et al.*, 2021). The relative position of lignin, hemicellulose and cellulose before and after pre-treatment is shown in Figure 2.3.

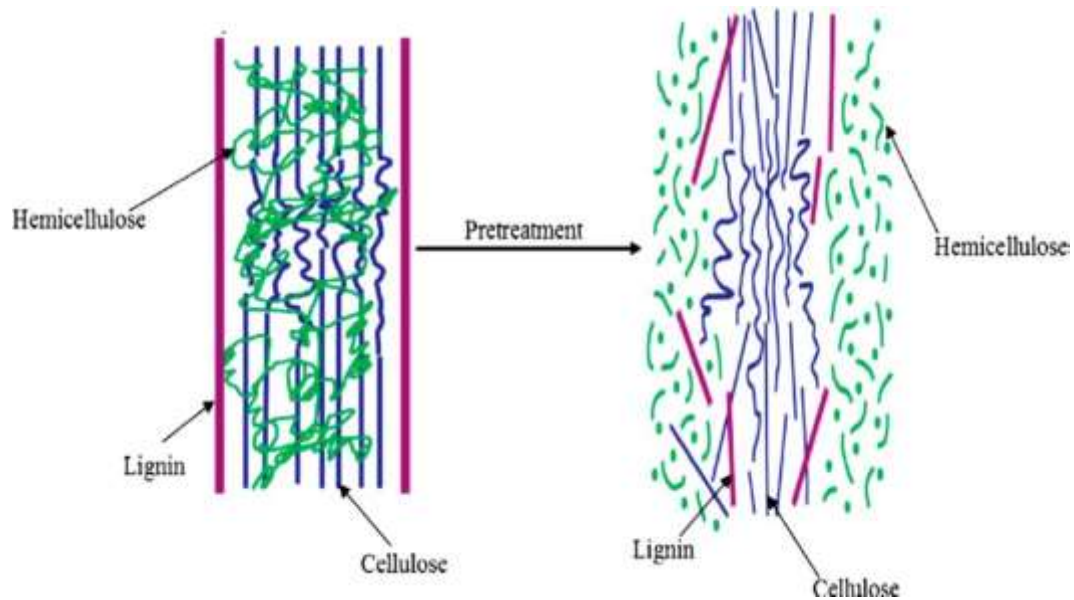


Figure 2.3: Effect of Pre-treatment on Lignocellulosic Materials
Source: Mosier *et al.* (2004)

An effective pre-treatment must be capable of preserving both pentose (hemicellulose) and hexose (cellulose) fractions and as well be able to avoid, to the barest minimum, formation of toxic components which can negatively affect the growth of fermentative microorganisms (Balasundaram *et al.*, 2022.). However, there is no known perfect pre-treatment method because the suitability of one method for different materials varies (Wyman *et al.*, 2005). Pre-treatment methods are in the category of physical, chemical, physicochemical and biological pre-treatment as shown in Figure 2.4.

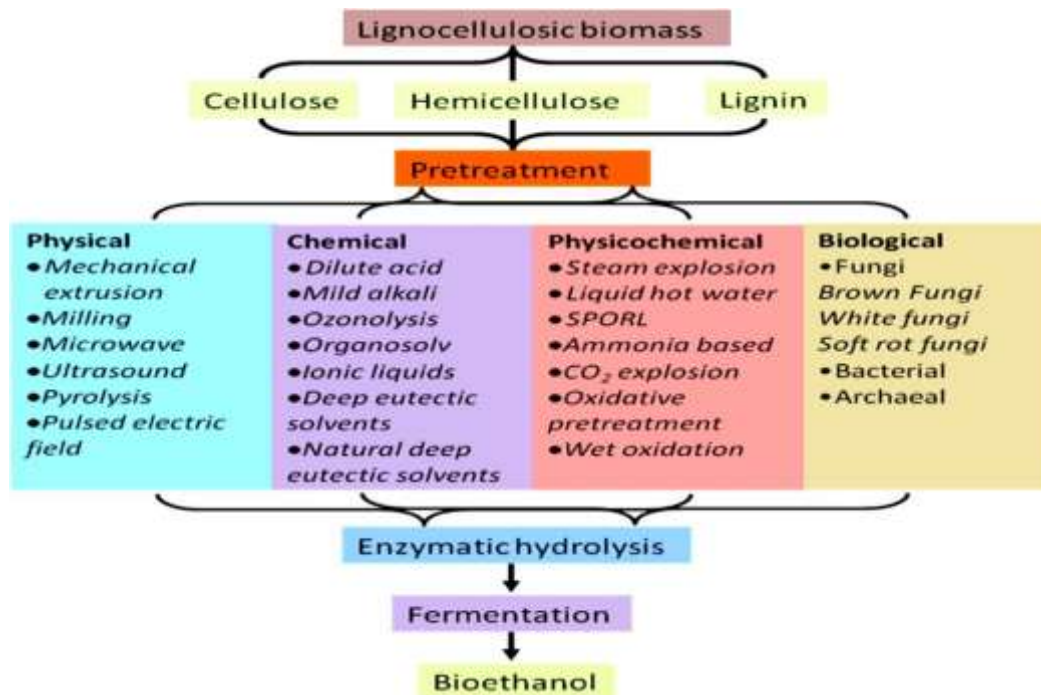


Figure 2.4: An Overview of Various Pre-treatment Processes
Source: Dias *et al.* (2011)

2.3.1.1 Physical pre-treatment

Physical pre-treatment includes mechanical pulverization, steam explosion, microwave, radiation and so on (Karimi and Taherzadeh, 2016). Here are a few examples:

i. Mechanical pulverization

Mechanical pulverization can bring about a noticeable change in the physical properties of biomass. These changes may include reduction in particle size, and smaller degree of crystallinity as well as polymerization. It is a common method used in the corn-ethanol conversion process, enabling efficient enzymatic action on corn kernel (Yu *et al.*, 2019). However, lignocellulosic biomass requires significantly more mechanical energy than corn.

ii. Steam explosion (autohydrolysis)

The rapid thermal expansion provided by steam explosion enabled the opening of target biomass structure. It has been shown to work more effectively for hardwoods and agricultural residues, but less so for softwoods (Yu *et al.*, 2019).

iii. Microwave

The impact of temperature is a major determining factor in microwave pre-treatment method. The fact that the required temperature is mostly more 180°C makes it very effective in softening cell wall and reduce cellulose crystallinity. Previous research on rice agricultural residue has confirmed that microwave has a good record of removing lignin and changing the crystalline structure of cellulose, thereby granting easy access to enzyme (Lai and Idris, 2013). In contrast to conduction/convection heating, microwave heating generates heat by direct interaction between a heated target and an electromagnetic field. When microwave is used to treat lignocellulosic materials, the heating is volumetric and rapid. It is assumed that this unique heating feature has an 'explosive effect' among particles and improves disruption of recalcitrant structure of lignocelluloses. Furthermore, the electromagnetic field of microwave may cause non-thermal effects that accelerate the destruction of crystalline structures. Some authors have also reported that microwave/alkali pre-treatment can remove more lignin and hemicellulose from rice straw in less time than alkali alone. For example, combining microwave treatment with alkali (NaOH) has been shown to be more effective than using the alkali alone for lignin removal (Egwim *et al.*, 2015). Microwave-based technologies have other benefits such as reduction in energy needed in the process, uniform and specific processing and also the equipment is user friendly (Lai and Idris, 2013).

2.3.1.2 Pre-treatment with chemicals

i. Pre-treatment with acid

It is a long-time practice to use concentrated acid, particularly sulphuric acid, to degrade cellulose (Wyman and Yang, 2017). Dilute acid pre-treatment has recently been well developed to cater for the intense effects of concentrated acid such as corrosion and extra effort needed to recover the acid (Sun and Cheng, 2002; Yildirim *et al.*, 2021). The primary function of dilute acid pre-treatment is to effectively remove the hemicellulose sheathing over cellulose while loosening the lignin structure (Wyman and Yang, 2017).

ii. Pre-treatment with alkaline

Alkali pre-treatment is performed under milder conditions with lower temperature and pressure. However, alkali pre-treatment takes much longer depending on the operation temperature chosen (Wyman *et al.*, 2005; Lai and Idris, 2013). For biomass pre-treatment, bases such as NaOH, KOH, and NH₄OH can be used (Kim *et al.*, 2016). The main function of alkali is to saponify the ester bonds linking lignin and carbohydrates thereby resulting into increased porosity and internal surface area of the material (Tahezadeh and Karimi 2008). NaOH is more effective than the other bases studied (Sun *et al.*, 2016; Kumar *et al.*, 2009). However, the effect of dilute NaOH on softwood is not felt when lignin content is higher than 26% (Kumar *et al.*, 2009; Zhu *et al.*, 2010; Wang *et al.*, 2020). Singh and Trivedi (2013) conducted a comparative study between acid and alkaline pre-treatment effect on lignocellulosic biomass. After pre-treatment with 3% sulphuric acid, cellulose was found to be in the range of 55-62%, while hemicelluloses and lignin were found to be in the ranges of 6-12% and 15-31%, respectively. A comparison of different alkaline pre-treatments was also made, and it was discovered that NaOH is more effective than KOH and Ca(OH)₂. The

percentage of glucose produced by alkali pre-treatment with NaOH was found to be 58%, which was higher than the percentages produced by KOH (54%) and Ca(OH)₂ (40%). Sun *et al.* (1995) investigated the efficacy of various alkaline solutions by examining its effect on lignin and hemicellulose in wheat straw. They discovered that 60% lignin and 80% hemicellulose were released by the use of 1.5% sodium hydroxide for 144 hs at 20 °C. Zhao *et al.* (2008) also reported that sodium hydroxide pre-treatment was very effective on hardwoods, wheat straw, switchgrass, and softwoods which has less than 26% lignin content. Pre-treatment with sodium hydroxide is also effective to increase biogas production from corn stover by 37% when compared to untreated cellulose (Zhu *et al.*, 2010).

Lime [Ca(OH)₂] is another common alkali which removes acetyl groups and the lignin-carbohydrate ester, as well as improve cellulose digestibility (Mosier *et al.*, 2004). It has been successfully used to pre-treat wheat straw, poplar wood, switchgrass, and corn stover (Kim and Holtzapfle 2006; Rodrigues *et al.*, 2016). In addition, compared to NaOH or KOH pre-treatments, this pre-treatment has lower reagent costs, more user friendly, and it can be easily re-collected after use when the hydrolysate is reacted with CO₂ (Mosier *et al.*, 2004; (Carvalho *et al.*, 2008). Alkaline pre-treatment takes a longer time when done at low temperature, combining it with other methods such as microwave irradiation has been shown to shorten the process time. (Meng and Ragauskas, 2014; Wang *et al.*, 2020).

iii. Pre-treatment with cellulose solvent

Another chemical additive used for pre-treatment are chemicals that are capable of dissolving cellulose (Mosier *et al.*, 2004). These solvents work by disrupting the structure of cellulose in biomass feedstocks and increasing enzyme digestibility during hydrolysis. Examples of such solvents are alkaline H₂O₂, ozone, and glycerol, can (Satari *et al.*, 2019).

2.3.1.3 Pre-treatment with biological agents

In order to remove lignin from the plant cell wall in biological pre-treatment, genes are modified and enzymes are used. Biological pre-treatment is more time-consuming and involves more complicated reactions than physical or chemical processes (Moreno *et al.*, 2015).

2.3.2 Hydrolysis

The effectiveness of hydrolysis is determined by the outcome of the pre-treatment operation (Alvira *et al.*, 2010). Sugars are released which are then fermented and converted to bioethanol. Acidic (sulfuric acid) hydrolysis and enzymatic hydrolysis are the two main types of hydrolysis processes (Xie *et al.*, 2021).

2.3.2.1 Acidic hydrolysis

Hydrolysis can be carried out using either dilute or concentrated acids. To disrupt cellulose crystals in dilute acid hydrolysis (about 3% v/w) a high temperature of 200 °C to 240 °C is required. The disadvantage of dilute hydrolysis is the generation of harmful compounds such as HMF (Hydroxymethylfurfural) and phenolic, which can obstruct effective saccharification (Lenihan *et al.*, 2010).

Concentrated acid hydrolysis is widely used because it is more practical producing higher yield of sugar and lesser concentrations of inhibitors. The disadvantage of this approach is that it necessitates large amounts of acid, which makes the cost of production high as a result of recycling of the acid. To this end, it is not commercially viable, and much water molecules are being removed from the formed monosaccharides, resulting in aldehydes and other types of unwanted substances (Zhou *et al.*, 2021). The difficulties in acid hydrolysis have led to the advancement of research into cellulolytic enzymes.

2.3.2.2 *Enzymatic hydrolysis*

The use of enzyme in hydrolyzing biomass is thought to be critical to long-term cost-effective bioethanol production. The benefits that enzyme hydrolysis has over acid are that it eliminates corrosion problems, has higher substrate specificity, and lowers maintenance costs while producing high yields under mild processing conditions (Maitan *et al.*, 2015). Mechanical milling and grinding can increase the external surface area of lignocelluloses. More recently, the addition of xylanase has been shown to improve cellulase effectiveness (Moraïs *et al.*, 2010; Hu *et al.*, 2011; Prajapati *et al.*, 2018).

i. Cellulases

Cellulases are responsible for the hydrolysis of β -1,4-glucosidic bonds in cellulose thereby releasing the monomeric glucose as shown in Figure 2.5. The effect of the three major enzymes (endoglucanase [EC 3.2.1.4], exoglucanase [EC 3.2.1.91], and glucosidase [EC 3.2.1.21]) contained in cellulase results in cellulolytic activity (Sharma *et al.*, 2016). Cellulases are used in a variety of industrial applications, including the biofuel industry for biomass hydrolysis, as well as textile industry, animal feed industry, food industry, detergent industry (Ejaz *et al.*, 2021). These enzymes belong to the category of enzymes glycosyl hydrolase families based on similarity in sequence and cluster analysis.

Cellulase is a valuable commercial enzyme that can be isolated, extracted, and produced locally through fermentation, saving the country money on importation (Oyeleke *et al.*, 2012). Commercial cellulase preparations from *Trichoderma reesei* are popular because they have high exo-glucanase and endo-glucanase activities but low levels of β -glucosidases, hence other organisms like *Aspergillus* species are being explored (Bansal *et al.*, 2012). The cellulase produced by *Aspergillus fungi* is more preferred in industry because it has high

activity when compared to the enzyme produced by yeast and bacteria (Shah *et al.*, 2017). As a result, this genus has the potential to rule the enzyme industry. *Aspergillus niger* has been widely used because it contains all three essential components of the cellulase system (Salihu *et al.*, 2015).

The entire hydrolysis process is divided into two steps as shown in Figure 2.5. Primary hydrolysis is a depolymerization process which occurs on the surface of a solid substrate and involves endoglucanase and exoglucanase activities, it releases soluble sugars of up to 6 units into the liquid phase (Houfani *et al.*, 2020). The most important step in the process involved in the hydrolysis of cellulose is depolymerization. The next stage of hydrolysis which is secondary hydrolysis occurs in the liquid phase, with β -glucosidases primarily hydrolyzing cellobiose to glucose.

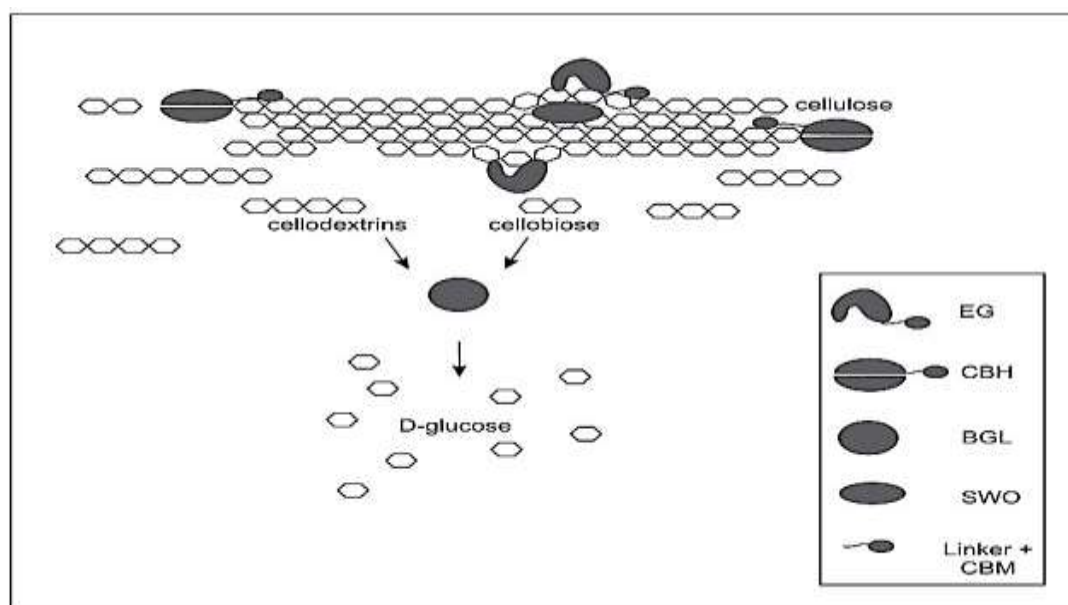


Figure 2.5: Mechanism of Action by Cellulase Enzyme
Source: Seiboth *et al.* (2011)

ii. Xylanases

Cellulose, hemicellulose, and lignin form the major part of plant cell wall (Rodrigues Mota *et al.*, 2018). Hemicelluloses in agrowaste residues are majorly xylan which are primarily composed of D-xylose, D-mannose, D-galactose, and L-arabinose (Qaseem *et al.*, 2021). The majority of xylan are heteropolysaccharides with various substituent groups (e.g., acetyl, arabinosyl, and glucuronyl residues) in the rachis and side chains (de Carvalho *et al.*, 2019). The decomposition of hemicelluloses to their constituent sugars is required for the conversion of xylan into useful end products (Biely *et al.*, 2016). Xylanases break down the linear polysaccharide β -1,4-xylan into xylose, thereby disrupting hemicellulose which is a major constituent of plant cell walls (Uday *et al.*, 2016).

Xylanases have received so much attention in recent years because they have uses in bleaching and pulping processes that use cellulose-free combinations, in the food processing industry, textile processes, enzymatic pre-treatment of lignocellulosic materials, and organic waste treatment (Shah and Vishwa, 2019). Using xylanases during enzymatic hydrolysis also aid the activity of cellulase since xylan which could block cellulase activity would have been removed by xylanase (Morais *et al.*, 2010). Some industrial sources of commercial xylanases include *Aspergillus niger*, *Trichoderma reesei*, *Bacillus*, and *Humicola insolens*, with optimum temperatures ranging from 40 °C–60 °C (Chadha *et al.*, 2019). Filamentous fungi are more useful xylanase producers because they can produce high levels of extracellular enzymes and are easier to cultivate than bacteria and yeast (Pal and Khanum, 2010; Chadha *et al.*, 2019).

Complete xylan hydrolysis brings multiple enzymes into action with overlapping but distinct roles (Biely *et al.*, 2016). These enzymes are made up a variety of hydrolytic enzymes (Figure 2.6), that work together to convert xylan to its constituent sugars (Uday *et al.*, 2016; Malgas *et al.*, 2019).

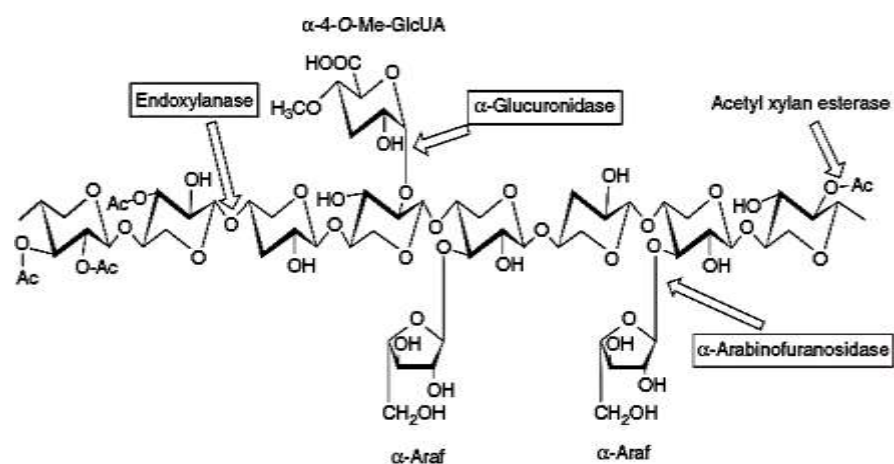


Figure 2.6: Mechanism of Action of Xylanase Enzyme; α -Araf, α -arabinofuranose; α -4-O-Me-GlcUA, α -4-O-methylglucuronic acid.
Source: Antil *et al.* (2015)

2.3.3 Immobilization of enzymes and cells

The process of immobilization generally involves locking up of an enzyme or cell physically in a specific defined region of space while they are still retaining their activities, and ability to be used repeatedly and continuously (Guzik *et al.*, 2014). This confinement of microbial cells and enzymes has both technical and economic benefits such as higher product purity, cleaner processes, and lower operational costs, but it also makes the use of enzymes or cells more cost effective and simple to manage (Brena *et al.*, 2013). Aside from making the enzyme easier to handle, it also improves the stability of enzyme under both storage and operational conditions (Hernandez and Fernandez-Lafuente, 2011; Saifuddin *et al.*, 2013). It is possible to conclude that enzyme immobilization reduces or eliminates protein

contamination of the products, increases biocatalyst productivity and improves their properties, making them more appealing for a variety of applications (Nguyen and Kim, 2017).

2.3.3.1 *Co-immobilization of enzymes and cells*

The confinement of two or more enzymes or cells in the same space is known as co-immobilization. Economic and environmental constraints are making way for the development of co-immobilized multiple-enzymatic systems. This approach mimics the biological nature in that, the desired products is formed within a cell thereby improving stability and also reaction kinetics by optimizing catalytic turnover due to the effect of substrate channeling and synergistic effects of the co-immobilized moieties (Saifuddin *et al.*, 2013).

Co-immobilized enzymes are used for three main reasons: to improve the efficacy of one of the enzymes as it produces its substrate in-situ, to make complex processes simple by carrying it in a single step, and also to eliminate unwanted by-products which may be produced during enzymatic reactions. As a result, the advantages of co-immobilization cannot be over emphasized ranging from biotechnological applications, to molecule biosensing.

2.3.3.2 *Immobilization techniques*

The enzyme and the matrix are very important in the immobilization set up but the way the enzyme is being attached to the matrix is also crucial for better efficiency. Improving enzyme stability, increasing enzyme loading, simplifying the recycling method are the driving forces behind enzyme immobilization (Liese and Hilterhause, 2013). The immobilization methods take advantage of the different types of amino acids present in proteins (Cantone *et al.*, 2013),

and that each amino acid has functional groups which can bind to the support in different manners depending on the linkages and interactions. The four methods mostly used for enzyme immobilization are shown in Figure 2.7, namely (1) non-covalent adsorption, (2) physical entrapment, (3) covalent attachment, and (4) cross linking (Brena *et al.*, 2013; Nguyen and Kim, 2017). Although there are many more methods, but these are combination of the methods listed above or very specific to a given support of enzyme. In any case, no single method or support is completely optimal for all enzymes and applications. This is due to the wide range of chemical properties and compositions of enzymes, as well as the unique properties of substrates and products, and the target applications of the products.

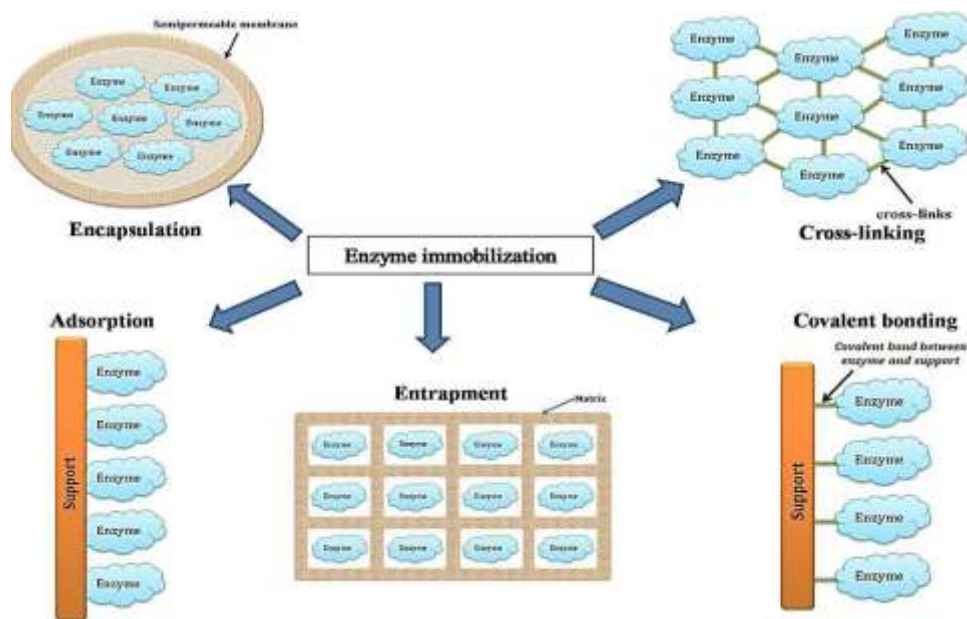


Figure 2.7: A Schematic Representation of the Various Methods of Immobilizing Enzymes or Cells. Source: Nguyen and Kim (2017)

2.3.3.3 Matrix or support for immobilization of enzymes

Confinement of enzymes on solid support makes the enzyme cost efficient in addition to other benefits such as repeated enzyme use and experimental control (Chapman *et al.*, 2018).

The emerging potential of this technology has necessitated the search for materials which can serve as support for enzyme immobilization. Many materials, including organic, inorganic, and hybrid materials, are involved in the formation of matrices which serve as support for enzyme immobilization (Zdarta *et al.*, 2018). The properties of the matrix are critical for good efficiency of immobilized enzyme system (Zdarta *et al.*, 2018). Some of the desirable properties of enzyme support are as shown in Figure 2.8.

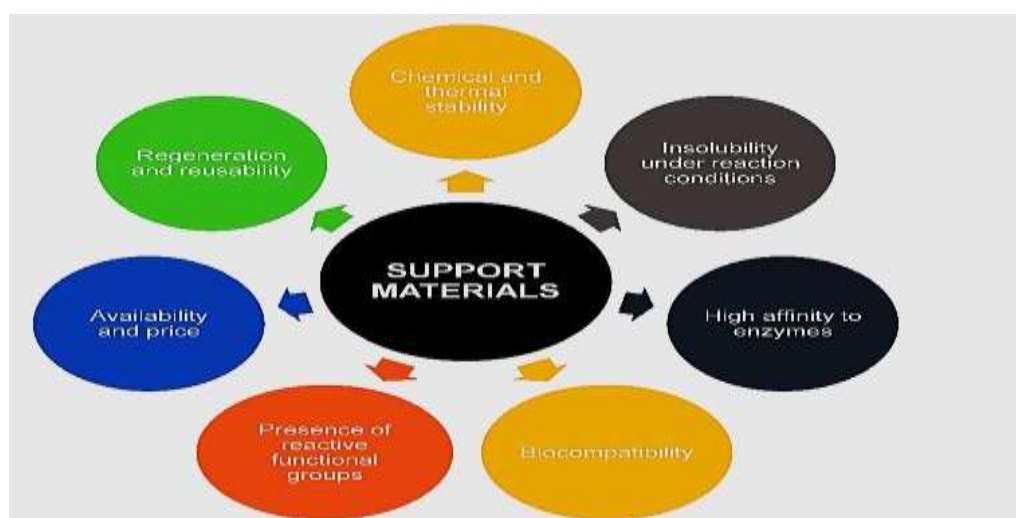


Figure 2.8: The Main Characteristics of Enzyme Immobilization Support Materials.
Source: Zdarta *et al.* (2018)

2.3.3.4 Porous biochar as support for enzyme immobilization

Lately, the choice of support has tended toward using environmentally friendly materials. Examples of such supports are, natural clays (Naghdi *et al.*, 2019), gels (Avnir *et al.*, 1994; Chen *et al.*, 2017), and porous materials. Natural materials are very compatible and also contain the needed functional groups for enzyme immobilization but their low surface area limits their application. Porous materials, on the other hand, possess enough specific surface

area which may conveniently occupy enzyme in immobilization. Popular supports in enzyme immobilization include mesoporous silica (Mehta *et al.*, 2016), metal-organic framework materials (Xu *et al.*, 2018), and zeolites (Cha *et al.*, 2016). These materials are difficult and expensive to prepare. Moreso adequate precision is also required.

The heating of biomass at a very high temperature in the absence of air (pyrolysis) results into biochar production. There is no combustion of carbon due to oxygen-limited conditions, and the materials that can be produced through this means include syngas, bio-oil, and biochar (Cha *et al.*, 2016).

The European Biochar Foundation (EBC) defined biochar as substance consisting of various proportions of aromatic carbon and minerals which is produced under controlled conditions using clean technology of pyrolysis sustainably obtained from biomass. Biochar can then be considered as a carbon storehouse (Smith, 2016), which has potential applications in a variety of fields due to its high carbon content. For instance, it is used as a soil supplement to increase soil fertility and nutrient retention capacity (Mohan *et al.*, 2018). It is also used to generate renewable energy such as thermal energy, bio-oils, and electricity (Waqas *et al.*, 2018; Regkouzas and Diamadopoulos, 2019).

2.3.3.5 Activation of biochar for enzyme immobilization

Biochar is a solid byproduct of biomass pyrolysis. After the pyrolysis, the biomass (bagasse, straw, and forest residue) is decomposed but retains the majority of the carbon content (Lehmann *et al.*, 2011; Cea *et al.*, 2019). It requires variation in temperature for each component of biomass to be decomposed. As a matter of fact, the temperature has a direct relationship with the specific surface area and carbon content and an inverse relationship with hydrogen/carbon and oxygen/carbon ratios (Weber and Quicker, 2018). This in turn results

in reduction of functional groups on the surface of the biochar, which makes it not very appropriate for enzyme immobilization. Although, biochar typically has pores and specific surface area, this needs to be improved to increase its specific surface area and pore fraction or to form reactive functional groups before it can be used as an immobilization support. The various methods of support activation that can be used are shown in Figure 2.9.

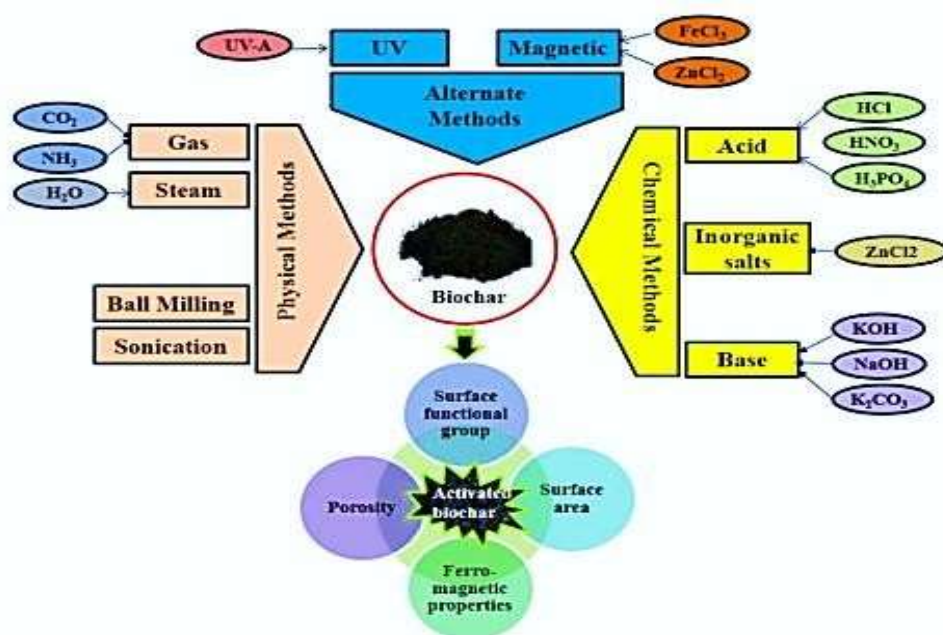


Figure 2.9: Methods of Activating Biochar for Enzyme Immobilization
Source: Pandey *et al.* (2020)

2.3.3.6 Biochar-chitosan composite preparations for enzyme immobilization

The lack of reactive and hydrophilic groups on porous biochar limits its use in the immobilization of water-soluble enzymes (Mo and Qui, 2020). Chitosan is a non-toxic biocompatible deacetylated chitin which has high affinity for proteins. It is cheap and also possesses some useful functional groups such as amino, hydroxyl, and hydroxymethyl groups (Krajewska, 1991; Guzik *et al.*, 2014; Zdarta *et al.*, 2018). Given these advantages, chitosan can serve as an ideal support for enzyme immobilization. Various chitosan-based supports in

various forms, such as beads, membranes, microspheres, fibers, or sponges, have been developed (Jesionowski *et al.*, 2014; Zargar *et al.*, 2015). Chitosan is soluble in acidic solutions due to its primary amino groups, which have a pKa value of 6.5, indicating that it is protonated below pH 6.5. Furthermore, chitosan can provide amino groups for covalent binding of porous biochar with enzymes (Sánchez-Ramírez *et al.*, 2017). The functional porous biochar--chitosan can then be used as an immobilization support for enzymes.

2.3.4 Ethanol production

Ethanol is produced through fermentation. Yeasts ferment sugars in the absence of oxygen to produce ethanol (Raj *et al.*, 2014). The conversion of sugars to ethanol and carbon dioxide in fermentation does not require oxygen, therefore it is called anaerobic fermentation. Alcoholic beverages and fuel ethanol are produced through anaerobic fermentation.

2.3.4.1 Principles of ethanol production through fermentation

Pyruvate is produced from glucose through Embden-Meyerhoff-Parnas pathway (EMP) Pyruvate, is a very important intermediate metabolite for most living organisms. The EMP pathway is divided into three stages: activation of glucose, division of hexose, and energy extraction.



The EMP pathway produces ethanol as a byproduct (Seol *et al.*, 2016). A single glucose molecule is first broken down into two pyruvates in an energy releasing reaction. The released energy can then bind inorganic phosphates to ADP and convert NAD^+ to NADH resulting into the breakdown of the two pyruvates into two acetaldehydes, which emit two CO_2 as a byproduct. Finally, using the hydrogen ions from NADH, the two acetaldehydes

are converted to two ethanol, converting NADH back into NAD⁺. Lactic acid, in addition to ethanol, is a byproduct of microbial fermentation as shown in Figure 2.10

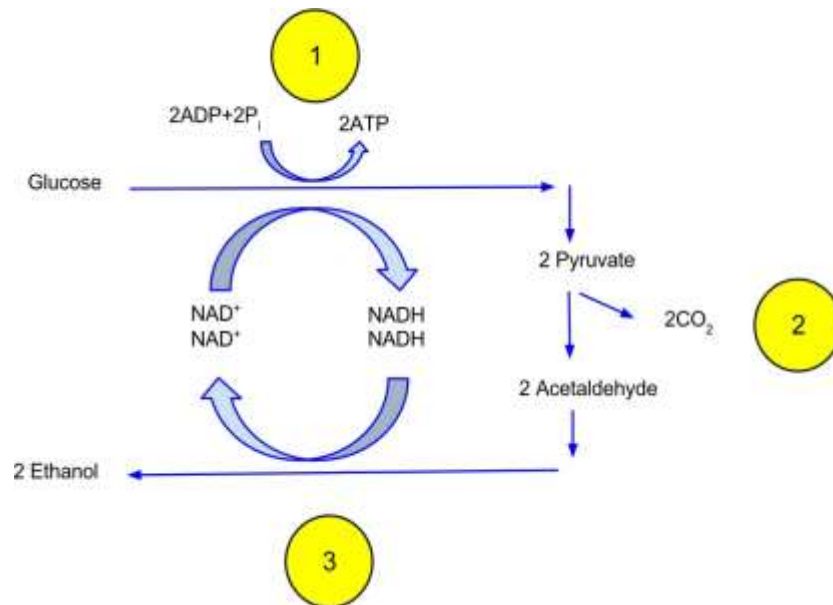


Figure 2.10: Processes of Ethanol Fermentation
Source: Seol *et al.* (2016).

2.3.4.2 *Microbes for fermentation*

Lignocellulosic material which is so abundantly available for ethanol production contains polysaccharides that can be converted to various hexoses and pentoses such as glucose, mannose, galactose, xylose, and arabinose. One of the major ways of obtaining high bioethanol yield from lignocellulose biomass is by the fermentation of both hexose and pentose sugars to ethanol (Maurya *et al.*, 2015). As a result, the chosen microorganism should have the potential to ferment both hexoses and pentoses, otherwise, microorganisms that can ferment each of the pentose or hexose can also be combined in fermentation. Ability to tolerate various toxic compounds found in the hydrolysate is also very important (Sues *et al.*, 2005; Methner *et al.*, 2022).

2.3.4.3 Fermentation of hexose and pentose sugars

Currently, *S. cerevisiae* is used primarily in the industrial production of ethanol (Dmytruk *et al.*, 2016). It is used because of its exceptional qualities of growing at high sugar concentrations and producing ethanol with high yields (Favaro *et al.*, 2019). One disadvantage is that it can only use glucose and other hexose sugars as substrate and cannot use pentose sugars (Dmytruk *et al.*, 2016). Non-Saccharomyces yeasts such as *pichia* and *candida spp*, like *S. cerevisiae*, can be used to produce bioethanol and are capable of fermenting hexose sugars; however, they have a low tolerance to ethanol yield when compared to *S. cerevisiae* (Padilla *et al.*, 2018). Recently, the ability of zygomycetes such as *Mucor indicus* to produce ethanol was investigated. *Mucor indicus* (formerly *M. rouxii*) has the ability to grow with or without air utilizing simple sugars such as glucose and xylose to produce bioethanol the same way *Saccharomyces cerevisiae* does in terms of yield and productivity (Karimi and Zamani, 2013; Molaverdi *et al.*, 2019). Its potential to tolerate high sugar concentration, ethanol, and a variety of potential inhibitors suggests that it may have industrial applications (Christia *et al.*, 2016; Molaverdi *et al.*, 2022). This class of filamentous fungi are saprophytic organisms which are capable of producing a variety of metabolites, including ethanol. Millati *et al.* (2005) reported ethanol yield of 0.39, 0.22, and 0.44 g/g from glucose, xylose, and dilute-acid hydrolysate of spruce respectively at 37 °C by *M. indicus* under aerobic conditions. Under aerobic and anaerobic conditions, *M. indicus* have several industrial advantages over *S. cerevisiae*, including (a) the ability to utilize xylose, which is the major part of hemicellulose, and (b) *S. cerevisiae's* optimum temperature is in the range of 28-35 °C, whereas *M. indicus* demonstrated ethanol production which is relatively high at 37 °C (Sues *et al.*, 2005); (c) it is resistant to several inhibitory compounds

found in pre-treated hydrolyzates, including furfural, hydroxymethylfurfural (HMF), acetic acid, and vanillin (Millati *et al.*, 2005; Karimi and Karimi, 2018). Furthermore, the fungus is easily cultured, requires only basic nutrients, and is safe for humans.

2.4 Strategies for Bioethanol Production

Several integrated methods employed for the conversion of lignocellulosic material to ethanol have been proposed as shown Figure 2.11. This involves Separate Hydrolysis and Fermentation (SHF); Separate Hydrolysis and Co-fermentation (SHCF); Simultaneous Saccharification and Fermentation (SSF); Simultaneous Saccharification and Co-fermentation (SSCF); and Consolidated Bioprocessing CBP).

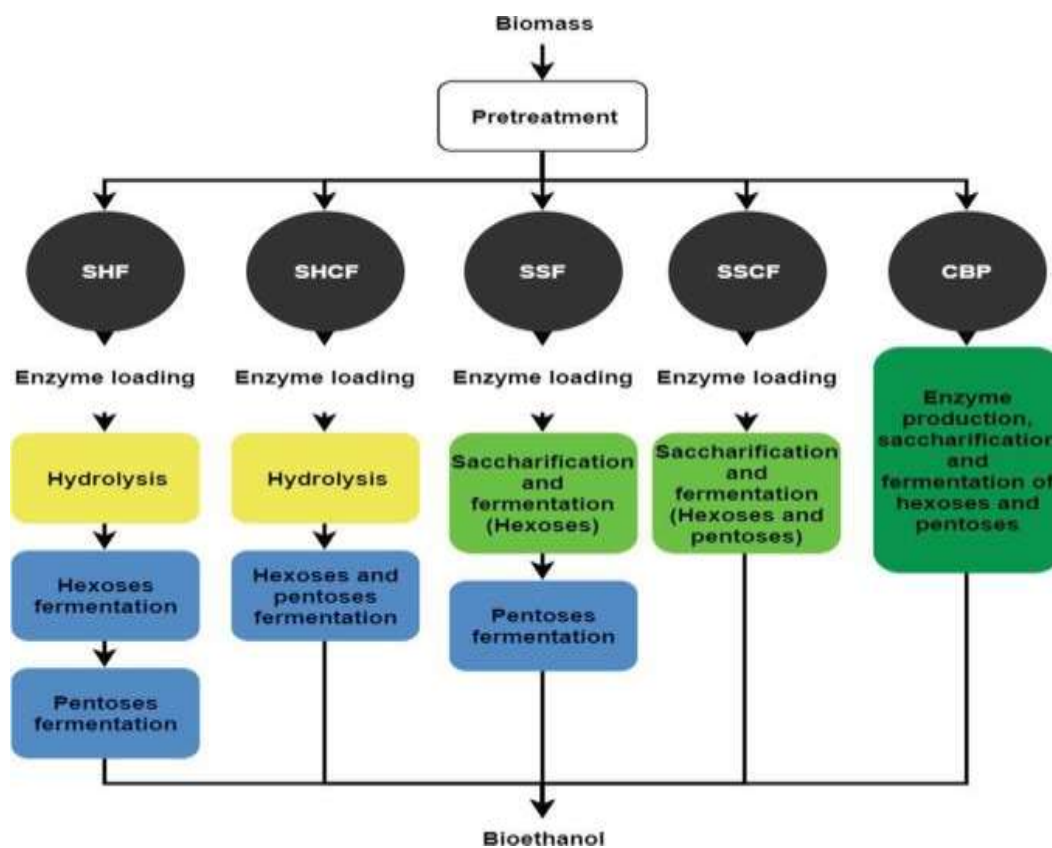


Figure 2.11: Bioethanol Production Strategies.
Source: Mejía-Barajas *et al.* (2018)

2.4.1 Separate hydrolysis and fermentation (SHF)

Separate hydrolysis and fermentation (SHF) involve two different stages of first breaking down the pre-treated biomass into monomeric sugars (glucose and xylose) by enzymatic saccharification, and secondly, the sugar released are then converted into ethanol (Zabed *et al.*, 2017) as shown in Figure 2.12. The fact that these two steps are done differently makes it very effective. However, this has the disadvantage of accumulation of hydrolysis products in the hydrolysis vessel, thereby preventing enzyme to function well which makes the reaction rate generally slow.

In the case of Separate Hydrolysis and Co-fermentation, the hydrolysis is done first in a separate vessel after which both hexose and pentose sugars are fermented together in another vessel. This has the advantage of higher ethanol yield since more sugars are being fermented at the same time but the disadvantage of product inhibition is also present here just as in separate hydrolysis and fermentation.

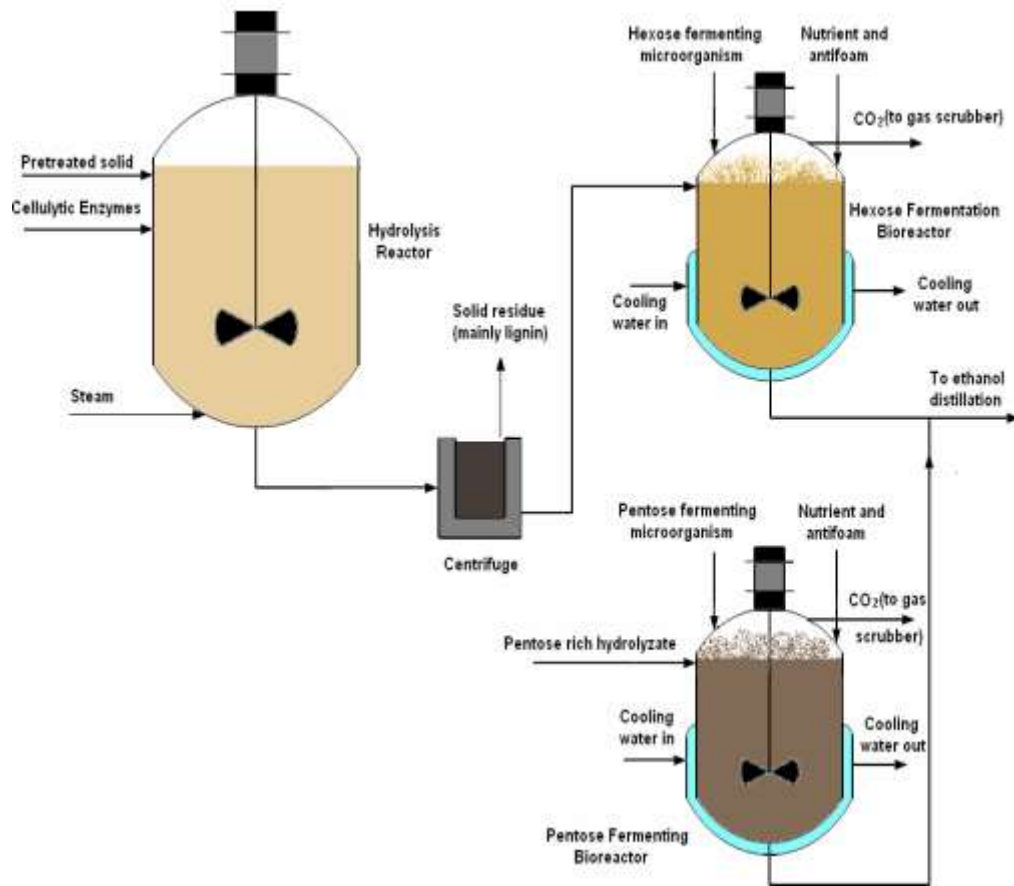


Figure 2.12: Flow Diagram for Separate Enzymatic Hydrolysis and Fermentation (SHF)

Source: Taherzadeh and Karimi, (2008)

2.4.2 Simultaneous saccharification and fermentation (SSF)

Simultaneous saccharification and fermentation (SSF) is another method used to compensate for the shortcomings of SHF. In SSF, the first stage of releasing simple sugars (saccharification) from biomass is done together with fermentation of the released sugars at the same time in the same compartment as shown in Figure 2.13. As a result, once the sugar is released, it gets converted to ethanol, reducing the tendency of the sugar to accumulate in the medium. Furthermore, because ethanol is present in the medium, there is less possibility of contamination (Zabed *et al.*, 2017; Vohra *et al.*, 2014). Nevertheless, making use of the best conditions for each stage of reaction is challenging because both enzymes and microorganisms must work simultaneously. However, the two types of sugars (hexose and pentose) are fermented in two different bioreactors with different organisms only hexoses are converted to ethanol, whereas pentoses can be fermented in another bioreactor with different microorganisms (Mood *et al.*, 2013).

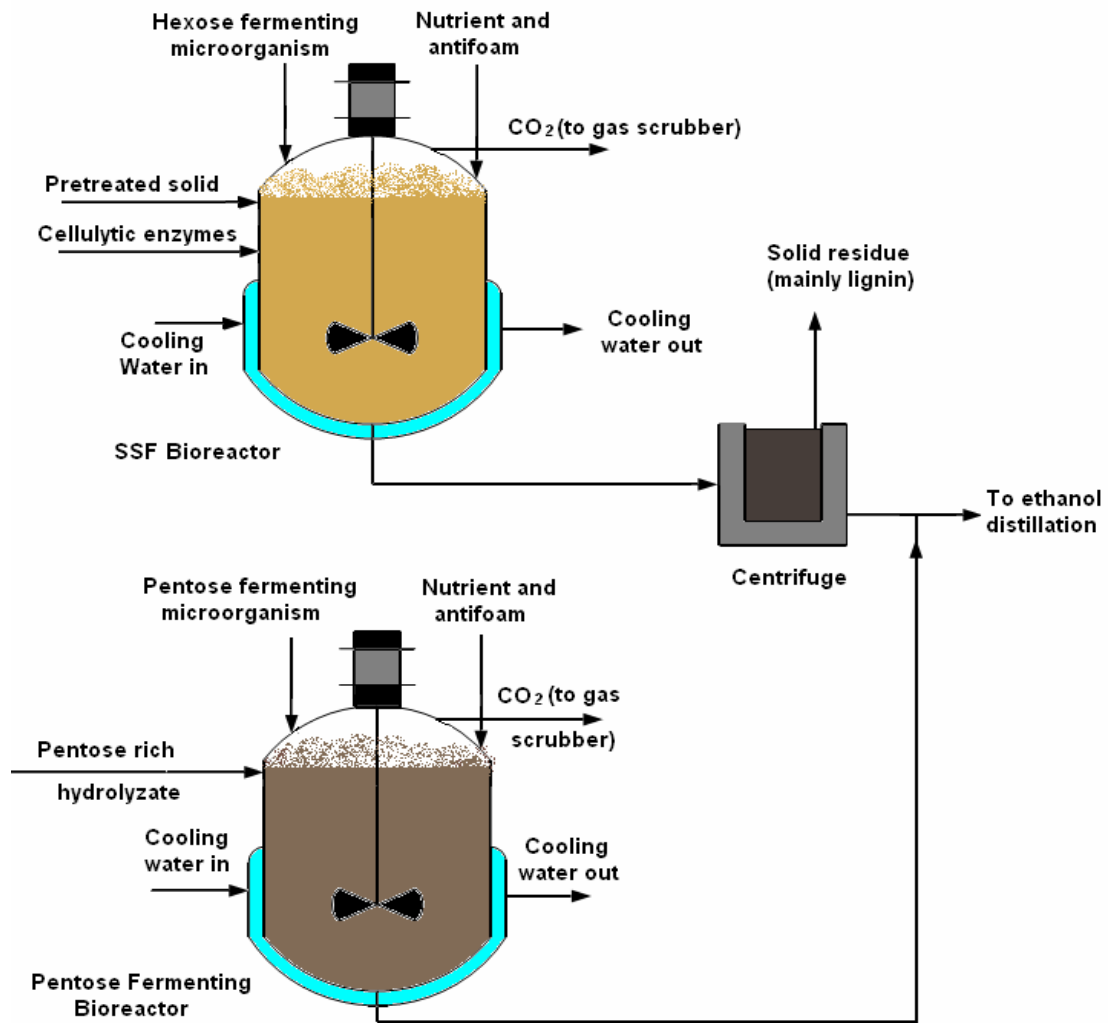


Figure 2.13: Process Flow Diagrams for Simultaneous Saccharification and Fermentation
Source: Taherzadeh and Karimi, (2008).

2.4.3 Simultaneous saccharification and co-fermentation (SScF)

Simultaneous Saccharification and Co-Fermentation (SSCF) is an integrated process that aims at utilizing all the sugars released during hydrolysis after pre-treatment of the biomass has taken place, which are then converted to ethanol in a single vessel (Sindhu *et al.*, 2016) as shown in Figure 2.14. One strategy is to use mixed cultures of organism that have the potential to ferment both hexose and pentose sugars, or to use a single organism capable of utilizing the two kinds of sugars together. The only challenge with

this method is that organisms fermenting hexose sugars tend to grow faster than the organisms which ferment pentose, resulting in higher hexose-to-ethanol conversion. This method has several advantages, including a shorter operation time, lower costs, as well as little or no contamination of medium and fewer generation of inhibitory products during enzymatic hydrolysis.

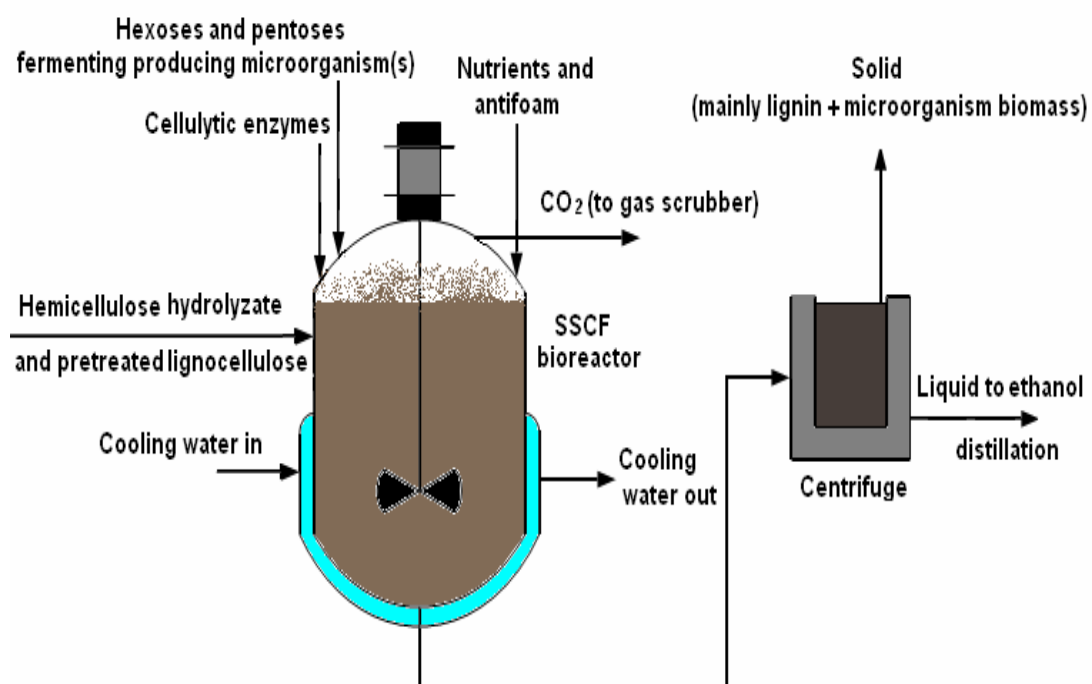


Figure 2.14: Flow Diagram for Simultaneous Saccharification and Co-fermentation (SScF)
Source: Taherzadeh and Karimi, (2008).

2.4.4 Consolidated bioprocessing (CBP) or Direct microbial conversion (DMC):

In this most recent approach called consolidated bioprocessing or direct microbial conversion, all of the steps involve in the production of bioethanol are done in a single reaction vessel at the same time (Tanimura *et al.*, 2015). Consolidated bioprocessing is a process in which a single microorganism produces enzymes, hydrolyzes cellulose, and

ferments it (Figure 2.15). In addition to being capable of carrying out fermentation, the microorganisms chosen for CBP must be capable of producing enzymes for hydrolyzing cellulose (i.e. cellulases) as well as enzymes for converting xylose to ethanol. The kind of microorganism that will do such consolidated process is not common naturally, therefore such organisms can be cloned genetically (Jouzani and Taherzadeh, 2015).

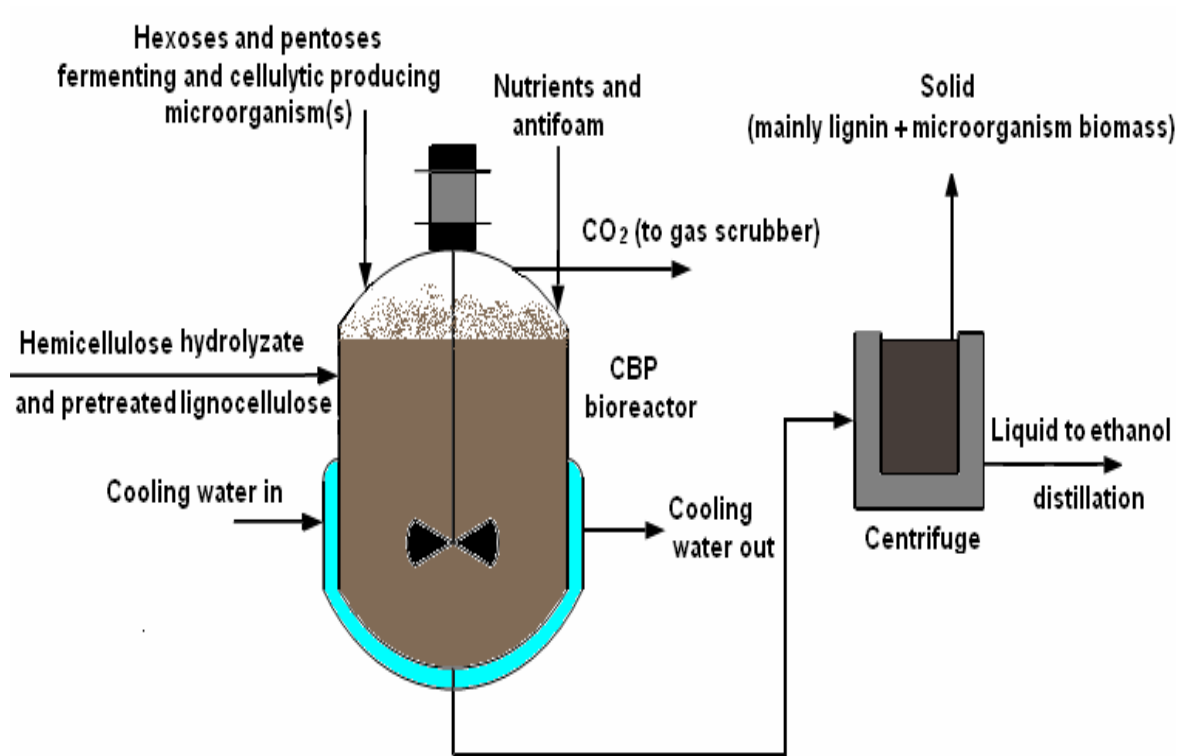


Figure 2.15: Flow Diagram for Simple Consolidated Bioprocessing (CBP)
Source: Taherzadeh and Karimi, (2008).

2.5 Alcohol Recovery

Distillation is the most common method for recovering ethanol from fermented media (Vane *et al.*, 2013). Alcohol distillation is the process of recovering alcohol from fermented broth or other alcohol-based mixture by taking advantage of their differences in boiling points. Distillation has many advantages, recovery of near absolute ethanol concentration (>99%), sufficient energy efficiency at moderate feed concentrations, and

possibility of using computer to simulate the process using process simulation software (Zentou *et al.*, 2019).

2.6 Selected Agricultural Wastes

The agrowastes of interest in the present study are discussed in the following section.

2.6.1 Maize plant

Maize, which has its scientific name as *Zea mays*, is also known generally as corn, is a cereal that indigenous people in southern Mexico first domesticated around 10,000 years ago. In Nigeria, maize began as a non-commercial crop but has now become a commercial crop which many agro-based industries use as raw materials.

2.6.1.1 Description

The leaf of the plant stalk produces pollen inflorescences as well as ovuliferous inflorescences (ears) which are produced separately. The ear produces fruits in form of kernels or seeds. Maize is one of the most consumed foods in many parts of the world, and it is cultivated more than rice. Nigeria is currently the world's tenth largest maize producer and Africa's largest maize producer with an average production of about 10 million tons as of 2013 as shown in Figure 2.16 (Abdoulaye *et al.*, 2018). By estimated calculation, it was found that 70% of farmers operate a small-scale maize farming, and these are majority of total farm output (Cadini and Angelucci, 2013).

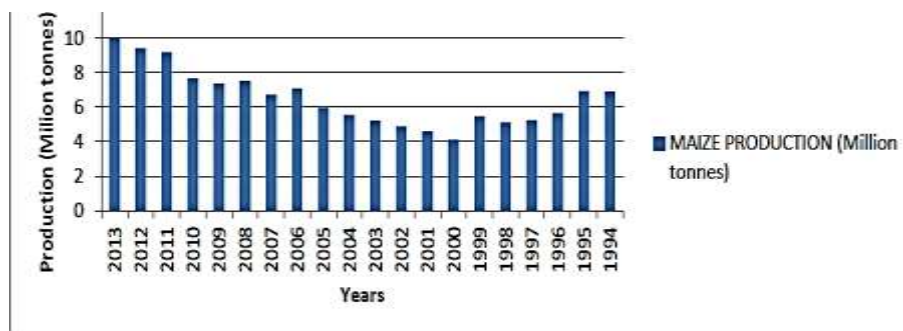


Figure 2.16: Maize Production in Nigeria (million tonnes) Between 1994 and 2013
Source: Umar *et al.* (2015)

2.6.1.2 Corncobs

Corncobs, also known as maize cobs, are a byproduct of the maize crop that consist of the female inflorescence's central fibrous rachis (the maize "ear"). Each ton of maize shelled yields approximately 180 kg of cobs, with the majority of them being left on the field (Adebayo *et al.*, 2016). The most generated by-product in many maize-producing countries is corncob. Despite their low economic value, they are used in agriculture as fuel, beddings for poultry and other animals, mulch and soil conditioner, and fodder for ruminants (Jansen and Lübberstedt, 2011).



Figure 2.17 Corncobs Obtained from Shelled Corn
Source: Umar *et al.* (2015)

Maize cobs have recently been reported as a potentially cheap and promising source of sustainable energy production (Jansen and Lübberstedt, 2011). Maize cobs are available at every site that maize is cultivated and, in all households, where maize is consumed.

2.6.2 Plantain (*Musa paradisiaca*)

Plantain, also known as cooking bananas, is a member of the Musaceae family and the genus *Musa*. Plantain cultivation is appealing to farmers because it requires less labor than cassava, maize, rice, and yam.

2.6.2.1 Description

This is a tree-like perennial herbaceous plants that grow to be 2 to 9m tall which has an underground rhizome or corn. The most common species are *Musa paradisiaca* (French plantain), *M. acuminata* (Gross plantain) and *M. corniculata* (Horn plantain). Nigeria is a major producer of plantain in Africa and ranks sixth in the world, producing 3,164,878 metric tonnes in 2017 as shown in Figure 2.18 (Akinyemi *et al.*, 2017). After harvesting the edible fruit, the plantain stem generated per hectare is approximately 100 metric tons (Tripathi *et al.*, 2021). Ondo, Ogun, Osun, Oyo, Cross River, Imo, and Abia State are among the producing states (Akinyemi *et al.*, 2017). In Nigeria, the availability of banana/plantain of good quality is primarily from October to February each year, despite the fact that there is a year-round demand for banana/plantain.



Figure 2.18: Plantain Production (tons) in Nigeria from 1961 to 2017.
Source: www.factfish.com .

2.6.2.2 Plantain pseudostem

Plantain pseudostem (Figure 2.19) is the trunk-like part of the plantain plant which is generated when the overlapping leaf sheaths are tightly packed. Despite the fact that the pseudostem is very fleshy and contains majorly moisture, it is still very strong and can support the heavy weight of the bunch of plantain.



Figure 2.19: Plantain Pseudostem Biomass Obtained from Plantain Farm
Source: Ai *et al.* (2021)

Plantain pseudostem biomass is a potential lignocellulosic biomass that could be used to produce biofuel due to its high concentration of holocellulose (72%) and relatively low percentage of lignin content (about 10%) (Ai *et al.*, 2021) The plantain pseudo-stem has a high cellulosic content (42.2 – 63%), which can be used to produce fermentable sugars for bioethanol.

2.6.3 Sugarcane (*Saccharum officinarum*)

It is a perennial crop that resembles a bamboo cane and thrives in tropical climates. Sugarcane has traditionally been grown at subsistence level (typically 0.2 to 1.0 ha) for consumption and preparing livestock feed. However, as the demand for sugar in the country rises, the crop is being grown on a large scale and now used as raw material for the sugar industry.

2.6.3.1 Description

The stalk is fibrous and stoutly joined, and it is high in sucrose, which accumulates in the internodes of the stalk. Sugarcane can be grown in almost all West African states, including Nigeria, but it is commercially produced in Kastina, Adamawa, Kebbi, and Sokoto (Issa *et al.*, 2020). Sugarcane was introduced to Nigeria by European sailors through the country's eastern and western coasts in the fifteenth century (Galadima *et al.*, 2011).

According to national statistics, more than 400,000 hectares of land in the country could support high yield sugarcane operations (Newton *et al.*, 2017). Sugarcane and cassava are clearly identified as the primary raw materials for the bioethanol production programme by the NNPC (Galadima *et al.*, 2011).

2.6.3.2 Sugarcane bagasse

Bagasse, as shown in Figure 2.20, is the material that remains after sugarcane juice is extracted from a cane stalk and from a ton of sugarcane, about 270-280 kg of bagasse can be obtained (Lachos-Perez *et al.*, 2016). Usually the bagasse is left to decay, or sometimes burnt to generate the energy required for the process of sugar production (Mokhena *et al.*, 2018; Motta *et al.*, 2020)



Figure 2.20: Sugarcane Bagasse Obtained from Sugarcane Stem after Extracting the Juice from the Stem
Source: Alokika *et al.* (2021)

Sugarcane bagasse contains cellulose (32-45%), hemicellulose (20-32%), and lignin (17-32%), as well as 1.0-9.0% ash and some extractives (Alokika *et al.*, 2021). The trend of bagasse production in Nigeria between 1990 to 2016 is shown in Figure 2.21. With the vast agricultural resource in Nigeria, biodiversity and suitable climate for sugarcane cultivation, the country could direct her focus at producing highly productive type of sugarcane for sugar and ethanol production through conventional breeding and using the tools of biotechnology

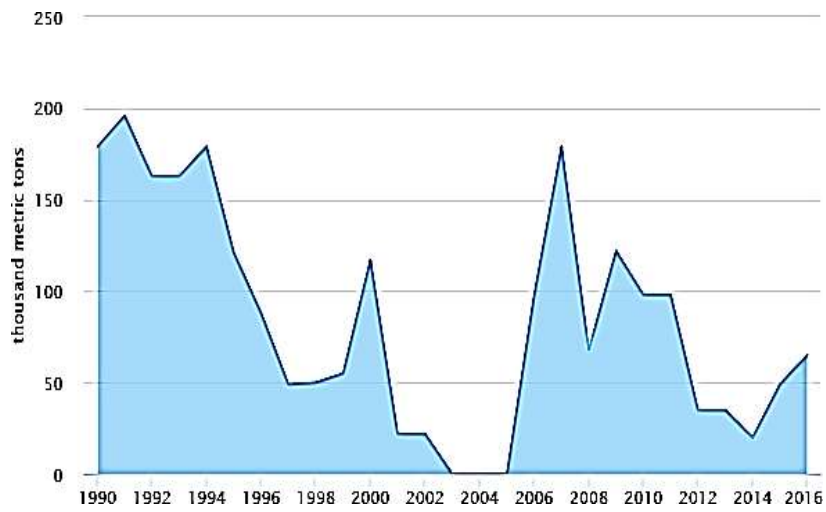


Figure 2.21: Production of Sugarcane Bagasse in Nigeria
Source: www.factfish.com

CHAPTER THREE

3.0 MATERIALS AND METHOD

3.1 Materials

3.1.1 Agrowaste samples

Samples of plantain pseudostem biomass, sugarcane bagasse, and corncob biomass were collected from farms and dumpsite in Bosso, Minna, Niger State, Nigeria.

3.1.2 Equipments

The equipment used are: Domestic thermocool microwave oven with model frequency of 2450 MHz. Gene Amp 9700 PCR System Thermal cycler (Applied Biosystem Inc., USA), Bruker AXS D8 X-ray diffractor, Zeiss Auriga HRSEM, FTIR Thermo Nicolet, Avatar 370, Big Dye terminator version 3.1 cycle sequencing kit, TGA-4000; PerkinElmer, Quantachrome (model: NOVA4200e) BET analyzer, Agilent 6890 N gas chromatography system (Agilent, Santa Clara), Agilent 5973 N mass spectrometer (Agilent, Santa Clara). The Centre for Genetic Engineering and Biotechnology, Federal University of Technology, Minna, Niger State, Nigeria, kindly provided an autoclave machine, industrial oven, rotary shaker, Shimadzu ultraviolet spectrophotometer (1800 series), and furnace for the research

3.1.3 Reagents and chemicals

Industrial grade NaOH (caustic soda) was a product of Global Chem Tech, was obtained from chemical vendors in Minna, Niger State, Nigeria.

3.2 Methods

3.2.1 Overall process description

The flowchart for overall methodology in cellulosic bioethanol production using agrowaste biomasses is as shown in Figure 3.1. The process includes biomass preparations, microwave-alkaline pre-treatment, enzyme production, simultaneous saccharification and co-fermentation, ethanol distillation and characterization.

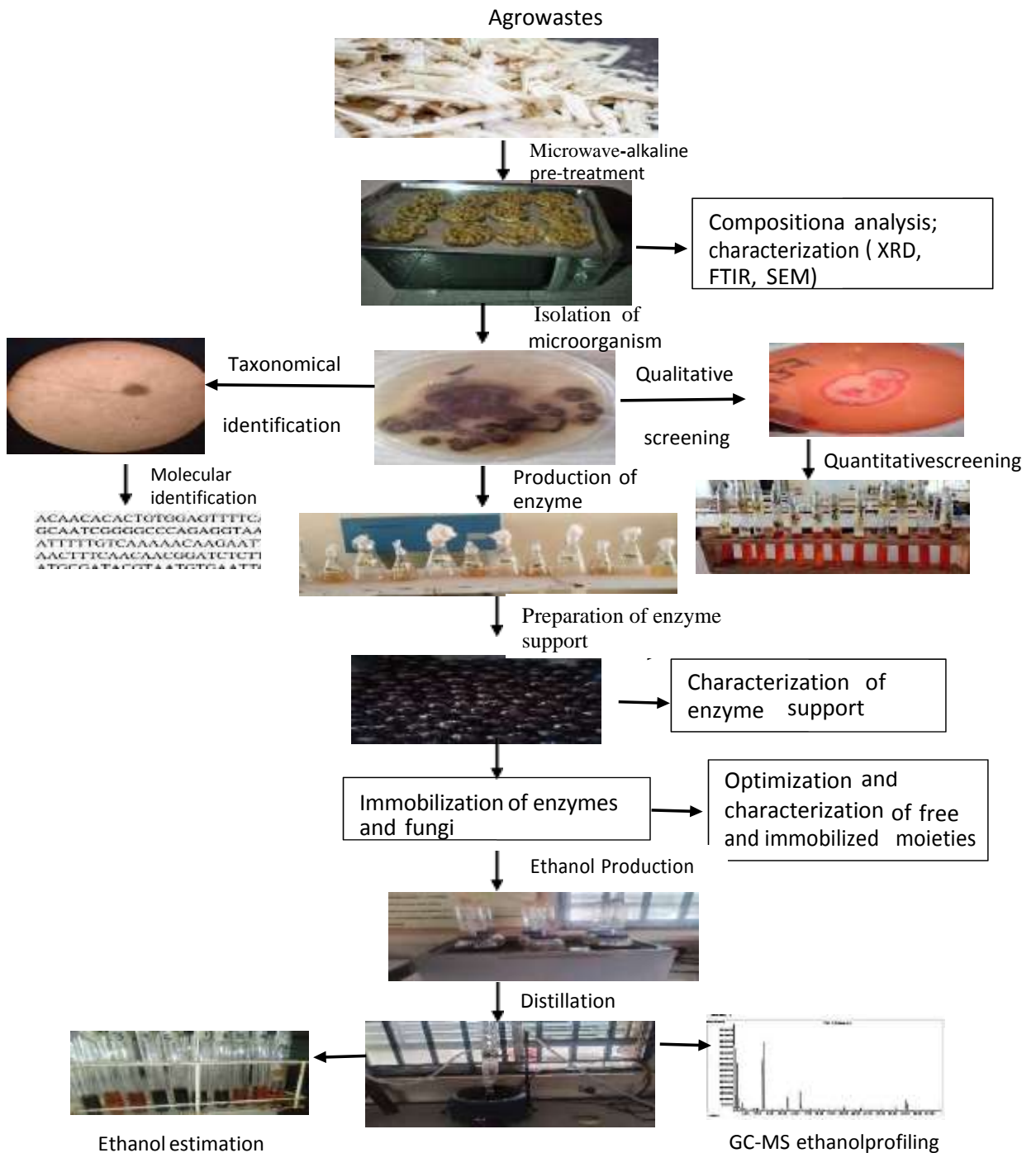


Figure 3.1: Flowchart of Methodology for the Production of Cellulosic Bioethanol by Simultaneous Saccharification and Co-fermentation.

3.2.2 Preparation of agrowaste samples

The selected agrowaste samples were thoroughly washed, cut into pieces, and then dried in atmospheric conditions until constant weight was achieved. The dried sample was

pulverized and weighed. The samples were then kept in tightly covered containers at room temperature until needed for further analysis (Asikoko *et al.*, 2023).

3.2.3 Microwave-Alkaline (MA) pre-treatment of biomass

The experimental runs for Microwave -Alkaline pre-treatment of the agrowaste samples was generated by Box-Behnken model of Design Expert software (Version 11). The chosen variables were NaOH solution concentration (A), the microwave power (B) and the treatment time of the pre-treatment process (C) and the process conditions are as shown in Table 3.1. The dried pulverized agrowaste samples was first soaked in 0.5%, 1%, 1.5%, 2%, 2.5% and 3% NaOH solution in the ratio of 10:1 of liquid to solid (v/w) for 10 min (Hu and Wen, 2008). The mixture was then placed in a microwave oven for 1, 2, 3, 4 and 5 minutes at power levels ranging from 70 W to 700 W.

Table 3.1: Variable Factors and Runs Generated by Design Expert Software For the Optimization of Microwave-alkaline Pre-treatments of Agrowaste

		Factor 1	Factor 2	Factor 3	Response 1	Response 2	Response 3
Std	Run	A: Conc. NaOH %	B: Power Watts	C: Time Min	Delignification %	Cellulose content %	Hemicellulose content %
11	1	2	70	5			
2	2	3	70	3			
17	3	2	385	3			
12	4	2	700	5			
10	5	2	700	1			
7	6	1	385	5			
6	7	3	385	1			
14	8	2	385	3			
15	9	2	385	3			
13	10	2	385	3			
5	11	1	385	1			
1	12	1	70	3			
3	13	1	700	3			
8	14	3	385	5			
9	15	2	70	1			
16	16	2	385	3			
4	17	3	700	3			

Key: Std -Standard

These variables were experimented in the laboratory by using the software-generated process conditions as a guide. The mixture was then filtered, the residue was washed thoroughly with clean water so as to obtain a neutral pH, and then put in an oven to dry at 60 °C so as to remove moisture and then weighed (Singh *et al.*, 2020). The remaining dried biomass was safely stored for further experiment.

3.2.4 Compositional analysis

The cellulose, hemicellulose and total lignin contents of the untreated and biomass pre-treated under different process conditions were determined as follows:

3.2.4.1 Determination of total lignin content

All the sum of lignin present in the residue was determined by the addition of lignin that is not soluble in acid (also called Klason lignin) and lignin that is soluble in acid which are present in the unpre-treated and pre-treated agrowaste according to the method of Sluiter *et al.* (2012). In summary, about 1.5 g of dry pre-treated biomass was thoroughly mixed with 15 mL of 72% (w/v) tetra-oxo sulphate (VI) acid and stirred for one hour; then 420 mL of distilled water was also added to the mixture and then autoclaved at 121 °C for 1 h and filtered. The filtrate was read at 320 nm using UV spectrophotometer to quantify the acid soluble lignin portion present therein. Acid soluble lignin (ASL) concentration was also determined by using the following formulae (Sluiter *et al.*, 2012).

$$ASL = \frac{Abs \times Dillution}{s \times W} \times 100 \quad (3.1)$$

where; Abs = average UV-VIS absorbance for the sample at 320 nm;

ϵ = Absorptivity of lignin at specific 320 nm wave-length (30 L/g·cm);

W = total weight of sample in milligrams.

The residue was placed in the oven to dry at 105 °C for 4 h until a uniform weight was attained, ashed at 300 °C for 1 h (Plate 4) and then placed in a desiccator to cool before

weighing and then the quantity of Acid Insoluble Lignin (AIL) was calculated using the following equation

$$\text{AIL: } \frac{\text{weight of sample at } 105^{\circ}\text{C} - \text{weight of sample at } 300^{\circ}\text{C}}{\text{initial weight of dried sample}} \times 100 \quad (3.2)$$

$$\text{Total Lignin} = \text{ASL} + \text{AIL} \quad (3.3)$$

3.2.4.2 Determination of cellulose and hemicellulose content

The composition of cellulose and hemicellulose of unpre-treated and pre-treated agrowaste was determined by Chesson-Datta gravimetric method (Maryana *et al.*, 2014). In summary, 150 mL of distilled H₂O was added to 1 g (a) of the dried unpre-treated and pre-treated agrowaste sample. This was refluxed at 100 °C inside water bath for 1 h and then filtered. The residue was washed with hot water (300 mL), dried in an oven at 100 °C until constant weight (b) was attained. Then, 150 mL of 0.5 M H₂SO₄ was added to the dried residue and also refluxed in a water bath at 100 °C for 1h. The liquid portion of the mixture was removed through filter paper while the residue was washed with 300 mL of hot water and later dried at 60 °C to a constant weight (c). Afterwards, 10 mL of 72% H₂SO₄ was added to the already dried residue and then placed at room temperature for 4 h to soak before adding 150 mL of 0.5 M H₂SO₄. It was then refluxed in water bath for 1 h after which the residue was removed and thoroughly washed with hot H₂O to attain neutral pH, then it was dried in an oven at 105 °C for 6 h and weighed (d).

The cellulose and hemicellulose contents were calculated using the following formula:

$$\text{Hemicellulose content} = \frac{b-c}{a} \times 100\% \quad (3.4)$$

$$\text{Cellulose content} = \frac{c-d}{a} \times 100\% \quad (3.5)$$

However, the percentage of total lignin removed was calculated as percentage of lignin removed when compared to the unpre-treated biomass using the following equation:

$$\text{Percentage Total lignin removed (delignification)} = \frac{\text{lignin content in unpre-treated agrowaste} - \text{lignin content in pre-treated agrowaste}}{\text{lignin content in unpre-treated agrowaste}} \times 100 \quad (3.6)$$

3.3 Analysis of Data Generated by Design Expert for Pre-Treatment of Agrowaste

Design Expert statistical software version 11 was used in generating the analysis of variance (ANOVA) as well as model equation. Also, three-dimensional response surface plots were developed by the same software. Optimization of the results obtained was done using the numerical and graphical methods provided by Design-Expert statistical software in order to get the optimum values for the combination of the variable factors for the desired goal.

3.4 Characterization of Pre-Treated Agrowaste

For the present study, the agrowaste pre-treated at optimal conditions using microwave-alkaline pre-treatment were characterized using three analytical techniques. These characterization techniques included: X-ray Diffraction (XRD), high Resolution Scanning Electron Microscopy (HRSEM) and Fourier Transform Infrared Spectroscopy (FTIR). The method for each of the analytical techniques are provided in the following sections.

3.4.1 X-ray diffraction analysis (XRD)

X-ray diffraction analysis (XRD) is One of the powerful and safe non-destructive technique mostly used in the analysis of solid-state chemistry and material science. It is based on bombardment of a single crystal powder sample with X-rays photon to produce diffraction pattern (Okolo *et al.*, 2015). The patterns of the diffraction were recorded and analyzed so as to determine the nature of the crystal structure. For this study, the percent crystallinity was determined from the integrated peak intensities of the $[\bar{0}1]$, $[\bar{1}1]$ and

[002] diffraction planes in the 2θ range of $0^\circ - 90^\circ$. The conditions at which the analysis was done is as shown in Table 3.2

Table 3.2: Bruker D8 Advance XRD Operating Parameters

Operating Parameters	Condition
Time constant	0.5 s
Radiation	Cu.Ka
Wavelength	1.542λ
X-Ray Operating voltage	40 Kv
X-ray Operating current	40 Ma
Scanning angle Range	20°<2θ<90°
Scanning Step	0.2°
Scanning speed	60s/step

The crystal size from half height peak width was determined using scherer equation as shown below

$$D = \frac{k\lambda}{\beta \cos\theta} \quad (3.7)$$

Where **D** is crystalline size in nanometer, **K**= 0.94, λ is the wavelength of the X-ray which is 0.1541 nm θ is the half-diffraction angle, β is the full width at half-maximum in radian.

The crystalline index of cellulose, CrI, was determined based on the empirical Segal method as reported by Jamaldheen *et al.* (2018) in the equation below:

$$\text{CrI (\%)} = \frac{(I_{\text{crystalline}} - I_{\text{amorphous}}) \times 100}{I_{\text{crystalline}}} \quad (3.8)$$

Where, $I_{\text{crystalline}}$ is the intensity at $2\theta = 22.5^\circ$ corresponding to crystalline fraction and $I_{\text{amorphous}}$ is the intensity at $2\theta = 18.7^\circ$ corresponding to amorphous fraction

3.4.2 High resolution scanning electron microscopy (HERSM)

High Resolution Scanning Electron Microscopy (HERSM) is a tool used to characterize samples. It produces high-resolution images of a sample surface which reveals information on surface structure and morphology as well as the degree of aggregation of micro and macro materials. (Egerton, 2016). Morphology and microstructure of the synthesized products were determined using Zeiss Auriga HRSEM. The conditions at which the analysis was done is shown in Table 3.3

Table 3.3: Experimental Parameters for High Resolution Scanning Electron Microscopy

Operating parameters	Condition
Current	10 mA
Magnification	Varies
Aperture	0.4 mm
Resolution	1 nm but not constant
Emitter	Thermal field emission type
Working Distance	4-10.4 mm
Voltage	5 kV
Signal A	Inlens

3.4.3 Fourier transform infrared (FT-IR) spectroscopic analysis of pre-treated and untreated samples

This technique provides information about the chemical bonding or molecular structure of either material. The bonds and group of bonds vibrate at characteristic frequencies which is read at a spectral range $4000-400\text{ cm}^{-1}$ and 4 cm^{-1} resolution. The pre-treated and untreated samples were subjected to FTIR spectroscopic analysis (Thermo Nicolet,

Avatar 370), equipped with KBr beam splitter with DTGS (Deuterated triglycine sulphate) detector (7800- 350 cm⁻¹).

3.5 Screening of Fungi for Enzyme Production and Fermentation Process

Fungi for enzyme production and fermentation process were isolated from different soil samples in Minna, Niger State, Nigeria. The sources for enzyme producers were: refuse dump site, sewage sludge, corncob biomass dump site, rice husk dump site, decayed plantain soil, decayed corncob biomass soil and decayed sugarcane soil; while the fermenters were isolated from palm wine, rice husk dump site, fermented food, and termite hill. The organisms were isolated by preliminary screening where the dilution plating technique of Montenecourt and Eveleigh, as reported by Chamekh *et al.* (2019) was used. Furthermore, these organisms were screened qualitatively and quantitatively to select the best organisms for the purpose in view. Furthermore, the selected organisms were identified by molecular characteristics.

3.5.1 Screening of fungi for enzyme production

3.5.1.1 Qualitative screening of the isolated microorganisms for cellulase and xylanase production using agrowastes as carbon source

Agrowastes of interest (corncob biomass, plantain pseudostem biomass, and sugarcane bagasse) which has been treated with microwave-assisted sodium hydroxide were chosen as the only source of carbon for the screening of isolated microorganism for cellulase and xylanase activities. The pre-treated agrowaste samples were milled into powder and used as the sole carbon source for enzyme production. The medium comprises the following items (in g/l): peptone, 5.0; yeast extract, 5.0; K₂HPO₄, 0.2; agar 20.0 and 10.0 of agrowaste as carbon source. Birch wood xylan and carboxyl methyl cellulase (CMC) were also included as carbon source into a similar media to serve as control for xylanase and cellulase activities respectively. The media were put into the autoclave at 121 °C for

15 min. and then poured into petri dishes when they were cooled to about 30 °C so that they could form gel. Afterwards, each plate was inoculated with pure fungi isolate and incubated for 48 h at 25 ± 2 °C. Cellulolytic enzyme producing organisms hydrolysed the carbon source in the medium to form a zone of clearance. Detection of positive isolates was achieved when zones of clearance appeared on the agar plates after flooding the plates with 0.1% aqueous Congo red followed by repeated washing (to de-stain) with 1M NaCl as reported by Sukmawati *et al.* (2018). Organisms which have clear zones of hydrolysis around their colonies were selected and stored on Sabouraud Dextrose Agar (SDA) slant for further studies.

3.5.1.2 Quantitative screening of the selected organisms for cellulase and xylanase production using agrowaste as a carbon source

This involved:

1. Inoculum preparation

The cultures for inoculum preparations were prepared by subculturing the most hydrolytic organisms from organisms previously stored as slant cultures on SDA. A loopful of the revived organism which was inoculated into sterile 100 mL Sabouraud Dextrose Broth (SDB) and incubated at 30 °C in an orbital shaker at 125 rpm, was used as the inoculum after 48 h of incubation

2. Enzyme production

Enzymes were produced under submerged fermentation condition using microwave-alkaline pre-treated agrowaste as sole carbon source. Five gram (5 g) of each substrate (sugarcane bagasse, corncob biomass, plantain pseudostem biomass, CMC or xylan) was placed in Mandels and Weber basal media salt (250 mL) (Ismaiel *et al.*, 2022). The media were initially autoclaved at 121 °C for 15 min and allowed to cool down to 28 ± 2 °C before being aseptically inoculated with 10% of fungi inoculum (Antil *et al.*, 2015). The Mandel's medium consisted of following composition (g/l): urea, 0.3; peptone, 0.3;

yeast extract, 0.75; (NH₄)₂SO₄, 1.4; KH₂PO₄, 2.0; CaCl₂, 2.0; MgSO₄.7H₂O, 0.3; NaNO₃, 3.0; CaCl₂, 0.3 and trace elements (mg/l): FeSO₄.7H₂O, 0.5; MnSO₄.4H₂O, 1.6; ZnSO₄.7H₂O, 1.4 and CoCl₂.6H₂O, 20.0 and Tween-80, 0.1% (v/v) pH 5.5. Inoculated flasks were incubated at 28 ± 2 °C under static conditions for 5 days. Sample was aseptically withdrawn at 24 h interval to check the enzyme activity. The culture medium was initially filtered using Whatman no.1 filter paper, and the filtrate was centrifuged at 8000 rpm at 4 °C for 20 min. The clear supernatant was used as the crude extracellular enzyme source.

3. Assay for crude enzyme activity

Optimal activity of the enzymes produced were assayed as follows:

i. Assay for crude xylanase activity

The measurement of the quantity of xylanase produced was done by using birch wood xylan (1%) as the substrate (Meddeb-Mouelhi *et al.*, 2014). A total of 1.0 mL reaction mixture, consisting of 0.5 mL of crude extracellular enzyme source and 0.5 mL of 1% birch wood xylan (prepared in 0.05 M Na-acetate buffer, pH 4.8), was used to assay for xylanase activity. The reaction mixture which was incubated for 10 min at 50 °C was stopped by the addition of 1.0 mL of 3, 5- dinitrosalicylic acid (DNS) and the contents were boiled for 5 min as reported by Whangchai *et al.* (2021). Xylose standard curve (Appendix A, Figure 2) was used to quantify the amount of reducing sugar released at 540 nm, which is a measure of glucose equivalent of the reducing sugar released. A unit of xylanase activity was defined as the amount of enzyme required to liberate 1 µmol of xylose per minute under the assay conditions (Valliammai *et al.*, 2021).

ii. Assay for crude cellulase activity

The method of Wood and Bhat was used to assay for the activity of cellulase as cited by Valliammai *et al.* (2021). A total of 1.0 mL reaction mixture consisting of 0.5 mL of crude extracellular enzyme source and 0.5 mL of 1% carboxyl methyl cellulose (prepared in 0.05 M Na-citrate buffer, pH 5.0) was used to assay for cellulase activity. The reaction mixture which was incubated for 10 min at 50 °C was stopped by the addition of 1.0 mL of 3, 5- dinitrosalicylic acid (DNS) and the contents were boiled for 5 min as reported by Whangchai *et al.* (2021). Glucose standard curve (Appendix A, Figure 3) was used to quantify the amount reducing sugar released at 540 nm, which is a measure of glucose equivalent of the reducing sugar released. A unit of cellulase activity was defined as the amount of enzyme required to liberate 1µmol of glucose per minute under the assay conditions (Valliammai *et al.*, 2021).

3.5.2 Screening of fungi for fermentation process

3.5.2.1 Qualitative screening of the isolated microorganisms for fermentation (sugar fermentation test)

The ability of organism to ferment a specific carbohydrate/sugar was determined by the presence of acid or gas produced from fermentation of the carbohydrate. Reaction medium containing 1% each carbohydrate source (glucose, lactose, xylose, sucrose, fructose or maltose) and 0.01% phenol red (indicator) was prepared and sterilized in the autoclave at 121 °C for 15 min (Hemraj *et al.*, 2013). The medium was kept at 30 °C for seven days after being inoculated with a loopful of 24 h old culture of the organisms under investigation. There was a production of acid, consequently leading to reduction in the pH of the medium, during the reaction which is detectable by a pH indicator (phenol red) which was also added to the medium. Also, an inverted Durham tube which was

immersed into the reaction medium collected the gas (carbon dioxide) produced during the reaction (Varghese and Joy, 2014).

3.5.2.2 Quantitative screening of the isolated microorganisms for fermentation

process

Inoculum for fermentation was prepared by growing fungi cells in 250 mL sterilized YPD broth containing (g L^{-1}): yeast extract (10), peptone (20), dextrose (20), with pH 5.0 at 30°C (Fakruddin *et al.*, 2012) on an orbital shaker (150 rpm) for 16 h. After centrifugation at 8000 rpm for 15 min, the sediment which are the cells were resuspended in normal saline (0.85% NaCl) and diluted until an optical density ($\text{OD}_{600 \text{ nm}}$) of 2.0 was reached (Reis *et al.*, 2013) and this was used as inoculum for fermentation. Ten percent of inoculum was added to sterilized fermentation medium containing extra 20% dextrose. The experiment was performed at room temperature (27 ± 2.0 °C) (Tayel *et al.*, 2010) and a pH of 5.0 (Narendranath and Power, 2004; Germec *et al.*, 2023). The medium was agitated at 150 rpm so as to supply the initial oxygen needed for yeast growth (Sriputorn *et al.*, 2020). Agitation ensured the fermentation media was adequately aerated and maintained at the optimum temperature for fungi growth. Fermentation was allowed for 10 days and samples were aseptically withdrawn at 24 h intervals for analysis. The pH of the medium was maintained at 5.0 throughout the reaction with drops of 10% NaOH solution. Glucose was analyzed by DNS method (Ghose, 1987) , xylose was analyzed using bial's reagent (Pham *et al.*, 2011) and the concentration of ethanol in the fermented medium was determined by dichromate method (Anwar *et al.*, 2012). The amount of ethanol (g/L) in the samples was extrapolated from ethanol standard curve (Appendix A, Figure 5) which was initially prepared in different concentrations (0 – 10%). Acidified potassium dichromate was added to each concentration of ethanol and left for 30 min to

develop a greenish colour in a dark place at room temperature which was read at 590 nm. The organisms which had the best results were selected for further studies.

3.5.2.3 Determination of ethanol tolerance of the fermentation organisms

The method described by Zainab *et al.* (2019), with a slight modifications, was used to check for ethanol tolerance of the ethanogenic fungi. The turbidity of the medium which is an indication of the viability of the organisms was determined optically at 600 nm. The organism was grown in a basal medium containing 4 g/L (NH₄)₂SO₄; 2 g/L K₂O; 0.7 g/L MgSO₄·7H₂O; and 200 g/L glucose. Various concentrations of absolute ethanol (2% to 16% (2%, 4%, 6%, 8%, 10%, 12%, 14%, and 16%)) were autoclaved at 121 °C for 15 min in a tightly corked bijou bottles and transferred to a water bath (30 °C). The sterile media was inoculated with actively growing fungi cells at an initial optical density (OD_{600 nm}) of 2. The suspension was incubated at 30 °C for 48 h and the number of surviving cells was determined by checking the final OD at 600 nm after 48 h. The initial optical density of media with no added ethanol was taken as 100%, the turbidity corresponded directly to the organism biomass in the medium. The amount of ethanol in percentage at which the growth of microbe was just inhibited was asserted as its ethanol tolerance level.

3.5.3 Molecular characterization of organisms used for enzyme production and fermentation process

The organisms used for the production of enzyme and fermentation process were identified and molecularly characterized as described by Nilsson *et al.* (2019). The methods are explained as follows:

3.5.3.1 Molecular identification and characterization of organisms

i. Fungi DNA extraction protocol

The mycelia of fungi were grinded with Dellaporta extraction buffer (100 mM Tris pH 8, 51 mM EDTA pH 8, 500 mM NaCl, 10 mM mercaptoethanol) and the DNA was extracted as described by Nilsson *et al.* (2019). Prior to vortexing and incubating the sample mixture at 65 °C for 10 min, 40 µl of 20% SDS was added to it in a sterile Eppendorf tube. Furthermore, 160 µl of 5 M potassium acetate was then added to the resultant mixture which was vortexed and centrifuged at 10000 g for 10 min and the supernatant were collected in another Eppendorf tube. Cold iso propanol (400 µl) was then added to the mixture and kept at -20 °C for 60 min. Then, the DNA was precipitated from the mixture at 13000 g for 10 min, and washed with 500 µl of 70% ethanol by centrifuging at 10000 g for 10 min. The DNA was air-dried at room temperature to remove every trace of ethanol and then re-suspended in 50 µl of Tris EDTA buffer for preservation and suspension of the DNA.

ii. Polymerase Chain Reaction (PCR) analysis of fungi

Characterization of fungi was done using the internal transcribed spacer (ITS) universal primer set which flank the ITS1, 5.8S and ITS4 region. PCR sequencing preparation cocktail consisted of 10 µl of 5x GoTaq colourless reaction, 3 µl of 25 mM MgCl₂, 1 µl of 10 mM of dNTPs mix, 1 µl of 10 pmol each ITS 1: 5' TCC GTA GGT GAA CCT GCG G 3' and - ITS 4: 5' TCC TCC GCT TAT TGA TAT GC 3' primers (Aşgin and Değerli, 2019) and 0.3 units of Taq DNA polymerase (Promega, USA) made up to 42 µl with distilled water and 8 µl DNA template. PCR was carried out in a Gene Amp 9700 PCR System Thermal cycler (Applied Biosystem Inc., USA) with a PCR condition which included a cycle of initial denaturation at 94 °C for 5 min, followed by 35 cycles of each

cycle comprising of 30 sec denaturation at 94 °C, 30 sec annealing of primer at 55 °C, 1.5 min extension at 72 °C and a final extension for 7 min at 72 °C.

iii. Purification of amplified gene product from organisms

In order to remove the remnants of PCR reagents, the amplified fragments were purified with ethanol, and was allowed to dry in the fume cupboard at room temperature for 10-15 min, after which it was resuspended with 20 µl of sterile distilled water and kept at -20 °C prior to sequencing. In order to confirm the presence of the purified products, it was checked on a 1.5% agarose gel ran on a voltage of 110 V for about 1 h as previously indicated, and then quantified using a nanodrop of model 2000 from thermos scientific.

iv. Sequencing of the gene product from fungi and construction of phylogenic tree

The amplified fragments were sequenced using a Genetic Analyzer 3130xl sequencer from Applied Biosystems using manufacturers' manual while the sequencing kit used was that of Big Dye terminator v3.1 cycle sequencing kit. Bio-Edit software and MEGA x1 were used for all genetic analysis. The 16S rRNA gene sequence of the four isolates was used to carry out BLASTN with the database of NCBI GenBank. The ITS rDNA region was sequenced using two primers (ITS1 and ITS4) for every strain. Molecular characteristics of organisms that are closely related to the sample organisms was shown in Table 3.4, the pairwise alignment of each sample organism with the most closely related four organisms were done for each organism based on maximum identity score as shown in Appendix H (iii). Multiple alignment software programme (Clustal omega) was used to select the closely related organisms. The aligned ITS-rDNA gene sequences were then used to construct a phylogenetic tree by neighbor-joining (NJ) method using MEGA x1. (Zhang *et al.*, 2019b).

Table 3.4: Molecular Characteristics of Organisms that are Related to the Sample Organisms

sample ID	Scientific Name	Max Score	Total Score	Query Cover	E value	Per. Ident	Accession Length	Accession Number
FBL	<i>Aspergillus flavus</i>	1098	1098	100%	0	99.83%	600	MN844036
	<i>Aspergillus flavus</i>	1086	1086	100%	0	99.50%	642	MN844036
	<i>Aspergillus flavus</i>	1086	1086	100%	0	99.50%	642	MN238861
	Sample organism	1103	1103	100%	0	This study	597	OP107821
	<i>Aspergillus niger</i>	1033	1033	99%	0	99.82%	577	MW548412
RDS	<i>Aspergillus niger</i>	1031	1031	99%	0	99.82%	576	MT628904
	<i>Aspergillus niger</i>	1031	1031	99%	0	99.82%	603	MT6200753
	<i>Aspergillus niger</i>	1031	1031	99%	0	99.82%	603	MT597823
	Sample organism	1040	1040	100%	0	This study	563	OP107822
	<i>Mucor indicus</i>	1068	1068	100%	0	99.49%	664	OQ660484
RB	<i>Mucor indicus</i>	1068	1068	100%	0	99.49%	907	KT359356
	<i>Mucor indicus</i>	1068	1250	100%	0	99.49%	759	KY425744
	<i>Mucor sp</i>	1068	1068	100%	0	99.49%	630	KU571498
	Sample organism	1083	1083	100%	0	This study	586	OP107823
	<i>Saccharomyces cerevisiae</i>	1362	1362	99%	0	99.47%	752	NR111007
PP	<i>Saccharomyces cerevisiae</i>	1349	1349	99%	0	99.20%	773	Z95942
	<i>Saccharomyces cerevisiae</i>	1347	1347	99%	0	99.07%	819	MF375634
	<i>Saccharomyces cerevisiae</i>	1347	1347	99%	0	99.07%	814	MF276989
	Sample organism	1384	1384	100	0	This study	749	OP107824

3.5.3.2 Molecular identification of enzyme gene extracted from characterized organisms

Molecular investigations of enzyme-producing gene extracted from characterized organisms are described below.

i. Molecular identification of endo-beta-1,4-glucanase gene from *Aspergillus flavus* strain FBL

Molecular investigations of cellulase-coding gene in the *Aspergillus flavus* by simple PCR on the extracted DNA using endo-beta-1,4-glucanase B gene -coding regions specific primers. Reaction cocktail used for PCR included (Reagent Volume in μ l) - 5X PCR SYBR green buffer (2.5), $MgCl_2$ (0.75), 10 pM DNTP (0.25), 10 pM of each forward ACCACGGTAAGTTGCTCATC and backwards CCGACCTTCTTGTTGTCCTT primer (0.25), 8000 U of taq DNA polymerase (0.06) and made up to 10.5 μ l with sterile distilled water to which 2 μ l of DNA template was added. Buffer control was also added to eliminate any probability of false amplification. PCR condition included a cycle of initial denaturation at 94 °C for 5 min, followed by 35 cycles with each cycle comprising of 30 sec denaturation at 94 °C, 30 sec annealing of primer at 50 °C, 30 sec extensions at 72 °C and a final extension for 7 min at 72 °C. PCR was carried out in a GeneAmp 9700 PCR System Thermal cycler (Applied Biosystem Inc., USA) using the appropriate profile as designed for each primer pair.

ii. Molecular identification of endo-beta-1,4-xylanase 1 gene *Aspergillus niger* strain RD5

Molecular investigations of xylanase-coding gene in the *Aspergillus niger* by simple PCR on the extracted DNA using endo-beta-1,4- xylanase gene -coding regions specific primers. Reaction cocktail used for PCR included (Reagent Volume in μ l) - 5X PCR

SYBR green buffer (2.5), MgCl₂ (0.75), 10 pM DNTP (0.25), 10 pM of each forward GATCATCACGTCACCCGATAAA and backward AACTCTCCTCAGGCCGAATA primer (0.25), 8000 U of taq DNA polymerase (0.06) and made up to 10.5 with sterile distilled water to which 2 µl DNA template was added. Buffer control was also added to eliminate any probability of false amplification. The PCR condition included a cycle of initial denaturation at 94 °C for 5 min, followed by 35 cycles with each cycle comprising of 30 sec denaturation at 94 °C, 30 sec annealing of primer at 47 °C, 30 sec extensions at 72 °C and a final extension for 7 min at 72 °C. PCR was carried out in a GeneAmp 9700 PCR System Thermal cycler (Applied Biosystem Inc., USA) using the appropriate profile as designed for each primer pair.

3.5.4 Production of support for enzyme immobilization

Support for enzyme immobilization was prepared using sugarcane bagasse as described by Wu *et al.* (2020) and shown below.

3.5.4.1 Preparation of porous biochar as support for immobilization

Sugarcane bagasse was used to prepare the porous biochar as described by Wu *et al.* (2020) with modification to obtain a larger surface area as shown in Figure 3.2. Sugarcane bagasse was first cut in bits and heated in distilled water for a period of 8 h at 90 °C. The boiled sample was dried in the oven at 80 °C for 24 h. Secondly, 1 g each of boiled sugarcane bagasse and KOH were poured into 12 mL of absolute ethanol which was stirred for 6 h. The KOH activated bagasse was kept in oven to dry at 60 °C for a period of 12 h. The activated sugarcane bagasse was calcined at 450 °C for 40 min (protected with nitrogen at a heating rate of 10 °C/min), it was later cooled at room temperature. The impurities such as ash and alkali in the pyrolyzed bagasse was removed by the addition of 12.5 mL of 1.5M HCl. In the end, the residue remaining after the

removal of ash and alkali was washed with distilled water until there was no trace of acid in the sample, then it was dried at 60 °C for 24 h

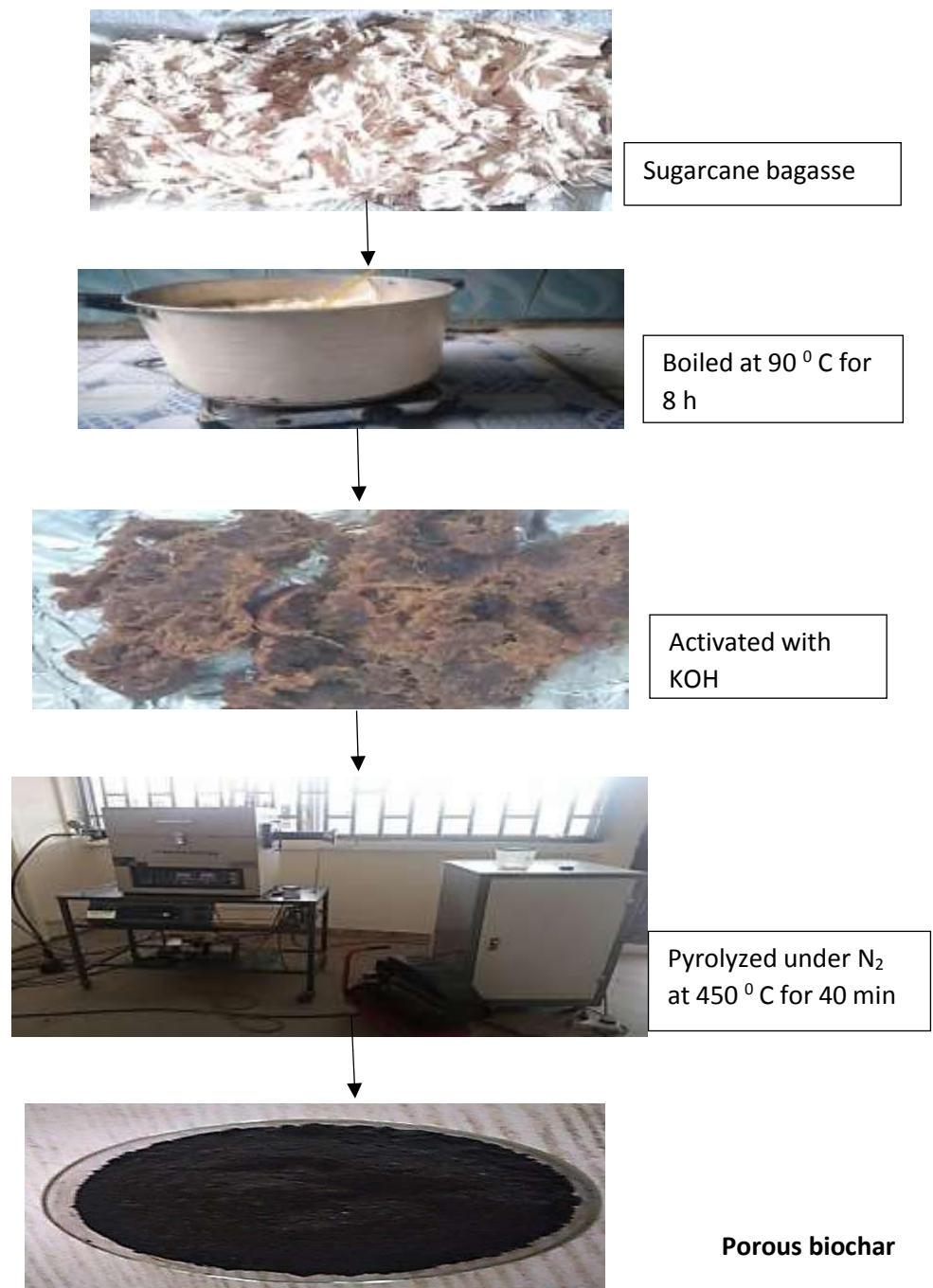


Figure 3.2: Preparation of Porous Biochar from Sugarcane Bagasse

3.5.4.2 Preparation of biochar-chitosan composite for enzyme immobilization

Biochar- chitosan composite bead was prepared by the method of Biró *et al.* (2008) with some modifications. A mixture of porous biochar (2% w/v) and Chitosan (2% w/v) was dissolved in an aqueous solution of acetic acid (1% v/v) and mixed thoroughly for 30 min to form a paste. The paste was extruded in drop through a syringe into a gently stirred coagulation liquid (A mixture of 10% CaCl₂ and 1 N, sodium hydroxide in 26% w/v ethanol) and left for 30 min to form beads. The obtained biochar-chitosan beads were filtered, washed with 1% acetate buffer thrice and then with distilled water until it attained neutral pH. Portions of the freshly prepared beads were dried at different temperatures (room temperature, oven-dried and freeze-dried) as shown in Figure 3. 3, so as to compare the activities of enzyme loaded on each support as well as to facilitate the ease of separation from the reaction medium. These beads were characterized to choose the best preparations for further studies.

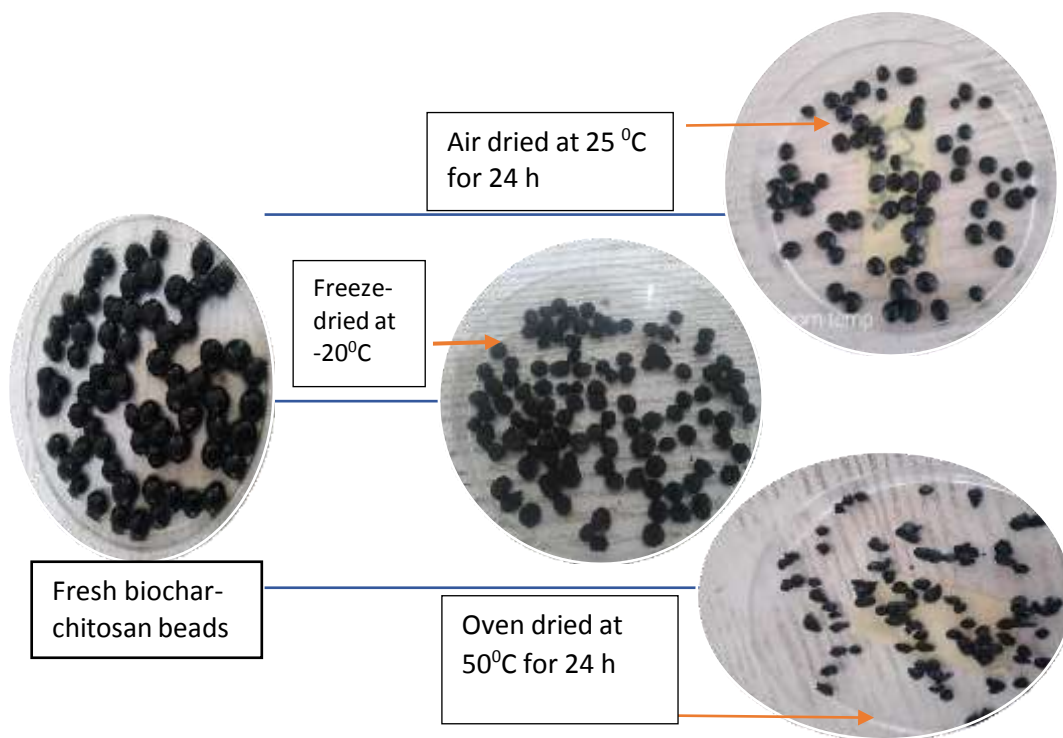


Figure 3.3: Biochar-chitosan Beads Prepared at Different Drying Conditions

3.5.5 Characterization of biochar-chitosan beads for enzyme immobilization

Biochar-chitosan beads prepared for enzyme immobilization were characterized as discussed below:

3.5.5.1 *Determination of the sizes of biochar-chitosan beads prepared at different drying temperatures*

The average of the diameter of 10 biochar-chitosan beads dried at different temperatures were measured with micrometer screw gauge as described by Jadhav and Nagarkar (2022).

3.5.5.2 Determination of the swelling behaviours of biochar-chitosan beads prepared at different drying temperatures

The ability of the biochar-chitosan composite beads to swell were determined by immersing in 10 mL of 50 mM citrate (pH 6) buffer at room temperature (25 °C) for 6 h (Parin *et al.*, 2020). The rate of swelling was checked at 30 min interval by weighing on analytical weighing balance. The swelling ratio was calculated by the following equation:

$$\text{Swelling ratio} = \frac{m_f - m_i}{m_i} \quad (3.9)$$

where m_i and m_f are the weights of the initial bead and final wet bead, respectively.

3.5.5.3 Thermogravimetric analysis (TGA) and derivative thermogravimetry (DTG) of biochar-chitosan beads

Thermogravimetric analyzer (TGA-4000; PerkinElmer) was used to determine the thermal stability of samples

i. Procedure:

Small quantities (5 mg) of the sample were placed into the sample holder and placed in the analysis chamber, then it was covered and allowed to cool to 15 degrees Celsius. All the information about the sample were inputed into the computer and the nitrogen flow was opened at the rate of 20 mL/min with heating rate of 10 °C/min between 30 °C to 800 °C, then finally the start button was clicked on to commence the analysis. The sample mass was recorded continuously by an analytical scale that was connected with a computer. The temperature of the gas was also noted at various segments by thermocouples. The result obtained appeared as a continuous chart record of temperature against time (Rasam *et al.*, 2020).

3.5.5.4 Determination of pore size, pore volume, and surface area of the biochar-chitosan beads prepared at different temperatures

The specific surface areas (SSA), total pore volume V_p , and average pore size of the biochar-chitosan composites were determined by Brunauer Emmett-Teller (BET) nitrogen adsorption-desorption method at the Centre for genetic engineering and biotechnology, Minna, Niger State, Nigeria. Quantachrome (model: NOVA4200e) BET analyzer was used for the analysis. The analysis involved:

ii. Procedure

Dewar was filled to the internal upper mark with liquid nitrogen, and the sample cell containing an out gassed and weighed sample was placed into the analysis station and all the fields/selections on the start analysis ‘‘Sample’’ menu was inputted. Also, point selection tagging and Equilibrium menu Fields were completely selected for BET measurements. Then, ‘‘Start’’ was clicked to begin the analysis. The specific surface area, particle size distribution and average pore diameter were obtained through the Barrett-Joyner-Halenda (BJH) method of the Brunauer Emmett-Teller.

3.6 Co-immobilization of enzyme

After characterization, the bead with the best characteristics was selected for co-immobilization of cellulase and xylanase for further studies.

3.6.1 Determination of activities of free and enzyme co-immobilized on beads prepared at different drying conditions

The enzymes were loaded in different categories on freeze-dried biochar-chitosan support to determine the loading method for further studies as described by Shi *et al.* (2011); Egwim *et al.* (2014); and Zawawi *et al.* (2020). The loading involved functionalization of support by soaking in 25% glutaraldehyde and then incubated on orbital shaker (150 rpm) for 24 h to functionalize the biochar-chitosan bead. The functionalized beads were

rinsed with distilled water to remove the excess glutaraldehyde before cross-linking the biochar-chitosan bead with the enzymes. Crosslinking of enzymes to the functionalized beads was done by soaking one gram of activated biochar-chitosan bead in 10 mL xylanase (38.63 IU/mL) and 10 mL cellulase (15.61 IU/mL) solution in 50 mM citrate buffer, pH 6.0, then it was incubated at 100 rpm and allowed to crosslink with the functionalized beads for 3 h. The activity of each constituent enzyme was determined by DNS method. Xylan was used as substrate for xylanase while carboxyl methyl cellulose was used as substrate for cellulase. The activities for cellulase and xylanase were recorded as micromole of reducing sugar released per milliliter of reaction volume per minute per gram of biochar-chitosan bead ($\text{IU}/\text{mLg}^{-1}$). The categories of loading were:

1. Xylanase was added to 1 g functionalized biochar-chitosan bead for 1 h before adding cellulase then, both were left to crosslink with the bead for 3 h
2. Cellulase was added to 1 g of functionalized biochar-chitosan bead for 1 h before adding xylanase then, both were left to crosslink with the bead for 3 h
3. Both xylanase and cellulase were added at the same time to 1 g functionalized biochar-chitosan bead and left to crosslink with the bead for 3 h

The category with the best total activity of loaded enzymes was selected for further study

3.6.2 Determination of total protein concentration, specific activity and immobilization efficiency of the co-immobilized crude enzyme

The protein concentration, specific activity and immobilization efficiency of the co-immobilized crude enzyme was determined as described by Bindu *et al.* (2018). The total protein contents of the free and co-immobilized enzymes were also determined by Bradford method at 595 nm to evaluate the specific activity of the enzyme. Bovine Serum Albumin (BSA) was used as standard to determine the protein concentration. The amount of bound enzyme was determined indirectly from the difference between the amount of

total protein in enzyme introduced (AEI) and the amount of total protein in enzyme remaining after immobilization (AER) (Egwim *et al.*, 2014).

$$\text{Total protein concentration} = \frac{AEI - AER}{AEI} \times 100 \quad (3.10)$$

AEI = total protein in enzyme introduced

AER = total protein in enzyme remaining after immobilization

The concentration of protein was calculated from the BSA standard curve (Appendix A)

Specific Enzyme activity, activity yield and immobilization yield were calculated for the free and co-immobilized enzymes by the following equations (Bindu *et al.*, 2018). Co-immobilized enzyme with the highest immobilization efficiency for both cellulase and xylanase was chosen for further study.

$$\text{Specific activity} = \frac{\text{Enzyme activity}}{\text{Total protein}} \quad (3.11)$$

$$\text{loading efficiency} = \frac{\text{Total amount of protein in immobilized enzyme}}{\text{Total amount of protein in free enzyme}} \times 100 \quad (3.12)$$

$$\text{Activity yield} = \frac{\text{activity of immobilized enzyme}}{\text{activity of free enzyme}} \times 100 \quad (3.13)$$

$$\text{Immobilization efficiency} = \frac{\text{Activity yield}}{\text{loading efficiency}} \times 100 \quad (3.14)$$

3.6.3 Effect of reaction temperature on the activity of free and co-immobilized enzymes

The enzymatic activity was assayed for free enzymes and co-immobilized enzymes (CIE) at the following reaction temperatures 20, 30, 40, 50, 60, 70, 80, and 90 degrees Celsius.

The optimum temperature obtained at this stage was used for subsequent test

3.6.4 Effect of pH on the activity of free and co-immobilized enzymes

The optimal activities of free and co-immobilized enzymes were determined at a pH range from 2 to 9 as described by Nguyen and Kim (2017), with some modifications. The buffers used were Sodium acetate buffer, (pH 3.0-6.0); Phosphate buffer, (pH 6.0-7.0); citrate phosphate (pH 8.0) and Carbonate buffer, (pH 9.0- 10.0). The optimum pH obtained at this stage was used for subsequent test.

3.6.5 Effect of substrate concentration on the activity of free and co-immobilized enzymes

The activities of free (Cellulase and xylanase) and co- immobilized cellulase and xylanase (CIE) were determined at different substrate concentrations using agrowaste samples at 0.25%, 0.5%, 1.0%, 2.0%, and 3.0% (w/v) in 50 mM sodium citrate buffer at pH 6.0 as described by Nguyen and Kim (2017). These were used to plot Michaelis-Menten and Line-weaver Burk plot so as to determine K_m and V_{max} .

3.6.6 Determination of half-life for free enzyme and enzyme co-immobilized on freeze-dried biochar-chitosan bead

The time it took for free and enzyme co-immobilized on freeze-dried biochar-chitosan bead to lose 50% of their activities was determined by incubating the enzymes at optimum temperature and pH without substrate for ten days. The residual activity was determined by DNS method using carboxyl methyl cellulose as substrate. Samples taken at 24 h interval was used to calculate the rate constant and half-life of free and co-immobilized enzymes.

3.6.7 Re-usability test for co-immobilized enzymes

In order to determine the operational stability of enzymes co-immobilized on freeze-dried support, it was reacted with agrowaste and reused repetitively for 10 times as described

by Nguyen and Kim (2017). The operational stability was evaluated by the percentage of residual enzyme activity from each cycle. The enzyme activity in the first cycle for the immobilized enzyme was taken as the control and correspond to 100% activity.

3.6.8 Determination of thermal stability of free and co-immobilized enzymes

The free (Cellulase and xylanase) and co-immobilized enzymes were incubated at varying temperatures between 40 °C and 90 °C for 3 h without substrate to determine the thermal stability as described by Weng *et al.* (2022). Samples were taken at 30 min interval to determine the residual enzyme activity by DNS method using carboxyl methyl cellulose as substrate.

Activation and Deactivation energy of free and co-immobilized enzymes was also determined from Arrhenius plot (Appendix I). Likewise, the half-life of the free and co-immobilized enzymes was determined for each Temperature.

3.6.9 Determination of storage stability of free and co-immobilized enzymes

The stability of the free (Cellulase and xylanase) and co-immobilized enzymes (CIE) were analyzed when stored at 25 °C and 4 °C as described by as described by Weng *et al.* (2022). The enzymes were incubated in 50 mM sodium citrate buffer at room temperature (25 °C) for 10 ten days and refrigerator (4 °C) for 45 days. The activity of each enzyme was measured at intervals of 24 h. Furthermore, the half-life of enzymes was also determined when stored at 25 °C and 4 °C.

3.7 Enzymatic hydrolysis of agrowaste using free and co-immobilized enzymes

Enzymatic hydrolysis of pre-treated and unpre-treated agrowaste samples were carried out in 250 mL Erlenmeyer flasks at 55 °C shaken at 150 rpm. Six grams of the agrowaste biomass was soaked in 100 mL of 50 mM sodium citrate buffer (pH 6.0) so as to maintain a pH of 6 (Gunam *et al.*, 2020). Cellulase was added at an enzyme loading of 13.63 IU/g

dry biomass, while xylanase was added to biomass in 50 mM acetate buffer (pH 5.0) at an enzyme loading of 27.61 IU/g dry biomass. Also, 1g/g dry biomass of co-immobilized enzyme (CIE) containing 9.5 IU/mL of cellulase and 19.3 IU/ mL of xylanase was used for the hydrolysis. In order to prevent microbial growth during the reaction, Sodium azide (0.02% (w/v)) was added to the mixture. The hydrolysis reaction was done for 96 h during which the samples were taken at 24 h intervals. The hydrolysate was boiled for 5 min at 100 °C to deactivate the enzymes, after which the sample was centrifuged so as to determine the reducing sugar content using DNS method. The experiments were repeated twice (duplicate) and the average reducing sugar value was reported as mg of equivalent glucose units per mL of hydrolysate (indicated as mg/mL).

3.8 Immobilization of Fungi

The immobilization of the fungi was made by encapsulation in biochar-chitosan beads as described by Sierra Solache *et al.* (2016), and Hutchinson *et al.* (2020), with some modifications. Briefly, 2.4 mL of biomass suspension ($OD_{600} = 2$) of fungi was added to the mixture of 30 mL solution of porous biochar (2% w/v) and Chitosan (2% w/v) which were dissolved in an aqueous solution of acetic acid (1 v/v%) and then mixed thoroughly for 30 min. The biomass suspension was in three categories: yeast only, mucor only, and equal volume of yeast and mucor. A 10 mL syringe was used to drop the mixture into a coagulating medium (A mixture of 10% $CaCl_2$ and 1 N sodium hydroxide in 26 v/v% ethanol) and left for 30 min. After encapsulation, the biochar-chitosan beads which contained fungi biomass was then thoroughly washed with sterile distilled water to attain pH of 7 which was later preserved in saline (0.9% NaCl solution) at 4 °C until needed for further analysis.

3.9 Production of Bioethanol

3.9.1 Experimental design for simultaneous saccharification and co-fermentation (SScF)

The SScF experiments were performed in 750 mL glass flasks with air-tight lid. The medium used for fermentation contained the same content as used for inoculum preparation except glucose that was swapped for 6% (w/v) of pre-treated sugarcane bagasse or plantain pseudostem biomass as carbon source. Therefore, the fermentation medium consisted of: Yeast extract (10 g/L); Peptone (20 g/L) and pre-treated agrowaste (60 g/L). The medium was maintained at pH 5 throughout the experiment. Six percent free enzyme and ten percent (v/v) fungi inoculum was introduced to the medium after sterilization to commence the SScF. However, one gram of loaded bead per gram of dry agrowaste sample was used in the case of co-immobilized enzyme, immobilized yeast; immobilized mucor and co-immobilized yeast and mucor. Initially, pre-hydrolysis was performed at 50 °C, using the enzyme loading earlier reported (Section 3.6.1), before the fermentation organisms were introduced (Adeniyi *et al.*, 2022). Then, the reaction mixture was incubated for 24 h in aerobic conditions, which is favorable for the growth of yeast cells and this was done by shaking the bioreactor on orbital shaker at 30 °C. After this process, anaerobic conditions were provided to the reaction media for the production of ethanol in static condition at room temperature for additional 72 h as described by Bhuyar *et al.* (2020).

The set up for the simultaneous saccharification and fermentation is as shown in Table 3.5. while the pictures for fermentation set-up are shown in Plates 6 and 7 (Appendix E).

Table 3.5: Constituents of Each Reaction Vessel for Bioethanol Production

Bioreactor	SScF medium
1	Free enzyme plus free yeast
2	Free enzyme plus free mucor
3	Co-immobilized enzymes plus free yeast
4	Co-immobilized enzymes plus free mucor
5	Co-immobilized enzymes plus immobilized yeast
6	Co-immobilized enzymes plus immobilized mucor
7	Co-immobilized enzymes plus co-immobilized yeast and mucor

The category with the best ethanol production was chosen for further studies.

3.9.2 Re-usability test for co-immobilized fungi and mucor

After the completion of the first fermentation cycle, biochar-chitosan beads were separated from the fermentation flasks using a sterile strainer and rinsed with distilled water. Subsequently, the biochar-chitosan beads were inoculated into flask containing fresh media and substrate and the SScF was repeated until the ethanol yield was below 50% of the initial yield and the number of cycles was noted.

3.10 Distillation of Fermented Broth

Distillation of the fermented broth was done in the laboratory by using distillation apparatus as described by Oyeleke and Jibrin (2009). After the fermentation process, the sample mixture was filtered to remove the solid biomass debris from the fermented mixture. The mixture was then distilled at a temperature of 78 °C which was the boiling point of ethanol. Then the ethanol was collected as the distillate.

3.11 Estimation of Ethanol Concentration

The concentration of distillate collected was measured in percentage ethanol content by dichromate method. Furthermore, the ethanol concentration was also determined in gram per litre (g/L) as described by Oyeleke and Jibrin (2009) by using a measuring cylinder

to measure the volume of the distillate and then multiplied the value by 0.8033 g/mL, which is the density of ethanol, to give the value of ethanol concentration in g/L.

3.12 Ethanol Characterization

The components of the bioethanol produced was profiled by GC-MS at Central Instrumentation Research Facility, Covenant University, Ota-Canaan land, Nigeria. An Agilent 6890 N model gas chromatography system which was coupled to an Agilent 5973 N model mass spectrometer containing an electron impact ion source was used for the analysis. Operating parameter and conditions for GC-MS analysis are shown in Table 3.6

Table 3.6: Operating Parameter and Conditions for GC-MS Analysis

Parameters	Operating Conditions
temperature T1 [time]	35 °C [10 min]
temperature ramp 1 [T1 – T2]	10 °C min ⁻¹ [35–100 °C]
temperature ramp 2 [T2 – T3]	20 °C min ⁻¹ [100–225 °C]
temperature T2 [time]	225 °C [10 min]
injector temperature	250 °C
Split	1:10
detector temperature	250 °C
carrier (helium) gas flow rate	1.3 mL min ⁻¹
Model	J&W DB-624 (Agilent)
stationary phase	6% cyanopropyl-phenyl–94% dimethylpolysiloxane cross-linked

3.13 Cost Estimation for the Production of 1.5 L of Bioethanol

The production cost of ethanol depends on several factors such as the cost of raw materials, labour, energy, and capital. The cost of production can be calculated by adding up all the costs involved in producing ethanol such as production cost, maintenance cost, labour cost, administrative cost and capital cost. Production costs, include both variable (feedstock and plant operation) while capital expenses involve fixed capital and working

capital. In the present study, the production process took about 12 days from collection of samples to obtaining the products as shown in Figure 3.4. For each of the box in the process flowchart, someone will be manning the operation in a large-scale production. The costs were estimated approximations of the values of the items while assumptions were made for the other items such as maintenance because they were either not bought or the items were not applicable for the present production. However, the contribution (in percentage) to the overall cost by each of the process was analyzed by Tao *et al.* (2014).

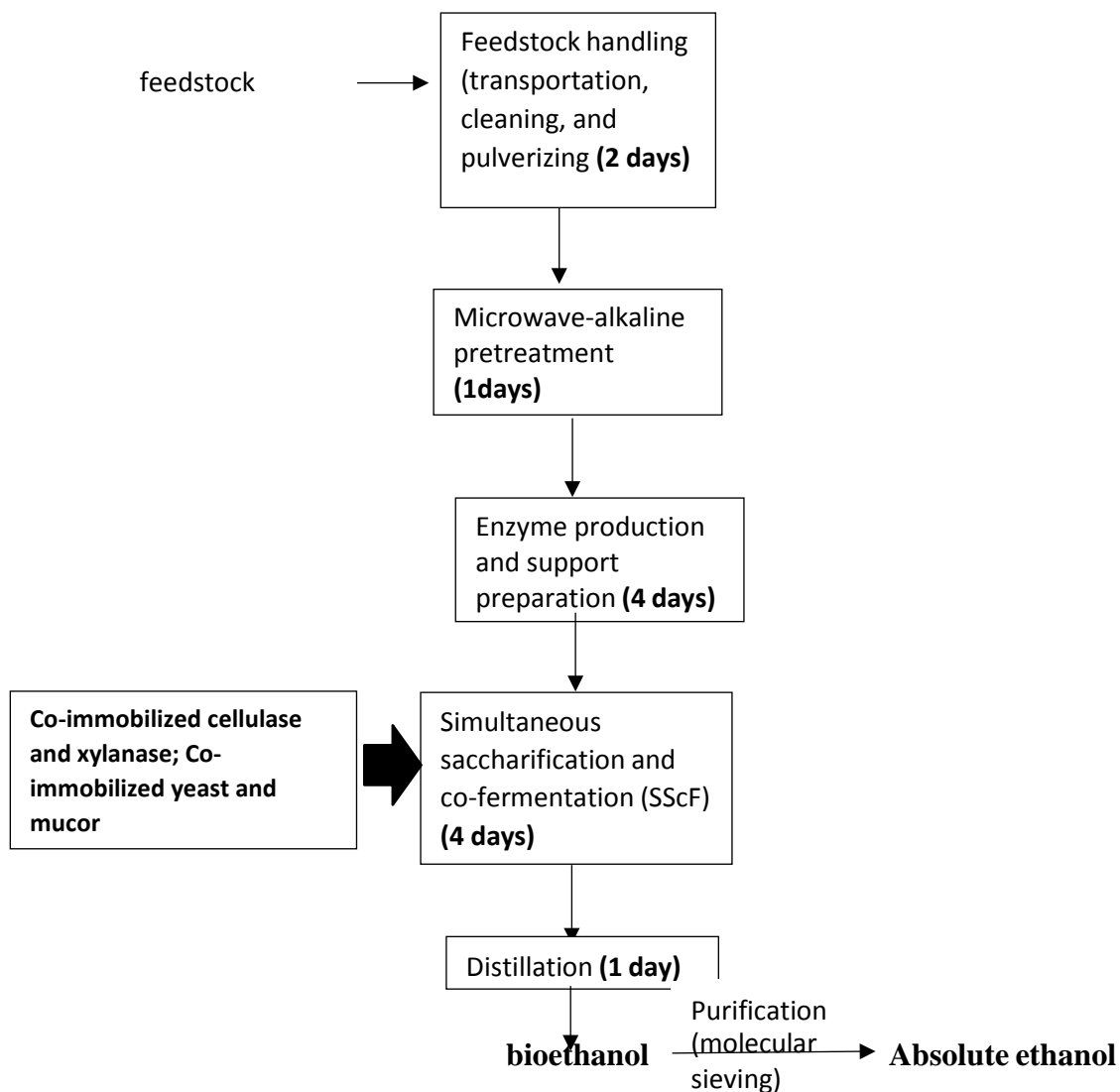


Figure 3.4: Flowchart for the Production of 1.5 L of Cellulosic Bioethanol

Although, the media components used for the present production were laboratory grade, the media component costs were calculated through the market prices and estimated in accordance to the amount used in the required volume.

Sixty gram of beads was used to co-immobilize enzyme and 30 g of biochar-chitosan beads containing encapsulated co-immobilized *S. cerevisiae* and *M. indicus* were added to 60 g of pretreated biomass in 1000 mL of YPD broth for simultaneous saccharification and co-fermentation to produce 1.5 L of bioethanol. This entails:

- i. 10mL each of enzyme (cellulase: 9.5 IU/mL; and xylanase: 19.3 IU/ mL) loaded on 1 g of biochar-chitosan bead.
- ii. Sixty grams of loaded beads were added to 60 g of pretreated biomass in 1000mL of YPD broth for SSCF to yield 150 mL of 81% bioethanol.
 - Cost of bead production of biochar chitosan beads
 - Chitosan (2 g) = ~ ₦ 1000
 - Biochar (2 g) = ~ ₦ 300
 - Coagulating medium = ~ ₦ 200
 - Cost of mineral salts used to produce 1 L of enzyme ~ ₦ 500
 - Cost of yeast extract and peptone water per 1 L of fermentation medium = ₦ 300

Immobilized moieties were used ten times in fresh fermentation medium, therefore cost of yeast and peptone water for ten times fermentation equals ₦ 3000.

3.14 Statistical Analysis

Analysis was conducted in duplicate. Values were analyzed using excel version 21, R software statistical package and Statistical Package for Social Science (SPSS) version 21 (IBM SPSS Incorporation, Chicago, USA). Results were presented as means \pm SE of the mean. Comparison of data was done using One Way Analysis of Variance (ANOVA) and Duncan Multiple Range Test (DMRT). Data were considered significant at $P < 0.05$.

CHAPTER FOUR

4.0 RESULTS AND DISCUSSION

4.1 Results

4.1.1 Composition of dried native (unpre-treated) agrowaste

The composition of dried raw unpre-treated agrowaste samples used for this research is shown in Table 4.1. Sugarcane bagasse was shown to have the highest concentration (percentage) of cellulose which was 48%, while plantain pseudostem biomass was shown to have the lowest concentration (percentage) of cellulose which was 35%. Hemicellulose content is highest in corncob biomass (35%) and lowest in sugarcane bagasse (24%). However, plantain pseudostem biomass contained the lowest percentage of lignin while sugarcane bagasse contained the highest percentage of lignin

Table 4.1: Cellulose, Hemicellulose and Lignin Content of Dried Unpre-treated Agrowaste

Agrowaste	Cellulose Content (%)	Hemicellulose Content (%)	Lignin Content (%)
Plantain pseudostem	35	30	11.49
Sugarcane bagasse	48	24	21.5
corncob biomass	42	35	19.3

4.1.2 Solid yield and composition of microwave-alkaline pre-treated agrowastes

The composition by weight and the total lignin content in the solid yield of agrowastes after microwave-alkaline pre-treatment are shown in Table 4.2 (a-c) for plantain pseudostem biomass, sugarcane bagasse and corncob biomass at different process conditions generated by design expert software. The tables show variation in sizes of the solid yield obtained at various process conditions. The reduction in sizes for all the agrowastes has a direct relationship with the percentage of total lignin content remaining after the biomass has undergone pre-treatment. For instance. In the case of plantain pseudostem biomass (Table 4.2a), the lowest solid biomass yield (1.85 g) which also corresponds to the lowest total lignin content (2.69%) was observed at run 15 while the highest solid biomass yield (3.64 g) was obtained when the highest percentage of total lignin (7.58%) after pre-treatment was retained at run 10. Likewise, in Table 4.2b, the lowest biomass yield (1.96 g) as well as lowest percentage of lignin (4.90%) remaining after the pre-treatment of sugarcane bagasse was at run 14, whereas, the highest solid biomass yield (4.16 g) as well as the highest percentage of total lignin retained (12.64%) after the pre-treatment of sugarcane bagasse was observed at run 7. Same trend can also be observed in the biomass yield and lignin retained after the pre-treatment of corncob biomass as shown in Table 4.2c. The lowest biomass yield (2.73 g) and lowest lignin retained (6.58%) was observed at run 15 while the highest biomass yields (4.14 g) and highest lignin remaining (14.30%) was observed at run 10

Table 4.2a: Effect of Microwave-alkaline Pre-treatment on the Weight and Percentage of Lignin in Plantain Pseudostem Biomass

Run	Treatment conditions	Weight (g) before delignification	Weight (g) after delignification	% total Lignin retained
	Unpre-treated	5.00	5.00	11.49
1	2%/70 W/5 min	5.00	3.49	5.33
2	1%/385 W/5 min	5.00	3.03	4.66
3	1%/700 W/3 min	5.00	2.69	3.56
4	3%/70 W/3 min	5.00	3.30	4.49
5	2%/385 W/3 min	5.00	2.63	4.69
6	2%/385 W/3 min	5.00	2.66	4.69
7	2%/70 W/1 min	5.00	3.16	6.78
8	3%/700 W/3 min	5.00	2.13	4.23
9	2%/700 W/1 min	5.00	3.04	4.66
10	1%/70 W/3 min	5.00	3.64	7.58
11	2%/385 W/3 min	5.00	2.61	4.25
12	2%/385 W/1 min	5.00	2.87	4.88
13	2%/385 W/3 min	5.00	3.51	4.71
14	2%/700 W/5 min	5.00	2.62	3.17
15	3%/385 W/5 min	5.00	1.85	2.69
16	1%/385 W/1 min	5.00	3.00	6.52
17	2%/385 W/3 min	5.00	2.62	4.69

Table 4.2b: Effect of Microwave-alkaline Pre-treatment on the Weight and Percentage of Lignin in Sugarcane Bagasse

Run	Treatment conditions	Weight (g)		% total Lignin retained
		before delignification	Weight (g) after delignification	
	Unpre-treated	5.00	5.00	21.50
1	2%/70 W/5 min	5.00	3.40	8.88
2	1%/385 W/5 min	5.00	3.15	7.07
3	1%/700 W/3 min	5.00	3.23	6.84
4	3%/70 W/3 min	5.00	3.24	9.74
5	2%/385 W/3 min	5.00	2.00	8.56
6	2%/385 W/3 min	5.00	2.85	9.70
7	2%/70 W/1 min	5.00	4.16	12.64
8	3%/700 W/3 min	5.00	2.91	6.21
9	2%/700 W/1 min	5.00	3.51	9.01
10	1%/70 W/3 min	5.00	3.85	11.35
11	2%/70 W/5 min	5.00	3.49	8.99
12	2%/385 W/1 min	5.00	3.81	10.69
13	2%/385 W/3 min	5.00	3.53	9.44
14	2%/700 W/5 min	5.00	1.96	4.90
15	3%/385 W/5 min	5.00	2.82	6.04
16	1%/385 W/1 min	5.00	3.81	11.31
17	2%/385 W/3 min	5.00	2.72	8.56

Table 4.2c: Effect of Microwave-alkaline Pre-treatment on the Weight and Percentage of Lignin in Corncob Biomass

Run	Treatment conditions	Weight (g)		% total Lignin Retained
		before delignification	Weight (g) after delignification	
	Unpre-treated	5.00	5.00	19.30
1	2%/70 W/5 min	5.00	3.92	9.11
2	1%/385 W/5 min	5.00	3.84	10.36
3	1%/700 W/3 min	5.00	3.84	8.61
4	3%/70 W/3 min	5.00	3.93	7.66
5	2%/385 W/3 min	5.00	3.42	9.61
6	2%/385 W/3 min	5.00	3.92	9.48
7	2%/70 W/1 min	5.00	3.69	13.07
8	3%/700 W/3 min	5.00	3.13	8.97
9	2%/700 W/1 min	5.00	3.71	10.52
10	1%/70 W/3 min	5.00	4.14	14.30
11	2%/70 W/5 min	5.00	3.63	9.92
12	2%/385 W/1 min	5.00	3.40	10.79
13	2%/385 W/3 min	5.00	3.11	10.48
14	2%/700 W/5 min	5.00	2.97	7.78
15	3%/385 W/5 min	5.00	2.73	6.58
16	1%/385 W/1 min	5.00	3.71	12.08
17	2%/385 W/3 min	5.00	3.23	9.65

4.1.3 Process variables and responses for microwave-alkaline pre-treatment of Agrowaste

The variable factors and the corresponding responses (percentages lignin removed, cellulose and hemicellulose retained) after microwave-alkaline pre-treatment of plantain pseudostem biomass, sugarcane bagasse, and corncob biomass are shown in Table 4.3 (a-c) respectively. After the pre-treatment of plantain pseudostem biomass (Table 4.3a) at different process conditions, the highest percentage of lignin (76.58%) was removed at run 15, the highest cellulose (65.70%) was retained at run 8 while the highest hemicellulose (25.54%) was retained at run 7. Also, as shown in Table 4.3b, for sugarcane bagasse, the highest percentage of lignin (77.2%) was removed at run 14, the highest cellulose (75.0%) was retained at run 4 while the highest hemicellulose (22.0%) was retained at run 1 and run 10. Likewise, Table 4.3c shows that after the exposure of corncob biomass to pre-treatment conditions, the highest percentage of lignin (65.9%) was removed at run 15, the highest cellulose (65.0%) was retained still at run 15 while the highest hemicellulose (34.0%) was retained at run 9 and run 16.

Table 4.3a: Process Variables and Responses for Microwave-alkaline Pre-treatment of Plantain Pseudostem Biomass

	Factor 1	Factor 2	Factor 3	Response 1	Response 2	Response 3
Run	A:NaOH Conc %	B:Power Watts	C:Reaction Time Min	Lignin removed %	Cellulose retained %	Hemicellulose retained %
1	2	70	5	53.61	61.00	21.00
2	1	385	5	59.43	63.00	16.00
3	1	700	3	69.00	55.00	21.00
4	3	70	3	60.91	60.00	25.00
5	2	385	3	59.21	62.00	18.00
6	2	385	3	59.21	61.45	17.00
7	2	70	1	41.00	60.00	25.54
8	3	700	3	63.21	65.70	13.40
9	2	700	1	59.46	59.00	20.00
10	1	70	3	34.00	62.65	21.00
11	2	385	3	63.00	59.90	19.00
12	3	385	1	57.53	65.00	20.00
13	2	385	3	59.00	60.00	17.60
14	2	700	5	72.41	61.00	16.00
15	3	385	5	76.58	59.00	18.00
16	1	385	1	43.28	53.00	23.00
17	2	385	3	59.21	60.00	20.00

Table 4.3b: Process Variables and Responses for Microwave-alkaline Pre-treatment of Sugarcane Bagasse

	Factor 1	Factor 2	Factor 3	Response 1	Response 2	Response 3
Run	A:NaOH Conc %	B:Power Watts	C:Time Mins	Lignin removed %	Cellulose retained %	Hemicellulose retained %
1	2	70	5	58.7	60	22
2	1	385	5	67.1	61	21
3	1	700	3	68.2	70	18
4	3	70	3	54.7	75	20
5	2	385	3	60.2	65	19
6	2	385	3	54.9	64	19
7	2	70	1	41.2	63	21
8	3	700	3	71.1	57	15
9	2	700	1	58.1	62	14
10	1	70	3	47.2	52	22
11	2	385	3	58.2	63	20
12	3	385	1	50.3	63	15
13	2	385	3	56.1	63	19
14	2	700	5	77.2	70	19
15	3	385	5	71.9	69	21
16	1	385	1	47.4	63	21
17	2	385	3	60.2	65	19

Table 4.3c: Process Variables and Responses for Microwave-alkaline Pre-treatment of Corncob

	Factor 1	Factor 2	Factor 3	Response 1	Response 2	Response 3
Run	A:Conc. NaOH %	B:Power Watts	C:Time Min	Lignin removed %	Cellulose retained %	Hemicellulose retained %
1	2	70	5	52.8	60	18
2	1	385	5	46.3	52	23
3	1	700	3	55.4	47	31
4	3	70	3	60.3	60	20
5	2	385	3	50.2	52	26
6	2	385	3	50.9	53	28
7	2	70	1	32.3	56	28
8	3	700	3	53.5	53	27
9	2	700	1	45.5	47	34
10	1	70	3	25.9	54	25
11	2	385	3	48.6	53	23
12	3	385	1	44.1	54	28
13	2	385	3	45.7	55	25
14	2	700	5	59.7	56	22
15	3	385	5	65.9	65	20
16	1	385	1	37.4	50	34
17	2	385	3	50.0	52	26

4.1.4 Optimal parameters for microwave-alkaline pre-treatment of agrowaste

The different criteria for the variable combinations and their responses are shown in Table 4.4 (a-c) for plantain pseudostem biomass, sugarcane bagasse and corncob biomass respectively. The run which used lowest power and lowest sodium hydroxide concentration to generate maximum percentages of cellulose and hemicellulose content while still removing optimal percentage of lignin were chosen for further studies. On this note, row 2 were selected for plantain pseudostem biomass (Table 4.4a) and sugarcane bagasse (Table 4.4b), while row 4 was selected for corncob biomass (Table 4.4c).

Table 4.4a: Some Criteria Considered for Process Optimization of Microwave-alkaline Pre-treatment of Plantain Pseudostem Biomass

S / N	FACTORS						RESPONSES		
	NaOH		Power		Time		Delignin	cellulose	H/cellulose
0	criteria	value	Criteria	value	criteria	value	Delignin	cellulose	H/cellulose
1	range	2.5	Mini	70	range	1.95	50	51	35
2	Mini	1.97	Mini	70	range	5	56	62	30
3	range	2.35	Mini	70	Max	5	62	60	22
4	Max	2.52	Mini	70	Max	4.99	55	49	32
5	range	3	Mini	70	Max	5	61	46	33
6	range	3	Mini	82.9	range	1.97	49	51	34.5
7	range	1	Range	700	Max	5	66	49	27

Table 4.4b: Some Criteria Considered for Process Optimization of Microwave-alkaline Pre-treatment of Sugarcane Bagasse Biomass

S / N	FACTORS						RESPONSES		
	NaOH		Power		Time		Delignin	cellulose	H/cellulose
0	criteria	value	Criteria	value	criteria	value	Delignin	cellulose	H/cellulose
1	range	1	Range	699	range	5	76	74	20
2	range	3	Mini	73	range	5	63	74	22
3	mini	2.3	Range	700	range	5	76	74	20
4	range	3	Mini	96	Max	5	63	74	22
5	Mini	1	Range	254	range	5	63	55	20

Table 4.4c: Some Criteria Considered for Process Optimization of Microwave-alkaline Pre-treatment of Corncob Biomass

S / N	FACTORS						RESPONSES		
	NaOH		Power		Time		Delignin	cellulose	H/cellulose
o	criteria	value	Criteria	value	criteria	value	Delignin	cellulose	H/cellulose
1	range	3	Mini	74	range	1.9	52	58	23
2	Max	3	Max	700	range	4.8	61	61	22
3	Mini	2.65	Mini	176.2	range	2.8	44	56	24
4	range	2.8	Mini	86	Max	4.4	66	64	18
5	mini	1	Range	700	range	5	59	49	24

4.1.5 Three-dimensional response surface plots for percentage delignification, cellulose and hemicellulose content of microwave-alkaline pre-treated plantain pseudostem biomass

The visual three-dimensional representation of interactive effects of the variable factors generated by design expert software is shown in Figures 4.1 (a-c) for microwave-alkaline pre-treated plantain pseudostem biomass. The colour displayed shows the values for the responses in the design space by the interactive effects of two factors when one factor is kept constant. The colour ranges from blue which was the lowest value of responses to red which was the highest value of responses observed in the design space. At microwave-alkaline pretreatment of plantain pseudostem, the minimum percentage of lignin removed was 34% while the maximum percentage of lignin removed was 76.58%; the minimum percentage of cellulose retained was 53% while the maximum percentage of cellulose retained was 65.7%; also the minimum percentage of hemicellulose retained was 13.4% while the maximum percentage of hemicellulose retained was 25.54%;

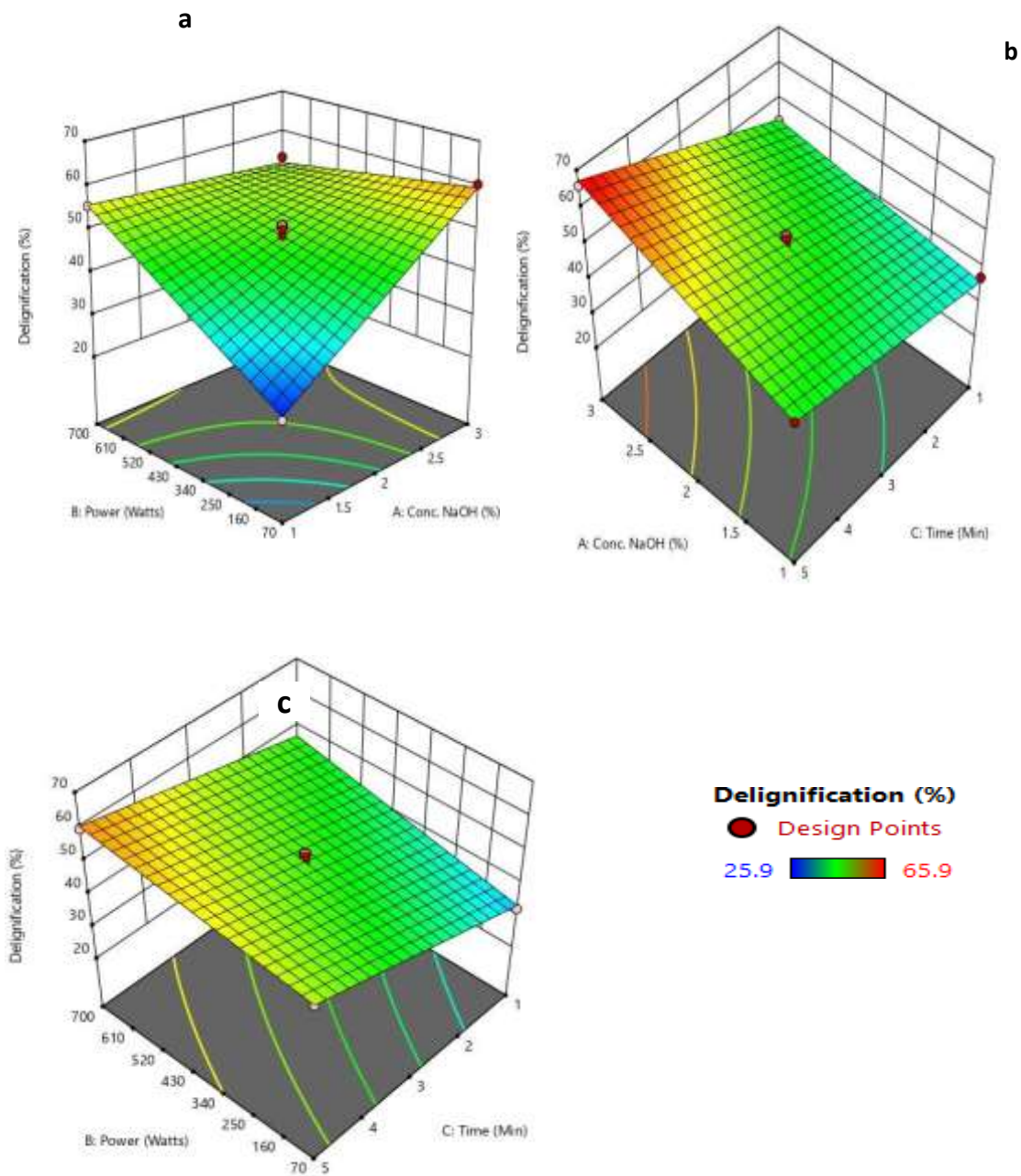


Figure 4.1a: Three-Dimensional Response Surface Plots of Plantain Pseudostem Biomass for: Percentage Delignification at (a) constant Time, (b) constant power (c) constant NaOH concentration.

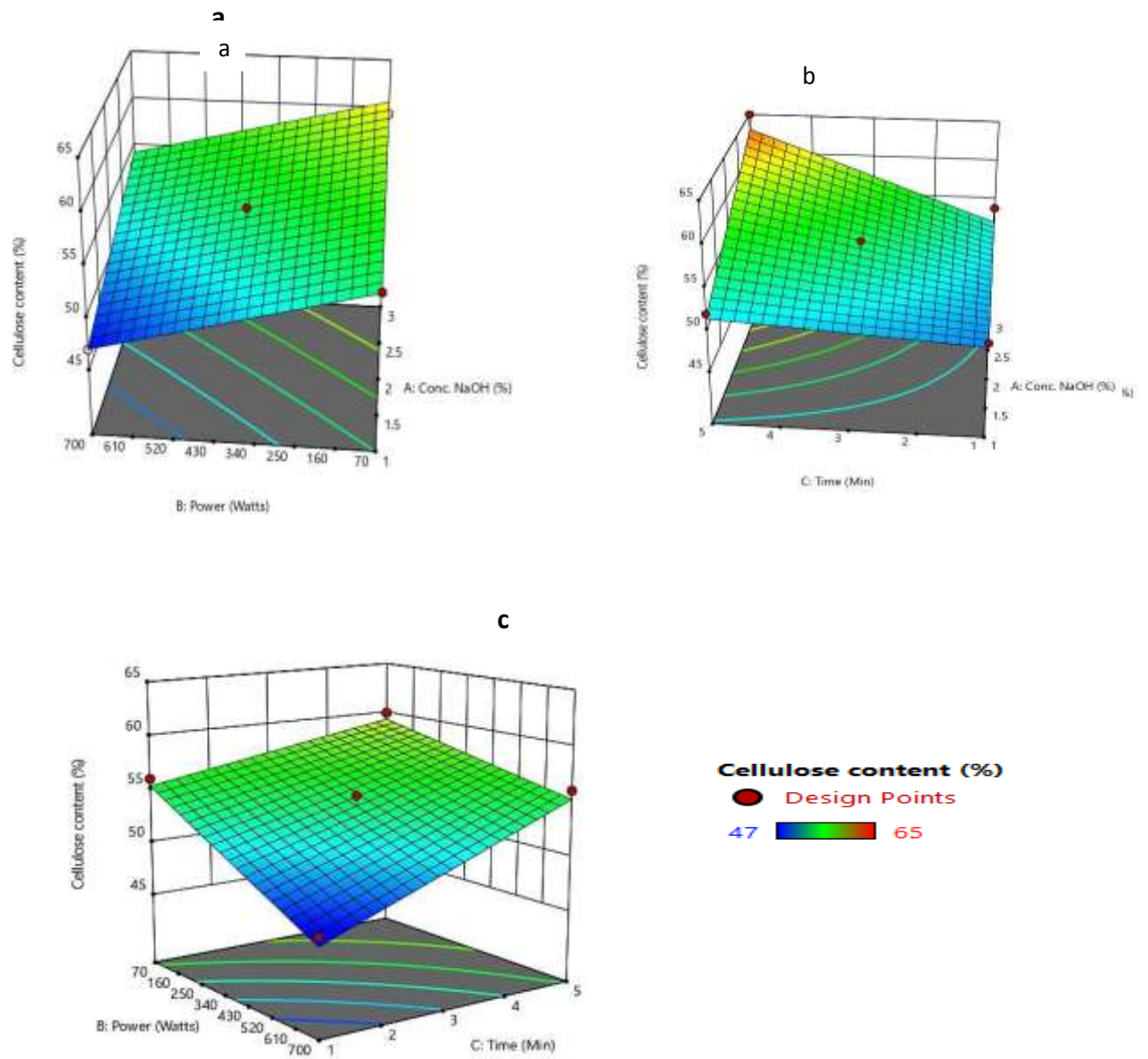


Figure 4.1b: Three-Dimensional Response Surface Plots of Plantain Pseudostem Biomass for: Percentage Cellulose Removed at (a) constant Time, (b) constant power (c) constant NaOH concentration.

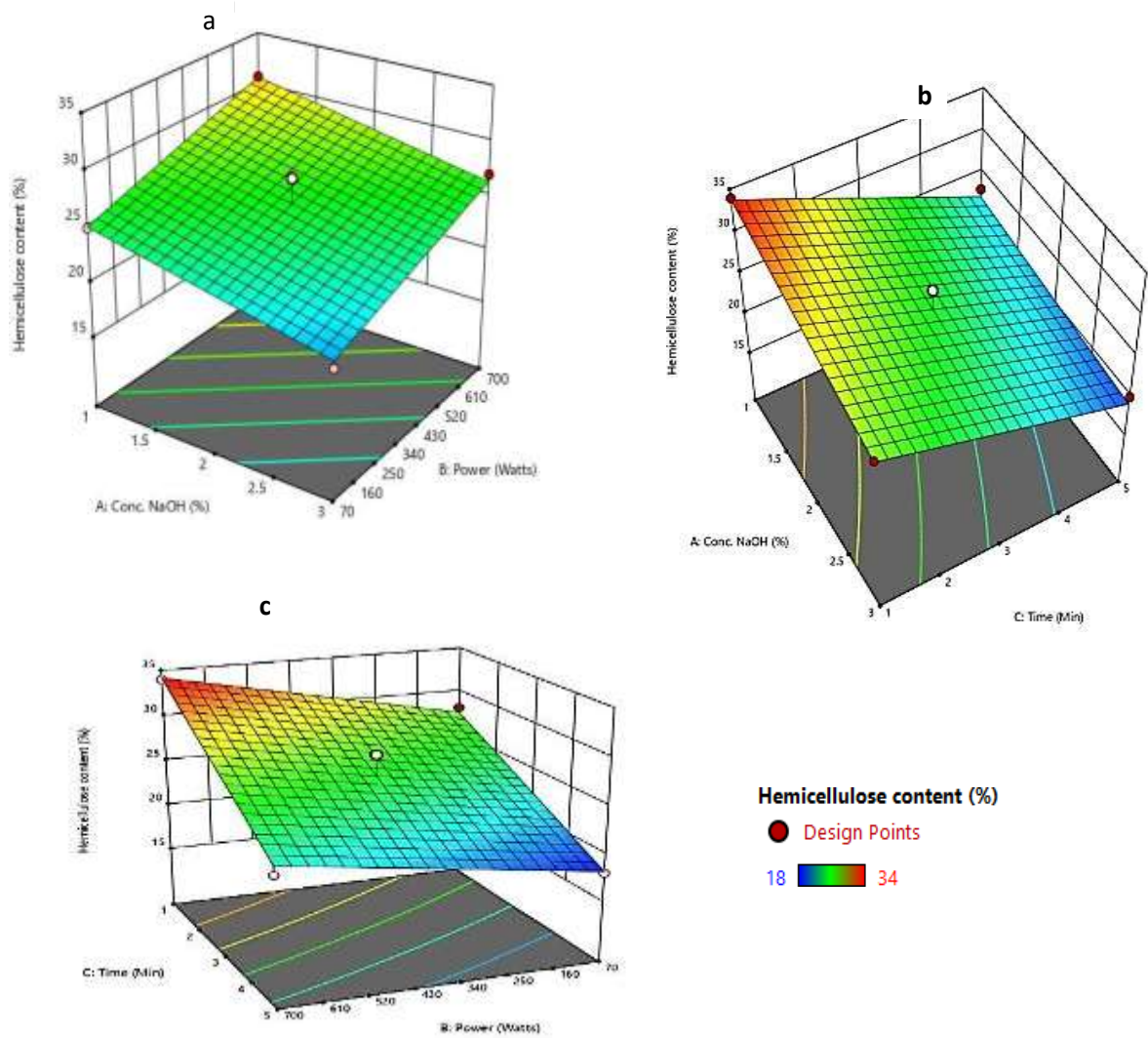


Figure 4.1c: Three-Dimensional Response Surface Plots of Plantain Pseudostem Biomass for: Percentage Hemicellulose Retained at (a) constant Time, (b) constant power (c) constant NaOH concentration.

4.1.6 Three-dimensional response surface plots for percentage delignification, cellulose and hemicellulose content of microwave-alkaline pre-treated sugarcane bagasse

The visual three-dimensional representation of interactive effects of the variable factors generated by design expert software is shown in Figures 4.2 (a-c) for microwave-alkaline pre-treated sugarcane bagasse. The colour displayed shows the values for the responses in the design space by the interactive effects of two factors when one factor is kept constant. The colour ranges from blue which was the lowest value of responses to red which was the highest value of responses observed in the design space. At microwave-alkaline pretreatment of plantain pseudostem, the minimum percentage of lignin removed was 25.9% while the maximum percentage of lignin removed was 65.9%; the minimum percentage of cellulose retained was 47% while the maximum percentage of cellulose retained was 65%; also the minimum percentage of hemicellulose retained was 18% while the maximum percentage of hemicellulose retained was 34%;

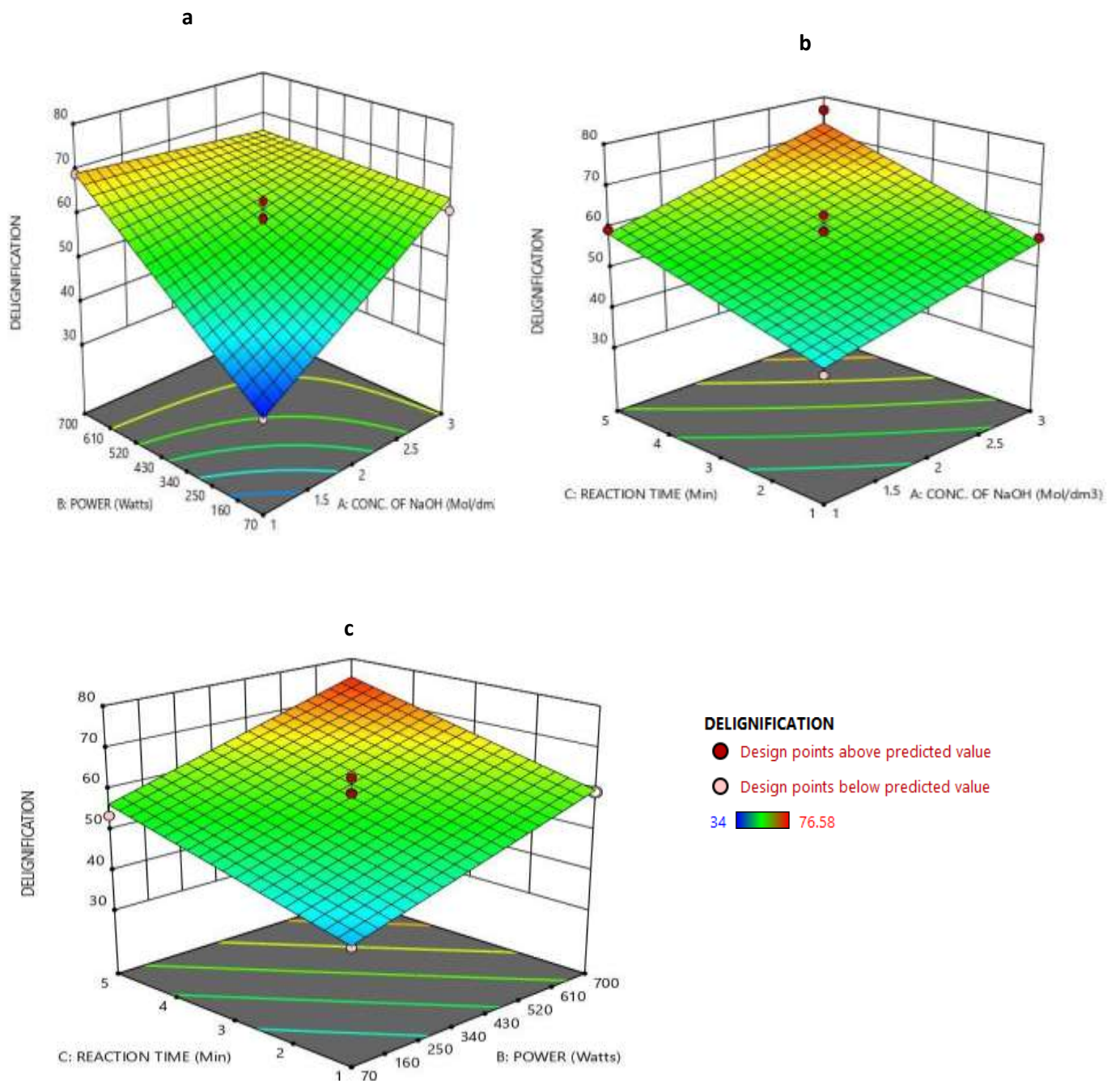


Figure 4.2a: Three-Dimensional Response Surface Plots of Sugarcane Bagasse for: Percentage Delignification at (a) constant Time, (b) constant power (c) constant NaOH concentration.

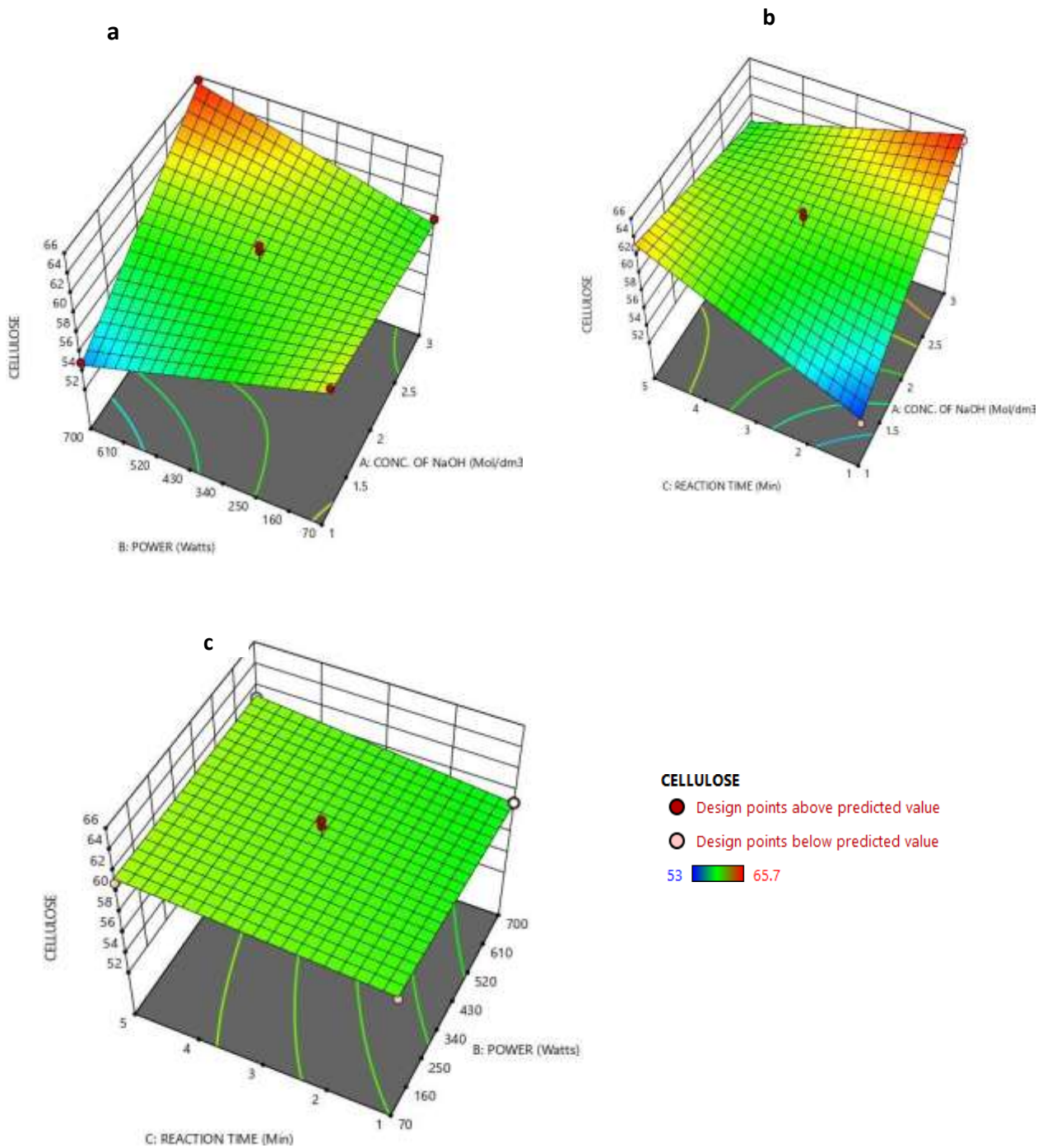


Figure 4.2b: Three-Dimensional Response Surface Plots of Sugarcane Bagasse for: Percentage Cellulose Removed at (a) constant Time, (b) constant power (c) constant NaOH concentration.

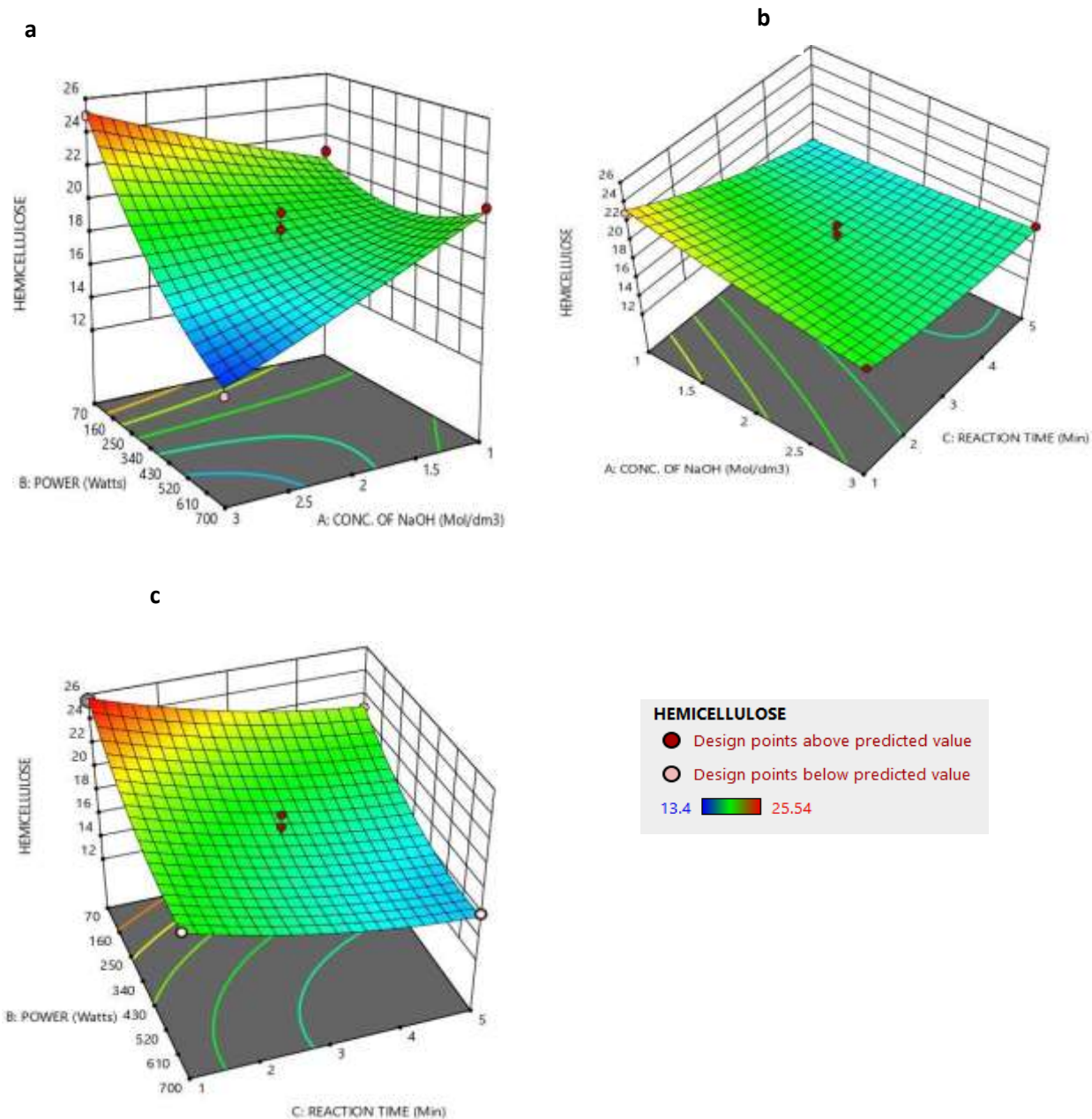


Figure 4.2c: Three-Dimensional Response Surface Plots of Sugarcane Bagasse Biomass for: Percentage Hemicellulose Retained at (a) constant Time, (b) constant power (c) constant NaOH concentration.

4.1.7: Three-dimensional response surface plots for percentage delignification, cellulose and hemicellulose content of microwave-alkaline pre-treated corncob biomass

The visual three-dimensional representation of interactive effects of the variable factors generated by design expert software is shown in Figures 4.3 (a-c) for microwave-alkaline pre-treated corncob biomass. The colour displayed shows the values for the responses in the design space by the interactive effects of two factors when one factor is kept constant. The colour ranges from blue which was the lowest value of responses to red which was the highest value of responses observed in the design space. At microwave-alkaline pretreatment of plantain pseudostem, the minimum percentage of lignin removed was 34% while the maximum percentage of lignin removed was 76.58%; the minimum percentage of cellulose retained was 52% while the maximum percentage of cellulose retained was 75%; also the minimum percentage of hemicellulose retained was 14.4% while the maximum percentage of hemicellulose retained was 22%;

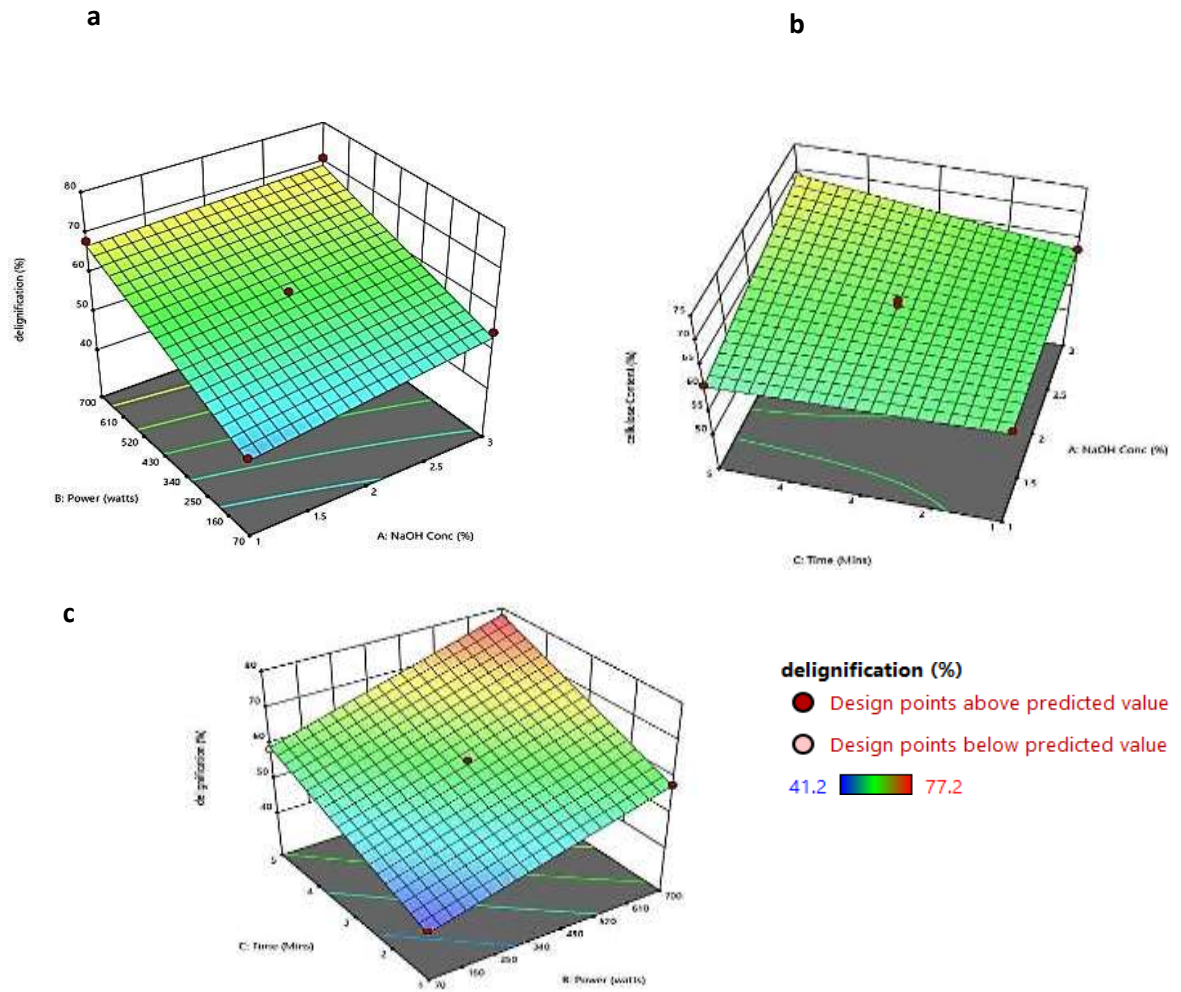


Figure 4.3a: Three-Dimensional Response Surface Plots of Corncob Biomass for: Percentage Delignification at (a) constant Time, (b) constant power (c) constant NaOH concentration.

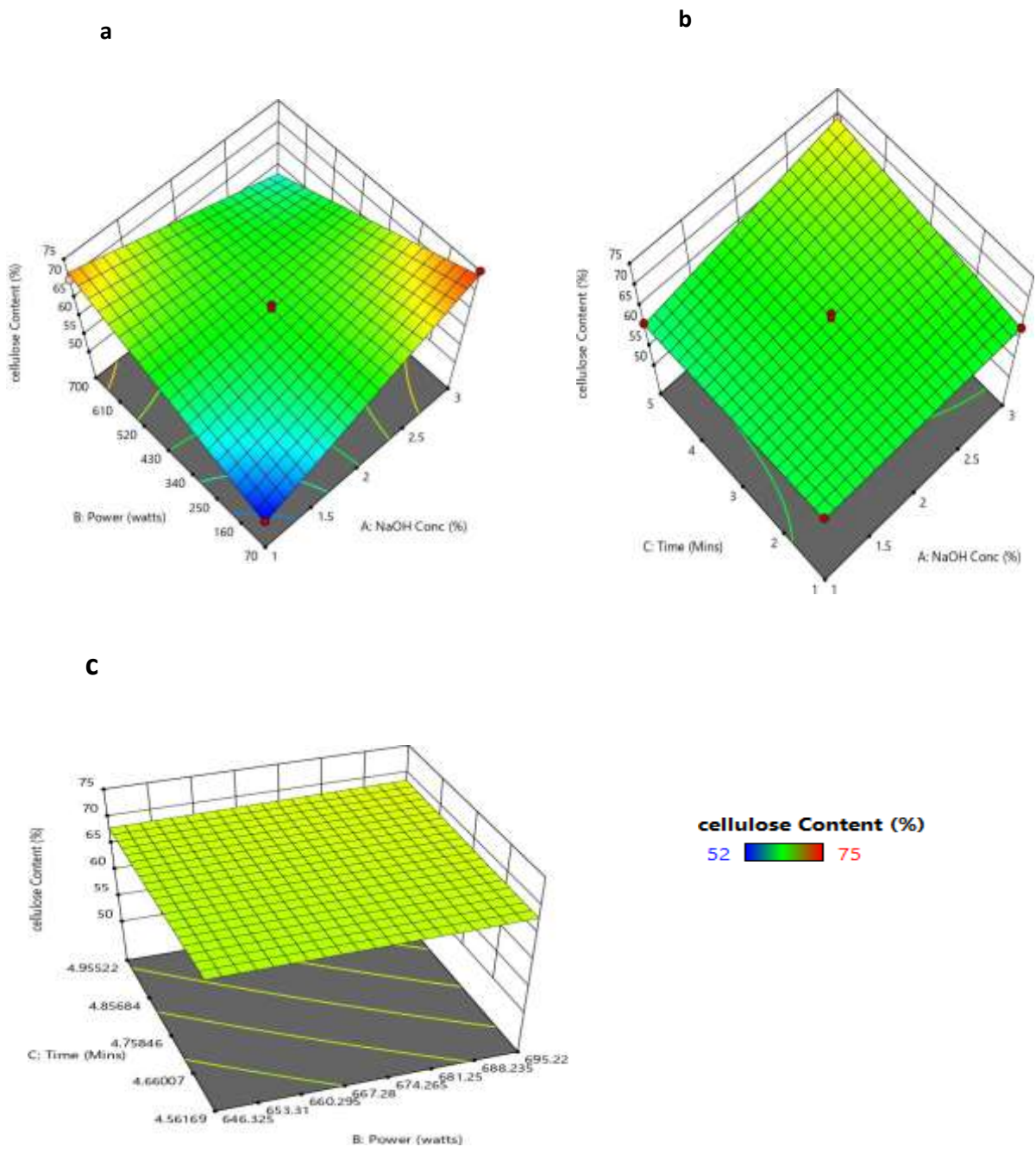


Figure 4.3b: Three-Dimensional Response Surface Plots of Corncob Biomass for: Percentage Cellulose Retained at (a) constant Time, (b) constant power (c) constant NaOH concentration

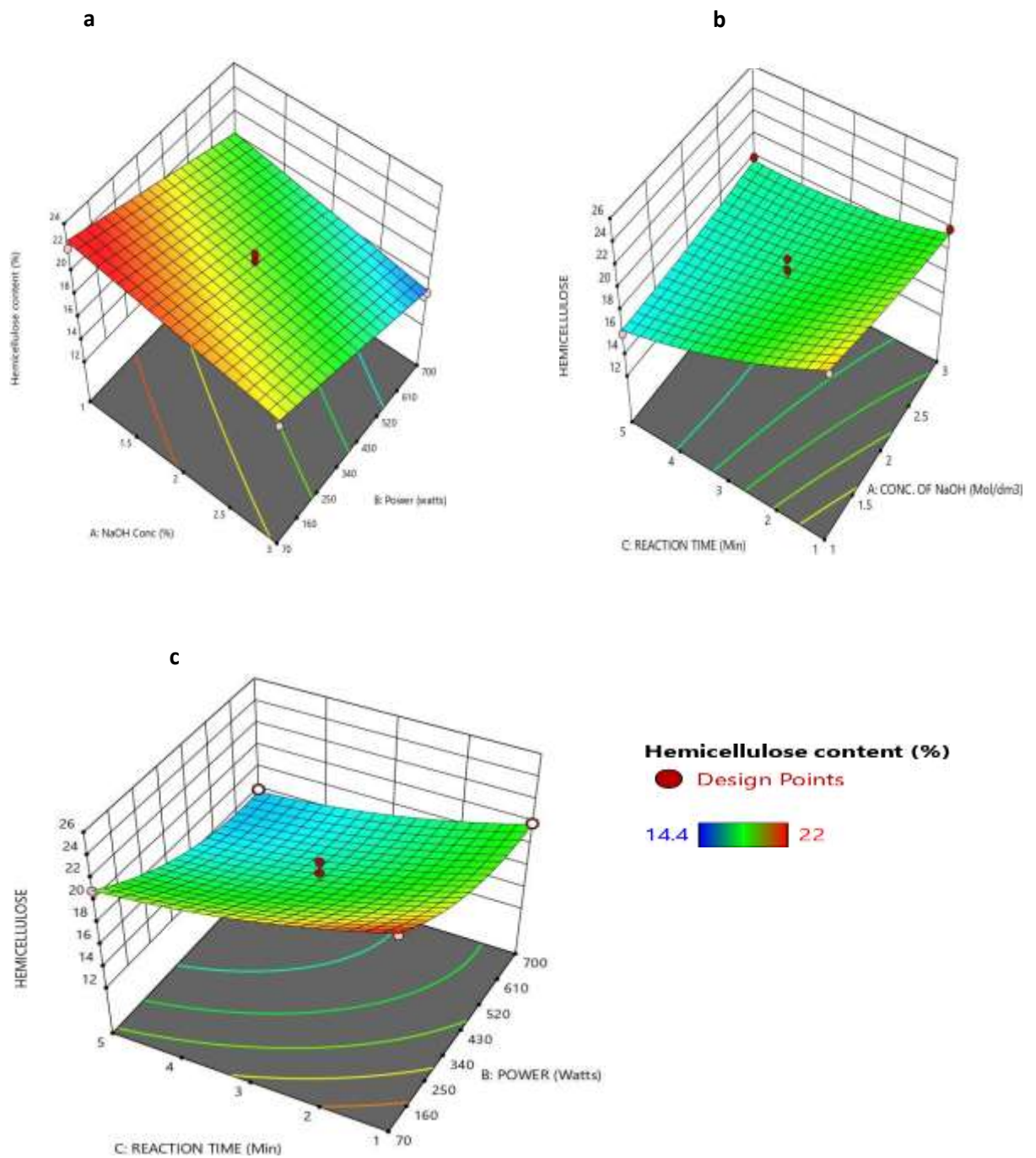


Figure 4.3c: Three-Dimensional Response Surface Plots of Corncob Biomass for: Percentage Cellulose Retained at (a) constant Time, (b) constant power (c) constant NaOH concentration

4.1.8 X-Ray Diffraction Pattern of the untreated and treated agrowastes

X-ray Diffraction of both untreated and treated agrowastes are shown in Figure 4.4 - 4.6 for plantain pseudostem biomass, sugarcane bagasse and corncob biomass respectively. The Bragg angles of 16° , 22° and 35° are characteristics of crystalline region which are located on the lattice plane of $\bar{1}01$, $\bar{1}11$ and $[002]$ respectively. The diffraction peak intensities for the samples in the present study were more distinct at $2\theta = 16.87^\circ$, 22.5° and 35.2° for both treated and untreated plantain pseudostem biomass (Figure 4.4), while the peak intensities were more distinct at $2\theta = 16.25^\circ$, 22.22° and 34.9° for both treated and untreated sugarcane bagasse (Figure 4.5). Also, the diffraction peak intensities of treated and untreated corncob biomass (Figure 4.6) were more distinct at $2\theta = 16.02^\circ$, 21.85° and 35.54° . However, the pre-treated samples had a higher intensity at these regions.

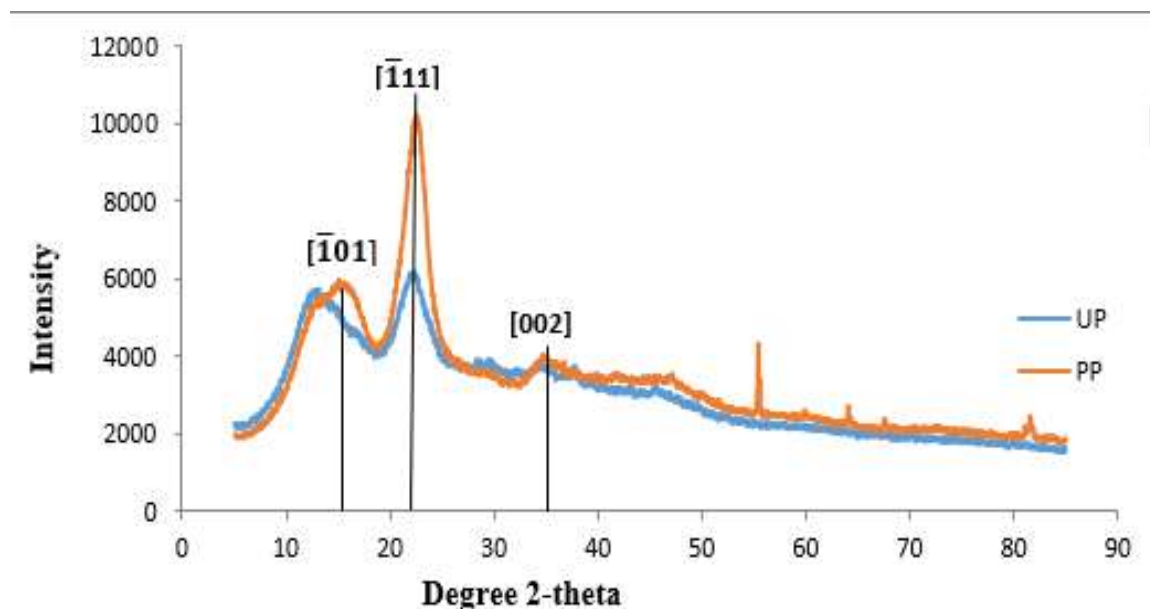


Figure 4.4: X-Ray Diffraction Pattern of the untreated (UP) and pre-treated plantain (PP)

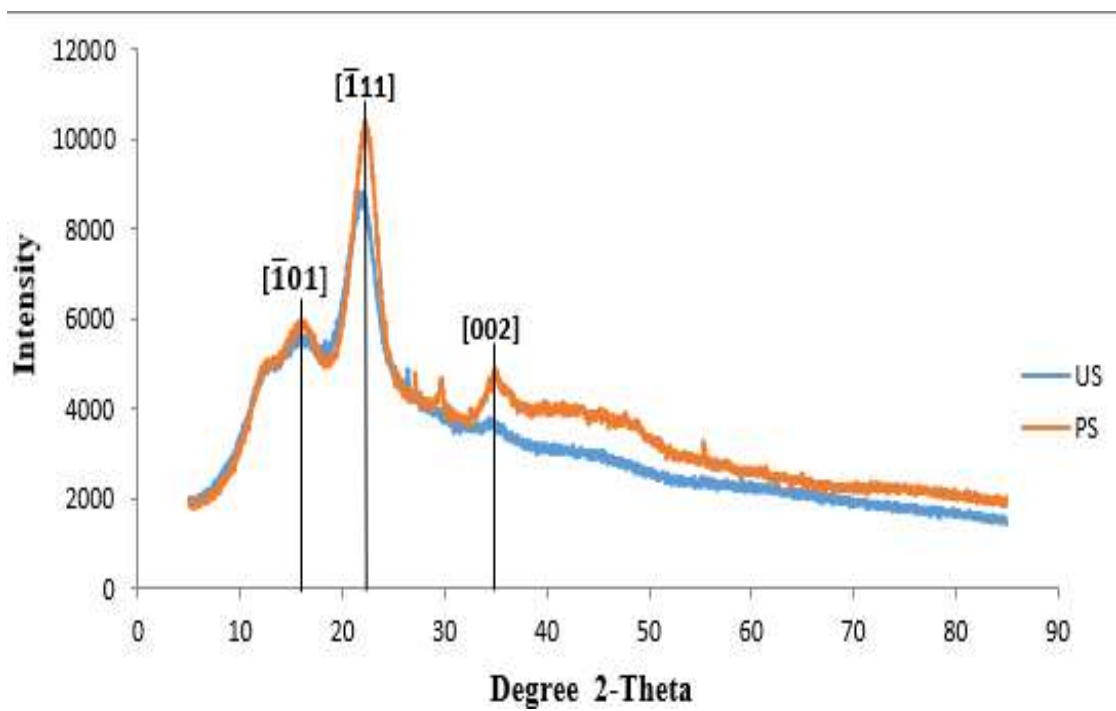


Figure 4.5: X-Ray Diffraction Pattern of the Untreated (US) and Pre-treated Sugarcane Bagasse (PS)

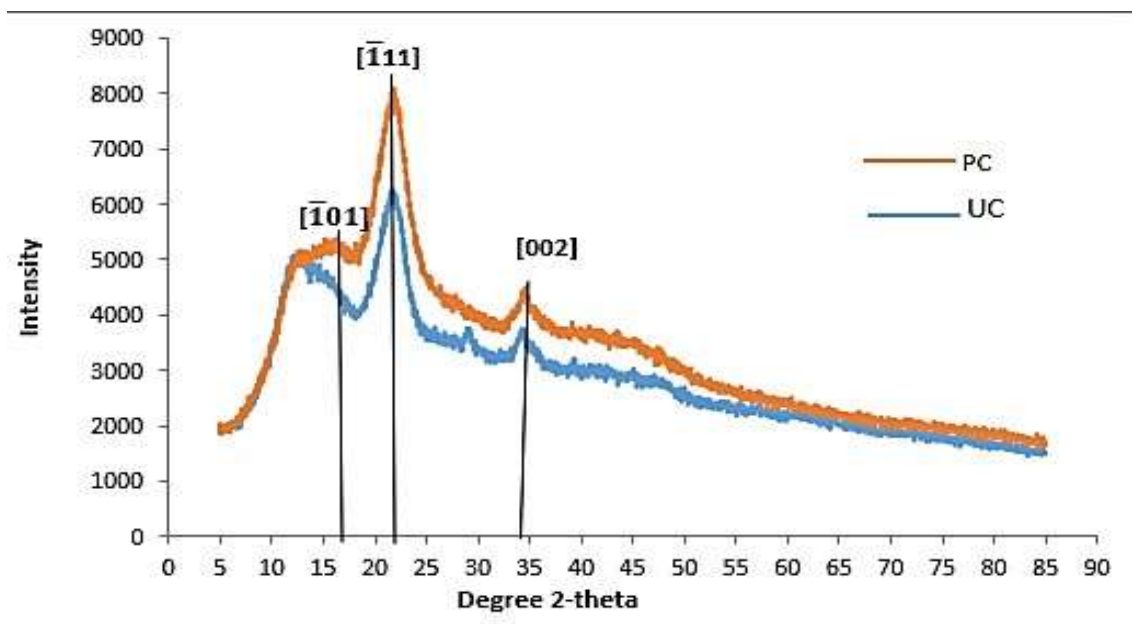


Figure 4.6: X-Ray Diffraction Pattern of the Untreated (UC) and Pre-treated Corncob Biomass (PC)

4.1.9 Infrared Spectra of the untreated and treated agrowaste samples

Infrared spectrum was observed in the range of $500\text{ cm}^{-1} - 4000\text{ cm}^{-1}$ to determine the functional groups present in pre-treated and untreated agrowaste samples as shown in Figures 4.7, 4.8, and 4.9 for plantain pseudostem biomass, sugarcane bagasse and corncob biomass respectively. The spectra wavelength in Figures 4.7, shows that the unpre-treated plantain pseudostem had a wider range of values from $711.5\text{ to }3954.2\text{ cm}^{-1}$ while the pre-treated plantain pseudostem biomass indicated a shorter range of values from $1571\text{ and }3954.2\text{ cm}^{-1}$ also, in Figures 4.8, the spectra wavelength of the untreated sugarcane bagasse showed wider range from $626.2\text{ to }3980\text{ cm}^{-1}$ while the treated sugarcane bagasse had shorter range of wavelength between $1119.5\text{ and }3980\text{ cm}^{-1}$, likewise, in Figures 4.9, the spectra wavelength of the unpre-treated corncob biomass showed wider range from $626.2\text{ to }3998.2\text{ cm}^{-1}$ while the pre-treated corncob biomass had shorter range of wavelength between $994.5\text{ and }3998.2\text{ cm}^{-1}$. Also, a higher absorbance intensity was observed in the spectra of the pre-treated agrowastes than the untreated samples.

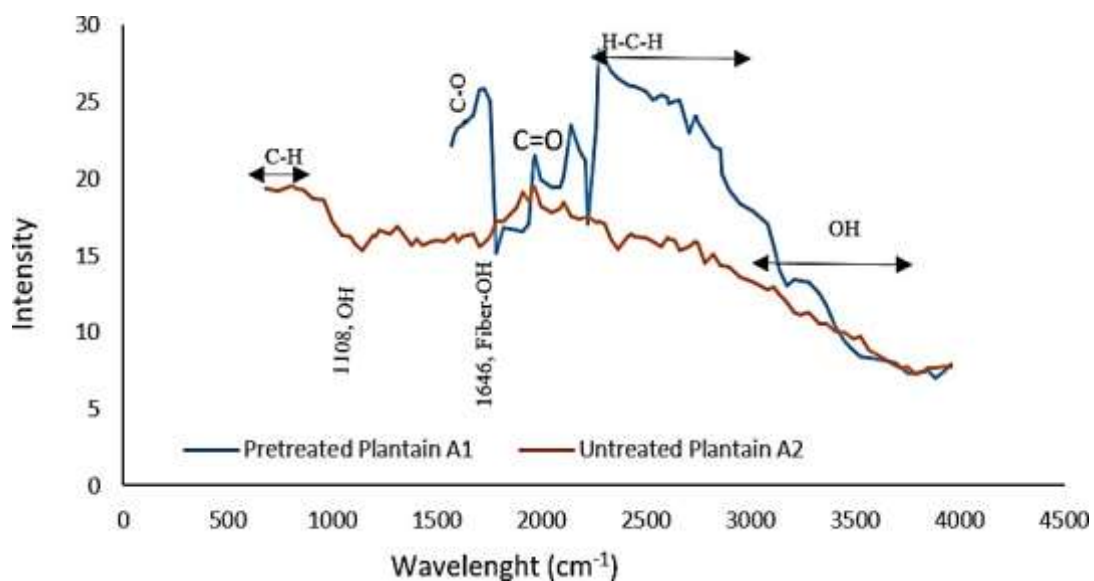


Figure 4.7: Infrared Spectra of the Untreated and Treated Plantain Pseudostem Biomass

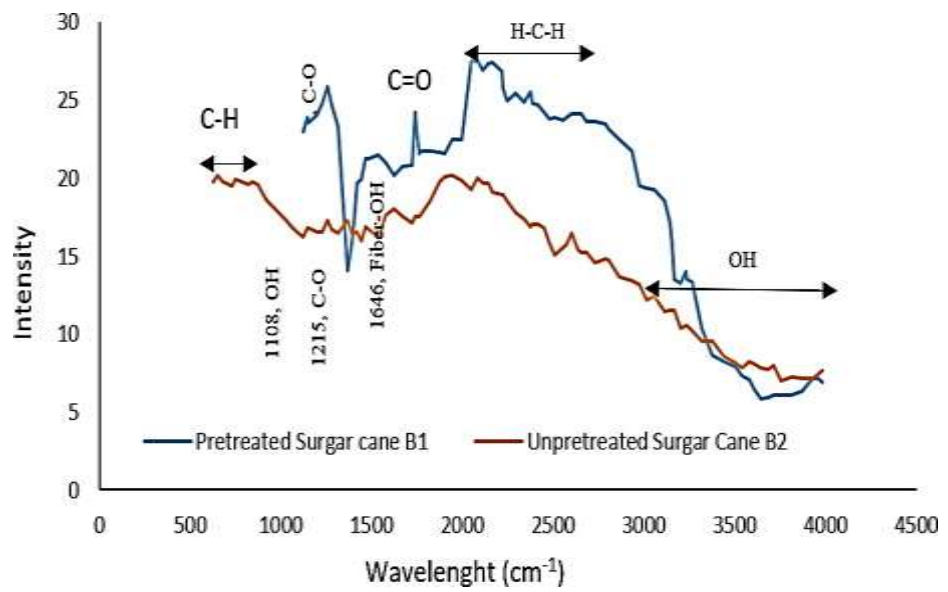


Figure 4.8: Infrared Spectra of the Untreated and Treated Sugarcane Bagasse

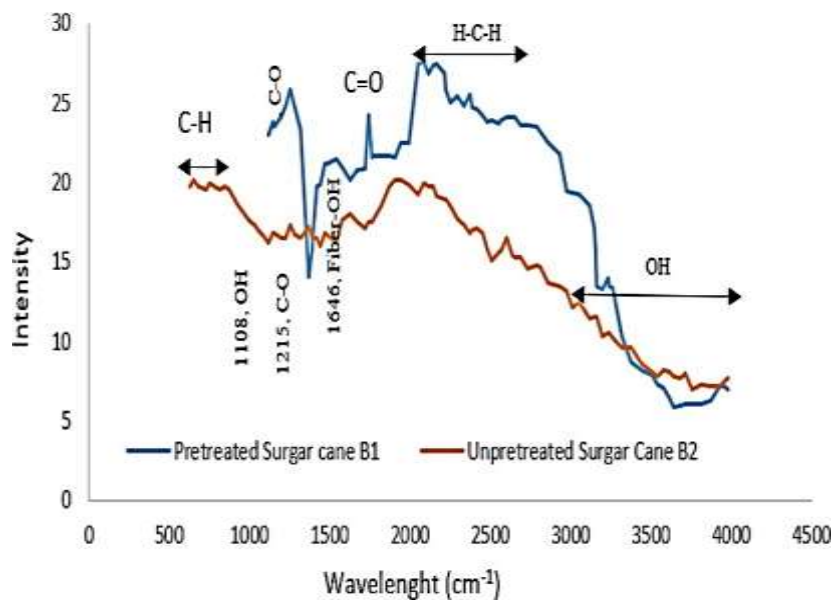


Figure 4.9: Infrared Spectra of the Untreated and Treated Corncob Biomass

4.1.10: Scanning Electron Microscopy of pre-treated and untreated agrowastes

The SEM images of both treated and untreated plantain pseudostem biomass, sugarcane bagasse and corncob biomass, are presented in Plate 4.1- 4.3 respectively. Microwave-alkaline pre-treatment of corncob, plantain pseudostem biomass and sugarcane bagasse resulted into a porous and smoother surface apparently eliminating the rough external surface. The structure becomes loose and less compact when compared to the untreated samples.

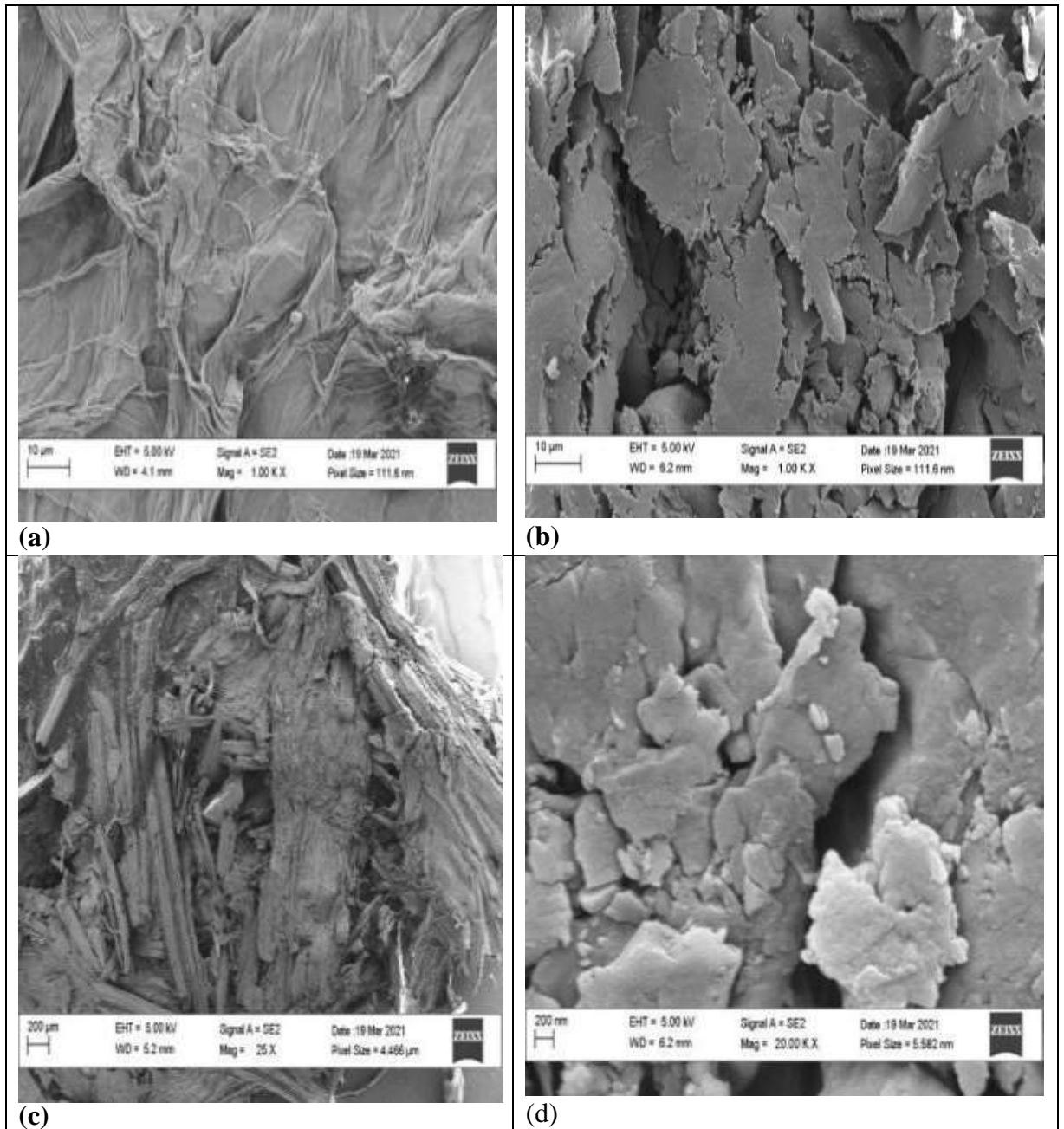


Plate 4.1: Scanning Electron Micrograph of Plantain Pseudostem Biomass for (a) unpre-treated sample at magnification of 10 μm; (b) pre-treated sample at Magnification of 10 μm; (c) unpre-treated sample at Magnification of 200 μm; (d) pre-treated sample at Magnification of 200 μm.

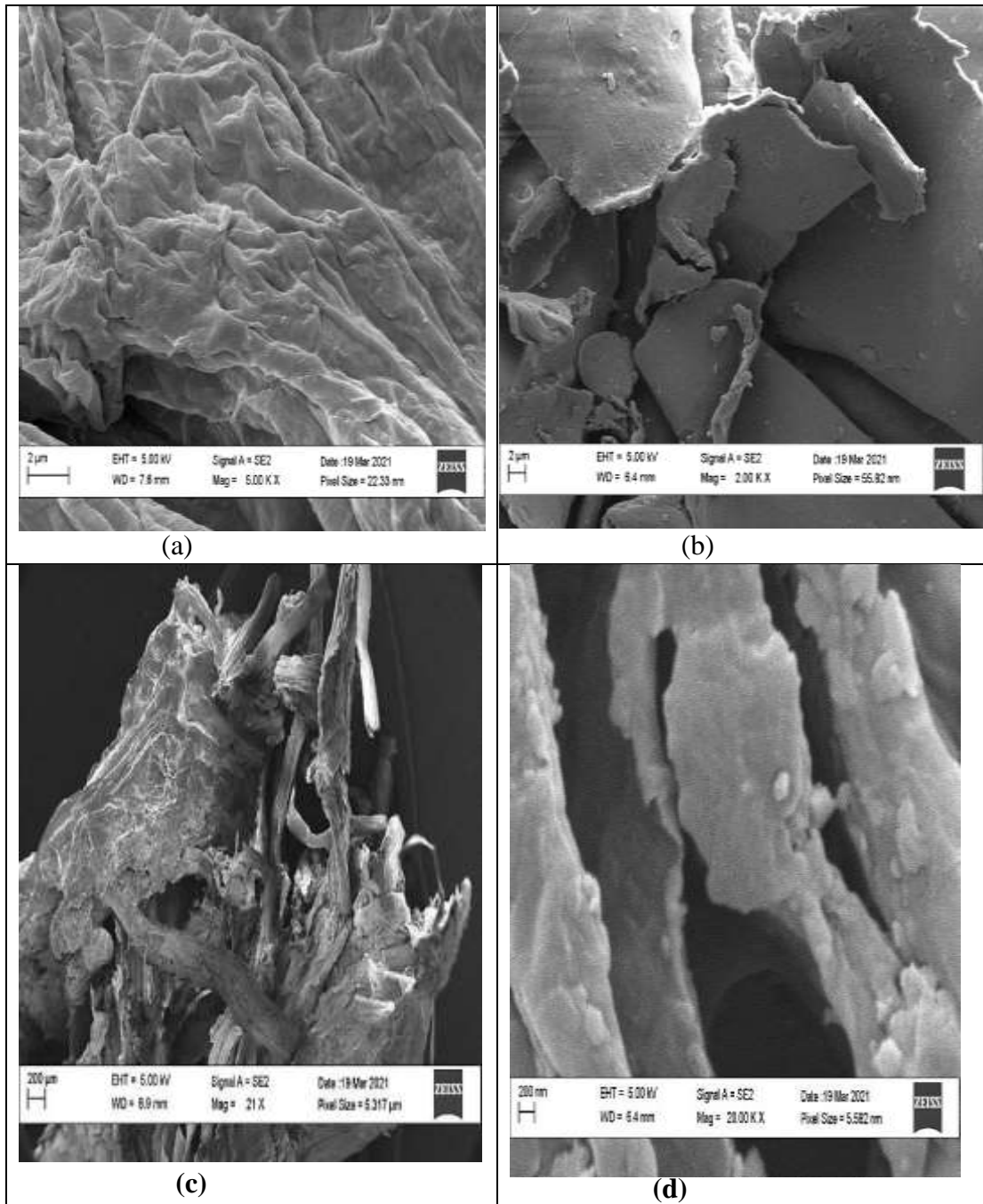
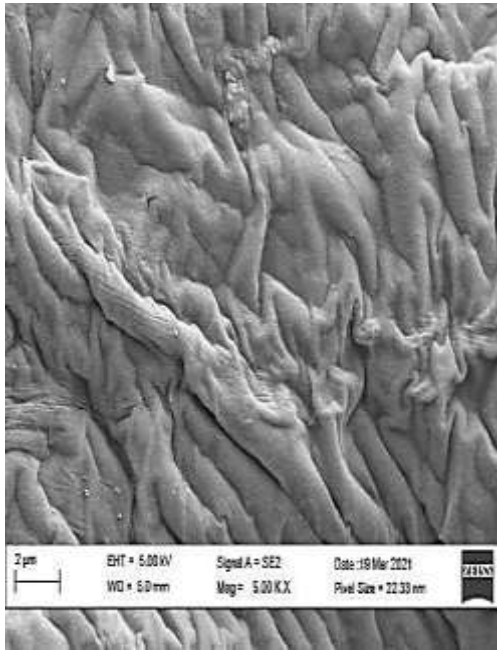
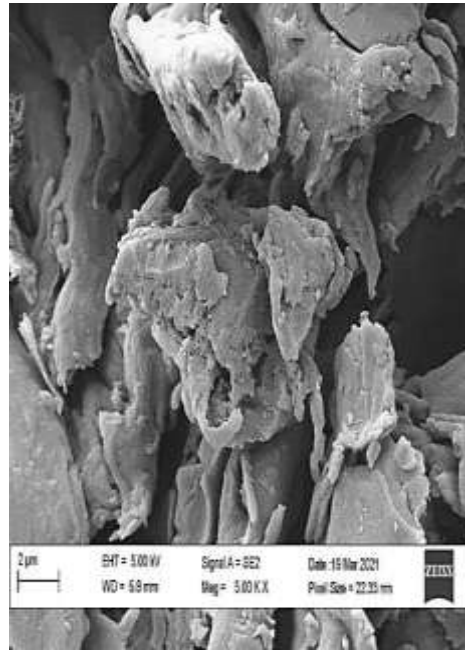


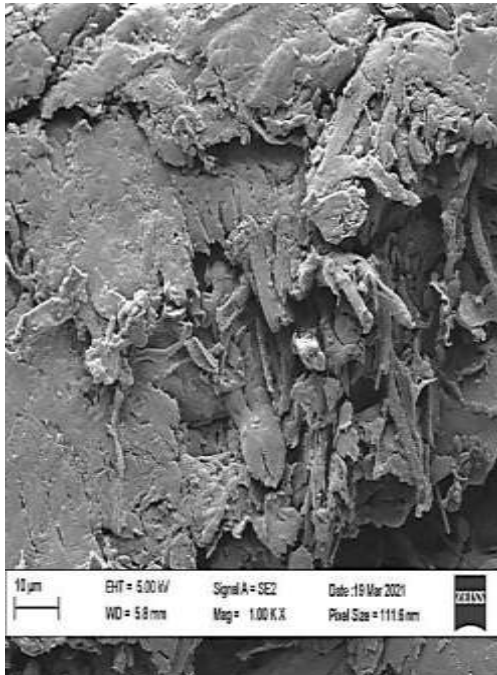
Plate 4.2: Scanning Electron Micrograph of Sugarcane Bagasse for (a) unpre-treated sample at magnification of 10 μm ; (b) pre-treated sample at Magnification of 10 μm ; (c) unpre-treated sample at Magnification of 200 μm ; (d) pre-treated sample at Magnification of 200 μm .



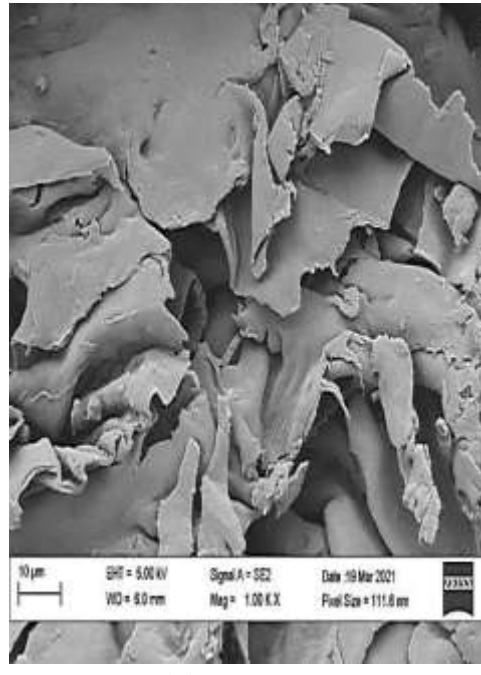
(a)



(b)



(c)



(d)

Plate 4.3: Scanning Electron Micrograph of Corn cob Biomass for (a) unpre-Treated sample at magnification of 10 μm ; (b) pre-treated sample at Magnification of 10 μm ; (c) unpre-treated sample at Magnification of 200 μm ; (d) pre-treated sample at Magnification of 200 μm .

4.1.11 Organisms and substrate for enzyme production and fermentation process

Organisms isolated from different soil sources for the production of enzymes and fermentation process are shown in Table 4.5. The macroscopic and microscopic features are also highlighted led to the suggested names for the organisms

Table 4.5: Macroscopic and Microscopic Features of Microorganisms Isolated for Enzyme Production

S/ N	Isolate code	Sample site	Macroscopic Features on SDA	Microscopic Features	Suggested organisms
1	CC1	corn cob dump	Produce a flat, cottony colony proceeding from a central button	Grape-like clusters of round microconidia, spiral hyphae in some culture	<i>Trycophyton sp</i>
2	PS2	plantain stem dump	Develops whitish black flat velvety growth.	Tear-shaped microconidia	<i>Trycophyton sp</i>
3	RH3	plantain stem dump	Whitish Fissured button-like centre velvety growth	Clusters of microconidia cigar shaped macroconidia	<i>Trycophyton sp</i>
4	SB4	sugarcane waste dumpsite ;	Produces white soft Fast growing cottony growth	Hyphal swelling, chlamydo spores, favic chandelier	<i>Trycophyton sp</i>
5	RD5	refuse dump	Growth is initially white but they change to black after a few days.	the conidial heads are radiate with conidiogenous cells biseriate. Conidia brown	<i>Aspergillus sp</i>
6	RH6	plantain stem dump	Produces a cottony growth, brown centre with white periphery	Distorted hyphae, conidia rare	<i>Trycophyton sp</i>
7	RH7	plantain stem dump	Fast growing, white cottony growth which turns brownish after 5 days	Non septate globular sporangia	<i>Mucor sp</i>
8	SW8	sewage sludge	Growth is initially white but they change to black after a few days	the conidial heads radiate with conidiogenous cells biseriate. Conidia brown	<i>Aspergillus sp</i>

S/N	Isolate code	Sample site	Macroscopic Features on SDA	Microscopic Features	Suggested organisms
9	RD9	refuse dump	Produces white soft velvety colonies that turn yellowish-green after 4 days	The conidial heads radiate with conidiogenous cells biseriate. Conidia brown	<i>Aspergillus sp</i>
10	FBL	sewage sludge	produces white soft fluffy colonies that turn yellowish-green after 4 days	Dark conidia heads with septate hyphae	<i>Aspergillus sp</i>
11	PS11	plantain stem dump	growth is initially white but they change to black after a few days. The edges of the colonies appear pale yellow.	The conidial heads are radiate with conidiogenous cells biseriate. Conidia brown	<i>Aspergillus sp</i>
12	CC12	corn cob dump	Velvet, short fluffy centre. Centre has intertwining fold with brownish periphery <u>finely fringed</u>	Distorted hyphae, conidia rare	<i>Trycophyton sp</i>

Table 4.6: Macroscopic and Microscopic Features of Microorganisms Isolated for Fermentation Process

S/N	Sample code	Sample site	Macroscopic Features on SDA	Microscopic Features	Suggested organisms
1	PW1	Palm wine	Confluent colonies, with shine surface and light yellow, sticky consistency.	Ovoid and spherical cells, with no forming filaments. Unipolar bud. Singular and grouped cells.	Yeast
2	PW2	Palm wine	Glossy colonies with cream-white colour with full edge and convex profile, sticky consistency	Ovoid cells with filamentous elements. Linear and branched filaments.	Yeast
3	PW3	Palm wine	White and non-shiny colonies, adherent to the medium, sticky consistency	Oval cells with various sizes. Isolated or grouped in small clusters.	Yeast
4	PP	Fermented food;	Oval knob-like cream consistent surface.	Oval cells without filaments. Unipolar bud. Isolated or grouped in small clusters	Yeast
5	T	Termite hill soil	Whitish Colonies grow rapidly to fill the plate with peripheral part growth sticky to the surface and turned yellowish brown within 4 days	Stolons and pigmented rhizoids	Rhizopus
6	PP1	Fermented food	Fast growing, brown cottony growth which turns wavy as it matures after 5 days	Non septate globular sporangia	Mucor
7	RB3	Rice bran dump site	Fast growing, white cottony growth which turns blackish after 5 days	Non septate globular sporangia	Mucor
8	RB2	Rice bran dump site	Fast growing, white cottony growth which turns blackish and wavy after 5 days	Non septate globular sporangia	Mucor
9	RB6	Rice bran dump site	Fast growing, white cottony growth.	Non septate globular sporangia	Mucor

4.1.12: The hydrolytic zone of clearance observed on agar plates prepared with different agrowaste substrates

The hydrolytic zone of clearance observed on agar plates prepared with different agrowaste substrates (corn cob biomass (CC), sugarcane bagasse (SB) and plantain pseudostem biomass (PS)) as well as carboxyl methyl cellulose (CMC) and xylan is shown in Plate 4.4. Congo red dye combine with polysaccharides to form orange colour. Hydrolytic enzymes produced by organisms converts polysaccharides to monosaccharides which cannot combine with Congo red dye. Therefore, a zone of clearance is formed. The more the cleared area the better the potential of the organisms to produce hydrolytic enzyme. The diameter of the zone of clearance is shown in Table 4.7. Organisms RD5 and FBL had the best hydrolytic zone of clearance on plantain pseudostem agar plate and sugarcane bagasse agar plate respectively.

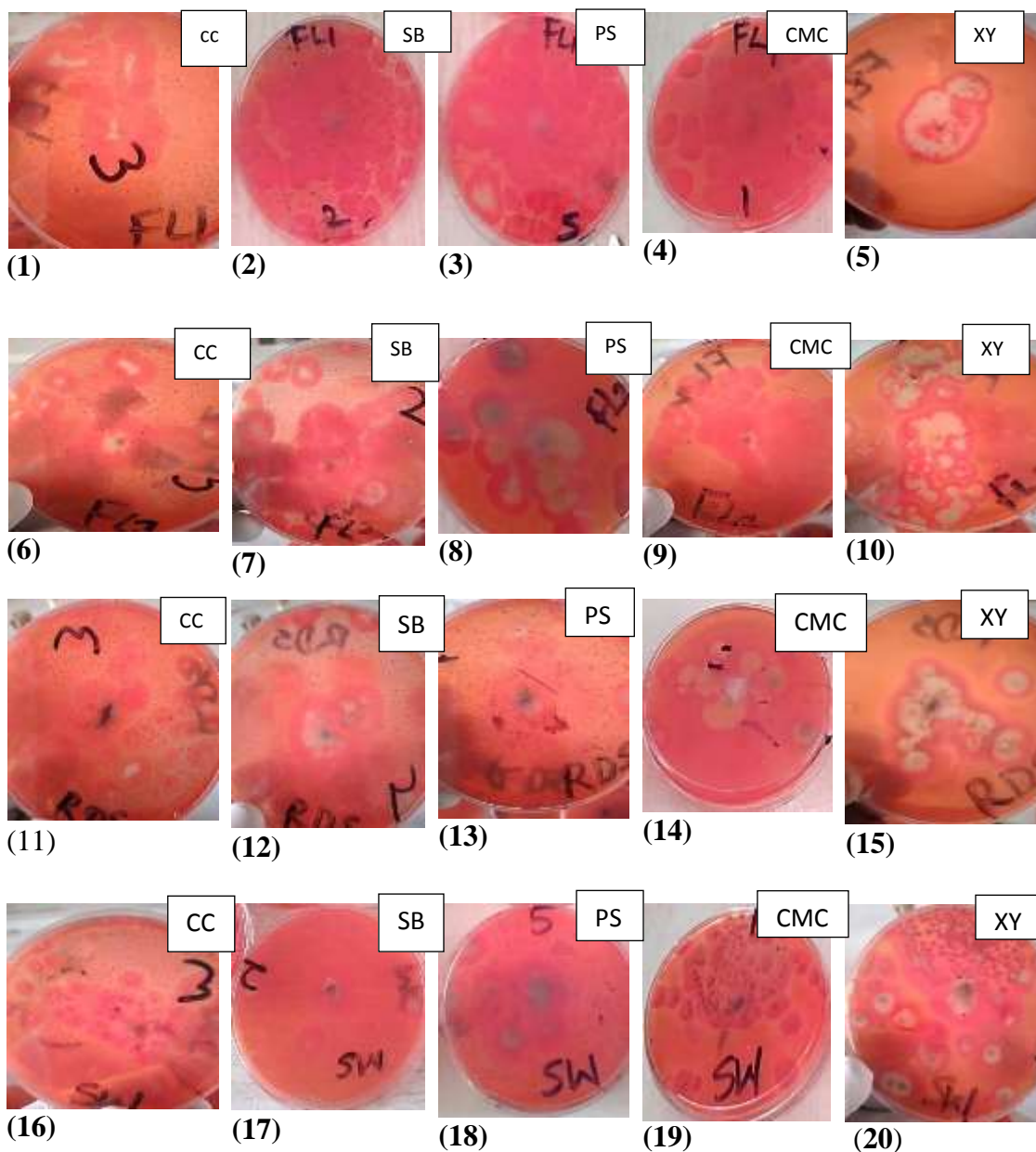


Plate 4.4: Hydrolytic zone of Clearance of Organisms on Agar Plate Prepared with Different Substrate after Staining with Congo Red.

1–5 : Hydrolytic zone of Clearance of **RD9**: isolate from refuse dump site;

6–10: Hydrolytic zone of Clearance of **FBL** isolate from sewage sludge;

11–15: Hydrolytic zone of Clearance of **SW8** isolate from sewage sludge;

16–20: Hydrolytic zone of Clearance of **RD5** isolate from refuse dump site.

CC: corncob; **SB:** sugarcane bagasse; **PS:** plantain pseudostem biomass; **CMC:** carboxyl methyl cellulose; **XY:** xylan.

Table 4.7: Dimensions of Hydrolytic Zones formed by Four Organisms Cultivated on Different Substrates in Congo Red Agar Plate

Substrate	Dimensions (millimeters) of hydrolytic zones			
	Organisms			
	SW8	FBL	RD9	RD5
Xylan	3.5	2.5	1.6	3.1
Carboxyl Methyl Cellulose	0.9	1.5	0.9	1.5
Corncob biomass	1.4	1.0	0.6	1.2
Plantain pseudostem biomass	1.0	1.1	0.6	2.5
Sugarcane bagasse	2.5	2.7	0.7	2.3

4.1.13: Activity of cellulase produced by different microorganism isolated from soil using three agrowaste as carbon source

The quantity of cellulase produced by each organism for five days is shown in Table 4.8. In comparing the highest enzyme activity for each of the carbon sources, when sugarcane bagasse (SB) was used as carbon source, cellulase with the highest activity (15.35 ± 0.48) was produced by FBL on the 2nd day. This was followed by the activity (8.08 ± 0.13) of the cellulase produced by RD9 when plantain pseudostem (PS) was used as carbon source on the 2nd day, and then followed by the activity (6.95 ± 0.08) of the enzyme produced by FBL when standard commercial substrate (CMC) was used as carbon source on the 5th day, while enzyme with lowest activity (5.53 ± 0.04) was produced on the 4th day by SW8 when corncob biomass was used as carbon source.

Table 4.8: Activity of Cellulase Produced by Different Microorganisms Isolated from Soil Using Three Agrowastes as Carbon Sources

Carbon Sources	Organisms	Cellulase Activities (IU/mL)				
		DAY 1	DAY 2	DAY3	DAY4	DAY 5
Carboxyl methyl cellulose	RD9	2.58±0.11	3.81±0.12	3.75±0.01	3.86±0.13	3.21±0.12
	FBL	2.86±0.02	4.20±0.12	4.00±0.08	3.56±0.08	6.95±0.12
	SW8	2.90±0.01	4.22±0.23	5.14±0.25	6.09±0.13	4.21±0.06
	RD5	2.88±0.02	3.82±0.02	4.31±0.15	4.26±0.11	2.85±0.26
Plantain pseudostem	RD9	5.77±0.01	8.08±0.13	4.81±0.01	4.22±0.11	3.12±0.13
	FBL	3.26±0.12	3.98±0.06	5.45±0.11	7.64±0.11	5.57±0.12
	SW8	2.91±0.11	4.51±0.01	4.40±0.12	5.66±0.11	4.38±0.06
	RD5	5.54±0.25	7.78±0.36	5.97±0.06	5.66±0.06	3.39±0.11
Sugarcane Bagasse	RD9	6.59±0.12	11.81±1.05	4.39±0.12	7.53±0.14	2.80±0.14
	FBL	12.12±0.15	15.35±0.48	9.62±2.08	4.41±0.34	5.45±0.75
	SW8	13.40±0.25	15.37±0.70	9.24±1.49	7.69±0.14	4.53±0.04
	RD5	9.19±0.11	13.82±0.00	5.73±0.14	7.84±0.46	3.48±0.04
Corncob	RD9	4.11±0.23	4.36±0.21	4.06±0.09	3.99±0.25	0.13±0.13
	FBL	4.10±0.25	4.43±0.10	4.44±0.09	4.20±0.35	0.13±0.13
	SW8	3.86±0.00	4.06±0.02	4.31±0.26	5.53±0.04	0.63±0.63
	RD5	3.21±0.17	3.35±0.37	3.98±0.27	4.08±0.03	0.12±0.12

Data are MEAN ± SEM of duplicate determinations

SW8, FBL- from sewage sludge; **RD5, RD9**- from refuse dump site; **SB4** - from sugarcane decayed soil.

4.1.14: Activity of xylanase produced by different microorganism isolated from soil using three agrowaste as carbon source

The quantity of xylanase produced by each organism for five days is shown in Table 4.9. Xylanase with the highest activity (38.04 ± 0.17 IU/mL) was produced by RD5 on the 3rd day when plantain pseudostem biomass (PS) was used as carbon source, this is comparable with the enzyme activity (38.84 ± 0.64 IU/mL) using the standard commercial substrate (xylan) while enzyme with the lowest activity (11.56 ± 0.72 IU/mL) was produced on the 1st day by the same organism (RD5) when corncob biomass was used as carbon source.

Table 4.9: Activity of Xylanase Produced by Different Microorganism Isolated From Soil Using Three Agrowastes as Carbon Source

Carbon sources	Organisms	Xylanase Activities (IU/mL)				
		DAY 1	DAY 2	DAY3	DAY4	DAY 5
Xylan	RD9	35.28±0.18	40.11±0.05	34.07±1.78	23.50±1.89	18.84±1.19
	FBL	38.17±0.54	38.32±0.05	37.37±0.52	37.75±0.13	21.46±0.88
	SW8	39.35±0.04	40.05±0.06	38.25±0.59	23.92±0.08	14.45±0.60
	RD5	36.84±0.01	37.96±0.53	38.84±0.64	33.90±0.53	19.30±0.12
PS	RD9	24.29±1.68	33.23±0.71	37.44±0.66	34.58±0.41	28.80±0.64
	FBL	23.53±1.75	33.41±0.58	34.59±0.54	31.42±1.24	28.70±0.77
	SW8	32.00±0.72	34.58±0.59	33.66±0.59	34.12±0.13	28.52±0.31
	RD5	23.53±1.76	30.12±0.59	38.04±0.17	33.66±0.60	28.28±0.04
SB	RD9	30.77±1.89	32.79±1.24	33.69±0.59	32.40±1.78	24.42±0.18
	FBL	29.70±0.65	35.90±0.12	34.48±0.05	33.52±0.71	27.47±0.65
	SW8	34.12±1.61	34.73±0.70	28.51±0.71	34.66±0.16	27.78±0.36
	RD5	22.92±1.05	31.12±1.24	27.16±0.01	27.99±1.37	25.80±0.01
CC	RD9	20.86±0.27	30.63±0.08	31.20±0.63	28.51±2.87	26.46±1.13
	FBL	20.56±1.59	21.03±0.69	25.79±0.02	34.13±0.70	16.75±0.18
	SW8	26.16±1.13	34.66±0.67	31.48±0.11	30.99±1.14	28.30±1.11
	RD5	11.56±0.72	30.82±1.18	34.58±0.68	28.74±0.66	26.46±1.24

Data are MEAN ± SEM of duplicate determinations.

SW8, FBL - from sewage sludge; **RD5, RD9**- from refuse dump site; **SB4** - from sugarcane decayed soil.

PS: plantain pseudostem; **SB**: sugarcane bagasse; **CC**: corncob

4.1.15: Qualitative profile of isolates for fermentative ability using sugar fermentation test

Qualitative profile of isolates for fermenting ability using sugar fermentation test is shown in Table 4.10. Isolates were designated as positive (+) or negative (-) based on their potential to assimilate and ferment the given sugar which is indicated by the ability to produce gas or able to change the colour of the media from orange to yellow during the incubation period. All the organisms assimilated and fermented glucose, fructose and sucrose while the other sugars were either assimilated or fermented. Organism PP fermented all the sugars except Lactose whereas organism RB6 fermented all the sugars except galactose and lactose.

Table 4.10: Qualitative Profile of Isolates for Fermenting Ability Using Sugar Fermentation Test

Organisms	Sources	SIMPLE SUGARS													
		Glucose		Galactose		Xylose		Sucrose		Fructose		Arabino		Lactose	
		Gas	colour	gas	colour	Gas	colour	gas	colour	gas	colour	Gas	colour	gas	Colour
PW1	PW	+	+	+	-	-	+	+	+	+	+	-	-	-	-
PW2	PW	+	+	+	+	-	-	+	+	+	+	-	+	-	+
PW3	PW	+	+	+	-	-	+	+	+	+	+	-	+	-	-
PP1	PP	+	+	-	-	-	+	+	+	+	+	+	+	-	-
PP	PP	+	+	+	+	+	+	+	+	+	+	+	+	-	+
T	T	+	+	-	+	-	+	+	+	+	+	-	+	-	-
RB6	RB	+	+	-	+	+	+	+	+	+	+	+	+	-	+
RB2	RB	+	+	-	-	-	-	+	+	+	+	-	+	-	-
RB3	RB	+	+	-	-	-	+	+	+	+	+	-	-	-	-

PW: Palm wine; **PP:** Fermented food; **T:** Termite hill; **RB:** Rice bran dump site

Responses: +: positive; -: negative

4.1.16: Quantitative profile of isolates for fermenting ability using Dichromate test

A preliminary study was carried out to determine the amount of fermentable sugar utilized and the concomitant amount of ethanol produced by each screened organism as shown in Figure 4.10. A progressive reduction in the concentration of simple sugar with a concomitant increase in the concentration of ethanol was noticed up to the fourth day (96th h) of fermentation, after which there was little or no change in the concentration of both simple sugar. At 96th h organism, T and organism RB6 utilized most of the xylose but organism RB6 produced higher yield of ethanol. Hence organism RB6 was chosen for further study. Also, for the fermentation of glucose, all the organisms, utilized glucose efficiently but the highest yield of ethanol was produced by Organism PP. Therefore, this organism was selected for further study

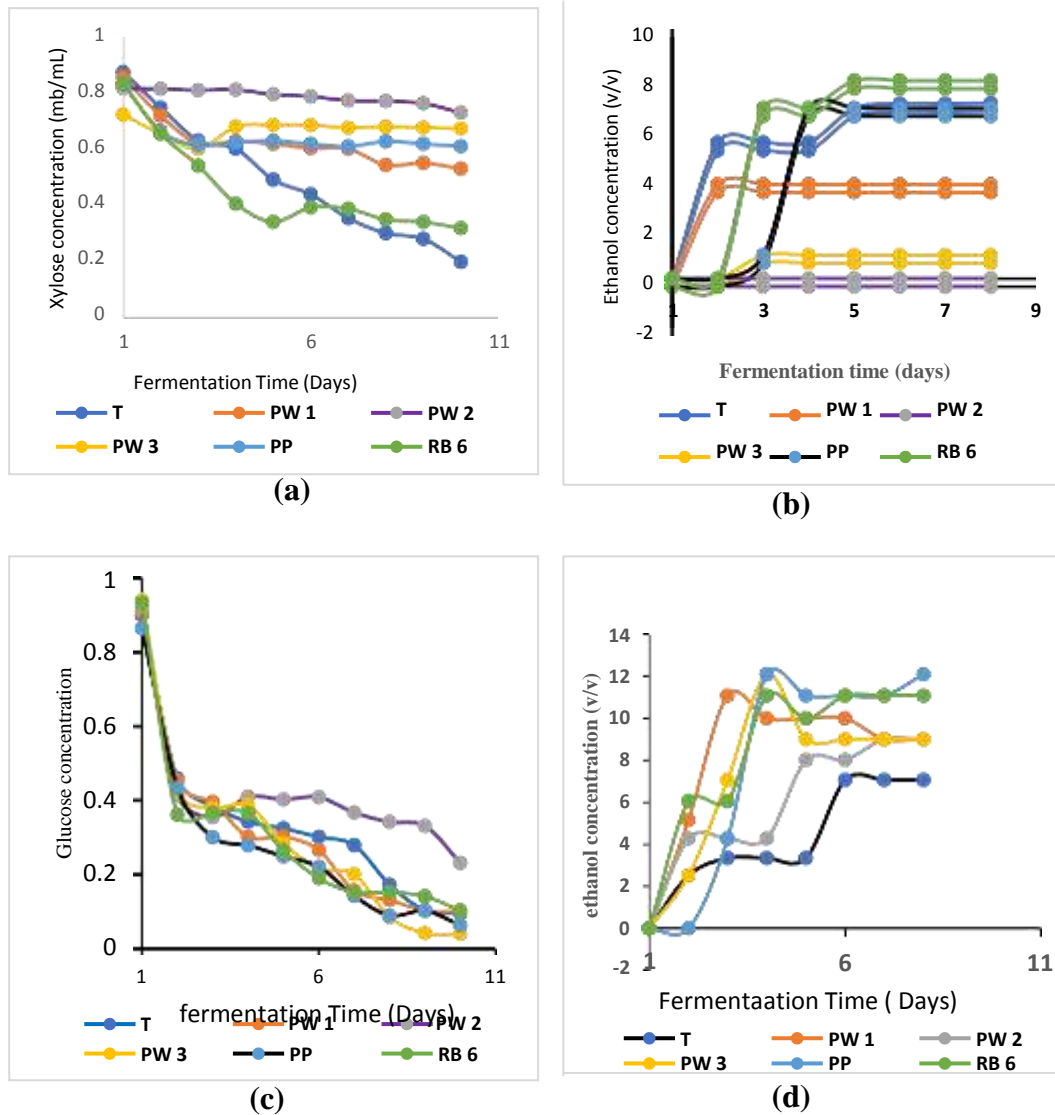


Figure 4.10: Quantitative Profile of Isolates for Fermentative Ability Using Dichromate Test. Xylose Fermentation (a); Ethanol Production from Xylose (b); Glucose Fermentation (c); Ethanol Production from Glucose (d)

Note: T, PW, PP and RB 6 are assigned names to unknown organisms

4.1.17: Ethanol tolerance test

The ability of the isolates to tolerate different concentrations (0-16%) of ethanol was determined by optical density method as shown in Figure 4.11. From the ethanol tolerance study, the tolerance levels of all the strains were found to be in varying capacities up to 12%; but Organism RB 6 and organism PP had a better tolerance level than all the other organisms, with organism T having the least tolerance level for ethanol at every ethanol concentration when compared to other organisms. Even though the organisms had a slight growth at 14%, the level of growth were not comparable to the growth up to 12%. The experiment was done in duplicates and the standard error of mean was used to indicate the error bar.

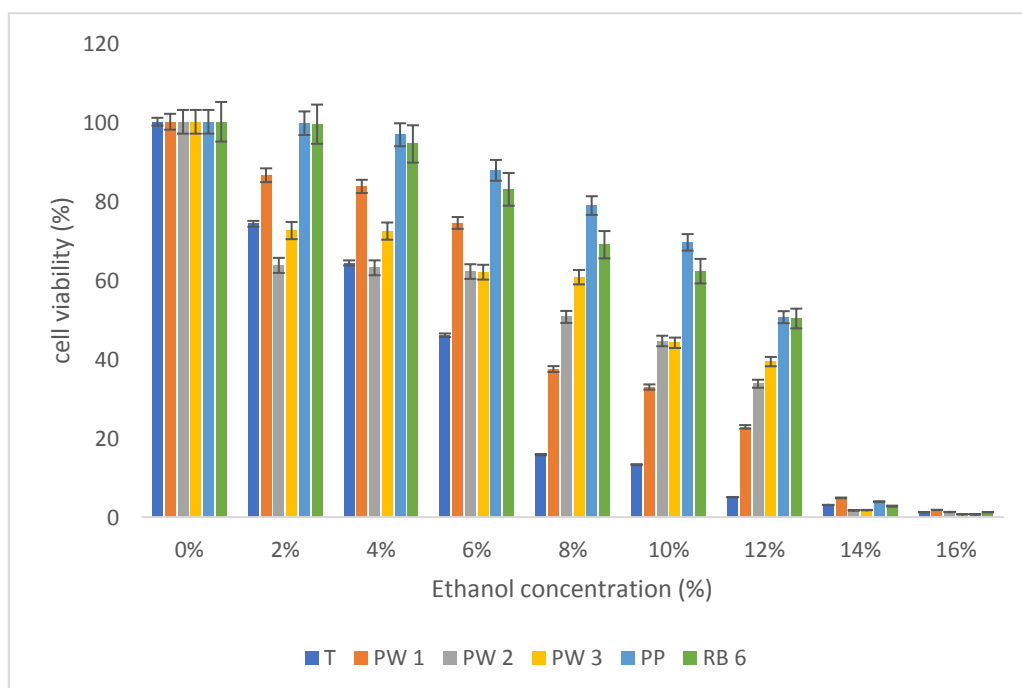


Figure 4.11: Effect of Different Concentrations of Ethanol on the Viability of Screened Organisms.

Note: Values are mean of duplicate readings

4.1.18: Molecular identification of screened organisms for enzyme production and fermentation process

The organisms which produced enzymes with highest activity as well as the organisms which optimally produced ethanol were selected for molecular identification and characterization. The organisms were first identified based on percentage similarity as presented in Table 4.11, then a phylogenic tree was constructed to determine the relationship of the screened organisms with other organisms on the basis of ITS sequence as shown in Figure 4.12. Finally, the organisms were amplified and sequenced for enzyme producing gene, the band obtained in each case was found to be 690 bp and 400 bp for cellulase and xylanase gene respectively as shown in Plate 4.5 and Plate 4.6.

Table 4.11: Molecular Identification and Classification of Organisms Screened for Enzyme Production and Fermentation Process by Percentage Similarity Index and Accession Number

sample ID	Max Score	Total Score	Query Cover	Accession Number of samples organisms	Reference organism	Identification (%)	Accession Number of reference organism
FBL	1098	1098	100%	OP107821	<i>Aspergillus flavus</i>	99.83	MN844036
RD5	1033	1033	99%	OP107822	<i>Aspergillus niger</i>	99.82	MW548412
RB	1068	1250	100%	OP107823	<i>Mucor indicus</i>	99.49	OQ660484
PP	1362	1362	99%	OP107824	<i>Saccharomyces cerevisiae</i>	99.47	MF276989

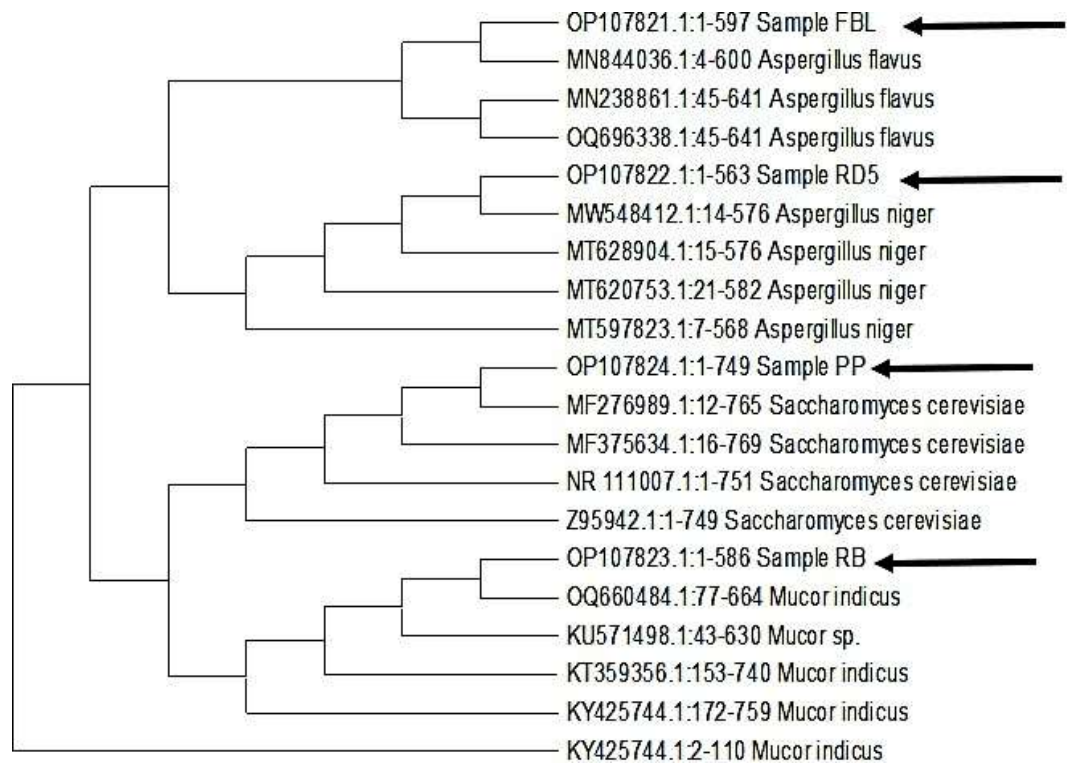


Figure 4.12: Phylogenetic Tree Showing the Relationship Between Screened Organisms for Enzyme Production and Fermentation With Other Organisms on the Basis of ITS Sequence

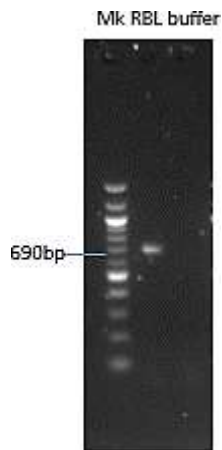


Plate 4.5: Agarose Gel Showing the Positive Amplification of the Endo-beta-1,4-glucanase Cellulase Precursor *ceE* Gene Amplified From *Aspergillus flavus* Strain RBL

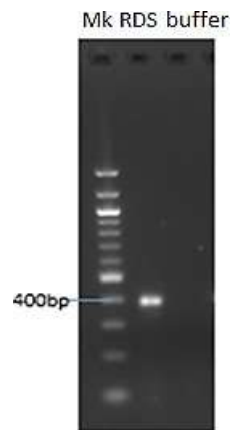


Plate 4.6: Agarose Gel Showing the Positive Amplification of the Endo-1,4-beta-Xylanase Precursor (*xyn11B*) Gene Amplified From *Aspergillus niger* Strain RDS

4.1.19: Average diameter of biochar-chitosan beads prepared at different drying conditions

The average diameters of fresh biochar-chitosan beads and beads dried at different conditions were measured and the values were presented in millimeter as shown in Table 4.12. The oven-dried beads have the smallest average diameter among all the dried beads when compared to the fresh biochar-chitosan beads.

Table 4.12: Average Diameter of Biochar-chitosan Beads Dried at Different Drying Conditions

biochar-chitosan beads	Average diameter (mm)
Fresh	2.67 ± 0.32^b
Air-dried	2.54 ± 0.21^b
Freeze- dried	2.55 ± 0.41^b
oven-dried	1.97 ± 0.17^a

4.1.20: The swelling behaviours of biochar-chitosan beads

The effects of time on the swelling capacity of fresh biochar-chitosan beads and biochar-chitosan beads dried at different temperature were shown in Figure 4.13. After soaking for 6 h, Freeze- dried beads had the highest swelling ratio of about 7.21 while fresh beads have the least swelling ratio of about 0.31. So, freeze dried composite bead was chosen for enzyme immobilization

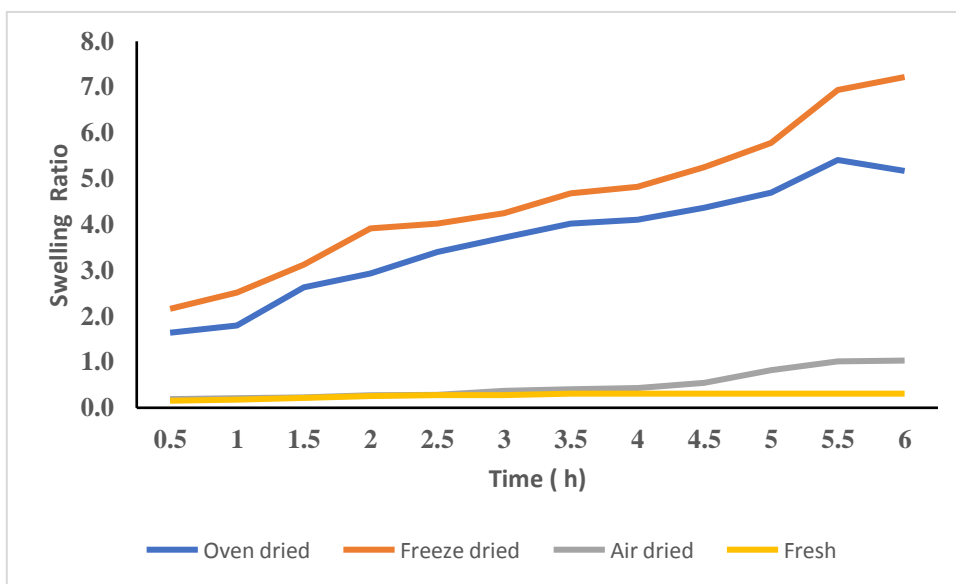


Figure 4.13: Effect of Soaking Time on the Swelling Capacity of Biochar-chitosan Beads Dried at Different Temperature Conditions

4.1.21: Thermogravimetric curves (TGA) and the derivative Thermogravimetric analysis (D TGA) curves of biochar-chitosan beads

The TGA and DTG curves of biochar-chitosan beads dried at various drying temperature conditions are shown in Figure 4.14a and Figure 4.14b. All the dried beads were stable up to 200 °C after which thermal degradation began. The temperature at which the beads degraded most was shown by DTG curve in Figure 4.14b. The biochar-chitosan beads in this study had the highest degradation at 400 °C.

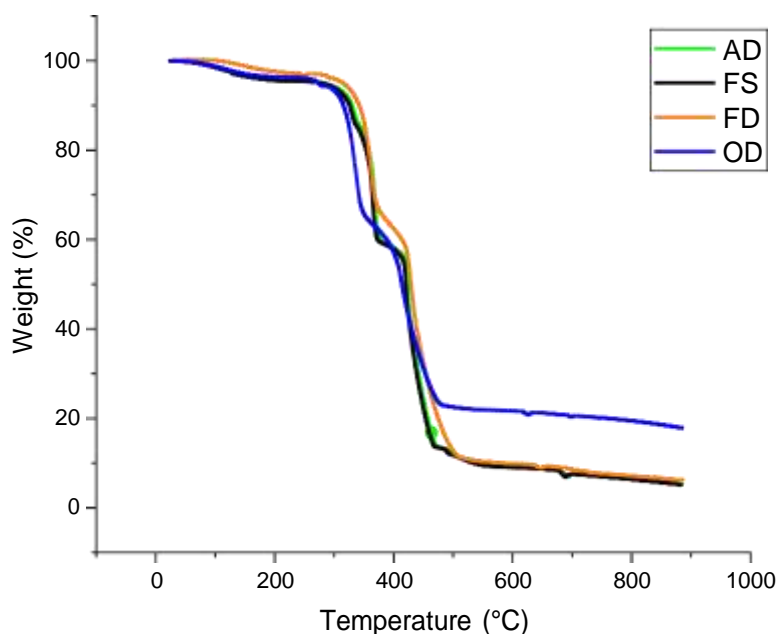


Figure 4.14a: Thermogravimetric (TG) Curves Showing the Effect of Temperature on Weight loss of Biochar-chitosan Beads Prepared at Various Drying Conditions.

FS: Fresh sample; **FD:** Freeze-dried sample; **OD:** oven-dried sample; **AD:** Air-dried sample

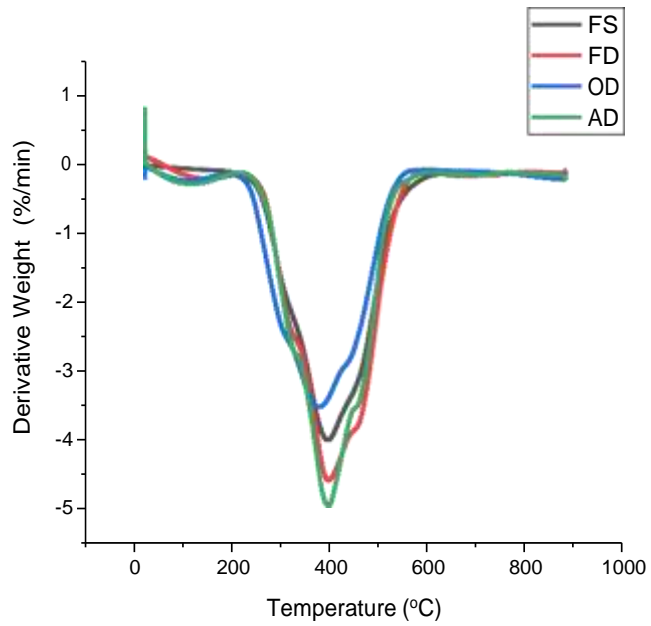


Figure 4.14b: Derivative Thermogravimetric (DT) Curves Showing the Effect of Temperature on Weight Loss of Biochar-chitosan Beads Prepared at Various Drying Conditions.

FS: Fresh sample; **FD:** Freeze-dried sample; **OD:** oven-dried sample; **AD:** Air-dried sample

4.1.22 : Specific surface area, pore size and pore volume of biochar-chitosan composite

The calculated surface area, pore volume and pore size obtained through the Barrett-Joyner-Halenda (BJH) method of Brunauer Emmett-Teller (BET) analyzer is as shown in Figure 4.15. The pore volume and pore sizes were in opposite trend for the biochar-chitosan composite. The free porous biochar had the highest surface ($375.8 \text{ m}^2/\text{g}$) area, pore volume (0.1839 cc/g), and pore size (2.138 nm). However, among the biochar-chitosan composite beads, freeze-dried beads had the highest surface area ($276.3 \text{ m}^2/\text{g}$) and pore volume (0.1361 cc/g) while the air-dried had the highest pore size.

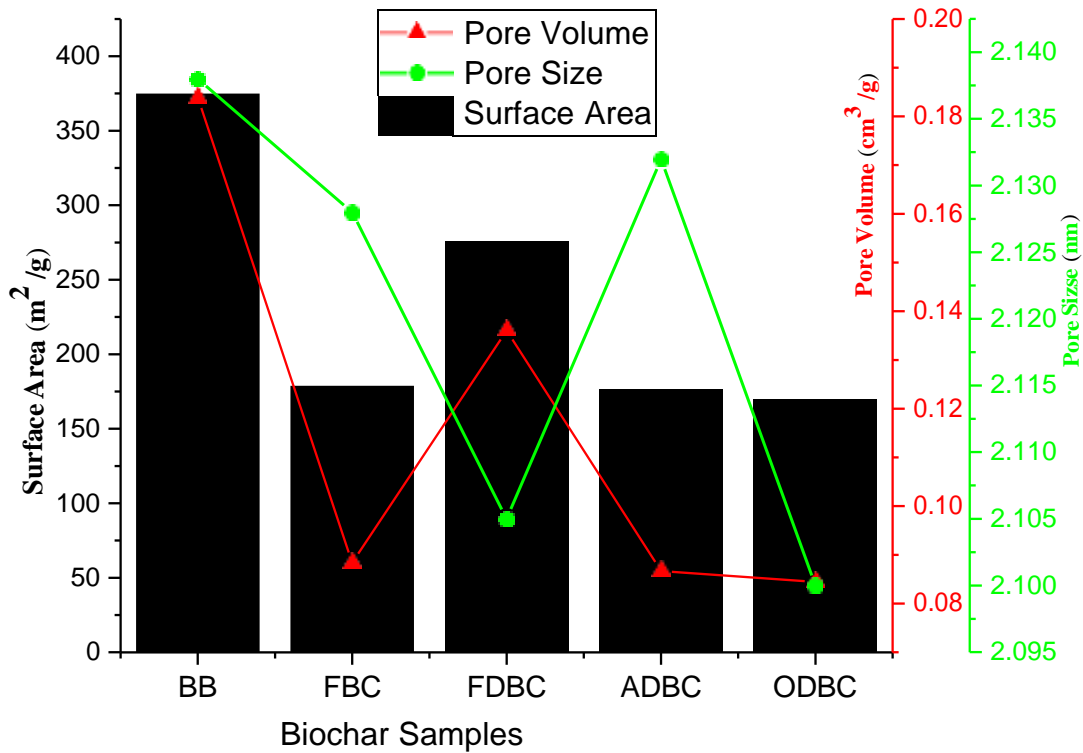


Figure 4.15: Effect of Different Drying Temperature Conditions on the Pore Size, Pore Volume and Surface Area of Biochar-chitosan Composites.

BB: porous bagasse biochar; **FBC:** Fresh biochar-chitosan composite; **FDBC** Freeze-dried biochar-chitosan composite; **ADBC:** Air-dried biochar-chitosan composite; and **ODBC:** Oven-dried biochar-chitosan composite

4.1.23 : Enzyme loading and activity assay

The categories of enzymes loading for co-immobilization is shown in Table 4.13. Xylanase and cellulase loaded at the same time on freeze-dried beads had the highest immobilization efficiency activity of 89.29% and 82.16% respectively. Therefore, freeze-dried bead was chosen for enzyme co-immobilization

Table 4.13: Cellulase and Xylanase Activities of Free and Co-immobilized Enzymes Loaded in Different Categories on Various Biochar-chitosan Beads Used as Support

category	xylanase activity (IU/mLg ⁻¹)	SA of xylanase (mg/mL)	IE of xylanase	cellulase activity IU/mLg ⁻¹	SA of cellulase (mg/mL)	IE of cellulase
Xylanase before cellulase						
free	35.49	8.60	NI	18.35	1.84	NI
F	14.49	5.00	70.25	8.53	1.49	81.38
AD	13.29	5.73	56.24	7.98	1.25	68.31
OD	19.97	6.65	72.72	9.21	1.53	83.33
FD	20.05	5.77	84.19	10.69	1.56	84.73
cellulase before xylanase						
free	33.65	7.68	NI	18.97	1.99	NI
F	14.44	4.74	74.42	6.65	1.59	79.64
AD	14.57	5.00	66.57	6.76	1.20	60.47
OD	17.95	5.22	78.46	8.55	1.64	82.26
FD	18.04	4.79	53.61	12.70	1.67	84.12
Both cellulase and Xylanase						
free	36.28	8.40	NI	19.70	2.34	NI
F	14.10	6.24	63.69	8.23	1.88	80.17
AD	14.29	5.90	60.26	8.21	1.61	68.78
OD	20.66	6.29	76.35	11.66	1.85	79.05
FD	28.51	7.42	89.29	15.48	1.93	82.16

Fresh bead (F); air-dried bead (AD); oven-dried bead (OD); freeze-dried bead (FD).

Specific activity (SA); Immobilization yield (IE); Not immobilized (NI)

4.1.24 : Effect of reaction Temperature and pH on the activity of free and co-immobilized enzymes

The effects of temperature and pH on the activity of free and co-immobilized enzymes are shown in Figures 4.16 and Figure 4.17 respectively; while the optimum pH and temperature extrapolated from the graphs are shown in Table 4.14. Free xylanase had its optimal activity at 50 °C, free cellulase had its optimal activity at 60 °C, while co-immobilized enzymes had their optimal activity at 70 °C. However, free enzymes lost their activities to about 10% at 90 °C while about 50% of activity of co-immobilized enzyme was remaining at 90 °C. The co-immobilized enzymes had a broader optimal pH between 5 to 7 while the optimal pH of free cellulase was 5 and that of free xylanase was 6.

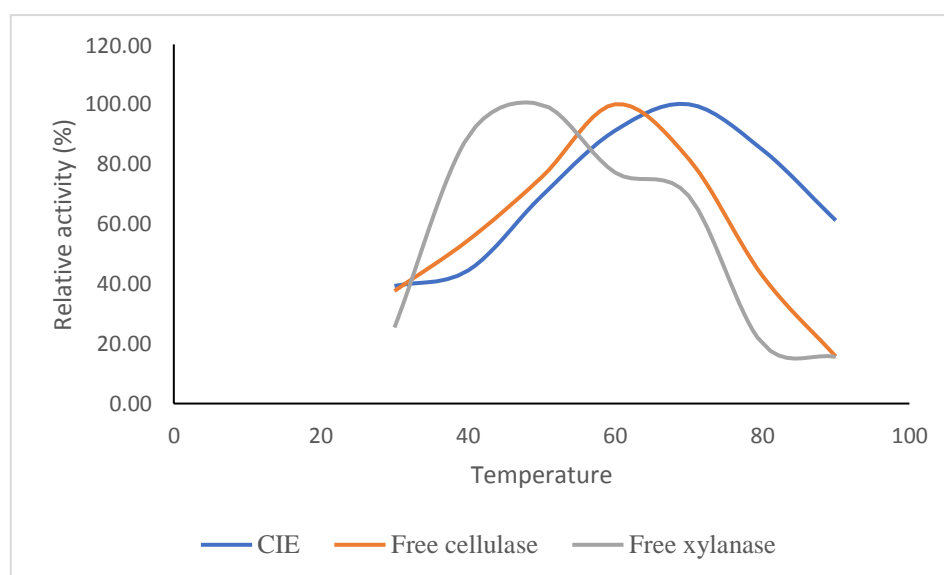


Figure 4.16: Effect of Temperature on the Activity of Co-immobilized Enzymes (CIE), Free Cellulase, and Free Xylanase

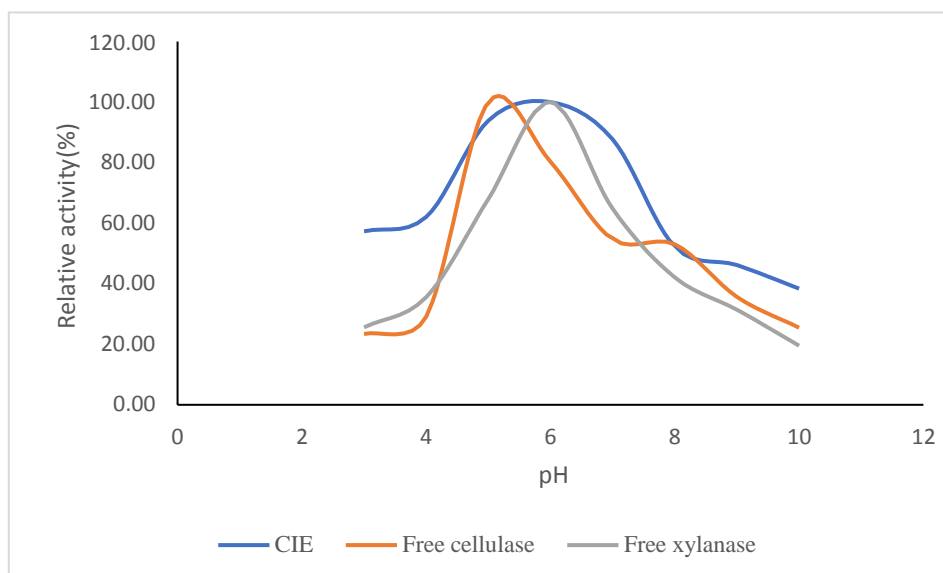


Figure 4.17: Effect of pH on the Activity of Co- immobilized Enzymes (CIE), Free Cellulase and Free Xylanase.

Table 4.14: Optimum pH and Temperature for Free Cellulase, Free Xylanase and Co-immobilized Enzymes

Enzyme Type	Optimum pH	Optimum Temperature (°C)
Free Cellulase	6	60
Free Xylanase	5	50
Co-mmobilized enzyme	5-7	70

4.1.25 : Effect of different agrowaste substrate concentrations on the kinetic parameters of free and co-immobilized cellulase and xylanase

Effects of different agrowaste as enzyme substrate on kinetic parameters as estimated by Michaelis-Menten and Line-weaver Burk plot are shown in Figure 4.18. Different concentrations of the agrowaste samples (sugarcane bagasse, corncob biomass and plantain pseudostem biomass)

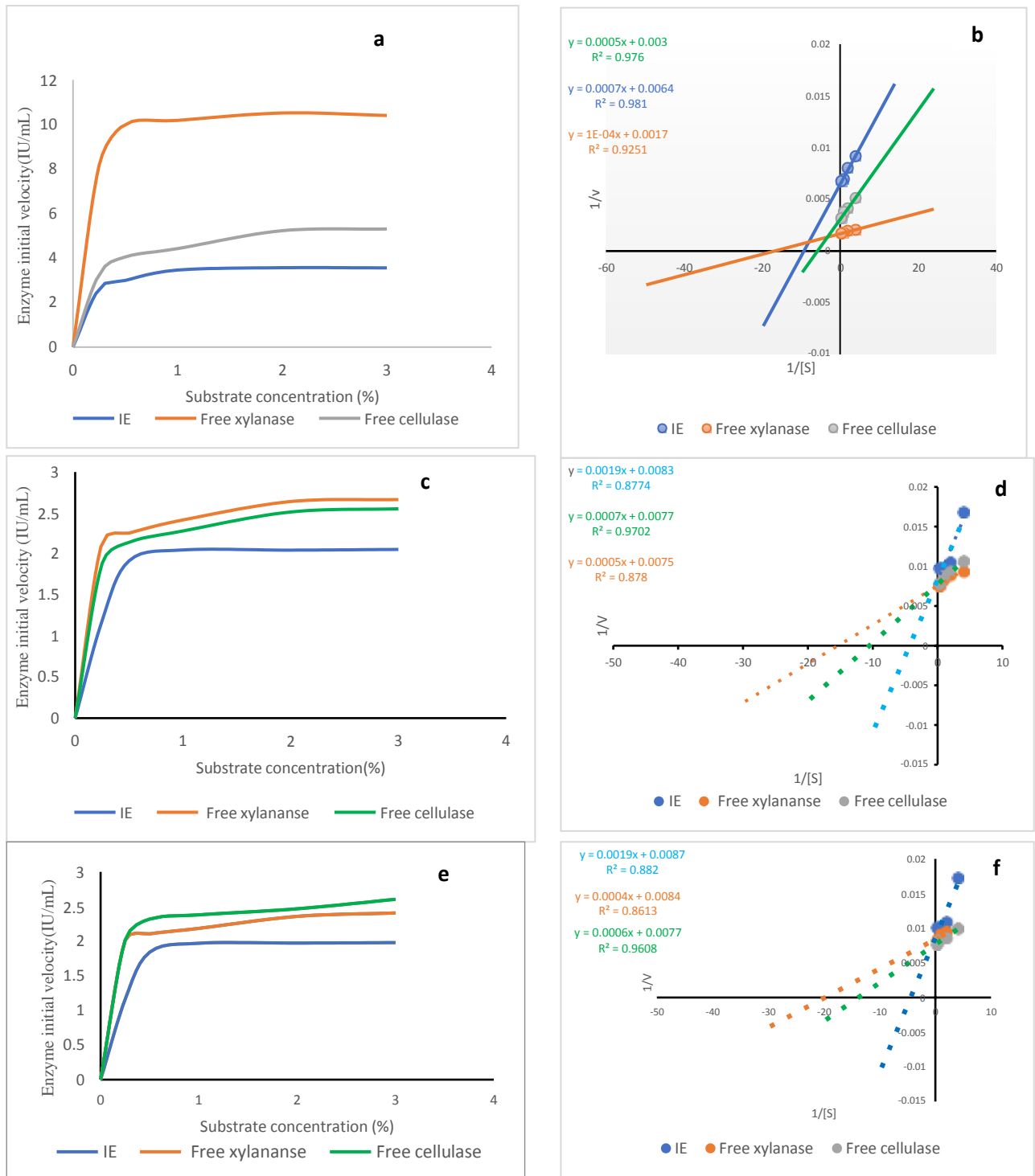


Figure 4.18: Effects of Substrate Concentration on the Kinetic Parameters for Free and Co-immobilized Cellulase and Xylanase

Michaelis Menten plot with sugarcane bagasse as substrate (a); Line weaver-Burk plot with sugarcane bagasse as substrate (b); Michaelis Menten plot with corncob biomass as substrate (c); Line weaver-burk plot with corncob biomass as substrate (d); Michaelis Menten plot with plantain pseudostem biomass as substrate (e); Line weaver-Burk plot with plantain pseudostem biomass as substrate (f).

4.1.26 : Kinetic parameters (K_m and V_{max}) of free and co-immobilized enzymes using different agrowaste as substrate

The summary of K_m and V_{max} values of free cellulase, free xylanase and co-immobilized cellulase and xylanase when different agrowaste samples were used as substrates are shown in Table 4.15. The K_m of free cellulase and the K_m of co-immobilized enzymes were 0.017 mg/mL and 0.018 mg/mL respectively, with sugarcane bagasse as substrate. Also, when plantain pseudostem biomass was used as substrate, the K_m of free xylanase was 0.028 mg/mL and this is comparable to 0.022 mg/mL which was the K_m of co-immobilized enzymes

Table 4.15: K_m and V_{max} Values for Free and Co-immobilized Enzymes

Substrate	Enzyme	K_m (mg/mL)	V_{max} (μMmin^{-1})
Sugarcane bagasse	Free cellulase	0.017	333.33
	Free xylanase	0.006	555.47
	Co-mmobilized cellulase and xylanase	0.018	227.25
corncob biomass	Free cellulase	0.009	129.87
	Free xylanase	0.007	133.33
	Co-mmobilized cellulase and xylanase	0.019	120. 48
Plantain pseudostem biomass	Free cellulase	0.008	129.87
	Free xylanase	0.028	119.05
	Co-Immobilized cellulase and xylanase	0.022	114.94

4.1.27 : Effects of incubation time and conditions on the storage stability of free and co-immobilized enzymes

The effect of storage conditions and time on the activities of free and co-immobilized enzymes at 4 °C and 25 °C are shown in Figure 4.19 and 4.20 respectively. Exactly 79.63% of the initial activity of co-immobilized enzymes was retained after 45 days when stored at 4 °C, while 10.05% and 5. 26% activity remained for free cellulase and free xylanase at the same condition. The activity remaining were 35.64%, 5.01% and 1.05% for co-immobilized enzymes, free cellulase, and free xylanase respectively when the enzymes were stored at room temperature. Half-lives (days) of free and co-immobilized enzymes at this storage temperature were also estimated as shown in Table 4.16.

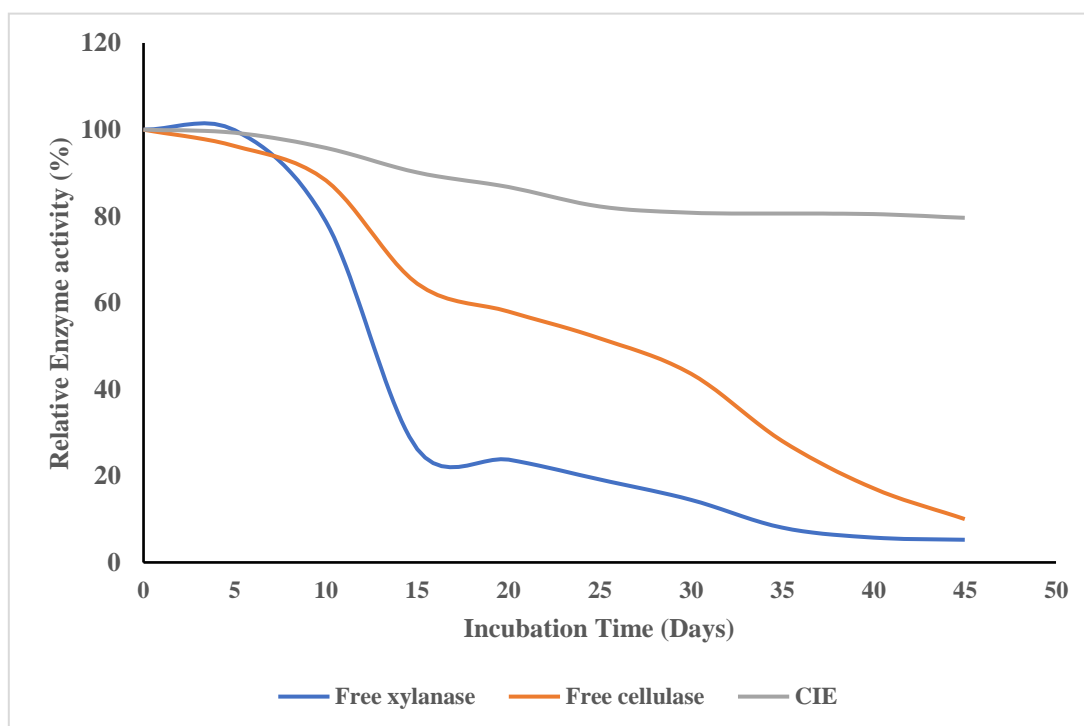


Figure 4.19: Effect of Incubation Time on the Stability of Free and Co- immobilized Enzyme (CIE) Stored in the Refrigerator (4 °C) for 45 days

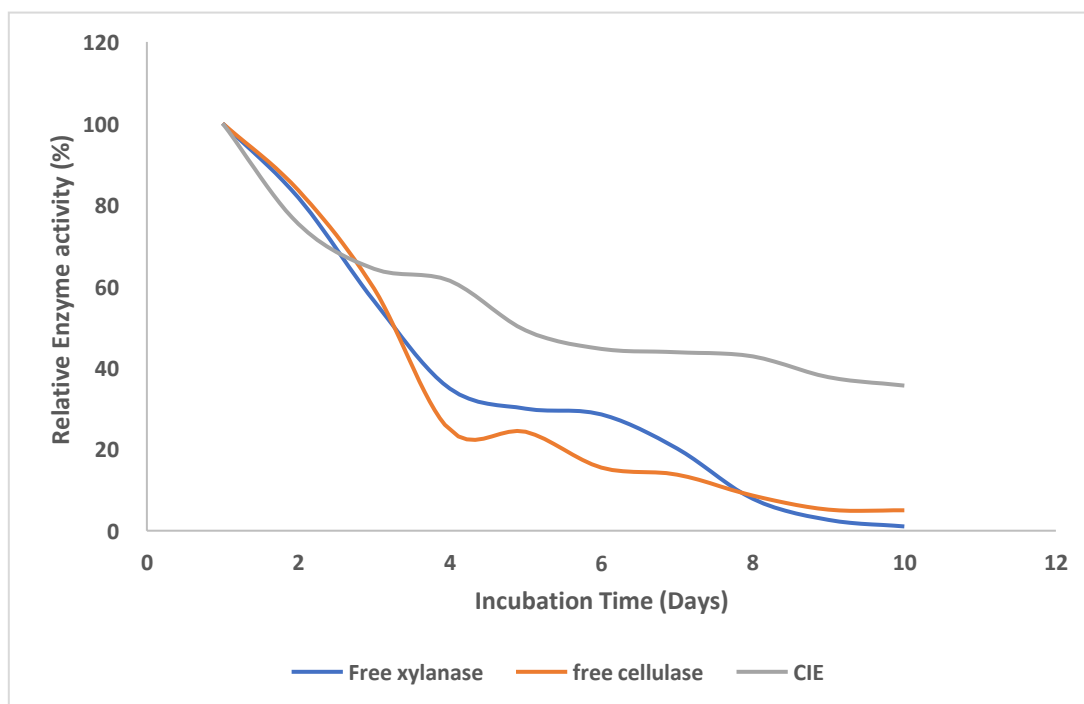


Figure 4.20: Effect of Incubation Time on the Stability of Free and Co-immobilized Enzyme (CIE) Stored at Room Temperature (25 °C) for 10 days

Table 4.16: Half-life of Free and Co-immobilized Enzymes (CIE) Stored at 4 °C and 25 °C

Thermal Condition	Half-life of Enzymes (Days)		
	Free Cellulase	Free xylanase	Immobilized Enzyme
Refrigerator (4 °C)	5.02	4.15	29.37
Room Temperature (25 °C)	4.15	2.50	11.95

4.1.28 : Thermal stability of free and co-immobilized enzymes

The effect of various storage temperature on the stability of free cellulase, free xylanase and co-immobilized cellulase and xylanase is shown in Figure 4.21. The co-immobilized enzymes maintained its highest activity (97%) at 60 °C for the period of 4 h, whereas only 16% of the activity of free cellulase and free xylanase remained at the same period. Also, co-immobilized enzymes retained 93% of its activity at 70 °C for 2 h before the activity gradually reduced to 61.7% whereas free cellulase retained 6% of its initial activity while free xylanase retained 1% of its initial activity. Furthermore, the half -life of co-immobilized enzymes and free cellulase and xylanase at the temperature under study (30 °C -90 °C) was also determined and the values are shown in Table 4.17. Co-immobilized enzymes had longer half-life at every temperature considered. The activation energy and deactivation energy of co-immobilized and free cellulase and xylanase was also determined from Arrhenius plot (appendix I) and the values are presented in Table 4.18. The co-immobilized enzyme has the lowest activation energy (3.450 kJ/MOL) when compared to the activation energy of the free cellulase (15.899 kJ/MOL) and free xylanase (29.218 kJ/MOL). Also, the deactivation energy of the co-immobilized enzyme (52.145 kJ/MOL) was higher than the deactivation energy of free cellulase (48.235 kJ/MOL) and free xylanase (39.596 kJ/MOL)

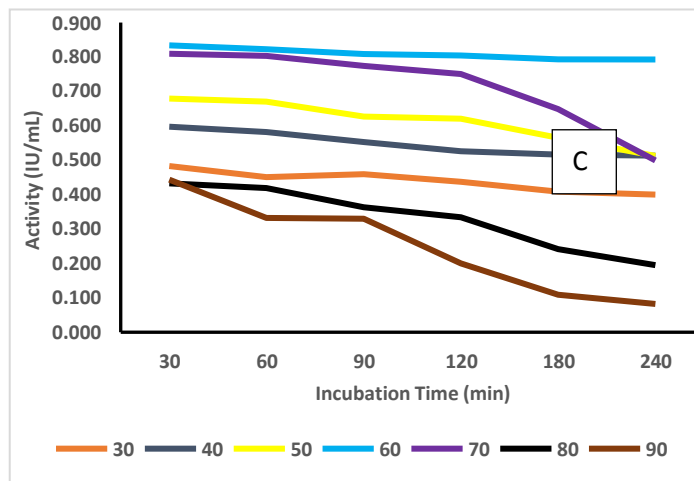
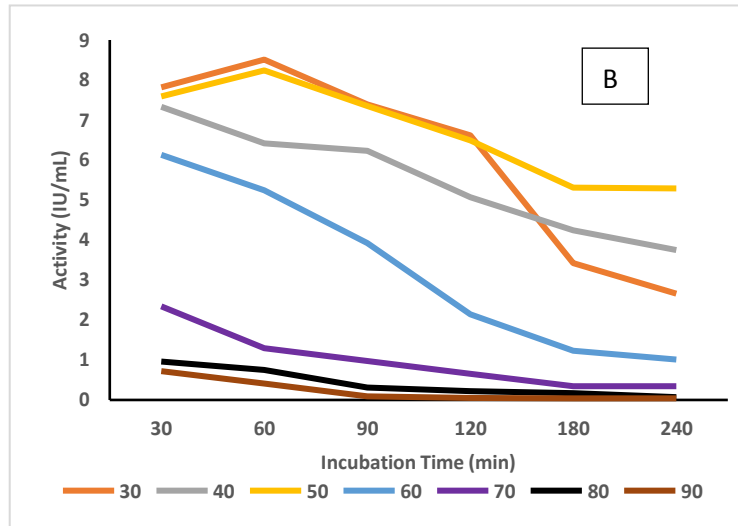
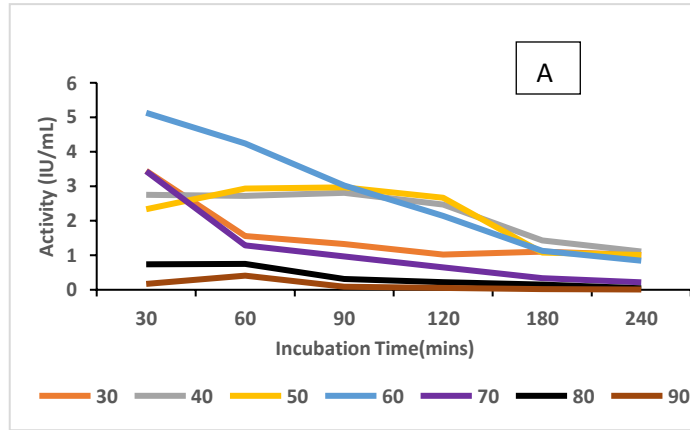


Figure 4.21: Effects of Different Storage Temperatures on the Stability of Free Cellulase (A); free xylanase (B) and co-immobilized cellulase and Xylanase (C) when incubated for 240 minutes from 30 °C to 90 °C

Table 4.17: Half-life of Free and Immobilized Enzymes at Different Thermal Conditions

Temperature (degrees)	Half-life of Enzymes (Hour)		
	Free Cellulase	Free xylanase	Immobilized Enzyme
30	1.38	0.80	27.87
40	1.28	1.38	10.57
50	3.30	4.16	30.09
60	8.69	2.90	59.70
70	1.22	0.45	39.64
80	0.96	0.67	9.52
90	0.55	0.39	6.63

Table 4.18: Activation and Deactivation Energy of Free and Co-immobilized Enzymes

Enzyme	Activation Energy (kJ/MOL)	Deactivation Energy (KJ/MOL)
free cellulase	15. 899	48. 235
free xylanase	29. 218	39.596
Co-immobilized enzymes	3. 450	52.145

4.1.29 : The effect of number of usages on the relative efficiency of the co-immobilized enzymes

The co-immobilized enzymes were used repeatedly for 10 times in fresh substrate for each cycle and the residual enzyme activity after each cycle is as shown in Figure 4.22. The experiments were carried out in duplicate and the standard error of mean was used to indicate the error bar. The co-immobilized enzymes retained 55.13% of its initial activity after the 10th used.

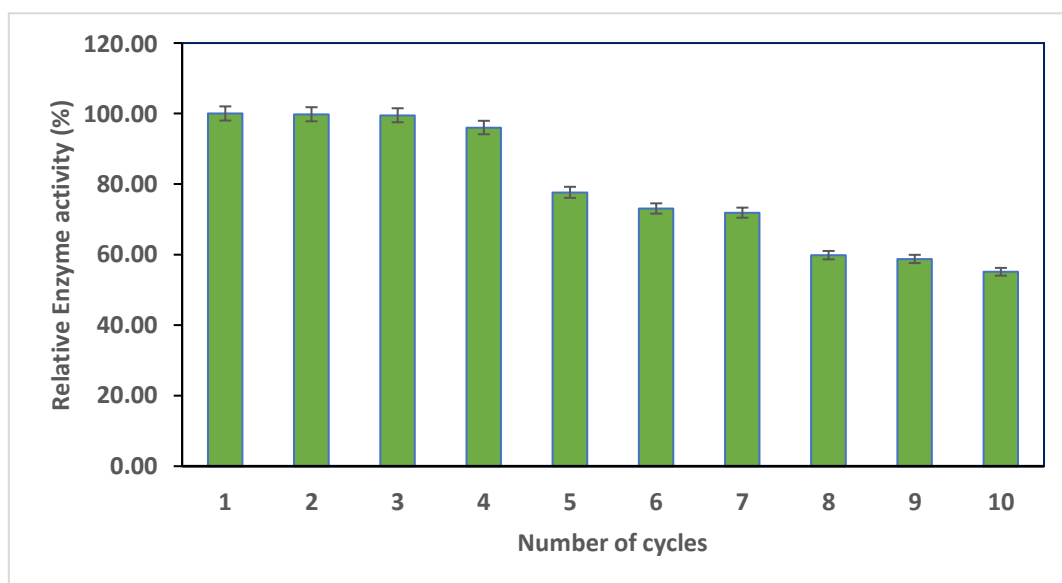


Figure 4.22: Effect of Number of Usages on the Relative Efficiency of the Co-immobilized Enzymes on Freeze-dried Biochar-chitosan Beads

Note: Data are MEAN \pm SEM of duplicate determinations

4.1.30 : Enzymatic hydrolysis of agrowaste using free and immobilized enzymes

The reducing sugar, otherwise called fermentable sugar, released during enzymatic hydrolysis of pre-treated agrowaste with free and co-immobilized enzymes is as shown in Table 4.19. The highest amount (45.99 ± 0.58 mg/mL) of reducing sugar was obtained at the 72nd hour when the mixture of free cellulase and free xylanase was used to hydrolyze sugarcane bagasse. Also, plantain pseudostem biomass released a very high amount of fermentable sugar (43.34 ± 0.27 mg/mL) at the 72nd hour when the mixture of cellulase and xylanase was used to hydrolyze it. However, the number of fermentable sugars produced by corncob biomass at the same experimental conditions was about 60% lower (18.98 ± 0.91 mg/mL) than the fermentable sugar produced by sugarcane bagasse and plantain pseudostem biomass. Also, the amount of fermentable sugar released by co-immobilized enzymes were 32.47 ± 0.89 mg/mL, 36.62 ± 1.90 mg/mL, and 17.42 ± 0.41 mg/mL for plantain pseudostem, sugarcane bagasse and corncob biomass respectively.

Table 4.19: Fermentable Sugar Produced from the Hydrolysis of Different Agrowaste Using Free Cellulase, Free Xylanase and Co-immobilized Enzymes for 4 Days (96 h)

Substrate	Enzyme	Day 0	Day 1	Day 2	Day 3	Day 4
		Reducing sugar (mg/mL)	Reducing sugar (mg/mL)	Reducing sugar (mg/mL)	Reducing sugar (mg/mL)	Reducing sugar (mg/mL)
PS	Free Cellulase	0.41 ± 0.01	9.80 ± 0.51	23.70 ± 1.01	26.14 ± 1.18	25.07 ± 1.18
PS	Free Xylanase	0.34 ± 0.02	6.41 ± 0.47	16.62 ± 0.51	19.50 ± 0.23	17.90 ± 0.77
PS	Free Cellulase and xylanase	0.62 ± 0.02	11.82 ± 1.04	40.0 ± 0.42	43.34 ± 0.27	42.81 ± 0.27
SB	Free cellulase	0.77 ± 0.02	16.26 ± 0.33	32.80 ± 0.90	34.92 ± 0.66	33.58 ± 0.14
SB	Free xylanase	0.61 ± 0.01	10.57 ± 0.04	27.65 ± 0.85	28.50 ± 0.89	26.90 ± 0.36
SB	Free cellulase and xylanase	0.88 ± 0.09	21.70 ± 0.28	43.84 ± 0.06	45.99 ± 0.58	43.86 ± 0.58
CC	Free cellulase	0.42 ± 0.06	5.94 ± 0.52	17.63 ± 0.10	17.15 ± 0.68	16.88 ± 0.66
CC	Free xylanase	0.33 ± 0.06	4.33 ± 0.49	11.91 ± 0.42	12.13 ± 0.85	11.06 ± 0.85
CC	Free cellulase and free xylanase	0.61 ± 0.01	6.67 ± 0.75	18.98 ± 0.91	18.50 ± 0.07	17.44 ± 0.07
PS	Co-immobilized cellulase and xylanase	0.57 ± 0.02	12.71 ± 0.38	25.97 ± 0.79	32.47 ± 0.89	31.36 ± 0.53
SB	Co-immobilized cellulase and xylanase	1.00 ± 0.09	19.28 ± 1.57	34.14 ± 1.49	36.62 ± 1.90	37.12 ± 0.80
CC	Co-immobilized cellulase and xylanase	0.58 ± 0.02	7.91 ± 0.38	12.32 ± 0.54	17.42 ± 0.41	17.26 ± 0.27

PS: Plantain pseudostem biomass; **SB:** Sugarcane bagasse; **CC:** corncob biomass

Note: Results are in mean ± SEM of duplicate values

4.1.31 : Amount of bioethanol produced determined by potassium dichromate method

The concentrations (g/L) of ethanol produced with different combinations of enzyme and fermenters as determined by potassium dichromate method are shown in Table 4.20. The combination of co-immobilized enzymes and co-immobilized *S. cerevisiae* and *Mucor indicus* produced the highest concentration of ethanol for both sugarcane bagasse (76.09 ± 0.15 g/L) and plantain pseudostem biomass (68.93 ± 0.33 g/L).

Table: 4.20: Concentration of Ethanol (g/L) Produced with Different Combinations Enzyme and Fermenters

Enzymes	fermenters	Concentration of Ethanol produced with sugarcane bagasse (g/L)	Concentration of Ethanol produced with plantain pseudostem biomass (g/L)
Co-immobilized cellulase and xylanase	Free <i>S. cerevisiae</i>	47.49 ± 0.34	44.33 ± 0.28
Co-immobilized cellulase and xylanase	Free <i>Mucor indicus</i>	39.95 ± 0.04	37.71 ± 0.01
free cellulase and xylanase	free <i>Mucor indicus</i>	64.20 ± 0.54	60.55 ± 0.96
free cellulase and xylanase	Free <i>S. cerevisiae</i>	65.73 ± 0.04	63.65 ± 0.04
Co-immobilized cellulase and xylanase	immobilized <i>Mucor indicus</i>	50.92 ± 0.42	45.46 ± 0.19
Co-immobilized cellulase and xylanase	Co-immobilized <i>S. cerevisiae</i> and <i>Mucor indicus</i>	76.09 ± 0.15	68.93 ± 0.33
Co-immobilized cellulase and xylanase	Immobilized <i>S. cerevisiae</i>	55.08 ± 0.51	55.75 ± 0.19

4.1.32 : Characterization of bioethanol by GC-MS

The percentages of compound identified by GC-MS in the distillate of bioethanol produced by co-immobilized enzymes and co-immobilized yeast and fungi is shown in Table 4.21 and Table 4.22 for sugarcane bagasse and plantain pseudostem biomass respectively. Other components such as toluene, hexanol, butanol, Heptane were also identified in the distillate. However, ethanol had the highest percentages of 80.87% and 71.15% for sugarcane bagasse, and plantain pseudostem biomass respectively

Table 4.21: Compounds Identified by GC-MS in the Distillate of Bioethanol Produced by Co-immobilized Enzymes and Co-immobilized Yeast and Fungi Using Sugarcane Bagasse

Retention Time (min)	Area (Ab*s)	Hit Name	Composition (%)
2.351	938888	Butane, 1-ethoxy-	1.79
3.063	1426714	Toluene	2.72
3.453	1179061	Heptane, 3-methylene-	2.25
6.965	42420237	Ethanol	80.87
10.901	3362900	1-Hexanol, 2-ethyl-	6.41
30.218	3124716	1,2-Benzenedicarboxylic acid,	5.96

Table 4.22: Compounds Identified by GC-MS in the Distillate of Bioethanol Produced by Co-immobilized Enzymes and Co-immobilized Yeast and Fungi Using Plantain Pseudostem Biomass

Retention Time (min)	Area (Ab*s)	Hit Name	Composition (%)
2.361	939,634	Butane, 1-ethoxy-	1.56
2.715	2,518,218	1-Butanol, 3-methyl-	4.22
2.757	1,261,507	1-Butanol, 2-methyl	2.11
3.065	1,427,355	Toluene	2.39
3.459	1,147,837	Heptane	1.93
6.965	42,420,237	Ethanol	71.15
10.903	4,102,462	1-Hexanol, 2-ethyl-	6.88
28.498	2,615,401	Tropidine, 2-acetyl-	4.39
30.204	3,190,810	1,2-Benzenedicarboxylic acid, mono(2-ethylhexyl) ester	5.35

4.1.33 : Infrared spectra of free biochar-chitosan and biochar-chitosan loaded with co-immobilized enzymes and co-immobilized yeast and fungi

The functional group identified in infrared spectra of free biochar-chitosan bead (F), biochar-chitosan loaded with co-immobilized enzymes (CIE) and biochar-chitosan bead loaded with co-immobilized fungi are shown in Table 4.23. The variation in the spectra relative to the position and intensity of the characteristic peaks (Appendix J) and the functional groups for unloaded biochar-chitosan beads especially within the wavenumber of 2000 cm^{-1} and 1000 cm^{-1} is a confirmation of successful co-immobilization.

Table 4.23: Functional Groups Identified in Infrared Spectra of Free Biochar-Chitosan Bead (F), Biochar-chitosan Loaded with Co-immobilized Enzymes (CIE) and Biochar-chitosan Beads Loaded with Co-immobilized Yeast and Fungi

Free biochar-chitosan bead			Biochar-chitosan bead loaded with co-immobilized cellulase and xylanase			Biochar-chitosan bead loaded with co-immobilized mucor and yeast		
Wave-number (cm ⁻¹)	Intensity	Functional group	Wave-number (cm ⁻¹)	Intensity	Functional group	Wave-number (cm ⁻¹)	Intensity	Functional group
1028.74	44.44	C-N	1032.472	50.060	C-N	1036.199	52.454	C-N
1066.01	46.13	C-N	1066.018	50.701	C-N	1241.203	71.958	C-N
1151.74	62.48	C-N	1151.739	68.466	C-N	1312.022	72.156	N=O
1263.56	66.53	C-O	1248.658	72.333	C-N	1379.115	69.598	N=O
1379.11	55.45	C-H ₂	1312.022	73.550	N=O	1457.389	71.338	N=O
1461.11	64.62	CH ₃	1379.115	70.227	N=O	1543.117	64.189	C=C
1576.66	52.76	-NH	1546.845	65.208	-NH	1636.301	65.711	-NH
1640.02	56.75	C=N	1640.028	54.132	C=N	2117.127	92.817	C≡O
2113.40	91.03	-CH ₂	2117.127	92.896	-CH ₂	2325.858	93.087	N=C=O
2292.31	90.90	C-H	2929.687	75.966	C-H	2929.687	75.244	C-H
3287.51	42.61	-NH	3280.057	44.643	-NH	3272.602	44.162	-NH

4.1.34 : Scanning electron micrograph (SEM) of free biochar-chitosan bead

The SEM images for the samples of unloaded biochar-chitosan beads (Free), co-immobilized enzymes loaded biochar-chitosan beads (CIE), and co-immobilized yeast and fungi biochar-chitosan beads (CMY) are shown in Figure 4.23. The differences in the morphology of the loaded beads are clearly seen when compared to the unloaded bead. The visible pores or cavities in the free biochar-chitosan beads have been blocked by the attachment of either enzyme or cells.

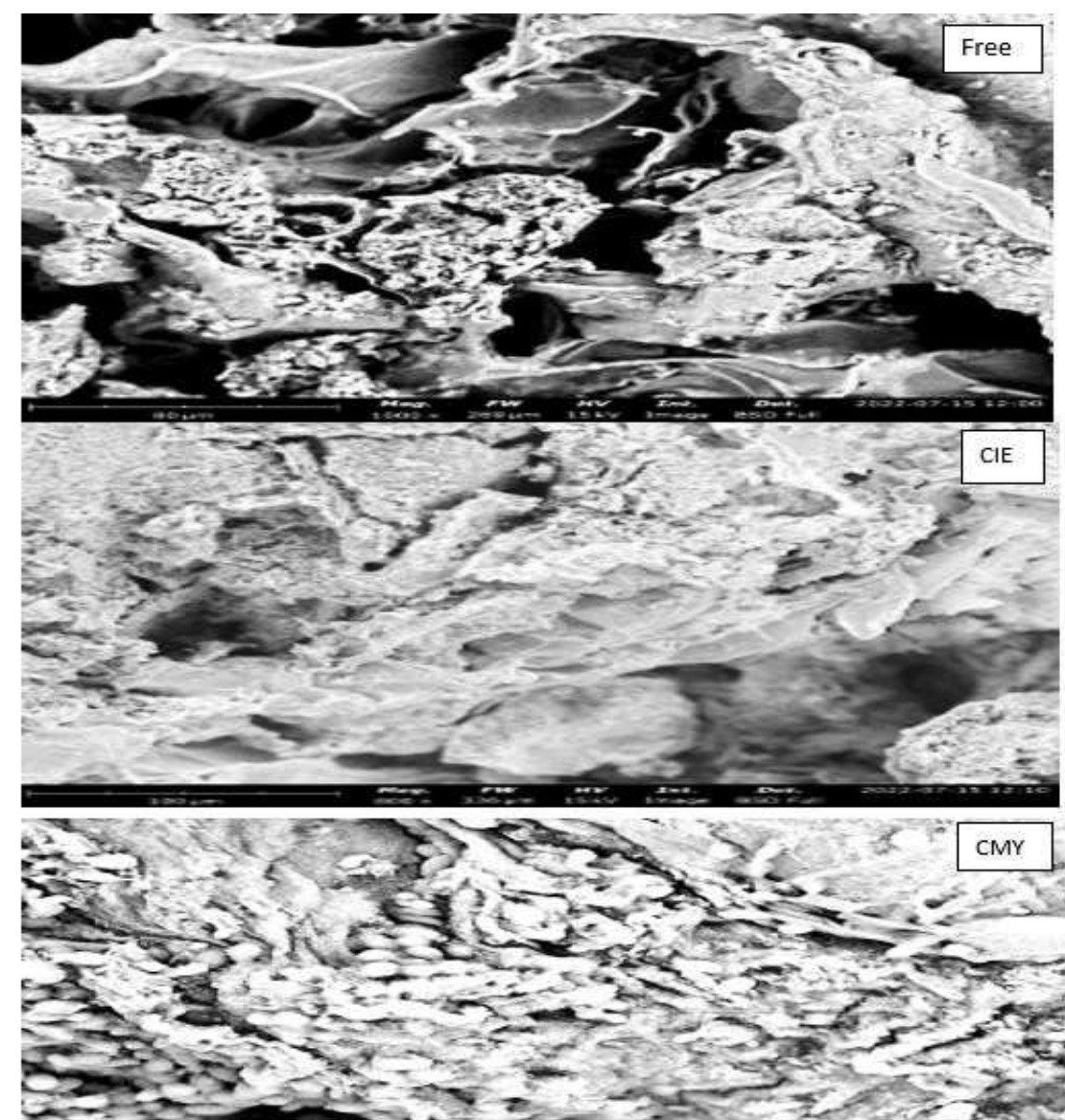


Figure 4.23: Scanning Electron Micrograph of Free Biochar-chitosan Bead (Free); Biochar-chitosan Beads Loaded with Co-immobilized Enzymes (CIE); and Co-immobilized *Mucor indicus* and *Saccharomyces cerevisiae* (cMY)

4.1.35 : Re-usability test of co-immobilized mucor and yeast

Co-immobilized *S. cerevisiae* and *Mucor indicus* together with co-immobilized cellulase and xylanase which had the highest yield of bioethanol was used repeatedly in fresh substrate and the concentration of ethanol produced at the end of each cycle was recorded in g/L as shown in Figure 4.24

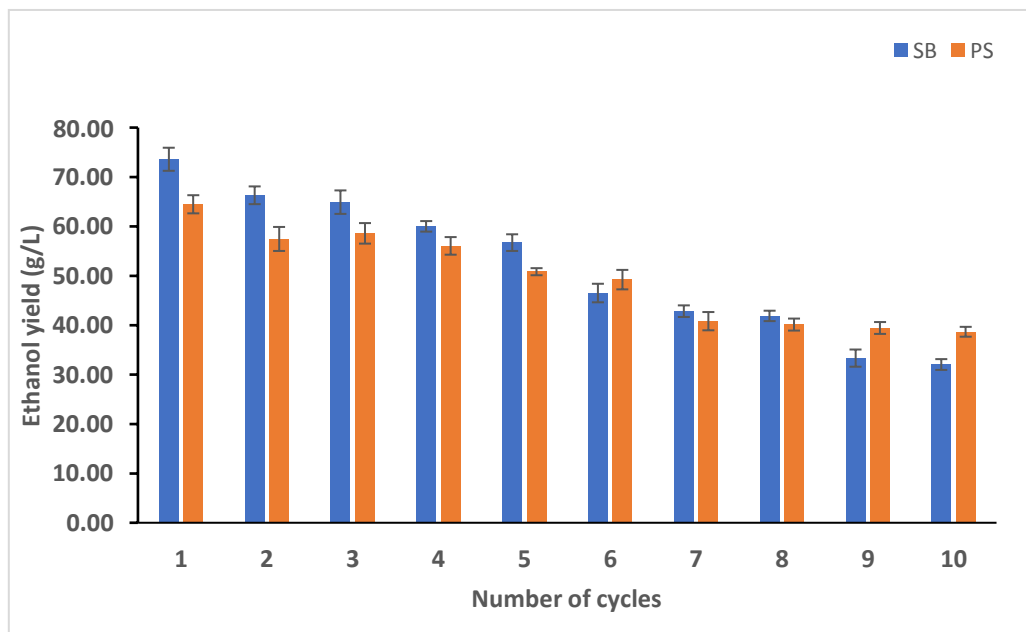


Figure 4.24: Effect of Number of Usages on the Relative Efficiency of the Co-immobilized *Saccharomyces cerevisiae* and *Mucor indicus*

4.1.36 : Estimated cost for the production of 1.5 L of lignocellulosic bioethanol

The cost of production of lignocellulosic bioethanol can be estimated by adding up all the costs involved in producing bioethanol as shown in Table 4.24. The costs are estimated approximations of the values of the items while assumptions were made for the other items such as maintenance because they were either not bought or the items were not applicable for the present production. However, Tao *et al.* (2014) reported the contribution (in percentage) by each of the process to the overall cost as shown in Table 4.24. A sum of ₦ 6800 was estimated for the production of 1.5 L of lignocellulosic bioethanol.

Table 4.24: Estimated Cost for the Production of 1.5 L of Lignocellulosic Bioethanol

Cost category	Type	Item	Estimated cost (₹)	Percentage in the overall cost
Variable cost	feedstock	Feedstock purchase	~300/ kg	
		Feedstock Transportation	~300	32%
		Feedstock preparation	B	
	Chemicals	Feedstock and product storage		1%
		Pretreatment	~500	13%
		Enzyme production	~500	16%
		Fermenters isolation	~300	
		Immobilization support	~1500	
		SScf nutrient	~3000	11%
		Denaturant	C	
Labour	Process operators	D		
	Laboratory Technicians	E	3%	
	Cleaners	F		
Fixed cost	Administration		G	15%
	Capital	Fixed capital investment	H	
		Working capital investment	I	6%
	Utility	Electricity (centrifugation, agitation, autoclaving, drying, storage)	J	3%
		Water	~400	
ESTIMATED COST FOR ETHANOL PRODUCTION (1.5 L)			6,800	~₹ 4500/L

4.2 Discussion

4.2.1 a: Optimal conditions for the pre-treatment of agrowaste using microwave – assisted-alkaline pre-treatment methods

The production of bioethanol from lignocellulosic agricultural waste, known as second generation bioethanol, has a significant advantage in terms of sustainability over first generation bioethanol, which is produced from starchy food items. However, different agrowaste contains varying amount of cellulose, hemicellulose and lignin. Therefore, different conditions of pre-treatments are required for optimal removal of lignin as well as retention of high percentage of cellulose and hemicellulose. In the present study, bioethanol was produced from sugarcane bagasse and plantain pseudostem as discussed in the following sections. The combination of cellulose with hemicellulose is called holocellulose. Holocellulose is the polysaccharide part of the lignocellulosic material that can be converted to fermentable sugars. So, indirectly, the quantity of holocellulose could determine the ethanol yield from a particular lignocellulosic agrowaste. However, the compositional analysis of the sample used for the present study is shown in Table 4.1. plantain pseudostem biomass contained 35%, 30% and 11.49% cellulose, hemicellulose and lignin respectively while sugarcane bagasse contained 48%, 24%, and 21.5% cellulose, hemicellulose and lignin respectively, whereas, corncob biomass contains 42%. 35% and 19.3% for cellulose, hemicellulose and lignin respectively. This is in line with the reports from the reviews by Gonzalez-Rentería *et al.* (2011), and Boneberg *et al.* (2016), on the percentage composition of the contents of lignocellulosic materials in which (32-48%), (11-35%) , and (9- 27%) were reported as the percentages of cellulose, hemicellulose, and lignin respectively. According to Xu *et al.* (2016b) and Rezanian *et al.* (2020), the variations in the composition of the lignocellulosic agrowaste can be related to many factors such as the plant genetics, growth environment, processing conditions as well as the method used in the composition analysis.

A close examination of the relative percentages of the contents of the agrowastes used in this study (Table 4.1) suggests that the pre-treatment conditions required to optimally remove lignin in order to access the cellulose and hemicellulose contents may be mildest in plantain pseudostem biomass because it contained the least amount of lignin, whereas a harsher pre-treatment condition was required to optimally remove lignin from sugarcane bagasse. However, based on the holocellulose (cellulose plus hemicellulose) content of each agrowaste, corncob biomass (with a holocellulose content of 77%) is expected to produce the highest ethanol yield, followed by sugarcane bagasse (with a holocellulose content of 72%), and plantain pseudostem biomass is expected to give the lowest yield of bioethanol.

In this study, pre-treatment of lignocellulosic material resulted in a reduction in the material's initial weight, as shown in Table 4.2. (a-c). The lowest solid biomass (1.85 g) was obtained in the pre-treatment of plantain pseudostem biomass (Table 4.2a) when the sample was treated with 3% NaOH at 385 W for 5min; also, the lowest percentage total lignin retained (2.29%) was evaluated at this process condition. This is also true for pre-treated sugarcane bagasse (Table 4.2b), where the lowest solid biomass yield (1.96 g) after pre-treatment was obtained at run 14 when the sample was treated with 3% NaOH at 700 W for 5 min, resulting in the lowest percentage (4.90%) of lignin retained. Similarly, Table 4.2c shows that the lowest solid biomass yield (2.73 g) from corncob biomass after pre-treatment was obtained at run 15, when the sample was treated with 3% NaOH at 385 W for 5 min, as well as the lowest percentage lignin (6.58%) retained under these process conditions. This finding was consistent with the findings of Wang *et al.* (2020), who found that higher NaOH concentrations and longer pre-treatment times resulted in lower solid recovery and higher lignin removal. Furthermore, Kim *et al.* (2016) attributed the size reduction of pre-treated lignocellulosic materials to the removal of

lignin, which eventually led to a decrease in the degree of cellulose crystallinity and an increase in specific surface area, allowing the plant cell walls to separate into liquid and thus increasing cellulose accessibility to hydrolytic enzymes. Furthermore, even when both samples were treated under the same conditions, the percentage of lignin remaining after pre-treatment was lowest in plantain pseudostem biomass and highest in corncob biomass. This supports the findings in the compositional analysis of the raw (untreated) biomass, which confirmed that, due to the initial low lignin content in plantain pseudostem biomass, the process conditions required to optimally remove lignin may be the mildest. As a result, plantain pseudostem biomass is more responsive to treatment conditions in which more lignin is removed.

The experimental responses (percentage cellulose retained, hemicellulose retained and lignin removed) as well as the three independent variables for the microwave-alkaline pre-treatment of the three lignocellulosic agrowastes under study are shown in Table 4.3 (a-c). The goal was to remove as much lignin as possible while retaining as much cellulose and hemicellulose as possible. However, the conditions under which this goal was met differ for each component in the agrowaste sample. For example, the highest percentage of lignin (65.9%) was removed from corncob biomass (Table 4.3c) at run 15 (3% NaOH/ 385 W/5 min), while the highest percentage of cellulose was retained at the same process conditions. However, at different process conditions, the highest percentage of hemicellulose (34%) was obtained. Variability in the most efficient process conditions was observed for sugarcane bagasse and plantain pseudostem pre-treatment as well, such that the conditions under which the highest percentage of cellulose was retained differed from those under which the highest percentage of hemicellulose was obtained. This variability is unsuitable for industrial processes because it may waste time and resources. Therefore, the microwave-alkaline pre-treatment process conditions were optimized

using design expert software to obtain the optimum values for the combination of the variable factors in order to achieve the desired goal.

The goal of pre-treatment is to maximize lignin removal from biomasses while obtaining the highest recovery yield of cellulose and hemicellulose that can be used to produce ethanol. The best combinations of variable factors as generated by design expert software for the optimal yield of percentage delignification, cellulose content, and Hemicellulose content for the industrial process in the model investigated are as shown in Tables 4.4(a-c), for Plantain pseudostem biomass, corncob biomass, and sugarcane bagasse, respectively. The selection criteria were based on obtaining a solid with a high percentage of delignification (lignin removal) and a high content of polysaccharides (cellulose and hemicellulose) in the defined interval of conditions. The chosen optimal conditions for each of the agrowaste were 1.97% NaOH, 70 W power and 5 min treatment time for plantain; 3% NaOH concentration, 73 W power, and 5-min treatment time for sugarcane bagasse; 2.8% NaOH concentration, 86 W power, and 4.4 min treatment time for corncob biomass. At these optimal conditions the percentage delignification was 56% while the cellulose and hemicellulose yields were 62% and 30% respectively for plantain pseudostem; the percentage delignification was 63% while the cellulose and hemicellulose yields were 74% and 22%, respectively for sugarcane bagasse whereas the percentage delignification was 66%, while the cellulose and hemicellulose yields were 64% and 18%, respectively for corncob biomass.

The optimal yield with microwave-alkaline pre-treatment of plantain pseudostem obtained in this study is much higher than the yield reported by Sawarkar *et al.* (2022) in which cellulose content of banana stem was increased from 60.84% to 75.48% (increase of 14.64%) after being treated in autoclave with 7.15% NaOH at 71.83 °C for 7.97 hrs, whereas cellulose yield in this study was increased from 35% to 62% (increase of 27%).

Because microwave-alkaline removes lignin, exposing more cellulose, the 27% increase in cellulose observed in the current study (which was not observed in the previous study when autoclave was used) could be attributed to microwave-alkaline effectiveness in removing lignin. Although the percentage of lignin removed in this study is lower than that reported by Gazliya and Aparna (2021) who reported that microwave-alkaline pre-treated banana peduncle showed 60.86% delignification at 6.25N NaOH, the lower concentration of sodium hydroxide used in this study is preferable for a safer and cleaner environment. Shimizu *et al.* (2018) also reported a significant loss in hemicellulose percentage (from 19.32% to 4.38%) due to the use of a high percentage (25%) of NaOH solution. Although a higher percentage of delignification (61%) was reported, this increase is not industrially justifiable given the significant loss of hemicellulose, which is critical for bioethanol production, and, more importantly, the environmental hazards that a 25% NaOH solution could cause. Furthermore, Narron *et al.* (2016) reported that using severe conditions during a NaOH treatment resulted in ineffective lignin removal due to repolymerization or condensation reactions of lignin when using high NaOH concentrations. The optimal conditions generated in this study are preferable because the power required is low, the NaOH concentration is low, and the treatment time is short. Most importantly, there is an abundance of cellulose and hemicellulose, both of which are required for bioethanol production.

A study by Rezende *et al.* (2018) on the pre-treatment of sugarcane bagasse found a 40% (35% to 85%) increase in cellulose content of sugarcane bagasse after acid-alkali pre-treatment, whereas the current study found a 36% increase in cellulose content. Meanwhile, the optimal yield with microwave-alkaline pre-treatment in this study is significantly higher than the yield reported by Wang *et al.* (2019), in which the cellulose content of sugarcane bagasse was increased from 60.84% to 75.48% after being

autoclaved with 7.15% NaOH at 71.83 °C for 7.97 h. Furthermore, the current study is clearly more environmentally friendly (lower NaOH concentration) and more industrially viable with a shorter time and lower power of 86 W used as opposed to 500 W used in the previous study. In another study, Binod *et al.* (2012), pre-treated sugarcane bagasse biomass with 1% NaOH at 100-900 W for 1- 30 min, and the optimal conditions of 1% NaOH, 600W microwave power, and 4 min resident time yielded the highest reducing sugar. Despite the fact that the sodium hydroxide concentration in the previous study was much lower than the concentration used in the current study, the microwave power in the current study is significantly lower, which may make the present study more industrially feasible.

The optimal yields with microwave-alkaline pre-treatment of corncob biomass obtained in this study were lower than those reported by Pei *et al.* (2014), who reported values of 79.4%, 86.18%, and 10.68% for percentage delignification, cellulose content, and hemicellulose content when 8% NaOH was used to pre-treat plantain pseudostem biomass at 500 W for 3 min. Although the previous study obtained a higher yield in less time than the current study, it is clear that the current study is more environmentally friendly (lower NaOH concentration) and more industrially viable with a lower power of 86 W used as opposed to 500 W. In another study, Chongkhong and Tongurai (2018) pre-treated corncob biomass at 1% NaOH using 900 W for 20 min to obtain a yield of 52.9% cellulose, which was significantly lower than the yield obtained in the current study despite the higher power used.

When the yield from each agrowaste was evaluated under optimal conditions, the percentage holocellulose contents were 92%, 96%, and 92% for plantain pseudostem biomass, sugarcane bagasse, and corncob biomass, respectively. Meanwhile, the total lignin removal percentage was 56%, 63%, and 66% for Plantain pseudostem biomass,

sugarcane bagasse, and corncob biomass respectively. When compared to other pre-treated agrowaste, sugarcane bagasse has the highest holocellulose yield and the least amount of lignin remaining. However, despite the higher initial holocellulose content (77%) in Table 4.1, and harsher pre-treatment conditions (2.8% NaOH, 86 W, 4.4 min) in Table 4.4c for corncob biomass, the yield was not significantly higher than the yield obtained from plantain pseudostem biomass, which had a lower initial holocellulose content (65%) when a milder (1.97% NaOH, 70 W, and 5.0 min) pre-treatment conditions were used. As a result, plantain pseudostem biomass may be considered a better option than corncob biomass.

A confirmatory test to validate the optimal conditions is shown in Appendix B while the statistical significance (Table 2, Appendix C) for the models shows that the design expert software suggested two factor interaction (2FI) models for all responses in the pre-treatment of plantain pseudostem biomass, sugarcane bagasse, and corncob biomass, while a quadratic model was suggested for only the percentage hemicellulose retained in plantain pseudostem biomass. Therefore, in the model developed for each of the responses in the present study, a significant effect was obtained when two variables interact with each other.

The R^2 correlation coefficient, which is the ratio of regression sum to overall sum of squares, is used for overall model prediction compatibility. Furthermore, R^2 calculates the overall deviation of predicted model values from the mean. In order to describe excellent prediction efficiency, the R^2 value must be close to 1.0. The models developed for this study were significant at $p < 0.05$, and the R^2 obtained for the models in this study ranged from 0.92 to 0.98, implying that the models explained more than 90% of the variation observed in the response, indicating that all of the models developed in this study have statistical relevance for the experimental design. This is consistent with the

model developed by Hamouda *et al.* (2015), who obtained an R^2 value of 0.953 which is an indication of high model significance when sugarcane molasses was used to produce bioethanol.

Model equation (Table 3 a-c, Appendix C) establishes the foundation for future reproducibility of the experiment under consideration, with no expected significant difference in response. The software presents the equations in coded factors and in actual factors. The coded equations are determined first, and then the actual equations are derived from them. The coded equation is useful for determining the relative importance of the factors by examining the coefficients of the factors. Also, the value of the coefficient is an indication of the extent of influence such factor has on the responses.

The interaction between variable factors as depicted visually by design expert software is shown in Figure 4.1, to Figure 4. 3 for plantain pseudostem biomass, sugarcane bagasse and corncob biomass respectively. The difference in response value is represented by the colour variation. The red colour represents the highest value in the current study, while the blue colour represents the lowest value. The results of the surface plot of response for each agrowaste are discussed further below.

a. Plantain pseudostem

The interactive effects of variable factors on percentage delignification of plantain pseudostem biomass is shown in Figure 4.1(a-c) When the treatment time was kept constant, the interaction of NaOH concentration and microwave power resulted in the highest percentage delignification of 67% at 1.08% sodium hydroxide and 680 W microwave power. Furthermore, a high percentage (63%) of lignin removal was observed when sodium hydroxide and microwave power were 2.96% and 83 W, respectively, whereas the lowest percentage delignification (35%), was observed when NaOH

concentration and microwave power were 1.05% and 80 W, respectively. This indicates that high delignification in plantain pseudostem biomass at constant time was obtained when the relationship between NaOH concentration and microwave Power was inversely proportional, whereas percentage lignin removal was low when both NaOH concentration and microwave Power were either low or high. This confirms the finding in the model equation for the delignification of plantain pseudostem biomass where the coefficient of AB (NaOH concentration and microwave Power) was negative (-8.17). As a result, depending on the resources available, a decision will be made to use either a high NaOH concentration or a high microwave power to obtain a high percentage lignin removal at constant time from plantain pseudostem biomass at an industrial level.

When the microwave power was kept constant, highest percentage of cellulose (65%) was retained when NaOH concentration and treatment time were in inverse relationship, whereas when both factors were either low or high, the percentage of cellulose retained in plantain pseudostem biomass was low. This supports the negative AC (NaOH concentration and treatment time) coefficient observed in the model equation for percentage cellulose retained in plantain pseudostem biomass. When the treatment time was set to 3 min, a high NaOH concentration (2.95%) at a high microwave power (685 W) resulted in a high percentage of cellulose retained. No difference at $p < 0.05$ was observed, in the yield of percentage cellulose retained when microwave power and treatment time interacted at constant NaOH concentration based on the uniform colour observed in the response plot of the interaction between microwave power and treatment time. As a result, to retain a high cellulose content in plantain pseudostem biomass, the most important factor is NaOH concentration, which can be directly proportional to microwave power but inversely proportional to treatment time, as observed in the current study. This supports the findings of Ethaib *et al.* (2017), who found that an extended

treatment time in microwave-alkaline treated wheat straw resulted in a low cellulose yield due to the degradation of cellulose inhibitory products.

At constant time, the percentage hemicellulose yield increased with NaOH concentration but decreases with power. When the NaOH concentration was held constant at 2%, the hemicellulose yield increases as the Power and treatment time were reduced. This supports the findings of Ethaib *et al.* (2017), who discovered that cellulose and hemicellulose degrade into inhibitory products when exposed to high microwave power for an extended period of time.

b. Sugarcane bagasse biomass

The interactive effects of variable factors on percentage delignification of sugarcane bagasse biomass are shown in Figure 4.2 (a-c). When the power was kept constant at 385 W, the percentage delignification of sugarcane bagasse biomass was highest (77%) at high NaOH concentration (2.98%) and extended time of 4.81 min, but it was lowest when both NaOH concentration and treatment time were low. This same trend (direct relationship with yield) was observed for other variable factors when the third factor was kept constant.

The interactive effects of variable factors on cellulose content showed that at constant time of 3 min, maximum percentage Cellulose yield (>70%) can be obtained when the relationship between NaOH concentration and treatment time are in the inverse. However, when power is kept constant at 385 W, cellulose yield increased with increase in both treatment time and NaOH concentration. Similar to the observation in plantain pseudostem biomass, at constant NaOH (2%), statistical difference was not observed in the retention of cellulose when both treatment time and microwave power were interacted. This is evident in the uniform colour of the response surface plot.

The interactive effects of variable factors on percentage hemicellulose yield of sugarcane bagasse biomass showed that when treatment time was kept constant at 3mins, highest hemicellulose yield of 22% was obtained when both NaOH concentration and microwave power were low while the lowest hemicellulose was retained when both NaOH concentration and microwave power were high. However, when the power was kept constant at 385 W, high percentage of hemicellulose was retained either at low or high NaOH concentration in an extended time.

c. Corncob biomass

The interactive effects of variable factors on percentage delignification of corncob biomass are shown in Figure 4.3 (a-c). The interactive effect of sodium hydroxide concentration and power while the time was kept constant at 3 min showed that the highest percentage delignification of 59% was observed at 2.98% of sodium hydroxide when operated at 87 W, but a low percentage of lignin was removed when both microwave power and NaOH concentration were low. Therefore, it can be seen from the plot that, percentage delignification increased with increase in NaOH concentration and reduction in power when the time is kept constant. The interactive effects of sodium hydroxide concentration and time when the power was kept constant at 385 W showed that a percentage delignification of 66% was observed from the plot at 2.95% sodium hydroxide concentration in 4.96 min, while, 39.7% delignification was observed at 1.2% NaOH at 1.97 min. Hence when power was kept constant, percentage delignification of corncob biomass was directly proportional to time and sodium hydroxide concentration. The interactive effects of power and time when NaOH was kept constant showed that the highest percentage delignification (60%) of corncob biomass was obtained when microwave power was 690 W and treatment time was 4.96 min whereas, the lowest percentage delignification (34%) was obtained at 91 W and 1.08% of NaOH. This

indicated that percentage delignification increased with increase in time and power when the concentration NaOH was kept constant.

The percentage cellulose content increased as NaOH concentration increased (2.96%) and power was reduced (102 W) at constant time. When power was kept constant at 385W, percentage cellulose retained in corncob biomass increased with increase in both treatment time and NaOH concentration. A further increase in NaOH concentration beyond 2% at this power (385 W) may result in cellulose content reduction with time. However, the interactive effects of power and reaction time at constant NaOH concentration resulted into the highest percentage of cellulose retained (58%) when power was low (107 W) and time was high 4.85 min.

The interactive effects of variable factors on percentage hemicellulose yield of corncob biomass showed that at constant time (3 min), the highest percentage hemicellulose retained (30%) was obtained when power was high (675 W) and NaOH concentration was low (1.04 min). However, when power was kept constant, 33% hemicellulose was retained when both NaOH concentration and treatment time were low. Also, when NaOH was kept constant, highest hemicellulose (33%) was retained when high microwave power (692 W) was applied for a short time (1.16 min).

Therefore, from the interactive effects of variable factors on the responses from microwave-alkaline pre-treatment of the chosen agrowastes, it is possible to conclude that percentage lignin removal has a direct relationship with treatment time and microwave power. This supports the findings of Jablonowski *et al.* (2022), who found a positive correlation between microwave power and lignin removal in rice straw. However, the highest cellulose yields (71%, 62%, and 64% for SB, CC, and PS, respectively) were obtained when NaOH concentration was high and power was low, but in either case the

treatment time must be kept short because extended time reduces yield. The general observation for hemicellulose retained in agrowaste is that high yield was obtained when the power was low, but if high power is to be applied, as in the case of corncob biomass, then it must be at low NaOH concentration for a short time. This supports the findings of Ethaib *et al.* (2017), who discovered that cellulose and hemicellulose degrade into inhibitory products when exposed to high microwave power for an extended period of time.

4.2.1 b: Characteristics of agrowaste pre-treated at optimal conditions

i. Crystallinity index microwave-alkaline pre-treated and unpre-treated agrowastes

The primary goal of chemical pre-treatment steps is to increase the surface area and porosity of the substrate, remove amorphous portions to expose cellulose crystallinity, and maximize sugar production during the saccharification process (Zhang *et al.*, 2021). Microwave irradiation with aqueous NaOH degrades lignin and hemicelluloses and exposes the crystalline region of the cellulose fibril. This is accomplished through the cleavage of intermolecular ester bonds, which crosslink lignin and other components such as hemicelluloses.

The lignocellulosic biomass (sugar cane bagasse, plantain pseudostem biomass and corncob biomass) used in this study contained mainly cellulose, hemicellulose and lignin. The higher the lignin and hemicellulose contents of a lignocellulosic material, the lower its crystallinity index. Figures 4.4 – 4.6 show the crystallinity index from the XRD profiles of untreated and treated plantain pseudostem biomass, sugarcane bagasse, and corncob biomass. The percentage crystallinity index (C.I) was calculated for this study using the integrated peak intensities of the $\bar{1}01$, $\bar{1}11$ and 002 diffraction planes for all the agrowaste. There are increases in the intensities of the peak in the diffractogram

of pre-treated agrowastes at $\bar{1}01$, $\bar{1}11$ and $[002]$ diffraction planes at 2 thetas when compared to the unpre-treated agrowastes.

The diffraction angles of untreated plantain pseudostem (12.96° , 22.29° and 35.7°) is closer to the diffraction angles of pre-treated plantain (15.02° , 22.25° and 35.2°); also the diffraction angles of untreated sugarcane bagasse (16.67° , 22.05° and 35.2°) are closer to the diffraction angle of pre-treated sugar cane (16.25° , 22.22° and 35.9°), and the diffraction angle of untreated corncob biomass (16.11° , 21.68° and 34.47°) are close to the diffraction angle of pre-treated corncob biomass (12.96° , 21.85° and 34.54°). The closeness of the diffraction angles of both treated and untreated samples is an indication that there is no conversion from native cellulose I to cellulose II or cellulose III. All these angles correspond to the lattice planes of $\bar{1}01$, $\bar{1}11$ and $[002]$ respectively, which are specific to the crystalline region of cellulosic materials.

The Crystallinity Index (C.I) of the untreated plantain pseudostem biomass in this study was 35.66% while pre-treated plantain pseudostem biomass was 58.36%, this is slightly higher than the 46.76% C.I reported for pre-treated plantain pseudostem biomass residue when enzyme pre-treatment was used by Luz *et al.* (2020). This implies that the pre-treatment conditions in the present study removed more lignin from the agrowaste thereby exposing more of the crystalline part of agrowaste sample to enzymatic hydrolysis.

The C.I of the untreated sugarcane bagasse and microwave-alkaline pre-treated sugarcane bagasse in this study were 35.94% and 43.31%, respectively. This is below 41.41% and 46.76% C.I reported for untreated and alkaline pre-treated sugarcane bagasse respectively by Luz *et al.* (2020). However, it is clear that the difference in the crystallinity index of treated and untreated samples in the current study (7.32%) was greater than the difference (5.35%) in the crystallinity index of treated and untreated samples in the previous study.

This suggests that the pre-treatment conditions in the current study had a greater positive influence on the crystallinity of pre-treated sugarcane bagasse. The results showed that microwave-alkaline pre-treatment of sugarcane bagasse biomass increases cellulose crystallinity effectively. According to Ovalle-Serrano *et al.* (2018), treatment with hydrogen peroxide in basic medium allows the removal of amorphous constituents such as lignin and hemicellulose, thereby increasing the crystallinity of these lignocellulosic materials. As a result, more internal surface area of the crystalline region would be exposed to enzymatic hydrolysis, resulting in a high bioethanol yield.

In this study, the C.I of the untreated corncob biomass was 17.13%. This is less than the 33.32% C.I of the pre-treated corncob biomass, indicating that the microwave-alkaline pre-treatment removed lignin from the corncob biomass, exposing the crystalline part of the agrowaste. Jamaldeen *et al.* (2018) also reported an increase in C.I of pre-treated agrowaste as a result of the effect of the pre-treatment conditions.

In conclusion, a critical examination of the XRD results of the three agrowastes chosen for this study may indicate that there is a better improvement in the crystallinity of corncob biomass because the difference (16.19%) in the C.I of the unpre-treated when compared to the pre-treated is the highest among the three agrowaste, whereas the difference (11.6%) in the C.I of treated and untreated plantain pseudostem biomass sample was higher than the difference (7.32%) in the C.I of treated and untreated sugarcane bagasse. This could imply that more polysaccharides will be available for hydrolysis in corncob biomass, resulting in a higher bioethanol yield. This further confirms the results of the compositional analysis in this study where corncob biomass was found to contain the highest number of polysaccharides among the three agrowaste of choice.

ii. Infrared Spectra of microwave-alkaline pre-treated and unpre-treated agrowastes

Infrared Spectra of the untreated and treated plantain is presented in Figure 4.7. The waveband of the unpre-treated plantain pseudostem biomass showed wider wavelength ranging from 711.5 to 3954.2 cm^{-1} while the treated plantain has shorter wavelength between 1571 and 3954.2 cm^{-1} . Infrared Spectra of the untreated and treated sugarcane bagasse is presented in Figure 4.8. The waveband of the pre-treated sugarcane bagasse had wider wavelength ranging from 626.2 to 3980 cm^{-1} while the treated sugar cane had shorter wavelength between 1119.5 and 3980 cm^{-1} . Also, infrared Spectra of the untreated and treated corncob biomass is presented in Figure 4.9. The waveband of the pre-treated corncob biomass how wider wavelength ranging from 626.2 to 3998.2 cm^{-1} while the treated corncob biomass has shorter wavelength between 994.5 and 3998.2 cm^{-1} . The OH-vibration (acid and methanol) was observed between 2995 cm^{-1} to 4000 cm^{-1} . This functional group is present in cellulose, hemicellulose and lignin. The treated agrowastes had a higher absorbance intensity from 2995 cm^{-1} to 3401.54 cm^{-1} , but the absorbance intensity decreased as it approached 4000 cm^{-1} . The change was caused by the variation of binding energy of hydrogen in the system of internal and intermolecular interactions. The decline in the intensity at 3401.54 cm^{-1} is an indication that lignin and hemicellulose had experienced bond loss due to the change in the hydrogen bond. A strong broad band of H-C-H functional group with an increased intensity in pre-treated agrowaste existed between 2208 cm^{-1} to 2995 cm^{-1} . This stands for alkyl and aliphatic compounds. The H-C-H group is present in cellulose, hemicellulose, and lignin, but symmetric and asymmetric methyl and methylene cellulose groups are stretched (Boukir *et al.*, 2019). The treated agrowaste biomasses had higher absorbance intensity within this region than the agrowaste biomasses. This is due to loss of lignin during pre-treatments as it leads to

the removal of the aromatic structure of lignin thereby increasing the crystallinity of the pre-treated sample (Luz *et al.*, 2020). The band between 1765 cm^{-1} to 1715 cm^{-1} corresponds to the C=O functional group. It stands for the ketone and carbonyl compound and it is only present in hemicellulose. The band at 1646 cm^{-1} corresponds to the fiber-OH group which stands for the bending vibration of the absorbed water and it is only present in cellulose. It has a more prominent absorbance peak in the treated agrowaste biomasses than the untreated agrowaste biomasses as a result of the delignification. (Luz *et al.*, 2020; Anggono *et al.*, 2019).

Conclusively, the reduction in the band width, which corresponds to the amount of lignin removed, for both treated and untreated agrowastes, tend to be more prominent in plantain pseudostem biomass (711.5- 1571) cm^{-1} when compared to sugarcane bagasse (626.2-119.5) cm^{-1} and corncob biomass (626.2-994.5) cm^{-1} . This implies that the pre-treatment conditions were more favourable to plantain pseudostem biomass as it removed more lignin from the agrowaste. Therefore, plantain pseudostem biomass could be a better biomass for good ethanol production.

iii. Morphological change of microwave-alkaline pre-treated and unpre-treated agrowastes

The Scanning Electron Microscopy (SEM) image of both the treated and the untreated agrowaste are presented in Plate 4.1 to Plate 4.3. The untreated agrowaste has a compact homogeneous structure of raw biomass, with no visible pores within the structure. On the contrary, microwave-alkaline pre-treated agrowaste exhibited a distortion in the structure of the biomass. NaOH causes the conformation of the fiber to expand, the structure to loosen, and the surface area of the fibers to increase (Sahare *et al.*, 2012). These modifications primarily facilitate the exposure of the cell to subsequent enzymatic

hydrolysis. The disruption of the cross linkage between the linear cellulose chains causes the formation of such hollow spaces. According to Haldar *et al.* (2018), pre-treatment causes lignocellulosic structure degradation, resulting in maximum cellulose linear chain deformation and the formation of pores that release reducing sugars. These modifications improve enzyme accessibility to cellulose and hemicellulose, thereby improving enzyme hydrolytic performance. As a result, microwave-alkali pre-treatment can improve the overall saccharification rate of enzymatic hydrolysis and ensure a high ethanol yield

4.2.2 a: Qualitative and quantitative potentials of microorganisms for enzyme production and fermentation process

Microorganisms are the most powerful and convenient sources of industrial enzymes, fungi has been established as the source of a wide range of extracellular enzymes including cellulases and xylanases (Golgeri *et al.*, 2022). Fungal cellulases and xylanases are two of the most widely used microbial enzymes in a variety of industrial and environmental applications, including biofuel production (Saini and Sharma, 2021). In the present study, the macroscopic and microscopic features of pure isolates of fungi used for enzyme production and ethanol fermentation are shown in Table 4.5 and 4.6 respectively while the appearance on SDA plate is shown in Appendix E (Plate 4 and 5 respectively). These organisms were screened both quantitatively and qualitatively for the ability to perform the desired duties.

According to research, one of the most important aspects of enzyme production is the type of substrate used as a carbon source (Liu *et al.*, 2021). In the present study, Pre-treated agrowastes of choice (plantain pseudostem biomass, sugarcane bagasse, and corncob biomass) were used as carbon sources in the qualitative and quantitative screening of organisms for enzyme production. This decision was based on previous research that demonstrated the significance of using alternative substrates such as

lignocellulosic agrowaste as a carbon source for enzyme production . This will help to reduce the cost of enzyme production while also ensuring the availability of the substrate. In their study, Bhatia *et al.* (2012) discovered that agricultural waste, particularly lignocellulosic biomass, is an excellent source of microbial cellulase production. Previously, Abu (2005) reported that crude enzyme produced using sorghum pomace as substrate was more active than enzyme produced using commercial carboxyl methyl cellulose. Da Silva *et al.* (2005), also reported the production of cellulase and xylanase by Fungi in solid state fermentation using various agricultural residues as substrates (wheat bran, sugarcane bagasse, orange bagasse, corncob, green grass, dried grass, sawdust, and corn straw) and characterized the enzymes

i. Qualitative profile of organism for Enzyme production

In this study, ability of different lignocellulosic substrates to elicit the production of lignocellulosic enzymes by the microorganisms was made visible by the formation of zone of clearance using Congo red test. The organisms which showed considerable zone of clearance during the Congo red test are shown in Plate 4.4. The dimensions of hydrolytic zone of clearance are shown in Table 4.7. Organisms RD5 and FBL which had the best hydrolytic zone of clearance on plantain pseudostem agar plate and sugarcane bagasse agar plate were chosen for further studies.

ii. Quantitative profile of organisms for enzyme production

The activity of the enzyme produced by the isolated organisms are shown in Table 4.8 and Table 4.9 for cellulase and xylanase respectively. Cellulase with the highest activity (15.35 ± 0.48 IU/mL) was produced by FBL which used sugarcane bagasse as carbon source after 48 h. This value was higher than the highest value (6.95 ± 0.12 IU/mL) obtained when carboxyl methyl cellulase was utilized as carbon source by the same organisms. This confirms the report by Abu (2005) and Ravindran *et al.* (2018), that

lignocellulose materials are better carbon sources than commercially available carboxyl methyl cellulose because significant amounts of glucose isomerase were not detected in cultures grown on pure cellulosic substrates. However, when agricultural plant residues were used, the glucose isomerase enzyme was produced rapidly and in significant amount because glucose isomerase interconverts aldoses to ketoses (Zhang *et al.*, 2019a). This enzyme is produced by most bacteria and fungi to utilize cellulose as food thereby producing extracellular enzymes such as cellulase and xylanase. The value of cellulase activity obtained in this study is higher than the values reported by Golińska and Dahm (2011), who estimated cellulase activity in different *Streptomyces* sp. at different pH and temperature and found enzyme activity in the range of 8-13 IU/mL using sugarcane bagasse as substrate. The value of enzyme activity obtained in this study is, however, lower than the value (20 IU/mL) reported by Verma *et al.* (2018) , when 1.5% lignocellulosic substrates (*Luffa cylindrica* and *Litchi chinensis* peel) were used as carbon source.

The xylanase with the highest activity (38.04 ± 0.17 IU/mL) which was obtained after 96 hs was produced by RD5 isolated from refuse dump site which used plantain pseudostem biomass as carbon source. The value obtained for enzyme activity is comparable to the value (38.84 ± 0.17 IU/mL) obtained when commercial birch wood xylan was used as the carbon source. This activity is greater than the value reported by Singh *et al.* (2012b), who used rice bran as a carbon source and obtained a maximum xylanase activity of 30.15 IU/mL after 48 h of incubation. However, the value obtained in this study is lower than the value reported by Raj (2016), who found the highest xylanase activity to be 56.21 IU/mL when wheat bran was used as carbon source and also 50.89 IU/mL when birchwood xylan was used as a carbon source. The difference in enzyme production by different organisms on a variety of lignocellulosic materials could be due to a variety of

factors such as variable cellulose content in lignocellulose obtained from different plant sources, heterogeneity of structure and cellulolytic abilities of the organisms at different degrees, and culture conditions (Chinedu *et al.*, 2016)

iii. Qualitative profile of organisms for fermentation process

The organism isolated for the fermentation process (Plate 5, Appendix E) was qualitatively tested for their ability to ferment simple sugars using a physiological test, as shown in Table 4.10. All of the strains fermented glucose, sucrose, and fructose with gas production and colour change, except PP, which fermented all simple sugars except lactose. Only PP and RB6 were able to ferment xylose and arabinose; the medium containing xylose sugar into which organism T was inoculated also changed colour, but there was no evidence of gas production in the Durham tube. As a result of the aforementioned observations all the organisms that fermented hexose sugars, as well as organisms RB6 and T, were chosen for quantitative examinations in the current study.

iv. Quantitative profile of organisms for fermentation processes

Organisms PW1, PW2, PW3, PP and two organisms that showed potential to ferment pentose sugars (T and RB6) were chosen for quantitative screening to monitor their ability to utilize hexose (glucose sugar) and pentose (xylose sugar) for bioethanol production, and the results are shown in Figure 4.10. Maximum sugar consumption and ethanol yield were observed at the 96th h. This is similar to the work of Zabed *et al.* (2014), who performed fermentation at 30 °C and obtained the highest ethanol concentration yield (52.1 g/L) at the 96th h of the experiment. Meanwhile, Al-Judaibi (2011) achieved maximum ethanol yield from beet molasses fermentation after 48 h of incubation at 28°C using *S. cerevisiae*. At the 96th h, organism T used the most glucose, but organism RB 6 produced a higher concentration of ethanol. Furthermore, all of the yeast produced a high ethanol yield from glucose, but organism PP produced the highest yield. According to

Tulashie *et al.* (2021), the decreasing concentration of glucose as fermentation progresses over four days is due to the presence of Zymase, a naturally occurring enzyme complex that is responsible for the reduction of sugar during fermentation as it converts it to ethanol. Organisms PP and RB 6 produced the highest concentrations of ethanol from glucose and xylose, respectively, suggesting that they may be capable of effectively utilizing the fermentable sugars in lignocellulose to produce bioethanol.

v. Ethanol tolerance of fermentation organisms

Furthermore, as shown in Figure 4.11. an ethanol tolerance test was performed on each organism to determine their ability to withstand different concentrations of ethanol. According to Ukwuru and Awah (2013), ethanol tolerance is a unique property of organisms that makes it exploitable for industrial applications. Organisms RB6 and PP had a high tolerance of 50.55% and 50.2% respectively for ethanol concentration up to 12%. This supports the findings of Tikka *et al.* (2013), who isolated fifteen yeast strains using various fruit extracts as carbon sources, seven of which could tolerate ethanol concentrations up to 12.5%. The ethanol tolerance observed for the organisms in this study was higher than the tolerance level (8%) reported by Aminu *et al.* (2018) for *S. cerevisiae* isolated from palm wine, but lower than the tolerance level (14.7%) reported by Ukwuru and Awah (2013). This means that the organisms chosen for this study can stay metabolically active in the fermentation medium and tolerate up to 12% alcohol during the fermentation process.

4.2.2 b: Molecular identification of screened organisms for enzyme production and fermentation process

The two organisms, FBL and RD5 selected for the production of cellulase and xylanase respectively as well as the two organisms (RB6 and PP), for glucose and xylose fermentation respectively were identified at molecular level. The names, percentage similarity as well as the accession numbers of the identified organisms are shown in Table 4.11. The sample organism (accession number OP107821) for cellulase production had 99.83% similarity with *Aspergillus flavus*, while the sample organism (accession number OP107822) for xylanase production had 99.82% similarity with *Aspergillus niger*. This supports the findings of da Silva *et al.* (2019), who found that filamentous fungi, particularly *Aspergillus* sp., are more useful producers of xylanase and cellulase because they can produce high levels of extracellular enzymes and are easier to cultivate than bacteria and yeast. Also, the sample organism (accession number OP107823) for xylose fermentation had 99.47% similarity with *Mucor indicus*, while the sample organism (accession number OP107824) for glucose fermentation had 99.47% similarity with *Saccharomyces cerevisiae*. This study confirms the fact that *Saccharomyces cerevisiae* is very good at fermenting hexose sugar (Dmytruk *et al.*, 2016). Also, *Mucor indicus* has been reported to ferment xylose and glucose sugars to produce high bioethanol yield (Sharifyazd and Karimi, 2017; Karimi and Karimi, 2018)

Phylogenetic analysis was carried out using maximum identity scores; the phylogenetic tree comprised 20 taxa including the strains isolated in this study as shown in Figure 4.12. The 16S rRNA gene has become a reliable tool for the identification and classification of fungi because studies of 16S rRNA are necessary to achieve unambiguous identification at the species level. Each forward ACCACGGTAAGTTGCTCATC and backward CCGACCTTCTTGTTGTCCTT primer amplified a fragment of the 16S rRNA gene, and a single discrete PCR amplicon band of 690 bp and 400 bp was observed from *Aspergillus*

flavus and *Aspergillus niger* when resolved on agarose gel for both isolates, as shown in Plates 4.5 and Plate 4.6. CelE gene from *Aspergillus flavus* was found to be 99.56% similar to endo-beta-1,4-glucanase, while xyn11B gene from *Aspergillus niger* was found to be 100% similar to endo-1,4-beta-xylanase. This validates the findings of da Silva *et al.* (2019) that filamentous fungi, particularly *Aspergillus sp.*, are more useful producers of xylanase and cellulase.

4.2.3 a: Immobilization techniques developed for the co-immobilization of xylanase, cellulase, and suitable pentose and hexose sugar fermenters

i. Porous biochar as support for enzyme immobilization

The efficiency of immobilized enzyme is determined by the nature of the enzyme and the support material. The interaction between the enzyme and the support gives the immobilized enzyme specific chemical, biochemical, mechanical, and kinetic properties (Lee *et al.*, 2021). Therefore, it is very important to choose a suitable support for the immobilization of enzyme. Porous materials such as biochar are commonly used for enzyme immobilization because it is thermally, mechanically and chemically stable and insoluble in the solution for the immobilization and catalytic process. Also, biochar possesses the additional feature of cation exchange capacity owing to the presence of residual carboxylic acid functionalities on its graphitic backbone making it an attractive material for immobilization support. Furthermore, ability of biochar to accept and donate electrons makes it an ideal candidate for biocatalytic support (Pandey *et al.*, 2020)

Chemical activation of biochar with acids, bases, or oxidizing agents has been demonstrated to introduce the desired surface functional groups (Sajjadi *et al.*, 2019). Alkali treatment increases surface basicity through the introduction of hydroxyl groups, as well as increase its surface area and porosity (Kumar *et al.*, 2022). In the present study, biochar was prepared from alkali activated sugarcane bagasse and the biochar yield (Plate

6, Appendix F) was 33.5% of the initial sugarcane bagasse pyrolyzed at 450 °C. This yield is higher than that reported by Manyatshe *et al.* (2022), who obtained 22.57% and 16.79% of biochar after pyrolysis of sugarcane bagasse at 400 °C and 600 °C, respectively. According to Wang *et al.* (2021), the biochar yield varies greatly depending on the pyrolysis temperature as well as the feedstock materials. Al-Wabel *et al.* (2013) found that increasing the pyrolysis temperature reduced the yield of conocarpus biochar, with yields of 51.33%, 31.86%, 27.22%, and 23.19% obtained at 200 °C, 400 °C, 600 °C, and 800 °C, respectively. The decreasing biochar yield as the pyrolysis temperature increased was ascribed to the loss of cellulose and hemicellulose as well as a high number of aromatic lignin being converted into biochar during the process of pyrolysis (Manyatshe *et al.*, 2022). Furthermore, Ghani *et al.* (2013) demonstrated that lignin is not converted into a hydrophobic polycyclic aromatic hydrocarbon (PAH) at lower temperatures (less than 500 °C), and biochar becomes more hydrophilic. As a result, the biochar obtained in this study, which was pyrolyzed at 450 °C, is very suitable for enzyme immobilization.

ii. Biochar-chitosan composite support for immobilization of enzyme

Despite the availability and sustainability of biochar, some limitations, such as a lack of reactive and hydrophilic groups and the inability to recover easily, are major barriers to its use in enzyme immobilization (Mo and Qiu, 2020). Chitosan is added to biochar powder and used as a dispersing and stabilizing reagent to form biochar-chitosan composites in order to conveniently and quickly recycle and reuse enzymes (Xu *et al.*, 2020). Chitosan is a non-toxic, biocompatible, and biodegradable chitin deacetylated product with reactive amino and hydroxyl groups (Li *et al.*, 2020). According to studies, chitosan powders alone are non-porous materials with a low surface area (less than 10 m²g⁻¹) and poor mechanical and thermal stability (Li *et al.*, 2018). However, when

chitosan and biochar are combined, the adsorption capacity of both biochar and chitosan is increased, and the separation of the composite from the reaction medium is facilitated. Chitosan-based composites have attracted great attention in various applications due to their impressive characteristics such as mechanical strength, chemical stability, surface area and structural properties. (Li *et al.*, 2018). In the present study, biochar-chitosan composite beads were prepared freshly and also dried at various thermal conditions to enhance the ease of separation from reaction medium. The characteristics of the beads that led to the selection of the support for enzyme immobilization are discussed further below.

4.2.3b: Characteristics of biochar-chitosan support prepared for co-immobilization

i. Average diameter of biochar-chitosan beads prepared at different drying conditions

The average diameters of biochar-chitosan composites prepared at different thermal conditions are shown in Table 4.12. The average diameters of the biochar-chitosan bead composites were 2.67 ± 0.32 mm, 2.54 ± 0.21 , 2.55 ± 0.41 mm, and 1.97 ± 0.17 mm, for fresh beads, air-dried beads, freeze-dried beads and oven-dried beads respectively. There was no significant difference in the average diameter of the beads except for oven-dried beads which were slightly lower than the other beads. This corroborates the study by Bilal *et al.* (2019) who reported that chitosan beads of average size 2.0 mm was effective for laccase immobilization.

Since the diameter of the beads obtained in this study fall within the range of diameter reported as suitable for laccase immobilization, this suggests that the biochar-chitosan beads prepared in this study may be suitable for the immobilization of cellulase and xylanase for the hydrolysis of lignocellulosic agrowaste. However, among the dried beads, freeze-dried beads had the largest average diameter (2.55 ± 0.41 mm), which is

consistent with the findings of Martin *et al.* (2019), who found that freeze-dried beads have the largest diameter among calcium-alginate beads prepared for pectinase immobilization. This was attributed to inability of the freeze-dried bead to shrink, transforming the areas of the former ice crystals into cavities cell-like structures as a result of frozen water sublimation within the matrix. Iliescu *et al.* (2014) reported in a similar study that lyophilization of freeze-dried beads resulted in stratified cell-like structure, which may enhance swelling capacity and also enable controlled release of its loaded content. As a result, the freeze-dried beads prepared in this study may further be suggested as a better candidate for enzyme loading.

ii. The swelling behaviours of biochar-chitosan beads

The swelling ability of hydrogel beads is an important feature to evaluate because it may influence the application of the product, which can range from drug delivery systems to adsorbents (Parin *et al.*, 2020). It can also indicate the number of available pores in the matrix. In this study, the swelling behavior fresh biochar-chitosan beads as well as biochar-chitosan beads dried at different drying conditions is as shown in Figure 4.13. Swelling ratio measurements are a straightforward method for characterizing crosslinked polymer networks, with a focus on liquid-retention capacities (Li *et al.*, 2020).

Solvent penetration into the polymer causes swelling because the solvent fills the void space between the polymeric chain network. External triggers such as pH, ionic strength, and environmental temperature can all influence swelling behavior in some cases (Flemming *et al.*, 2020). The major mechanism of reversible swelling ability is based on chemical bonds and physical interactions (Yang *et al.*, 2021). Fresh beads had the lowest swelling ratio of 0.31, while freeze dried beads had the highest percentage swelling ratio of 7.21. This confirms the report of Iliescu *et al.* (2014) on the ability of freeze-dried beads to have a higher swelling capacity. The high swelling capacity of freeze-dried beads

indicates that they have the capacity, in terms of large surface area and high pore volume which may enable high enzyme loading for hydrolytic processes thereby releasing optimal fermentable sugars for high bioethanol yield.

iii. Thermogravimetric curves (TGA) and the derivative thermogravimetric (DTG) curves of biochar-chitosan beads

The thermal properties of the biochar-chitosan composites beads were studied using TGA analysis at the temperature range of 30 to 800 °C. TGA and DTG thermograms of biochar-chitosan beads are shown in Figure 4.14 (a and b). Figure 4.14a shows the TGA curves and while Figure 4.14b shows the DTG result. The biochar-chitosan beads were more thermally stable at lower temperatures (< 200 °C) since the graph did not show a dramatic decline at this stage. The curves sloped downward with increasing temperature, indicating that the beads were less stable at higher temperatures. Initially, a 5% weight loss in biochar was observed, which was due to the release of water molecules from the pores and surface of the biochar (Adeniyi *et al.*, 2022). The second stage of degradation began at 180 °C and continued until 420 °C, when samples lost approximately 77.38% of their total weight due to the decomposition of biochar and chitosan main chains (Roy *et al.*, 2022). The burning of the char formed during analysis in the N₂ atmosphere was the final step in the decomposition of the biochar-chitosan bead samples.

Collectively, the thermal degradation behavior of all the four biochar-chitosan composites samples showed minor differences to each other. The oven-dried biochar-chitosan bead showed slightly higher thermal stability than the other three biochar samples at higher temperatures. TGA curves of the biochar-chitosan beads indicated that there was no phase separation between chitosan and biochar composite. It can be said that the obtained blends of beads are compatible. This is highly related to the interactions between biochar and chitosan through hydrogen bonding formation between their functional groups (-OH and

-NH₂ groups) which will then work synergistically to bind with the loaded enzyme, allowing the enzyme to be stable. The temperatures at which the mass change is most noticeable can be determined from the DTG curve as shown in Figure 4.14b. The graph shows that the majority of the mass change occurred around 400 °C. This is consistent with the findings of Iliescu *et al.* (2014), who found that the maximum degradation of freeze-dried Montmorillonite-alginate beads occurred at 490 °C. The ability of the beads prepared in this study to withstand high temperatures up to 400 °C without deterioration indicates that the prepared matrix can withstand any reaction up to this high temperature at the industrial level.

iv. Specific surface area, pore size and pore volume of biochar-chitosan composite

Physical activation and pyrolysis of biochar influences the structural properties such as surface area, pore size and pore volume (Roy *et al.*, 2022),). The surface area of native inactivated sugarcane bagasse biochar has been reported to be 33.1 m²/g (Raul *et al.*, 2021). However, alkali activation of bagasse, according to Yang *et al.* (2022), increases the specific surface area of the resulting biochar. Furthermore, the increased temperature during the pyrolysis process forces volatile substances out of the char, resulting in the formation of pores and an increase in surface area (Shaaban *et al.*, 2014).

This is advantageous for enzyme immobilization because increased support surface area leads to increased enzyme loading on the support matrix (Bilal *et al.*, 2019). Although the enlarged surface area decreases when the biochar is combined with chitosan, the existing surface area after chitosan combination is usually greater than the surface area of the initial native bagasse. Textural properties such as surface area, average pore size, and pore volume were estimated in the current study using well-known calculation methods such as the Barrett- Joyner-Halenda (BJH) models of Brunauer-Emmett-Teller

(BET), as shown in Figure 4.15. After pyrolysis at 450 °C, the surface area of activated biochar was 378 m² /g, but this size was reduced to 178.6 m² /g, 276.3 m² /g, 177.1 m² /g, and 170.8 m² /g when the biochar was combined with chitosan to form fresh, freeze-dried, air-dried, and oven-dried beads, respectively. Tomczyk *et al.* (2020) reported specific surface areas of 185.6 m² /g for activated sugarcane bagasse biochar and 154.7 m² /g for rice husks-biochar.

Other authors have reported that chitosan-modified biochar from other feedstocks has lower surface areas than unmodified biochar (Zhou *et al.*, 2013; Creamer *et al.*, 2016; and Godwin *et al.*, 2019). This is most likely due to the incorporation of chitosan in the biochar matrix blocking partial pores or changes in the chemical compositions of the biochar surface causing nitrogen to have less affinity for surface adsorption (Loc *et al.*, 2022). It has also been reported that the feedstock type influences the surface area of the resulting biochar (Li *et al.*, 2019).

The chitosan modification also had an effect on the pore volume and pore size of the biochar. The pore volume of the unmodified biochar was 0.184 cc/g in the current study, but after chitosan modification, the pore volume decreased to 0.088 cc/g, 0.136 cc/g, 0.087 cc/g, and 0.084 cc/g for fresh bead, freeze-dried bead, air-dried bead, and oven-dried bead, respectively. These values are higher than the values reported (0.007 cc/g, 0.006 cc/g, and 0.004 cc/g) by Waqas *et al.* (2018). which were the pore volumes of agricultural waste biochar pyrolyzed at 250, 350, and 450 degrees Celsius, respectively.

Freeze-dried beads had the highest pore volume (0.184 cc/g) when compared to other modified beads. Angin *et al.* (2018), reported similar total pore volume results (0.180 cc/g) for biochar obtained from agricultural biomass at a pyrolysis temperature of 450 °C, implying that the biochar obtained in this study had a higher pore volume, which

may enhance more enzyme loading for effective hydrolysis. Furthermore, Varma *et al.* (2019) demonstrated that a high heating rate during the pyrolysis process increases biochar porosity due to the release of volatile compounds. However, the pore size in the current study is mainly inversely proportional to the pore volume results. This is consistent with the findings of a previous study by Waqas *et al.* (2018), who discovered that the trends of pore volume were mainly inversely proportional to the pore size, possibly due to the extremely small size particles formed by high temperature being pushed into the pores, resulting in a decrease in total pore volume as the size increases.

In this study, the average pore size of the biochar-chitosan composite was in the 2 - 8 nm range specified for small mesoporous regime suitable as efficient absorbent. As a result, the biochar-chitosan beads developed in this study may be able to accommodate enough enzyme to allow for effective agrowaste hydrolysis in bioethanol production.

4.2.3c: Loading strategy for co-immobilized enzymes

Immobilization is well known for its ability to protect enzymes from inactivation and, eventually, denaturation under extreme conditions by creating a stable microenvironment. In industrial processes, the effectiveness of immobilized enzyme is primarily determined by the method of immobilization and the amount of soluble enzyme used. Although the activity of immobilized enzymes is typically lower than that of free enzymes due to decreased availability of enzyme molecules within pores or from slowly diffusing substrate molecules (Fernandez-Lopez *et al.*, 2017), enzyme immobilization remains desirable for industrial processes due to numerous benefits such as stability, specificity, reusability, and little or no contamination by the resulting product. Furthermore, studies have shown that multi-enzymes have a much higher initial reaction rate and product yield than a single immobilized enzyme. For example, Han *et al.* (2020) reported that when multi-enzymes were co-immobilized on porous microspheres and used to produce inositol

from 1% maltodextrin, the activity of co-immobilized enzymes was higher than the activity of free enzyme. The efficiency of immobilized enzyme is determined by the method of loading and the support used to immobilize the enzyme. In the present study, free cellulase and free xylanase were co-immobilized on biochar-chitosan supports and the activities are shown in Table 4.13. The loading of equal volume of both enzymes at the same time had the highest activity for xylanase (28.51 IU/mL) and for cellulase (15.48 IU/mL), which is comparable to the activity of the free enzymes. According to one study, the initial reaction rate of co-immobilized enzymes is accelerated because there is less or no lag time, which prevents the immediate action of singly immobilized or even free enzymes (Hwang and Lee, 2019; Wu *et al.*, 2022). This lag time occurs because the concentration of the intermediate products is initially very low, preventing the other enzymes in the reaction chain from expressing their activities from the start of the reaction. The synergistic effect of the co-immobilized enzymes to release fermentable sugars is also noteworthy, particularly for the current study. According to Song *et al.* (2016), xylanase improves cellulase activity by allowing the cellulase to efficiently hydrolyze cellulose after the interlocking xylan (hemicellulose) has been hydrolyzed. In the current study, the activity of co-immobilized enzymes was approximately 40% lower than that of free enzyme, which could be attributed to the method of immobilization or the nature of the support used. When three enzymes (glucose mutase PGM, inositol 1-phosphate synthase IPS, and inositol monophosphatase (IMP) were co-immobilized, Muley *et al.* (2018), observed a 20% reduction in activity compared to individual free enzymes; this reduction was reported to occur due to alterations in enzyme conformation caused by removal of water from the exterior surface during immobilization. A 40% reduction in activity of co-immobilized enzymes as compared to free enzymes observed in the current study may be considered acceptable in light of the other benefits of co-

immobilized enzymes such as reusability, which allows the same co-immobilized enzymes to be re-used several times with fresh substrates at each use, as opposed to the free enzyme, which became mixed with the product after only one use and cannot be re-used again.

Also, the immobilization efficiency was 89.29% and 82.29% for xylanase and cellulase co-immobilized at the same time on freeze-dried support. This result is higher than the immobilization efficiency (71.8%) obtained by Sadaqat *et al.* (2022) when cellulase was loaded on chitosan beads whereas some other author such as Wu *et al.*, (2022), obtained a higher immobilization yield of 91.5%. The variations in the immobilization efficiency can be dependent on the assay method used, the physical properties of the immobilized biocatalyst and the type of support. The co-immobilized enzymes were further characterized and compared with free enzymes to check its suitability for industrial process as discussed in the next section.

4.2.4. Enzymatic properties, storage stability and re-usability of free and immobilized moieties

i. Effect of pH and temperature on the activity of free and immobilized enzymes

After immobilization, the structure of the enzymes may be altered, which would change the accessibility of the active site, stability, and specificity (Bolivar and Nidetzky, 2020). Therefore, it is necessary to investigate the influence of pH and temperature on the activity of free and immobilized enzymes. Effects of reaction temperature on the catalytic activities of free and co-immobilized cellulase and xylanase were carried out at 30–90 °C as shown in Figure 4.16. The optimal temperature for xylanase, cellulase and co-immobilized enzymes were 50 °C, 60 °C and 70 °C respectively. This shift in temperature optima for the co-immobilized enzymes might occur due to the impairment of hydrophobic and secondary interactions of the free enzyme molecules within the matrix

which was later improved at higher temperature to attain the maximum catalytic activity. It has been reported earlier that co-immobilized pectinase and cellulase showed maximum relative activity at 60 °C which was 10 °C increase in temperature as compared to free enzyme (Bié *et al.*, 2022) Same finding was reported by Dal Magro *et al.*(2018), when cellulase, xylanase and pectinase were co-immobilized within iron oxide magnetic nanoparticles functionalized with ATPES where temperature optima was shifted from 55 °C to 75 °C after immobilization. This implies that the co-immobilized enzymes developed in this study can accommodate variations in process temperature up to about 10 °C. However, it may not work optimally below the optimal temperature of 70 °C.

Effects of pH on the catalytic activities of free and co-immobilized cellulase and xylanase was also performed at different pH levels (2.0 – 9.0) as shown in Figure 4.17. The optimal pH of co-immobilized enzymes was found to be between 4.5 and 7.0, whereas the optimal pH of free cellulase and free xylanase were 6 and 5, respectively (Table 4.15). The increased activity observed for co-immobilized enzymes over a wide pH range when compared to free enzyme supports the findings of Bié *et al.* (2022), who reported that extended pH stability was observed when pectinase and cellulase were co-immobilized in ferrite-based nanoparticles. This means that the co-immobilized enzymes prepared in this study will remain optimally active over a wide pH range of 5 to 7. Immobilization has been shown to be more resistant to conformational changes caused by denaturing conditions such as temperature and pH. This is due to tertiary structure stabilization, which makes the enzyme more resistant to changes in reaction conditions (Guzik *et al.*, 2014).

ii. Effects of substrate concentration on the kinetic parameters for free and co-immobilized cellulase and xylanase

The enzyme kinetic parameters (K_m and V_{max}) are important for determining the affinity of enzyme for a specific substrate as well as the rate of the enzymatic reaction (Weng *et al.*, 2022). Figure 4.18 shows the kinetic study of free and co-immobilized enzymes with respect to substrate concentration using Michaelis-Menten kinetic derivation and Lineweaver-Burk plot. The plot was used to calculate the values of K_m and V_{max} for both free and co-immobilized enzymes, as shown in Table 4.15. Microbial enzyme kinetic parameters are known to be variable, and their values are strictly dependent on the specific nature of the substrate (Alatzoglou *et al.*, 2023). The K_m and V_{max} values in the current study varied with the agrowaste. However, for each agrowaste, the k_m value for both free and co-immobilized enzymes fell within the range proposed by Stryer (2002), which was reported by Matosevic, *et al.* (2010), that the k_m value of most enzymes falls between 10^{-1} and 10^{-7} mg/mL. In line with previous studies, the k_m values for free enzymes are lower than the k_m values obtained for co-immobilized enzymes while the values of V_{max} for co-immobilized enzymes are lower than that of the free enzymes. For instance, when sugarcane bagasse was used as the substrate, the K_m values for immobilized enzyme (0.018 mg/mL) was higher than the K_m values of free cellulase and xylanase which were 0.017 mg/mL and 0.0056 mg/mL respectively. The findings are in line with the previous study by Alatzoglou *et al.* (2023) who reported that an increase in K_m after enzyme immobilization might be due to the low diffusion rate of the substrate to the active site, as a result of the steric hindrance and diffusion resistance generated by the enzyme support. The V_{max} for co-immobilized enzymes (227.25 U/min g⁻¹) was lower than the V_{max} values for free cellulase and free xylanase which were 333.33 U/min g⁻¹, and 555.47 U/min g⁻¹ respectively. Awad *et al.* (2017) and Wehaidy *et al.* (2019), also

reported a decrease in V_{\max} which was ascribed to possible conformational change of the co-immobilized enzymes due to the immobilization process.

It is worth noting that the K_m values of both free and co-immobilized enzymes in this study were very close. This suggests that the co-immobilized enzymes had a similar affinity for the substrate as the free enzyme. This is in support of the enhanced catalytic potential of co-immobilized α -amylase, pectinase and cellulase reported by Muley *et al.* (2018), which was attributed to an increase in interaction frequency between the co-immobilized enzymes and their respective substrate as a result of higher substrate concentration in the limited space of the co-immobilized complex. This implies that the catalytic efficiency of both free and co-immobilized enzymes was similar. This finding lends credence to the previously reported catalytic efficiency of co-immobilized enzymes compared to free cellulase and free xylanase.

iii. Effect of incubation time and conditions on the storage stability of free and co-immobilized enzymes

The potential of enzyme to be stored for future use is an important industrial requirement since enzyme may not be produced at every industrial process. In the present study, the storage stability of co-immobilized cellulase and xylanase as compared to its free counterparts as shown in Figure 4.19 and Figure 4.20 for storage at 4 °C and 25 °C respectively. The immobilized enzyme stored at 4 °C (Figure 4.20) was able to retain 76.63% of its initial activity on the 45th day while just 10.05% and 5.26% of the initial activity was remaining for cellulase and xylanase respectively stored for the same period. As at 30th day at 4 °C, the residual activities of free cellulase and free xylanase were 63.6% and 43.8% respectively, whereas the co-immobilized enzyme has 95.8% of its initial activity retained. Furthermore, Zhang *et al.* (2020) reported that after 30 days of storage at 4 °C, covalently co-immobilized catalase and glucose oxidase retained

approximately 80% relative activity, whereas free catalase and free glucose oxidase retained no relative activity. This is most likely due to a decrease in the rate of peptide subunit dissociation and enzyme denaturation. It can be seen that, regardless of storage condition, the co-immobilized enzymes had higher activity than free cellulase and free xylanase. This is consistent with the report by Awad *et al.* (2017) that co-immobilized inulinase retained 100% of its initial activity after 30 days at 4 °C. Likewise, immobilized enzyme showed a better storage stability than free cellulase and xylanase when stored at 25 °C (Figure 4.21). On the tenth day of storage at room temperature, the remaining relative activities for free cellulase, and free xylanase were 5.01%, and 1.05%, respectively, whereas the co-immobilized enzyme retained 48.3% of its initial activity. These findings are consistent with the findings of Demirci *et al.* (2017), who reported 50% residual activity of immobilized α -glucosidase after 10 days of storage at 25 °C. This could be due to the formation of polyelectrolyte ionic complexes between the enzyme gel and the support matrix, which increased the shelf stability of the immobilized enzymes. This means that the co-immobilized enzymes can be stored in the refrigerator for 45 days and retain over 70% of its initial activity; this is advantageous for industry because it eliminates the need to prepare the enzyme every time, thereby saving money.

Furthermore, the half-life of the enzymes was calculated as shown in Table: 4.16 to determine how long (days) it will take for the enzymes to lose 50% of their initial activities. The half-lives of free cellulase, free xylanase and co-immobilized enzymes when stored in the refrigerator (4 °C) were 5.02 days, 4.15 days, and 29.37 days respectively. Furthermore, when stored at room temperature (25 °C), the half-lives of free cellulase, free xylanase, and co-immobilized enzymes were 4.15 days, 2.50 days, and 11.95 days, respectively. The co-immobilized enzymes had a longer half-life value in both storage conditions. These findings suggest that the immobilization strategy

employed in this study improved the storage stability of free cellulase and free xylanase. As a result, the co-immobilized enzymes could be stored at room temperature (25 °C) for 11 days and in the refrigerator (4 °C) for approximately 30 days while retaining 50% of its activity.

iv Thermal stability of free and co-immobilized enzymes

The thermal stability of free and co-immobilized enzymes is as shown in Figure 4.21. The co-immobilized enzymes maintained its highest activity (97%) at 60 °C for the period of 4 h, whereas only 16% of the activity of free cellulase and free xylanase remained at the same period. Also, co-immobilized enzymes retained 93% of its activity at 70 °C for 2 hs before the activity gradually reduced to 61.7% whereas free cellulase retained 6% of its initial activity while free xylanase retained 1% of its initial activity. The increase in thermal stability of co-immobilized enzymes is consistent with the findings of other authors (Giannakopoulou *et al.*, 2019; and Gao *et al.*, 2021). Increased thermal stability of enzyme after immobilization suggests that the immobilization process strengthened the enzyme structure. In general, immobilizing an enzyme protects it from heat inactivation.

Furthermore, the free and immobilized enzyme half-lives at each reaction temperature were also determined, as shown in Table 4.17. When compared to free cellulase and xylanase, the half-lives of co-immobilized enzymes increased dramatically. At 30 °C, for example, the half-lives of free cellulase, free xylanase, and co-immobilized enzymes were 1.38, 0.80, and 27.87 h, respectively. Furthermore, the half-lives of free cellulase, free xylanase, and immobilized enzymes at 90 °C were 0.55 h, 0.39 h, and 6.63 h, respectively. Because the enzyme reaction can be carried out at higher temperatures, co-immobilized enzymes stability at higher temperatures is advantageous for industrial applications. Additionally, high temperature reduces the risk of microbial contamination. This backs up a study published in a review by Bié *et al.* (2022), which found that the half-life of co-

immobilized α -amylase, pectinase, and cellulase at 70 °C increased by about 2.4-fold when compared to free enzymes.

It has been reported that various factors such as the number of bonds formed between the enzyme and the support, the nature of the bonds, the degree of confinement of an enzyme within the support, and the environmental conditions of an enzyme during covalent modifications may affect the stability of immobilized enzymes and co-immobilized enzymes. Earlier studies found that the extent of improvement varied from matrix to matrix and depend on the type of interaction between enzyme and matrix. (Fopase *et al.*, 2020).

v Activation and deactivation energy of free and co-immobilized enzymes

The activation energy (E_a) and deactivation energy (E_d) of the enzyme reaction were calculated to determine the quantitative evaluation of the thermal effect on free and co-immobilized enzymes. This was done by plotting the logarithm of inactivation constant (k_i) versus reciprocal of the absolute temperature (Arrhenius plot) as shown in Appendix I. The amount of energy required for a reaction to begin is referred to as activation energy, whereas the amount of energy required to denature the enzyme is referred to as deactivation energy (Sonkar and Singh, 2020). The activation energy (E_a) of free and immobilized cellulase and xylanase, as well as the deactivation energy (E_d), were calculated using the Arrhenius plot and are shown in Table 4.18. The activation energy of co-immobilized cellulase and xylanase (3.450 kJ/mol) was lower than that of free cellulase and free xylanase, which were 15.899 kJ/mol and 29.218 kJ/mol, respectively. This means that the reaction catalyzed by co-immobilized cellulase and xylanase requires less energy to initiate than reactions catalyzed by free cellulase and free xylanase. Furthermore, the deactivation energy (E_d) of immobilized enzyme was higher than that of free enzyme. This suggests that the co-immobilized enzymes were more compact,

stable, and resistant to heat denaturation than the free enzymes. A similar increase in thermal stability following multi enzyme immobilization was also reported by Kirupa-Sankar *et al.* (2018). Awad *et al.* (2017) also reported that covalent immobilization of inulinase reduced the E_a from 28.41 to 16.216 kJ/mol, resulting in increased catalytic efficiency of the immobilized inulinase. The higher deactivation energy and lower activation energy observed in the current study suggest that co-immobilized cellulase and xylanase are more thermally stable and will not be easily denatured in the reaction medium.

vi. The effect of number of usages on the relative efficiency of the co-immobilized enzymes

Once the immobilization techniques have been established, the operational stability of the immobilized enzyme must be tested. In the present study, the co-immobilized enzymes were able to retain more than 50% of its initial activity after ten cycles of hydrolysis as shown in Figure 4.22. The residual activity for immobilized enzyme at the end of the tenth cycle was 55.13%. This backs up the findings of Abou-Alsoaud *et al.* (2022), who found that the enzyme co-immobilized on biochar-chitosan composite beads retained approximately 60% of its initial activity after eight consecutive cycles. In another study, Bié *et al.* (2022) found that pectinase and cellulase co-immobilized on iron oxide magnetic nanoparticles retained 80% of their original activity after 10 uses. According to some reports, the observed decrease in catalytic properties of immobilized enzyme after repeated use is most likely due to factors such as product inhibition, structural modification of the enzyme, protein denaturation, and/or immobilized enzyme inactivation (Abraham *et al.*, 2014; Ladole *et al.*, 2021). The ability of the co-immobilized enzymes prepared in this study to retain more than 50% activity after the tenth use suggests that a single batch of co-immobilized enzymes can be used for multiple

hydrolysis using fresh agrowaste as substrate, releasing fermentable sugars sequentially for bioethanol yield.

4.2.5a: Fermentable sugar produced from agrowaste using free, immobilized and co-immobilized enzymes

The reducing sugar produced from agrowaste when free, immobilized and co-immobilized enzymes were used for hydrolysis is as shown in Table 4.19. Hydrolysis with the mixture of cellulase and xylanase produced the highest amount of reducing sugar. Furthermore, the reducing sugar produced by the co-immobilized enzymes was comparable to that produced by the combination of free cellulase and xylanase. This supports the findings of Shokrkar and Ebrahimi (2018), who discovered that hydrolysis with a mixture of cellulase and β -glucosidase resulted in higher reducing sugar production. Co-immobilized enzymes released 74.92%, 79.63% and 94.16% of the fermentable sugars released by free enzyme from plantain pseudostem, sugarcane bagasse and corncob biomass respectively at the 72nd h. Studies have shown that when multiple enzymes are immobilized at the same time, the distance between the cascade enzymes is reduced. This proximity effect may result in the rapid utilization of intermediates, giving the co-immobilized enzymes a higher activity than single immobilized enzymes (Ren *et al.*, 2019). Furthermore, some authors attribute the high hydrolytic efficiency of co-immobilized enzymes to the nature of the enzyme support, which provides an excellent microenvironment for the transfer of substrate, intermediates, and product, resulting in the high reaction rate of the co-immobilized multi-enzyme system (Han *et al.*, 2020; Song *et al.*, 2020).

Given that the amount of fermentable sugar produced is directly related to bioethanol yield, and that in this study, corncob biomass produced the least amount of fermentable

sugar when compared to other agrowaste samples, sugarcane bagasse and plantain pseudostem biomass were chosen for further research

4.2.5b: Quantity and quality of bioethanol produced using immobilized moieties

i. Quantity bioethanol produced using sugarcane bagasse and plantain pseudostem by co-immobilized enzymes and co-immobilized fungi

The concentration (g/L) of ethanol produced by different combinations of enzyme and yeast and mucor during simultaneous saccharification and fermentation is shown in Table 4.20. The highest concentration of bioethanol, 68.93 ± 0.33 g/L, and 76.09 ± 0.15 g/L for plantain pseudostem biomass and sugarcane bagasse respectively were produced by co-immobilized enzymes plus co-immobilized yeast and mucor. The yield obtained in this study is higher than the ethanol yield (57.6 g/L) obtained by Zabed *et al.* (2014). Similarly, the ethanol yield in this study is higher than the values reported by Irfan *et al.* (2014), who obtained the highest ethanol concentration (66 g/L) from sugarcane bagasse when co-immobilized cells were used in fermentation. The higher ethanol concentration obtained in this study could be another confirmation of co-immobilized enzymes and cells being more efficient than free and singly immobilized enzymes and cells. Other authors, such as Karagoz *et al.* (2019), found that when pentose and hexose ethanologenic *E. coli* strains were immobilized and co-immobilized in calcium alginate beads, co-immobilized cells produced more ethanol than free cells or singly immobilized cells. Earlier research attributed the increased productivity in the immobilized system to high cell density and immobilization-induced cellular or genetic changes (Nikolić *et al.*, 2009). Immobilized cells are also thought to be more tolerant of ethanol because the matrix protects them from ethanol toxicity.

ii. Profile of compounds in bioethanol produced using sugarcane bagasse and plantain pseudostem by co-immobilized enzymes and co-immobilized fungi

The components of bioethanol produced using sugarcane bagasse and plantain pseudostem is shown in Table 4.21 and Table 4.22 respectively. The retention times for the ethanol component was in the range of 6.965 min. This is in line with the retention time (6.9 min) reported by Tabah *et al.* (2017). However the value of the retention time in this study is higher than the value reported by Bhatt *et al.* (2012), who studied the ethanol production from the saccharified sugars of agricultural waste pearl millet bran through solid state fermentation by *A. flavus* FPDN1 and the concentration of resulted ethanol was noted as 88.0% with 3.31 min retention time. Likewise, Sanjivkumar *et al.* (2018), portrayed the chromatogram of GC-MS (RT) analysis of ethanol from *Tuber formosanum* and the functional ethanol groups were noted at the retention time of 2.58 min. Meanwhile, the retention time reported by Govindaraj *et al.* (2023), for ethanol was 15 min which is higher than the retention time for ethanol in the present study. Poor temperature control, the quality of the stationary phase, carrier flow instability, or contaminants in the sample could all contribute to variation in retention time (Al-Bukhaiti *et al.*, 2017). The distillate contained ethanol and other alcohols such as hexanol, 1-butanol, as well as some other useful compounds such as toluene and Heptane. For instance, hexanol is an organic alcohol with a six-carbon chain which is used as flavouring additives and in the manufacturing of perfumes, 1-Butanol or butyl alcohol is a metabolite produced by *Saccharomyces cerevisiae*. It is a 4-carbon primary alcohol used as a solvent and has the potential to be used as a biofuel. Toluene is used in oil refining and stain removal.

In this study, the highest percentages of ethanol identified by GC-MS were 80.87% and 71.15% from sugarcane bagasse and plantain pseudostem biomass, respectively. This supports the findings of Zhang *et al.* (2012), who reported that fermentation by co-

immobilized microorganisms was superior to immobilized single microorganism systems and also superior to free mixed microorganisms. According to Jiménez-Bonilla *et al.* (2022), immobilization protected microbial cells against the possible toxic effects during fermentation. As a result, the fermentation performance of the immobilized yeast was improved in comparison with that of the free yeast. Immobilized yeast cells have been shown to have advantages such as higher productivity and lower contamination when compared to free cells (Adelabu *et al.*, 2019).

4.2.5c. Characteristics of free biochar-chitosan and biochar-chitosan loaded with co-immobilized enzymes and co-immobilized yeast and mucor

The free biochar-chitosan support as well as biochar-chitosan support loaded with co-immobilized enzymes and co-immobilized fungi had different characteristics as discussed below

i. Infrared spectra of free biochar-chitosan and biochar-chitosan loaded with co-immobilized enzymes and co-immobilized fungi

The Infrared Spectra of free biochar-chitosan beads (F), beads co-immobilized with cellulase and xylanase (CIE) as well as beads co-immobilized with *mucor indicus* and *Saccharomyces cerevisiae* (CMY) between 500 cm^{-1} and 4000 cm^{-1} range is shown in figure 4.23. The variation in the spectra relative to the position and intensity of the characteristic peaks is shown in Appendix J. The FTIR results revealed that immobilization was successful. When compared to unloaded biochar-chitosan beads, the peaks of mucor and yeast co-immobilized on biochar-chitosan beads, as well as cellulase and xylanase co-immobilized on biochar-chitosan beads, showed changes in the position and intensity of the characteristic peaks within the wavenumbers of 2000 cm^{-1} and 500 cm^{-1} . These findings agreed with those of other authors, such as Guan *et al.* (2022), who reported a broad band of hydroxyl (-OH) groups in the three spectra between 3,000-3,500

cm⁻¹, indicating successful alkaline activation of the support. Also the stretching vibrations evident in the spectra of CIE and CMY in the range of 1650–1500 cm⁻¹ which corresponded to the C=O stretching and aromatic C=C vibrations (Polatoğlu, 2019) confirms the binding of the biochar-chitosan beads with the enzymes and cells. In the range of 3400 to 3100 cm⁻¹, peaks derived from the -NH groups of the amines are present which further confirms the presence of the enzyme (Dante *et al.*, 2011). At approximately 2000 cm⁻¹, the peaks are related to the stretching vibrations of -CH₂ groups in the long aliphatic chains of enzymes (Bak *et al.*, 2022), and the peaks at around 1400 cm⁻¹ can be attributed to the presence of stretching vibrations of symmetric carboxylate groups (Zhang *et al.*, 2016). The presence of the peaks at 1636 cm⁻¹ related to amide, 1543 cm⁻¹ (-NH group-second amine bending), while between 1000 and 1200 cm⁻¹ appears moderate signals corresponding to tertiary amide bonds of the immobilized enzyme (Negi and Kesari, 2022). Likewise, peaks at 1456 cm⁻¹ and 1377 cm⁻¹ correspond to -CH₂ stretching, and CH₃ group bending (Parin *et al.*, 2020). The absorption peak at 2292 cm⁻¹ in the free biochar-chitosan beads shifted slightly to 2929 cm⁻¹ in co-immobilized enzymes and co-immobilized fungi (Wojnarowska *et al.*, 2015; Yang *et al.*, 2021). The amide group were further confirmed with increased in peak intensities at 1576 cm⁻¹ in the co-immobilized enzymes cells spectra.

ii. Morphological change of free biochar-chitosan and biochar-chitosan loaded with co-immobilized enzymes and co-immobilized fungi

The SEM images for the samples of unloaded biochar-chitosan beads (Free), co-immobilized enzymes loaded biochar-chitosan beads (CIE), and co-immobilized fungi biochar-chitosan beads (CMY) are shown in Figure 4.23, the differences in the morphology of the loaded beads is clearly seen when compared to the unloaded bead. The visible pores or cavities in the free biochar-chitosan beads have been blocked by the attachment of either enzyme or cells. The SEM image of a biochar-chitosan bead loaded

with fungi shows encapsulated yeast in spherical form and encapsulated *Mucor* in thread-like shape (Vasilescu *et al.*, 2022), confirming the successful immobilization.

iv. Reusability of co-immobilized yeast and mucor

Given the importance of operational stability in industrial processes, the co-immobilized yeast and *mucor* were subjected to several fermentation cycles to determine their operational stability, as shown in Figure 4.24. The co-immobilized fungi were able to produce 43.53% and 59.97% ethanol from sugarcane bagasse and plantain pseudostem biomass, respectively, at the 10th fermentation cycle. According to (Liu and Lien, 2016), the co-immobilized cultivation system for co-cultured organisms had better synergistic effects and stability than the co-suspension system, resulting in increased ethanol yield.

4.2.5d: Estimated cost for the production of lignocellulosic bioethanol

The estimated cost of production of lignocellulosic bioethanol is shown in Table 4.24. In the present study, a total sum of ₦ 6800 (€ 8.26/ L) was estimated for the production of 1.5 L of lignocellulosic bioethanol. This is higher than the 0.54/L for ethanol production from starchy crops reported by Budimir *et al.* (2011). The production cost depends on the raw material and the country. Generally, the cost of producing lignocellulosic bioethanol may be high at the moments but the benefits anticipated from mandated use of cellulosic biofuels include energy security through domestic production of fuel and environmental improvement through the reduction of greenhouse gas and other particulate emissions associated with fossil fuel combustion. Additional benefits include creating new markets for agricultural products, keeping productive farmland in use, and improving trade balances.

CHAPTER FIVE

5.0 CONCLUSION AND RECOMMENDATIONS

5.1 Conclusion

The research was aimed at optimizing microwave-alkaline conditions in the pre-treatment of selected agrowastes for bioethanol production. The following conclusions were arrived at the end of the experiments

At optimal microwave-alkaline conditions of 1.97% NaOH at 70 W for 5 min, 56% lignin was removed from plantain pseudostem while 62% cellulose and 30% hemicellulose were retained for hydrolysis. Also, at optimal microwave-alkaline conditions of 3% NaOH at 96 W for 5 min, 63% of the lignin in sugarcane bagasse was removed, while 74% of the cellulose and 22% of the hemicellulose were retained. Similarly, at optimal microwave-alkaline conditions of 2.8% NaOH at 86 W for 4.4 minutes, 66% of lignin was removed from corncob biomass while 64% cellulose and 18% hemicellulose were retained.

A. flavus isolated from sewage sludge produced cellulase enzyme with the highest activity (15.35 ± 0.48 IU/mL) when sugarcane bagasse was used as a carbon source, whereas *A. niger* isolated from refuse dump site produced xylanase with the highest activity (38.04 ± 0.17 IU/mL) when plantain pseudostem was used as a carbon source. Therefore, it has been demonstrated in this study that indigenous approach to enzyme production using locally sourced microorganisms and abundantly available agrowastes as carbon source may reduce the high cost of hydrolytic enzymes.

Freeze-dried biochar-chitosan composite was used to co-immobilized cellulase and xylanase by covalent cross-linking method while biochar-chitosan slurry was used to co-immobilized *S. cerevisiae* and *M. indicus* by encapsulation method.

The co-immobilized enzymes are more thermally stable and had more potential to resist denaturation when compared to their free counterparts. Therefore, the use of co-immobilized enzymes as well as co-immobilized fungi on porous biochar-chitosan support may have a great potential for the production of high yield bioethanol, thereby making bioethanol available and accessible to the populace for a healthier environment

In simultaneous saccharification and co-fermentation (SScF), sugarcane bagasse had the highest bioethanol yield (76.09 ± 0.15 g/L), which is statistically ($p < 0.05$) different from the bioethanol yield (68.93 ± 0.33 g/L) obtained from plantain pseudostem biomass. However, it can be seen in the current study that both agrowastes had considerably high yields of bioethanol. Although sugarcane bagasse is a well-known substrate for secondary bioethanol production, this study sheds light on the potential of plantain pseudostem biomass as a substitute for sugarcane bagasse in bioethanol production.

5.2 Recommendations

In the concluded study, agrowaste was used to produce bioethanol. However, for the biorefinery to be sustainable, a large amount of agrowaste as feedstock is required. Given the seasonal availability of different agrowaste based on harvesting times, it is suggested that in a future study, a mixture of different agrowaste that are available at the same time be optimized for bioethanol production.

The study clearly demonstrated that hydrolysis is a rate-determining step in bioethanol production. This was demonstrated by corncob, which produced the least amount of fermentable sugar during hydrolysis despite having the highest initial holocellulose content. As a result, it is suggested that in future research, the hydrolysis of each agrowaste be optimized to obtain the best conditions for optimal fermentable sugar yield. Furthermore, it is suggested that recombinant DNA technology should be applied to the organisms so as to modify the gene for improved enzyme production and fermentation process

5.3 Contributions to Knowledge

The work established the production of lignocellulosic bioethanol from non-food-based feedstock from some locally available agrowastes (corncob biomass, sugarcane bagasse and plantain pseudo-stem biomass) using microwave-alkaline (MA) pretreatment conditions for the effective delignification. The results showed that optimal microwave-alkaline conditions of 1.97% NaOH/ 70 W/ 5 min, removed 56% lignin and retained 62 % cellulose and 30 % hemicellulose in plantain pseudo-stem; while 3% NaOH/ 96 W/ 5 min removed 63 % lignin and retained 74 % cellulose and 22 % hemicellulose in sugarcane bagasse; also, 2.8 % NaOH/ 86 W / 4.4 min removed 66 % lignin and retained 64 % cellulose and 18 % hemicellulose in corncob biomass. It also revealed that *Aspergillus flavus* isolated from sewage sludge produced cellulase enzyme with the highest activity (15.35 ± 0.48 IU/mL) when sugarcane bagasse was used as a carbon source, whereas *A. niger* isolated from refuse dump site produced xylanase with the highest activity (38.04 ± 0.17 IU/mL) when plantain stem was used as a carbon source. The study also showed that high concentration of ethanol was produced from both sugarcane bagasse (76.09 ± 0.15 g/L) and plantain pseudostem (68.93 ± 0.33 g/L).

However, the bioethanol produced from sugarcane bagasse was significantly ($p < 0.05$) higher than the bioethanol produced from plantain pseudostem.

REFERENCES

- Abas, N., Kalair, A., & Khan, N. (2015). Review of fossil fuels and future energy technologies. *Futures*, 69, 31–49. <https://doi.org/10.1016/J.FUTURES.2015.03.003>.
- Abdoulaye, T., Wossen, T., & Awotide, B. (2018). Impacts of improved maize varieties in Nigeria: ex-post assessment of productivity and welfare outcomes. *Food Security*, 10(2), 369–379. <https://doi.org/10.1007/S12571-018-0772-9>.
- Abou-Alsoaud, M. M., Taher, M. A., Hamed, A. M., Elnouby, M. S., & Omer, A. M. (2022). Reusable kaolin impregnated aminated chitosan composite beads for efficient removal of Congo red dye: isotherms, kinetics and thermodynamics studies. *Scientific Reports*, 12(1), 54-67. <https://doi.org/10.1038/s41598-022-17305-w>
- Abraham, R. E., Verma, M. L., Barrow, C. J., & Puri, M. (2014). Sustainability of magnetic nanoparticle immobilized cellulases in enhancing enzymatic saccharification of pretreated hemp biomass. *Biotechnology for Biofuels*, 7(1), 144-152. <https://doi.org/10.1186/1754-6834-7-90>.
- Abtahi, H., Ghazavi, A., & Karimi, M. (2011). Antimicrobial activities of ethanol extract of black grape. *African Journal of Microbiology Research*, 5(25), 4446-4448. <https://doi.org/10.5897/AJMR2010.9718>.
- Abu, E. (2005). Enzymatic saccharification of some agro-industrial cellulosic wastes by cellulose produced from a mixed culture of *Aspergillus niger* and *Saccharomyces cerevasae* grown on sorghum pomace. *Ife Journal of Science*, 6(1), 76-88. <https://doi.org/10.4314/ijis.v6i1.32128>.
- Adebayo, G., Adegoke, H., Jamiu, W., Balogun, B., & Jimoh, A. (2016). Adsorption of Mn(II) and Co(II) ions from aqueous solution using Maize cob activated carbon: Kinetics and Thermodynamics Studies. *Journal of Applied Sciences and Environmental Management*, 19(4), 737-749. <https://doi.org/10.4314/jasem.v19i4.22>
- Adegoke, O. J., Aluko, B. T., & Adegoke, B. F. (2017). Determinants of market value of residential properties in Ibadan Metropolis, Nigeria. *Journal of Economics and Sustainable Development*, 8(4), 167-181. <https://doi.org/10.4314/jased.v19i4.22>.
- Adelabu, B. A., Kareem, S. O., Oluwafemi, F., & Adeogun, I. A. (2019). Bioconversion of corn straw to ethanol by cellulolytic yeasts immobilized in *Mucuna urens* matrix. *Journal of King Saud University Science*, 31(1), 136-141. <https://doi.org/10.1016/j.jksus.2017.07.005>.
- Adeniyi, A. G., Ogunniyi, S., Iwuozor, K. O., & Emenike, E. C. (2022). Thermochemical Conversion of African balsam leaves- cow dung hybrid wastes into biochar. *Biofuels, Bioproducts and Biorefining*, 12, 625-878. <https://doi.org/10.1002/bbb.2453>.

- Aditiya, H. B., Mahlia, T. M. I., Chong, W. T., Nur, H., & Sebayang, A. H. (2016). Second generation bioethanol production: A critical review. *Renewable and Sustainable Energy Reviews*, 66, 631–653. <https://doi.org/10.1016/J.RSER.2016.07.015>.
- Agbro, E. B., & Ogie, N. A. (2012). A comprehensive review of biomass resources and biofuel production potential in Nigeria. *Research journal in engineering and applied sciences*, 1(3), 149-155. <http://dx.doi.org/10.4236/rjeas.2011.615247>.
- Ai, B., Zheng, L., Li, W., Zheng, X., Yang, Y., Xiao, D., Shi, J., & Sheng, Z. (2021). Biodegradable Cellulose Film Prepared from Banana Pseudo-Stem Using an Ionic Liquid for Mango Preservation. *Frontiers in Plant Science*, 12, 625-878. <https://doi.org/10.3389/fpls.2021.625878>.
- Akinyemi, S. O. S., Adejoro, M. A., Layade, A. A., & Adegbite, O. O. (2017). Market Structure and Performance for Plantain and Banana. *International Journal of Fruit Science*, 17(4), 440–450. <https://doi.org/10.1080/15538362.2017.1360231>.
- Alabi, O., & Safugha, F. (2022). Efficiency of Resource-Use and Marginal Value Productivity Analysis Among Maize Farmers, Abuja, Nigeria. *International Journal of Agriculture Forestry and Life Sciences*, 6(2), 28-33. <https://doi.org/10.1080/15538362.2017.1360231>.
- Alatzoglou, C., Patila, M., Giannakopoulou, A., Spyrou, K., Yan, F., Li, W., Chalmpes, N., Polydera, A. C., Rudolf, P., Gournis, D., & Stamatis, H. (2023). Development of a Multi-Enzymatic Biocatalytic System through Immobilization on High Quality Few-Layer bio-graphene. *Nanomaterials*, 13(1) 34-45.
- Al-Bukhaiti, W. Q., Noman, A., Qasim, A. S., & Al-Farga, A. (2017). Gas chromatography: Principles, advantages and applications in food analysis. *International Journal of Agriculture Innovations and Research*, 6(1), 2319-1473. <https://doi.org/10.2467/1jair.v19i4.22>.
- Al-Judaibi, A. A. (2011). Effect of some fermentation parameters on ethanol production from beet molasses by *Saccharomyces cerevisiae* CAIM13. *American Journal of Agricultural and Biological Science*, 6(2), 301–306. <https://doi.org/10.3844/ajabssp.2011.301.306>.
- Alokika, Anu, Kumar, A., Kumar, V., & Singh, B. (2021). Cellulosic and hemicellulosic fractions of sugarcane bagasse: Potential, challenges and future perspective. *International Journal of Biological Macromolecules* 169 (1), 564–582. Elsevier. <https://doi.org/10.1016/j.ijbiomac.2020.12.175>.
- Alvira, P., Tomás-Pejó, E., Ballesteros, M. J., & Negro, M. J. (2010). Pretreatment technologies for an efficient bioethanol production process based on enzymatic hydrolysis: a review. *Bioresource technology*, 101(13), 4851-4861. <https://doi.org/10.1016/j.biortech.2009.11.093>.

- Al-Wabel, M. I., Al-Omran, A., El-Naggar, A. H., Nadeem, M., & Usman, A. R. A. (2013). Pyrolysis temperature induced changes in characteristics and chemical composition of biochar produced from *conocarpus* wastes. *Bioresource Technology*, 131, 374–379. <https://doi.org/10.1016/j.biortech.2012.12.165>.
- Aminu, B. M., Bukar, A., Ado, A., & Bello, M. (2018). Bioethanol production from two varieties of mango kernel using co-culture of *Bacillus subtilis*, *Aspergillus niger* and *Saccharomyces cerevisiae*. *Bayero Journal of Pure and Applied Sciences*, 11(1), 349-356. <https://doi.org/10.4314/bajopas.v11i1.57S>.
- Anggono, J., Farkas, Á. E., Bartos, A., Móczó, J., Purwaningsih, H., & Pukánszky, B. (2019). Deformation and failure of sugarcane bagasse reinforced PP. *European Polymer Journal*, 112, 153-160. <https://doi.org/10.1016/j.eurpolymj.2018.12.033>
- Angin, M., Aburizaiza, A. S., Miandad, R., Rehan, M., Barakat, M. A., & Nizami, A. S. (2018). Development of biochar as fuel and catalyst in energy recovery technologies. *Journal of Cleaner Production*, 188, 477–488. <https://doi.org/10.1016/j.jclepro.2018.04.017>.
- Antil, P. S., Gupta, R., & Kuhad, R. C. (2015). Simultaneous saccharification and fermentation of pretreated sugarcane bagasse to ethanol using a new thermotolerant yeast. *Annals of Microbiology*, 65(1), 423–429. <https://doi.org/10.1007/s13213-014-0875-2>.
- Anwar, Z., Gulfraz, M., Imran, M., Asad, M. J., Shafi, A. I., Anwar, P., & Qureshi, R. (2012). Optimization of dilute acid pretreatment using response surface methodology for bioethanol production from cellulosic biomass of Rice Polish. *Pakistan Journal of Botany* 3 (9), 34-42, <https://doi.org/10.3390/fermentation9030289>.
- Arpia, A. A., Chen, W. H., Lam, S. S., Rousset, P., & De Luna, M. D. G. (2021). Sustainable biofuel and bioenergy production from biomass waste residues using microwave-assisted heating: A comprehensive review. *Chemical Engineering Journal*, 403, 126-233. <https://doi.org/10.1016/j.cej.2020.126233>.
- Aşgin, N., & Değerli, K. (2019). A comparison of the costs, reliability and time of result periods of widely used methods, new molecular methods and MALDI TOF-MS in the routine diagnosis of *Candida* strains. *Mikrobiyoloji Bulteni*, 53(2), 204-212. <https://doi.org/10.5578/mb.67952>.
- Asikoko, F., Okologume, W. C., Appah, D., & Aimikhe, V. (2023). Experimental investigation of cassava (*Manihot esculenta*) leaf extract as a green inhibitor of gas hydrate formation. *Biomass Conversion and Biorefinery*, 3 (2), 1-10. <https://doi.org/10.1007/s13399-023-04213-w>
- Atoyebi, O. D., Osueke, C. O., Badiru, S., Gana, A. J., Ikpotokin, I., Modupe, A. E., & Tegene, G. A. (2019). Evaluation of particle board from sugarcane bagasse and corn cob. *International Journal of Mechanical Engineering and Technology*, 10(1), 1193-1200. <http://www.iaeme.com/ijmet/issues.asp?JType=IJM ET&VType=10&IType=01>.
- Avnir, D., Braun, S., Lev, O., & Ottolenghi, M. (1994). Enzymes and Other Proteins Entrapped in Sol-Gel Materials. *Chemistry of Materials* 6 (10), 1605–1614. <https://doi.org/10.1021/cm00046a008>.

- Awad, G. E. A., Wehaidy, H. R., Abd El Aty, A. A., & Hassan, M. E. (2017). A novel alginate–CMC gel beads for efficient covalent inulinase immobilization. *Colloid and Polymer Science*, 295(3), 495–506. <https://doi.org/10.1007/s00396-017-4024-x>
- Bąk, J., Thomas, P., & Kołodyńska, D. (2022). Chitosan-Modified Biochars to Advance Research on Heavy Metal Ion Removal: Roles, Mechanism and Perspectives. *Materials*, 15(17), 6108. <https://doi.org/10.3390/ma15176108>.
- Balasundaram, G., Banu, R., Varjani, S., Kazmi, A. A., & Tyagi, V. K. (2022). Recalcitrant compounds formation, their toxicity, and mitigation: Key issues in biomass pretreatment and anaerobic digestion. *Elsevier*. Retrieved August 23, 2022, from: <https://www.sciencedirect.com/science/article/pii/S0045653521034020>.
- Bansal, N., Tewari, R., Soni, R., & Soni, S. K. (2012). Production of cellulases from *Aspergillus niger* NS-2 in solid state fermentation on agricultural and kitchen waste residues. *Waste Management*, 32(7), 1341–1346. <https://doi.org/10.1016/j.wasman.2012.03.006>.
- Behera, B. K., Varma, A., & Varma, A. (2019). Gasoline-Like Biofuel. *Bioenergy for Sustainability and Security*, 4(3), 79-158.
- Bergthorson, J. M., & Thomson, M. J. (2015). A review of the combustion and emissions properties of advanced transportation biofuels and their impact on existing and future engines. *Renewable and Sustainable Energy Reviews*, 42, 1393–1417. <https://doi.org/10.1016/j.rser.2014.10.034>.
- Bhatia, L., Johri, S., & Ahmad, R. (2012). An economic and ecological perspective of ethanol production from renewable agro waste: a review. *Express*, 2(1), 65. <https://doi.org/10.1186/2191-0855-2-65>.
- Bhatt, N., Adhyaru, D., & Thakor, P. (2012). Production of xylanase by *Aspergillus flavus* FPDN1 on Pearl millet bran: Optimization of culture conditions and application in bioethanol production. *Indian Journal of Environmental Protection*, 32(8), 639–647. <https://www.academia.edu/download/44974447/download.pdf>.
- Bhuyar, P., Shen, M. Y., Trejo, M., Unpaprom, Y., & Ramaraj, R. (2021). Improvement of fermentable sugar for enhanced bioethanol production from *Amorphophallus* spp. tuber obtained from northern Thailand. *Environment, Development and Sustainability*, 4(2), 1-12. <https://doi.org/10.1007/s10668-021-01786-2>.
- Bié, J., Sepodes, B., Fernandes, P. C., & Ribeiro, M. H. (2022). Enzyme immobilization and co-immobilization: Main framework, advances and some applications. *Processes*, 10(3), 494. <https://doi.org/10.3390/pr10030494>.
- Biely, P., Singh, S., & Puchart, V. (2016). Towards enzymatic breakdown of complex plant xylan structures: State of the art. In *Biotechnology Advances* 34 (7), 1260–1274. <https://doi.org/10.1016/j.biotechadv.2016.09.001>.
- Bilal, M., Asgher, M., Cheng, H., Yan, Y., & Iqbal, N. (2019). Multi-point enzyme immobilization, surface chemistry, and novel platforms: a paradigm shift in biocatalyst design. *Critical Reviews in Biotechnology* 39 (2), 202–219.

<https://doi.org/10.1080/07388551.2018.1531822>.

- Bilgili, F., Kocak, E., Kuskaya, S., & Bulut, U. (2022). Co-movements and causalities between ethanol production and corn prices in the USA: New evidence from wavelet transform analysis. *Energy*, 259, 124-874. <https://doi.org/10.1016/j.energy.2022.124874>.
- Bindu, V. U., Shanty, A. A., & Mohanan, P. V. (2018). Parameters affecting the improvement of properties and stabilities of immobilized α -amylase on chitosan metal oxide composites. *International Journal Biochemistry and Biophysics*, 6(1), 44-57. <http://dx.doi.org/10.15226/2374-8141/4/2/00146>.
- Binod, P., Satyanagalakshmi, K., Sindhu, R., Janu, K. U., Sukumaran, R. K., & Pandey, A. (2012). Short duration microwave assisted pretreatment enhances the enzymatic saccharification and fermentable sugar yield from sugarcane bagasse. *Renewable Energy*, 37(1), 109-116. <https://doi.org/10.1016/j.renene.2011.06.007>
- Biró, E., Németh, A. S., Sisak, C., Feczko, T., & Gyenis, J. (2008). Preparation of chitosan particles suitable for enzyme immobilization. *Journal of Biochemical and Biophysical Methods*, 70(6), 1240 – 1246. <https://doi.org/10.1016/j.jprot.2007.11.005>.
- Bolivar, J. M., & Nidetzky, B. (2020). On the relationship between structure and catalytic effectiveness in solid surface-immobilized enzymes: Advances in methodology and the quest for a single-molecule perspective. *Biochimica et Biophysica Acta Proteins and Proteomics* 1868 (2), 34-45. <https://doi.org/10.1016/j.bbaPP.2019.140333>.
- Boneberg, B. S., Machado, G. D., Santos, D. F., Gomes, F., Faria, D. J., Gomes, L. A., & Santos, F. A. (2016). Biorefinery of lignocellulosic biopolymers. *Revista Eletrônica Científica da UERGS*, 2(1), 79-100. <http://dx.doi.org/10.21674/2448-0479.21.79-100>.
- Boukir, A., Mehyaoui, I., Fellak, S., Asia, L., & Doumenq, P. (2019). The effect of the natural degradation process on the cellulose structure of Moroccan hardwood fiber: a survey on spectroscopy and structural properties. *Mediterranean Journal of Chemistry*, 8(3), 179–190. <https://doi.org/10.13171/mjc8319050801ab>
- Breig, S. J. M., & Luti, K. J. K. (2021). Response surface methodology: A review on its applications and challenges in microbial cultures. *Materials Today: Proceedings*, 42, 2277–2284. <https://doi.org/10.1016/j.matpr.2020.12.316>.

- Brena, B., González-Pombo, P., & Batista-Viera, F. (2013). Immobilization of enzymes: A literature survey. *Methods in Molecular Biology* 1051, 15–31. https://doi.org/10.1007/978-1-62703-550-7_2.
- Budimir, N., Jarić, M., Jaćimović, B. M., Genić, S., & Jaćimović, N. B. (2011). Rectified ethanol production cost analysis. *Thermal Science*, 15(2), 281-292. <https://doi:10.2298/tsci100914022b>.
- Cadini, P., & Angelucci, F. (2013). Analysis of incentive and disincentive for maize in Nigeria. *Monitoring African Food and Agricultural Policies (MAFAP)* 3(4), 41-53. Technical Report Series MAFAP/FAO Rome. <http://www.fao.org/mafap>
- Cantone, S., Ferrario, V., Corici, L., Ebert, C., Fattor, D., Spizzo, P., & Gardossi, L. (2013). Efficient immobilisation of industrial biocatalysts: Criteria and constraints for the selection of organic polymeric carriers and immobilisation methods. *Chemical Society Reviews*, 42(15), 6262–6276. <https://doi.org/10.1039/c3cs35464d>.
- Carvalho, F., Duarte, L. C., & Gírio, F. M. (2008). Hemicellulose biorefineries: a review on biomass pretreatments. *Journal of Scientific & Industrial Research*, 3(4), 849-864. <http://hdl.handle.net/10400.9/791>.
- Cea, M., González, M. E., Abarzúa, M., & Navia, R. (2019). Enzymatic esterification of oleic acid by *Candida rugosa* lipase immobilized onto biochar. *Journal of Environmental Management*, 242, 171–177. <https://doi.org/10.1016/j.jenvman.2019.04.013>.
- Cha, J. S., Park, S. H., Jung, S. C., Ryu, C., Jeon, J. K., Shin, M. C., & Park, Y. K. (2016). Production and utilization of biochar: A review. In *Journal of Industrial and Engineering Chemistry*, 40(1), 1–15. <https://doi.org/10.1016/j.jiec.2016.06.002>.
- Chadha, B. S., Kaur, B., Basotra, N., Tsang, A., & Pandey, A. (2019). Thermostable xylanases from thermophilic fungi and bacteria: Current perspective. *Bioresource Technology*, 277(2), 195–203. Elsevier. <https://doi.org/10.1016/j.biortech.2019.01.044>.
- Chamekh, R., Deniel, F., Donot, C., Jany, J. L., Nodet, P., & Belabid, L. (2019). Isolation, identification and enzymatic activity of halotolerant and halophilic fungi from the Great Sebkhia of Oran in Northwestern of Algeria. *Mycobiology*, 47(2), 230-241. <https://doi.org/10.1080%2F12298093.2019.1623979>
- Chapman, J., Ismail, A. E., & Dinu, C. Z. (2018). Industrial applications of enzymes: Recent advances, techniques, and outlooks. In *Catalysts*, 8 (6), 238-251. Multidisciplinary Digital Publishing Institute. <https://doi.org/10.3390/catal8060238>.
- Chen, B., Qiu, J., Mo, H., Yu, Y., Ito, K., Sakai, E., & Feng, H. (2017). Synthesis of mesoporous silica with different pore sizes for cellulase immobilization: Pure physical adsorption. *New Journal of Chemistry*, 41(17), 9338–9345. <https://doi.org/10.1039/c7nj00441a>.

- Chiaromonti, D., Prussi, M., Ferrero, S., Oriani, L., Ottonello, P., Torre, P., & Cherchi, F. (2012). Review of pretreatment processes for lignocellulosic ethanol production, and development of an innovative method. *Biomass and Bioenergy*, 46, 25-35. <https://doi.org/10.1016/j.biombioe.2012.04.020>.
- Chinedu, S., Okochi, V., & Omidiji, O. (2016). Cellulase production by wild strains of *Aspergillus niger*, *Penicillium chrysogenum* and *Trichoderma harzianum* grown on waste cellulosic materials. *Ife Journal of Science*, 13(1), 57–62. <https://www.ajol.info/index.php/ij/article/view/131277>.
- Chisti, Y. (2007). Biodiesel from Microalgae; *Biotechnology Advances*, 25, 294–306. <https://doi.org/10.1016/j.biotechadv.2007.02.001>.
- Chongkhong, S., & Tongurai, C. (2018). Optimization of glucose production from corncob by microwave-assisted alkali pretreatment and acid hydrolysis. *Songklanakarinn Journal of Science & Technology*, 40(3) 555-562. <https://api.semanticscholar.org/CorpusID:198992247>.
- Christia, A., Setiowati, A. D., Millati, R., Karimi, K., Cahyanto, M. N., Niklasson, C., & Taherzadeh, M. J. (2016). Ethanol production from alkali-pretreated oil palm empty fruit bunch by simultaneous saccharification and fermentation with *Mucor indicus*. *International Journal of Green Energy*, 13(6), 566-572. <https://doi.org/10.1080/15435075.2014.978004>.
- Creamer, A. E., Gao, B., & Wang, S. (2016). Carbon dioxide capture using various metal oxyhydroxide-biochar composites. *Chemical Engineering Journal*, 283, 826–832. <https://doi.org/10.1016/j.cej.2015.08.037>.
- da Silva, P. O., de Alencar Guimarães, N. C., Serpa, J. M., Masui, D. C., Marchetti, C. R., Verbisck, N. V., Zanoelo, F. F., Ruller, R., & Giannesi, G. C. (2019). Application of an endo-xylanase from *Aspergillus japonicus* in the fruit juice clarification and fruit peel waste hydrolysis. *Biocatalysis and Agricultural Biotechnology*, 21, 101312. <https://doi.org/10.1016/j.bcab.2019.101312>.
- Da Silva, R., Lago, E. S., Merheb, C. W., Macchione, M. M., Yong, K. P., & Gomes, E. (2005). Production of xylanase and CMCase on solid state fermentation in different residues by *Thermoascus aurantia*. *Brazilian Journal of Microbiology*, 36(3), 235–241. <https://doi.org/10.1590/s1517-83822005000300006>.
- Dal Magro, L., Silveira, V. C., de Menezes, E. W., Benvenuto, E. V., Nicolodi, S., Hertz, P. F., & Rodrigues, R. C. (2018). Magnetic biocatalysts of pectinase and cellulase: synthesis and characterization of two preparations for application in grape juice clarification. *International Journal of Biological Macromolecules*, 115, 35-44. <https://doi.org/10.4314/jasem.v19i4.22>.
- Dante, R. C., Martín-Ramos, P., Correa-Guimaraes, A., & Martín-Gil, J. (2011). Synthesis of graphitic carbon nitride by reaction of melamine and uric acid. *Materials Chemistry and Physics*, 130(3), 1094–1102. <https://doi.org/10.1016/j.matchemphys.2011.08.041>.

- de Carvalho, D. M., Berglund, J., Marchand, C., Lindström, M. E., Vilaplana, F., & Sevastyanova, O. (2019). Improving the thermal stability of different types of xylans by acetylation. *Carbohydrate Polymers*, 220, 132–140. <https://doi.org/10.1016/j.carbpol.2019.05.063>.
- Demirci, S., Sahiner, M., Yilmaz, S., Karadag, E., & Sahiner, N. (2020). Enhanced enzymatic activity and stability by in situ entrapment of α -Glucosidase within super porous cryogels during synthesis. *Biotechnology Reports*, 28 ((9), 534-546.
- Dias, M. O. S., Da Cunha, M. P., MacIel Filho, R., Bonomi, A., Jesus, C. D. F., & Rossell, C. E. V. (2011). Simulation of integrated first- and second-generation bioethanol production from sugarcane: Comparison between different biomass pretreatment methods. *Journal of Industrial Microbiology and Biotechnology*, 38(8), 955–966. <https://doi.org/10.1007/s10295-010-0867-6>.
- Dmytruk, K. V., Kshanovska, B. V., Abbas, C. A., & Sibirny, A. (2016). New methods for positive selection of yeast ethanol overproducing mutants. *Bioethanology*, 2(1). <https://doi.org/10.1515/bioeth-2015-0003>.
- Dutta, K., Daverey, A., & Lin, J. G. (2014). Evolution retrospective for alternative fuels: First to fourth generation. *Renewable Energy*, 69, 114-122. <https://doi.org/10.1016/j.renene.2014.02.044>.
- Egerton, R. F. (2016). Physical principles of electron microscopy: An introduction to TEM, SEM, and AEM, second edition. *Physical Principles of Electron Microscopy: An Introduction to TEM, SEM, and AEM, Second Edition*. Springer International Publishing. <https://doi.org/10.1007/978-3-319-39877-8>.
- Egwim, E. C., Adesina A., A., Oyewole, O. A., & Okoliegbe, I. N. (2014). Optimization of Lipase Immobilized on Chitosan Beads for Biodiesel Production. *Global Research Journal of Microbiology*, 2(2), 103–112. <http://repository.futminna.edu.ng:8080/jspui/handle/123456789/1084>.
- Egwim, E. C., Oluwatosin, S. K., & Deborah, K. (2015). Microwave-alkaline assisted pretreatment of banana trunk for bioethanol production. *Journal of Energy and Power Engineering*, 9, 705-13. <http://repository.futminna.edu.ng:8080/jspui/handle/123456789/1554>.
- Ejaz, U., Sohail, M., & Ghanemi, A. (2021). Cellulases: From bioactivity to a variety of industrial applications. *Biomimetics*, 6(3), 44. <https://doi.org/10.3390/biomimetics6030044>.
- Ethaib, S., Omar, R., Mustapa Kamal, S. M., Awang Biak, D. R., Syam, S., & Harun, M. Y. (2017). Microwave-assisted pretreatment of sago palm bark. *Journal of Wood Chemistry and Technology*, 37(1), 26-42. <https://doi.org/10.1080/02773813.2016.1224249>.
- Ezeoha, S. L., Anyanwu, C. N., & Nwakaire, J. N. (2017). The prospects, impacts, and research challenges of enhanced cellulosic ethanol production: a review. *Nigerian Journal of Technology*, 36(1), 267-275. <http://dx.doi.org/10.4314/njt.v36i1.35>.
- Fakruddin, M., Quayum, M. A., Ahmed, M. M., & Choudhury, N. (2012). Analysis of key factors affecting ethanol production by *Saccharomyces cerevisiae* IFST-

072011. *Biotechnology*, 11(4), 248–252. <https://doi.org/10.3923/biotech.2012.248.252>.

- Farkade, H. S., & Pathre, A. P. (2012). Experimental investigation of methanol, ethanol and butanol blends with gasoline on SI engine. *International Journal of Emerging Technology and Advanced Engineering*, 2(4), 205-215. <https://api.semanticscholar.org/CorpusID:18516632>.
- Favaro, L., Jansen, T., & van Zyl, W. H. (2019). Exploring industrial and natural *Saccharomyces cerevisiae* strains for the bio-based economy from biomass: the case of bioethanol. In *Critical Reviews in Biotechnology* 39(6), 800–816. <https://doi.org/10.1080/07388551.2019.1619157>.
- Fernandez-Lopez, L., Pedrero, S. G., Lopez-Carrobles, N., Gorines, B. C., Virgen-Ortíz, J. J., & Fernandez-Lafuente, R. (2017). Effect of protein load on stability of immobilized enzymes. *Enzyme and Microbial Technology*, 98, 18–25. <https://doi.org/10.1016/j.enzmictec.2016.12.002>.
- Flemming, P., Janke, A., Simon, F., Fery, A., Münch, A. S., & Uhlmann, P. (2020). Multiresponsive Transitions of *pdmaema* Brushes for Tunable Surface Patterning. *Langmuir*, 36(50), 15283–15295. <https://doi.org/10.1021/acs.langmuir.0c02711>.
- Fopase, R., Paramasivam, S., Kale, P., & Paramasivan, B. (2020). Strategies, challenges and opportunities of enzyme immobilization on porous silicon for biosensing applications. *Journal of Environmental Chemical Engineering*, 8(5). <https://doi.org/10.1016/j.jece.2020.104266>.
- Galadima, A., Garba, Z. N., Ibrahim, B. M., Almustapha, M. N., Leke, L., & Adam, I. K. (2011). Biofuels Production in Nigeria: The Policy and Public Opinions. *Journal of Sustainable Development*, 4(4). <https://doi.org/10.5539/jsd.v4n4p22>.
- Gao, X., Zhai, Q., Hu, M., Li, S., & Jiang, Y. (2021). Hierarchically porous magnetic Fe₃O₄/Fe-MOF used as an effective platform for enzyme immobilization: a kinetic and thermodynamic study of structure-activity. *Catalysis Science and Technology*, 11(7), 2446–2455. <https://doi.org/10.1039/d0cy02146f>.
- Gatdula, K. M., Demafelis, R. B., & Bataller, B. G. (2021). Comparative analysis of bioethanol production from different potential biomass sources in the Philippines. *Bioethanol Technologies*, 55, 345-367.
- Gavahian, M., Munekata, P. E., Eş, I., Lorenzo, J. M., Khaneghah, A. M., & Barba, F. J. (2019). Emerging techniques in bioethanol production: from distillation to waste valorization. *Green Chemistry*, 21(6), 1171-1185.
- Gazliya, N., & Aparna, K. (2021). Microwave-alkaline delignification of banana peduncle. *Journal of Natural Fibers*, 18(5), 664–673. <https://doi.org/10.1080/15440478.2019.1645786>.
- Germec, M., Ozcan, A., & Turhan, I. (2023). Effect of process parameters and media on the production of ethanol by *Scheffersomyces stipitis* in shake flask fermentation. *Biomass Conversion and Biorefinery*, 34(7), 234-251.
- Ghani, W. A. W. A. K., Mohd, A., da Silva, G., Bachmann, R. T., Taufiq-Yap, Y. H., Rashid, U., & Al-Muhtaseb, A. H. (2013). Biochar production from waste

- rubber-wood-sawdust and its potential use in sequestration: Chemical and physical characterization. *Industrial Crops and Products*, 44, 18–24. <https://doi.org/10.1016/j.indcrop.2012.10.017>.
- Ghose, T. K. (1987). Measurement of cellulase activities. *Pure and Applied Chemistry*, 59(2), 257–268. <https://doi.org/10.1351/pac198759020257>.
- Giannakopoulou, A., Patila, M., Spyrou, K., Chalmpes, N., Zarafeta, D., Skretas, G., Gournis, D., & Stamatis, H. (2019). Development of a four-enzyme magnetic nanobiocatalyst for multi-step cascade reactions. *Catalysts*, 9(12). <https://doi.org/10.3390/catal9120995>.
- Godwin, P. M., Pan, Y., Xiao, H., & Afzal, M. T. (2019). Progress in Preparation and Application of Modified Biochar for Improving Heavy Metal Ion Removal from Wastewater. *Journal of Bioresources and Bioproducts*, 4(1), 31–42. <https://doi.org/10.21967/jbb.v4i1.180>.
- Golgeri M, D. B., Mulla, S. I., Bagewadi, Z. K., Tyagi, S., Hu, A., Sharma, S., Bilal, M., Bharagava, R. N., Ferreira, L. F. R., Gurumurthy, D. M., & Nadda, A. K. (2022). A systematic review on potential microbial carbohydrases: current and future perspectives. *Critical Reviews in Food Science and Nutrition*, 4(7), 122-132.
- Golińska, P., & Dahm, H. (2011). Enzymatic activity of *actinomycetes* from the genus *streptomyces* isolated from the bulk soil and *rhizosphere* of the genus *sylvestris*. *Dendrobiology*, 65, 37–46. <https://api.semanticscholar.org/CorpusID:84545242>.
- Gonzalez-Renteria, S. M., Soto-Cruz, N. O., Rutiaga-Quinones, O. M., Medrano-Roldan, H., Rutiaga-Quinones, J. G., & Lopez-Miranda, J. (2011). Optimization of the enzymatic hydrolysis process of four straw bean varieties (Pinto villa, Pinto saltillo, Pinto mestizo and Flor de mayo). *Revista Mexicana de Ingeniería Química*, 10(1), 17-28.
- Govindaraj, V., Subramani, A. K., Gopalakrishnan, R., Kim, S. K., Raval, R., & Raval, K. (2023). Bioethanol: A New Synergy between Marine Chitinases from *Bacillus haynesii* and Ethanol Production by *Mucor circinelloides*. *Fermentation*, 9(1), 40. <https://doi.org/10.3390/fermentation9010040>.
- Grima, E. M., Belarbi, E. H., Fernández, F. A., Medina, A. R., & Chisti, Y. (2013). Recovery of microalgal biomass and metabolites: process options and economics. *Biotechnology Advances*, 20(7-8), 491-515. [https://doi.org/10.1016/S0734-9750\(02\)00050-2](https://doi.org/10.1016/S0734-9750(02)00050-2).
- Guan, W., Zhang, Y., Yan, C., Chen, Y., Wei, Y., Cao, Y., Wang, F., & Huo, P. (2022). Base-Free Aerobic Oxidation of Furfuralcohols and Furfurals to Furancarboxylic Acids over Nitrogen-Doped Carbon-Supported AuPd Bowl-Like Catalyst. *ChemSusChem*, 15(16). <https://doi.org/10.1002/cssc.202201041>.
- Gunam, I. B. W., Setiyo, Y., Antara, N. S., Wijaya, I. M. M., Arnata, I. W., & Putra, I. W. W. P. (2020). Enhanced delignification of corn straw with alkaline pretreatment at mild temperature. *Rasaya Journal of Chemistry*, 13(2), 1022-1029. <http://dx.doi.org/10.31788/RJC.2020.1325573>.
- Guzik, U., Hupert-Kocurek, K., & Wojcieszynska, D. (2014). Immobilization as a strategy for improving enzyme properties- Application to oxidoreductases. In *Molecules*, 19(7), 8995–9018. <https://doi.org/10.3390/>

molecules19078995.

- Haldar, D., Sen, D., & Gayen, K. (2018). Enzymatic hydrolysis of banana stems (*Musa acuminata*): Optimization of process parameters and inhibition characterization. *International Journal of Green Energy*, 15(6), 406–413. <https://doi.org/10.1080/15435075.2018.1467834>.
- Hamouda, H. I., Nassar, H. N., Madian, H. R., Amr, S. S. A., & El-Gendy, N. S. (2015). Response surface optimization of bioethanol production from sugarcane molasses by *Pichia veronae* strain HSC-22. *Biotechnology research international*, 8(7), 48–67
- Han, P., Zhou, X., & You, C. (2020). Efficient Multi-Enzymes Immobilized on Porous Microspheres for Producing Inositol from Starch. *Frontiers in Bioengineering and Biotechnology*, 8, 45–56. <https://doi.org/10.3389/fbioe.2020.00380>.
- Hemraj, V., Diksha, S. & Avneet, G. (2013). A review on commonly used biochemical test for bacteria. *Innovare Journal of Life Sciences*, 1(1), 1–7.
- Hernandez, K., & Fernandez-Lafuente, R. (2011). Control of protein immobilization: Coupling immobilization and site-directed mutagenesis to improve biocatalyst or biosensor performance. *Enzyme and Microbial Technology*, 48(2), 107–122. <https://doi.org/10.1016/j.enzmictec.2010.10.003>.
- Houfani, A. A., Anders, N., Spiess, A. C., Baldrian, P., & Benallaoua, S. (2020). Insights from enzymatic degradation of cellulose and hemicellulose to fermentable sugars a review. *Biomass and Bioenergy* 134(5), 345–367. <https://doi.org/10.1016/j.biom.bioe.2020.105481>.
- Hu, J., Arantes, V., & Saddler, J. N. (2011). The enhancement of enzymatic hydrolysis of lignocellulosic substrates by the addition of accessory enzymes such as xylanase: is it an additive or synergistic effect? *Biotechnology for biofuels*, 4(1), 36 - 44. <https://doi.org/10.1186/1754-6834-4-36>.
- Hu, Z., & Wen, Z. (2008). Enhancing enzymatic digestibility of switchgrass by microwave-assisted alkali pretreatment. *Biochemical Engineering Journal*, 38(3), 369–378. <https://doi.org/10.1016/j.bej.2007.08.001>.
- Hutchinson, U. F., Ntwampe, S. K. O., Chidi, B. S., Mewa-Ngongang, M., du Plessis, H. W., Booyse, M., & Jolly, N. P. (2020). Reusability of Immobilized Cells for Subsequent Balsamic-Styled Vinegar Fermentations. *Fermentation*, 6(4). <https://doi.org/10.3390/fermentation6040103>.
- Hwang, E. T., & Lee, S. (2019). Multienzymatic Cascade Reactions via Enzyme Complex by Immobilization. *Catalysis*, 9(5), 4402–4425.
- Iliescu, R. I., Andronescu, E., Ghitulica, C. D., Voicu, G., Ficai, A., & Hoteteu, M. (2014). Montmorillonite–alginate nanocomposite as a drug delivery system–incorporation and in vitro release of irinotecan. *International Journal of Pharmaceutics*, 463(2), 184–192. <https://doi.org/10.1016/j.ijpharm.2013.08.043>.
- Irfan, M., Nadeem, M., & Syed, Q. (2014). Ethanol production from agricultural wastes using *Saccharomyces cerevisiae*. *Brazilian Journal of Microbiology*, 45(2), 457–465. <https://doi.org/10.1590/S1517-83822014000200012>.
- Ismail, M. H., El Zanaty, A. M., & Abdel-lateif, K. S. (2022). Molecular and

- morphological identification of Trichoderma isolates from Egyptian agriculture wastes-rich soil. *Journal of Breeding and Genetics*, 54(3), 598-607. <http://dx.doi.org/10.54910/sabrao2022.54.3.12>.
- Issa, F. O., Kagbu, J. H., Sunusi, S., & Oba, A. I. (2020). profitability analysis of sugarcane production in Makarfi local government area of Kaduna State, Nigeria. *Journal of Applied Agricultural Research*, 8(1), 12-23. <https://doi.org/10.9734/jaar/2020/18987>.
- Jablonowski, N. D., Pauly, M., & Dama, M. (2022). Microwave Assisted Pretreatment of Szarvasi (*Agropyron elongatum*) Biomass to Enhance Enzymatic Saccharification and Direct Glucose Production. *Frontiers in Plant Science*, 12(1), 3177-3224. <https://doi.org/10.3389/fpls.2021.767254>.
- Jadhav, K. B., & Nagarkar, J. M. (2022). Development of karanj oil and castor oil nanoemulsions and its encapsulation into beads for controlled release larvicidal activity. *Journal of Advanced Scientific Research*, 13(02), 93-100. <https://doi.org/10.55218/JASR.202200000>.
- Jamaldheen, S. B., Sharma, K., Rani, A., Moholkar, V. S., & Goyal, A. (2018). Comparative analysis of pretreatment methods on sorghum (*Sorghum durra*) stalk agrowaste for holocellulose content. *Preparative Biochemistry and Biotechnology*, 48(6), 457-464. <https://doi.org/10.1080/10826068.2018.1466148>
- Jambo, S. A., Abdulla, R., Azhar, S. H. M., Marbawi, H., Gansau, J. A., & Ravindra, P. (2016). A review on third generation bioethanol feedstock. *Renewable and sustainable energy reviews*, 65, 756-769. <https://doi.org/10.1016/j.rser.2016.07.064>.
- Jansen, C., & Lübberstedt, T. (2011). Turning Maize Cobs into a Valuable Feedstock. *BioEnergy Research*, 5(1), 20–31. <https://doi.org/10.1007/S12155-011-9158-Y>.
- Jesionowski, T., Zdarta, J., & Krajewska, B. (2014). Enzyme immobilization by adsorption: A review. In *Adsorption*, 20(5), 801–821. Kluwer Academic Publishers. <https://doi.org/10.1007/s10450-014-9623-y>.
- Jiménez-Bonilla, P., Zhang, J., Wang, Y., Blersch, D., de-Bashan, L. E., Guo, L., & Wang, Y. (2022). Polycationic Surfaces Promote Whole-Cell Immobilization and Induce Microgranulation of *Clostridium saccharoperbutylacetonicum* N1-4 for Enhanced Biobutanol Production. *Applied Materials and Interfaces*, 14(44), 49555-49567. <https://doi.org/10.1021/acsami.2c14888>.
- Jönsson, L. J., & Martín, C. (2016). Pretreatment of lignocellulose: formation of inhibitory by-products and strategies for minimizing their effects. *Bioresource technology*, 199, 103-112. <https://doi.org/10.1016/j.biortech.2015.10.009>.
- Jouzani, G. S., & Taherzadeh, M. J. (2015). Advances in consolidated bioprocessing systems for bioethanol and butanol production from biomass: A comprehensive review. *Biofuel Research Journal*, 2(1), 152–195.
- Kadhun, H. J., Mahapatra, D. M., & Murthy, G. S. (2019). A novel method for real-time estimation of insoluble solids and glucose concentrations during enzymatic hydrolysis of biomass. *Bioresource Technology*, 275, 328-337. <https://doi.org/10.1016/j.biortech.2018.12.071>.

- Karagoz, P., Bill, R. M., & Ozkan, M. (2019). Lignocellulosic ethanol production: Evaluation of new approaches, cell immobilization and reactor configurations. *Renewable Energy*, 143, 741-752. <https://doi.org/10.1016/j.renene.2019.05.045>.
- Karimi, K., & Taherzadeh, M. J. (2016). A critical review of analytical methods in pretreatment of lignocelluloses: Composition, imaging, and crystallinity. *Bioresource Technology*, 200, 1008–1018. <https://doi.org/10.1016/j.biortech.2015.11.022>.
- Karimi, K., & Zamani, A. (2013). *Mucor indicus*: Biology and industrial application perspectives: A review. *Biotechnology Advances*, 31(4), 466–481. <https://doi.org/10.1016/j.biotechadv.2013.01.009>.
- Karimi, S., & Karimi, K. (2018). Efficient ethanol production from kitchen and garden wastes and biogas from the residues. *Journal of Cleaner Production*, 187, 37–45. <https://doi.org/10.1016/j.jclepro.2018.03.172>.
- Kim, J. S., Lee, Y. Y., & Kim, T. H. (2016). A review on alkaline pretreatment technology for bioconversion of lignocellulosic biomass. *Bioresource Technology*, 199(1), 42-48. <https://doi.org/10.1016/j.biortech.2015.08.085>.
- Kim, S., & Holtzapple, M. T. (2006). Delignification kinetics of corn stover in lime pretreatment. *Bioresource technology*, 97(5), 778-785. <https://doi.org/10.1016/j.biortech.2005.04.002>.
- Kim, T. H., & Kim, T. H. (2014). Overview of technical barriers and implementation of cellulosic ethanol in the US. *Energy*, 66, 13-19. <https://doi.org/10.1016/j.energy.2013.08.008>.
- Kirupa-Sankar, M., Ravikumar, R., Naresh Kumar, M., & Sivakumar, U. (2018). Development of co-immobilized tri-enzyme biocatalytic system for one-pot pretreatment of four different perennial lignocellulosic biomass and evaluation of their bioethanol production potential. *Bioresource Technology*, 269(1), 227–236. <https://doi.org/10.1016/j.biortech.2018.08.091>.
- Krajewska, B. (1991). Chitin and its derivative as support for immobilization of enzymes. *Acta Biotechnological*, 11(3), 269–277. <https://doi.org/10.1002/abio.370110319>.
- Kumar, A., Bhattacharya, T., Shaikh, W. A., Chakraborty, S., Sarkar, D., & Biswas, J. K. (2022). Biochar Modification Methods for Augmenting Sorption of Contaminants. *Current Pollution Reports*, 3(4), 45-59
- Kumar, R., Mago, G., Balan, V., & Wyman, C. E. (2009). Physical and chemical characterizations of corn stover and poplar solids resulting from leading pretreatment technologies. *Bioresource Technology*, 100(17), 3948–3962. <https://doi.org/10.1016/j.biortech.2009.01.075>.
- Lachos-Perez, D., Martinez-Jimenez, F., Rezende, C. A., Tompsett, G., Timko, M., & Forster-Carneiro, T. (2016). Subcritical water hydrolysis of sugarcane bagasse: An approach on solid residues characterization. *Journal of Supercritical Fluids*, 108, 69–78. <https://doi.org/10.1016/j.supflu.2015.10.019>.
- Ladole, M. R., Pokale, P. B., Varude, V. R., Belokar, P. G., & Pandit, A. B. (2021). One

- pot clarification and debittering of grapefruit juice using co-immobilized enzymes@chitosanMNPs. *International Journal of Biological Macromolecules*, 167, 1297–1307. <https://doi.org/10.1016/j.ijbiomac.2020.11.084>.
- Lai, L. W., & Idris, A. (2013). Disruption of oil palm trunks and fronds by microwave-alkali pretreatment. *Bio-Resources*, 8(2), 2792 - 2804. <http://dx.doi.org/10.15376/biores.8.2.2792-2804>.
- Lee, C. H., Lee, H. S., Lee, J. W., Kim, J., Lee, J. H., Jin, E. S., & Hwang, E. T. (2021). Evaluating enzyme stabilizations in calcium carbonate: Comparing in situ and crosslinking mediated immobilization. *International Journal of Biological Macromolecules*, 175, 341–350. <https://doi.org/10.1016/j.ijbiomac.2021.02.028>.
- Lehmann, J., Rillig, M. C., Thies, J., Masiello, C. A., Hockaday, W. C., & Crowley, D. (2011). Biochar effects on soil biota - A review. In *Soil Biology and Biochemistry* 43(9), 1812–1836. <https://doi.org/10.1016/j.soilbio.2011.04.022>.
- Lei, R., Feng, S., & Lauvaux, T. (2020). Country-scale trends in air pollution and fossil fuel CO₂ emissions during 2001-2018: Confronting the roles of national policies and economic growth. *Environmental Research Letters*, 16(1). <https://doi.org/10.1088/1748-9326/abc9e1>.
- Lenihan, P., Orozco, A., O’neill, E., Ahmad, M. N. M., Rooney, D. W., & Walker, G. M. (2010). Dilute acid hydrolysis of lignocellulosic biomass. *Chemical Engineering Journal*, 156(2), 395-403. <https://doi.org/10.1533/9781845699611.2.143>.
- Lennartsson, P. R., Erlandsson, P., & Taherzadeh, M. J. (2014). Integration of the first- and second-generation bioethanol processes and the importance of by-products. *Bioresource Technology*, 165, 3-8 <https://doi.org/10.1016/j.biortech.2014.01.127>.
- Li, B., Elango, J., & Wu, W. (2020). Recent advancement of molecular structure and biomaterial function of chitosan from marine organisms for pharmaceutical and nutraceutical application. *Applied Sciences*, 10(14), 75-87. <https://doi.org/10.3390/app10144719>.
- Li, R., Wang, J. J., Gaston, L. A., Zhou, B., Li, M., Xiao, R., Wang, Q., Zhang, Z., Huang, H., Liang, W., Huang, H., & Zhang, X. (2018). An overview of carbothermal synthesis of metal–biochar composites for the removal of oxyanion contaminants from aqueous solution. *Carbon*, 129, 674–687. <https://doi.org/10.1016/j.carbon.2017.12.070>.
- Li, S., Harris, S., Anandhi, A., & Chen, G. (2019). Predicting biochar properties and functions based on feedstock and pyrolysis temperature: A review and data syntheses. *Journal of Cleaner Production*, 215, 890–902. <https://doi.org/10.1016/j.jclepro.2019.01.106>.
- Liese, A., & Hilterhaus, L. (2013). Evaluation of immobilized enzymes for industrial applications. *Chemical Society Reviews*, 42(15), 6236 - 6249. <http://dx.doi.org/10.1039/c3cs35511j>.
- Limayem, A., & Ricke, S. C. (2012). Lignocellulosic biomass for bioethanol production: Current perspectives, potential issues and future prospects. *Progress in Energy and Combustion Science*, 38(4), 449–467. <https://doi.org/10.1016/j.pecs.2012.03>

.002.

- Liu, H., Kumar, V., Jia, L., Sarsaiya, S., Kumar, D., Juneja, A., Zhang, Z., Sindhu, R., Binod, P., Bhatia, S. K., & Awasthi, M. K. (2021). Biopolymer polyhydroxyalkanoates (PHA) production from apple industrial waste residues: A review. *Chemosphere*, 284, 45-67.
- Liu, Y. K., & Lien, P. M. (2016). Bioethanol production from potato starch by a novel vertical mass-flow type bioreactor with a co-cultured-cell strategy. *Journal of the Taiwan Institute of Chemical Engineers*, 62, 162–168. <https://doi.org/10.1016/j.jtice.2016.01.027>.
- Loc, N. X., Tuyen, P. T. T., Mai, L. C., & Phuong, D. T. M. (2022). Chitosan-Modified Biochar and Unmodified Biochar for Methyl Orange: Adsorption Characteristics and Mechanism Exploration. *Toxics*, 10(9), 54-76.
- Lü, J., Sheahan, C., & Fu, P. (2011). Metabolic engineering of algae for fourth generation biofuels production. *Energy & Environmental Science*, 4(7), 2451-2466. <http://dx.doi.org/10.1039/C0EE00593B>.
- Luz, E. P. C. G., Chaves, P. H. S., Vieira, L. D. A. P., Ribeiro, S. F., de Fátima Borges, M., Andrade, F. K., ... & Vieira, R. S. (2020). In vitro degradability and bioactivity of oxidized bacterial cellulose-hydroxyapatite composites. *Carbohydrate Polymers*, 237, 116-174. <https://doi.org/10.1016/j.carbpol.2020.116174>.
- Maitan, G. P., Visser, E. M., & Guimaraes, V. M. (2015). Enzymatic hydrolysis of lignocellulosic biomass: converting food waste in valuable products. *Current Opinion in Food Science*, 1, 44-49. <https://doi.org/10.1016/j.cofs.2014.10.001>
- Malgas, S., Mafa, M. S., Mkabayi, L., & Pletschke, B. I. (2019). A mini review of xylanolytic enzymes with regards to their synergistic interactions during hetero-xylan degradation. *World Journal of Microbiology and Biotechnology*, 35(12), 1–13). <https://doi.org/10.1007/s11274-019-2765-z>.
- Manyatshe, A., Cele, Z. E., Balogun, M. O., Nkambule, T. T., & Msagati, T. A. (2022). Chitosan modified sugarcane bagasse biochar for the adsorption of inorganic phosphate ions from aqueous solution. *Journal of Environmental Chemical Engineering*, 10(5), 108243. <https://doi.org/10.1016/j.jece.2022.108243>.
- Maryana, R., Ma'rifatun, D., Wheni, I. A., K.w., S., & Rizal, W. A. (2014). Alkaline pretreatment on sugarcane bagasse for bioethanol production. *Energy Procedia*, 47(1), 250–254. <https://doi.org/10.1016/j.egypro.2014.01.221>.
- Matosevic, S., Lye, G. J., & Baganz, F. (2010). Design and characterization of a prototype enzyme microreactor: quantification of immobilized transketolase kinetics. *Biotechnology Progress*, 26(1), 118-126. <https://doi.org/10.1002/btpr.319>.
- Maurya, D. P., Singla, A., & Negi, S. (2015). An overview of key pretreatment processes for biological conversion of lignocellulosic biomass to bioethanol. *Biotechnolgy*, 5(5), 597-609. <https://doi.org/10.1007/s13205-015-0279-4>.
- Meddeb-Mouelhi, F., Moisan, J. K., & Beauregard, M. (2014). A comparison of plate assay methods for detecting extracellular cellulase and xylanase activity. *Enzyme*

and *Microbial Technology*, 66(1), 16–19. <https://doi.org/10.1016/j.enzmictec.2014.07.004>.

- Mehta, J., Bhardwaj, N., Bhardwaj, S. K., Kim, K. H., & Deep, A. (2016). Recent advances in enzyme immobilization techniques: Metal-organic frameworks as novel substrates. *Coordination Chemistry Reviews*, 322, 30–40. <https://doi.org/10.1016/j.ccr.2016.05.007>.
- Mejía-Barajas, J. A., Alvarez-Navarrete, M., Saavedra-Molina, A., Campos-García, J., Valenzuela-Vázquez, U., Amaya-Delgado, L., & Arellano-Plaza, M. (2018). Second-Generation Bioethanol Production through a Simultaneous Saccharification-Fermentation Process Using *Kluyveromyces Marxianus* Thermotolerant Yeast. *Special Topics in Renewable Energy Systems*. <https://doi.org/10.5772/intechopen.78052>.
- Meng, X., & Ragauskas, A. J. (2014). Recent advances in understanding the role of cellulose accessibility in enzymatic hydrolysis of lignocellulosic substrates. *Current Opinion in Biotechnology*, 27(1), 150-158. <https://doi.org/10.1016/j.copbio.2014.01.014>.
- Methner, Y., Magalhães, F., Raihofer, L., Zarnkow, M., Jacob, F., & Hutzler, M. (2022). Beer fermentation performance and sugar uptake of *Saccharomyces fibuligera*—A novel option for low-alcohol beer. *Frontiers in Microbiology*, 13(1), 101-155. <https://doi.org/10.3389/fmicb.2022.1011155>.
- Millati, R., Edebo, L., & Taherzadeh, M. J. (2005). Performance of *Rhizopus*, *Rhizomucor*, and *Mucor* in ethanol production from glucose, xylose, and wood hydrolyzates. *Enzyme and Microbial Technology*, 36(2-3), 294-300. <https://doi.org/10.1016/j.enzmictec.2004.09.007>.
- Mo, H., & Qiu, J. (2020). Preparation of chitosan/magnetic porous biochar as support for cellulase immobilization by using glutaraldehyde. *Polymers*, 12(11), 1–14. <https://doi.org/10.3390/polym12112672>.
- Mohan, D., Abhishek, K., Sarswat, A., Patel, M., Singh, P., & Pittman, C. U. (2018). Biochar production and applications in soil fertility and carbon sequestration—a sustainable solution to crop-residue burning in India. *Advances*, 8(1), 508-520. <https://doi.org/10.1039/C7RA10353K>.
- Mokhena, T. C., Mochane, M. J., Motaung, T. E., Langaniso, L. Z., Thekiso, O. M., & Songca, S. P. (2018). Sugarcane Bagasse and Cellulose Polymer Composites. In *Sugarcane – Technology and Research*, 4(9), 567-611
- Molaverdi, M., Karimi, K., Mirmohamadsadeghi, S., & Galbe, M. (2019). High titer ethanol production from rice straw via solid-state simultaneous saccharification and fermentation by *Mucor indicus* at low enzyme loading. *Energy Conversion and Management*, 182, 520–529. <https://doi.org/10.1016/j.enconman.2018.12.078>.
- Molaverdi, M., Mirmohamadsadeghi, S., Karimi, K., Aghbashlo, M., & Tabatabaei, M. (2022). Efficient ethanol production from rice straw through cellulose restructuring and high solids loading fermentation by *Mucor indicus*. *Journal of Cleaner Production*, 339, 130702. <https://doi.org/10.1016/j.jclepro.2022.130702>.

- Mood, S. H., Golfeshan, A. H., Tabatabaei, M., Jouzani, G. S., Najafi, G. H., Gholami, M., & Ardjmand, M. (2013). Lignocellulosic biomass to bioethanol, a comprehensive review with a focus on pretreatment. *Renewable and Sustainable Energy Reviews*, 27, 77-93. <https://doi.org/10.1016/j.rser.2013.06.033>.
- Moraís, S., Barak, Y., Caspi, J., Hadar, Y., Lamed, R., Shoham, Y., Wilson, D. B., & Bayer, E. A. (2010). Cellulase-xylanase synergy in designer cellulosomes for enhanced degradation of a complex cellulosic substrate. *Microbiology*, 1(5). <https://doi.org/10.1128/mBio.00285-10>.
- Moreno, A. D., Ibarra, D., Alvira, P., Tomás-Pejó, E., & Ballesteros, M. (2015). A review of biological delignification and detoxification methods for lignocellulosic bioethanol production. *Critical Reviews in Biotechnology*, 35(3), 342-354.
- Mosier, N., Wyman, C., Dale, B., Elander, R., Lee, Y. Y., Holtzapple, M., & Ladisch, M. (2004). Features of promising technologies for pretreatment of lignocellulosic biomass. *Elsevier*. 15(3), 312-324. <https://doi.org/10.1016/j.biortech.2004.06.025>
- Motta, I. L., Arnold, R. A., Lopez-Tenllado, F. J., Filho, R. M., Wolf Maciel, M. R., & Hill, J. M. (2020). CO₂ gasification of sugarcane bagasse char: Consideration of pyrolysis temperature, silicon and aluminum contents, and potassium addition for recirculation of char. *Energy and Fuels*, 34(12), 16201–16211. <https://doi.org/10.1021/acs.energyfuels.0c02786>.
- Mu, D., Seager, T., Rao, P. S., & Zhao, F. (2010). Comparative life cycle assessment of lignocellulosic ethanol production: biochemical versus thermochemical conversion. *Environmental Management*, 46, 565-578. <https://doi.org/10.1007/s00267-010-9494-2>.
- Muley, A. B., Thorat, A. S., Singhal, R. S., & Babu, K. H. (2018). A tri-enzyme co-immobilized magnetic complex: Process details, kinetics, thermodynamics and applications. *International Journal of Biological Macromolecules*, 118(1), 1781-1795. <https://doi.org/10.1016/j.ijbiomac.2018.07.022>.
- Naghdi, M., Taheran, M., Brar, S. K., Kermanshahi-pour, A., Verma, M., & Surampalli, R. Y. (2019). Fabrication of nanobiocatalyst using encapsulated laccase onto chitosan-nanobiochar composite. *International Journal of Biological Macromolecules*, 124, 530–536. <https://doi.org/10.1016/j.ijbiomac.2018.11.234>.
- Najafi, G., Ghobadian, B., Yusaf, T., Ardebili, S. M. S., & Mamat, R. (2015). Optimization of performance and exhaust emission parameters of a SI (spark ignition) engine with gasoline–ethanol blended fuels using response surface methodology. *Energy*, 90, 1815-1829. <https://doi.org/10.1016/j.energy.2015.07.004>.
- Nanda, S., Rana, R., Sarangi, P. K., Dalai, A. K., & Kozinski, J. A. (2018). A broad introduction to first-, second-, and third-generation biofuels. *Recent Advancements in Biofuels and Bioenergy Utilization*, 6(7),1–25.
- Narendranath, N. V., & Power, R. (2004). Effect of yeast inoculation rate on the metabolism of contaminating lactobacilli during fermentation of corn mash. *Journal of Industrial Microbiology and Biotechnology*, 31(12), 581–584. <https://doi.org/10.1007/s10295-004-0191-0>.

- Narron, R. H., Kim, H., Chang, H. M., Jameel, H., & Park, S. (2016). Biomass pretreatments capable of enabling lignin valorization in a biorefinery process. *Current Opinion in Biotechnology*, 38, 39-46. <https://doi.org/10.1016/j.copbio.2015.12.018>.
- Negi, A., & Kesari, K. K. (2022). Chitosan Nanoparticle Encapsulation of Antibacterial Essential Oils. *Micromachines*, 13(8), 1265. <https://doi.org/10.3390/mi13081265>.
- Newton, S. M., Saidu, H., Galadima, A. I., Umar, D. M., Abubakar, K., Kefas, M., & Billah, C. (2017). Determination of physicochemical parameters and riparian land effect on Kwadon stream. *Journal of Advanced Research Design*, 36, 13-24. www.akademiabaru.com/jard.html.
- Nguyen, H. H., & Kim, M. (2017). An Overview of Techniques in Enzyme Immobilization. *Applied Science and Convergence Technology*, 26(6), 157–163. <https://doi.org/10.5757/asct.2017.26.6.157>.
- Nikas, A., Koasidis, K., Köberle, A. C., Kourtesi, G., & Doukas, H. (2022). A comparative study of biodiesel in Brazil and Argentina: An integrated systems of innovation perspective. *Renewable and Sustainable Energy Reviews*, 156, 112022. <https://doi.org/10.1016/j.rser.2021.112022>.
- Nikolić, S., Mojović, L., Rakin, M., & Pejin, D. (2009). Bioethanol production from corn meal by simultaneous enzymatic saccharification and fermentation with immobilized cells of *Saccharomyces cerevisiae* var. *ellipsoideus*. *Fuel*, 88(9), 1602–1607. <https://doi.org/10.1016/j.fuel.2008.12.019>.
- Nilsson, R. H., Larsson, K. H., Taylor, A. F. S., Bengtsson-Palme, J., Jeppesen, T. S., Schigel, D. & Abarenkov, K. (2019). The UNITE database for molecular identification of fungi: handling dark taxa and parallel taxonomic classifications. *Nucleic Acids Research*, 47(1), 259-264. <https://doi.10.1093/nar/gky1022>.
- Niphadkar, S., Bagade, P., & Ahmed, S. (2018). Bioethanol production: insight into past, present and future perspectives. *Biofuels*, 9(2), 229–238. <https://doi.org/10.1080/17597269.2017.1334338>.
- Nwangi, J. K., Lee, W. J., Chang, Y. C., Chen, C. Y., & Wang, L. C. (2015). An overview: Energy saving and pollution reduction by using green fuel blends in diesel engines. *Applied Energy*, 159, 214-236. <https://doi.org/10.1016/j.apenergy.2015.08.084>.
- Okolo, G. N., Neomagus, H. W. J. P., Everson, R. C., Roberts, M. J., Bunt, J. R., Sakurovs, R., & Mathews, J. P. (2015). Chemical-structural properties of South African bituminous coals: Insights from wide angle XRD-carbon fraction analysis, ATR-FTIR, solid state ¹³C NMR, and HRTEM techniques. *Fuel*, 158, 779–792. <https://doi.org/10.1016/j.fuel.2015.06.027>.
- Olofsson, J., Barta, Z., Börjesson, P., & Wallberg, O. (2017). Integrating enzyme fermentation in lignocellulosic ethanol production: life-cycle assessment and techno-economic analysis. *Biotechnology for Biofuels*, 10, 1-14. <https://doi.org/10.1186/s13068-017-0733-0>
- Olumba, C. C., & Onunka, C. N. (2020). Banana and plantain in West Africa: Production

- and marketing. *African Journal of Food, Agriculture, Nutrition and Development*, 20(2), 15474-15489. <http://ajfand.net/AJFAND/v19i4.19>.
- Ovalle-Serrano, S. A., Blanco-Tirado, C., & Combariza, M. Y. (2018). Exploring the composition of raw and delignified Colombian figue fibers, tow and pulp. *Cellulose*, 25(1), 151–165. <https://doi.org/10.1007/S10570-017-1599-9>.
- Oyeleke U., Sohail, M., & Ghanemi, A. (2012). Cellulases: From bioactivity to a variety of industrial applications. *Biomimetics*, 6(3), 44-58.
- Oyeleke, S. B., & Jibrin. (2009). Production of bioethanol from guinea cornhusk and millet husk. *African Journal of Microbiology Research*, 3(4), 147–152. <http://www.academicjournals.org/ajmr>.
- Ozdingis, A. G. B., & Kocar, G. (2018). Current and future aspects of bioethanol production and utilization in Turkey. *Renewable and Sustainable Energy Reviews*, 81, 2196-2203. <https://doi.org/10.1007/s00425-013-1921-1>.
- Padilla, B., Gil, J. V., & Manzanares, P. (2018). Challenges of the non-conventional yeast *wickerhamomyces anomalus* in winemaking. In *Fermentation*, 4(3), 68-79.
- Pal, A., & Khanum, F. (2010). Production and extraction optimization of xylanase from *Aspergillus niger* DFR-5 through solid-state-fermentation. *Bioresource Technology*, 101(19), 7563-7569.
- Pandey, D., Daverey, A., & Arunachalam, K. (2020). Biochar: Production, properties and emerging role as a support for enzyme immobilization. In *Journal of Cleaner Production*, 255, 69-77. <https://doi.org/10.1016/j.jclepro.2020.120267>.
- Parin, F. ., Yıldırım, K., & Terzioğlu, P. (2020). Biochar loaded chitosan/gelatin/poly (ethyleneglycol) biocomposite beads: Morphological, thermal and swelling properties. *Journal of Innovative Science and Engineering*, 4(2), 56–68. <https://doi.org/10.38088/jise.743635>.
- Pauly, M., Gille, S., Liu, L., Mansoori, N., de Souza, A., Schultink, A., & Xiong, G. (2013). Hemicellulose biosynthesis. *Planta*, 238(4), 627-642. <https://doi.org/10.1007/s00425-013-1921-1>.
- Pei, P., Zhang, C., Li, J., Chang, S., Li, S., Wang, J., & Chen, X. (2014). Optimization of NaOH pretreatment for enhancement of biogas production of banana pseudo-stem fiber using response surface methodology. *BioResources*, 9(3), 5073-5087. <https://doi.org/10.4314/biores.v19i4.14>.
- Pham, P. J., Hernandez, R., French, W. T., Estill, B. G., & Mondala, A. H. (2011). A spectrophotometric method for quantitative determination of xylose in fermentation medium. *Biomass and Bioenergy*, 35(7), 2814–2821. <https://doi.org/10.1016/j.biombioe.2011.03.006>.
- Polatoğlu, İ. (2019). Electrochemical Sensing Platform Based on Tyrosinase Immobilized Magnetite Chitosan Nanobiocomposite Film and Its Application as Catechol Biosensor. *Journal of The Electrochemical Society*, 166(15), B1620–B1629. <https://doi.org/10.1149/2.1041915jes>.
- Prajapati, A. S., Panchal, K. J., Pawar, V. A., Noronha, M. J., Patel, D. H., &

- Subramanian, R. B. (2018). Review on cellulase and xylanase engineering for biofuel production. *Industrial Biotechnology* 14(1), 38–44. <https://doi.org/10.1089/ind.2017.0027>.
- Qaseem, M. F., Shaheen, H., & Wu, A. M. (2021). Cell wall hemicellulose for sustainable industrial utilization. *Renewable and Sustainable Energy Reviews*, 144, 110996. <https://doi.org/10.1016/j.rser.2021.110996>.
- Raj, A. (2016). Immobilization and Biochemical Properties of Purified Xylanase from *Bacillus amyloliquefaciens* SK-3 and Its Application in Kraft Pulp Biobleaching. *Journal of Clinical Microbiology and Biochemical Technology*, 4, 026–034. <https://doi.org/10.17352/jcmbt.000012>.
- Raj, S. B., Ramaswamy, S., & Plapp, B. V. (2014). Yeast Alcohol Dehydrogenase Structure and Catalysis. *Biochemistry*, 53(36), 5791–5803. <https://doi.org/10.1021/bi5006442>.
- Raja, W., Kanth, R. H., & Singh, P. (2018). Validating the Aquacrop model for maize under different sowing dates. *Water Policy*, 20(4), 826-840. <https://doi.org/10.1007/s00425-013-1921-1>.
- Rasam, S., Haghghi, A. M., Azizi, K., Soria-Verdugo, A., & Moraveji, M. K. (2020). Thermal behavior, thermodynamics and kinetics of co-pyrolysis of binary and ternary mixtures of biomass through thermogravimetric analysis. *Fuel*, 280, 118665.
- Rasool, U., & Hemalatha, S. (2016). A review on bioenergy and biofuels: sources and their production. *Brazilian Journal of Biological Sciences*, 3(5), 3-9. <https://doi.org/10.21472/bjbs.030501>.
- Raul, C., Bharti, V. S., Dar Jaffer, Y., Lenka, S., & Krishna, G. (2021). Sugarcane bagasse biochar: suitable amendment for inland aquaculture soils. *Aquaculture Research*, 52(2), 643-654. <https://doi.org/10.1111/are.14922>.
- Ravindran, R., Hassan, S. S., Williams, G. A., & Jaiswal, A. K. (2018). A review on bioconversion of agro-industrial wastes to industrially important enzymes. *Bioengineering* ,5(4), 45-67. <https://doi.org/10.3390/bioengineering5040093>.
- Regkouzas, P., & Diamadopoulou, E. (2019). Adsorption of selected organic micro-pollutants on sewage sludge biochar. *Chemosphere*, 224, 840–851. <https://doi.org/10.1016/j.chemosphere.2019.02.165>.
- Reis, V. R., Bassi, A. P. G., Silva, J. C. G. D., & Ceccato-Antonini, S. R. (2013). Characteristics of *Saccharomyces cerevisiae* yeasts exhibiting rough colonies and pseudohyphal morphology with respect to alcoholic fermentation. *Brazilian Journal of Microbiology*, 44, 1121-1131. <https://doi.org/10.1590/s1517-83822014005000020>.
- Ren, S., Li, C., Jiao, X., Jia, S., Jiang, Y., Bilal, M., & Cui, J. (2019). Recent progress in multienzymes co-immobilization and multienzyme system applications. *Chemical Engineering Journal*, 373, 1254–1278. <https://doi.org/10.1016/j.cej.2019.05.141>.
- Rennie, E. A., & Scheller, H. V. (2014). Xylan biosynthesis. *Current Opinion in Biotechnology*, 26, 100–107. <https://doi.org/10.1016/j.copbio.2013.11.013>.

- Rezania, S., Oryani, B., Cho, J., Talaiekhosani, A., Sabbagh, F., Hashemi, B., Rupani, P. F., & Mohammadi, A. A. (2020). Different pretreatment technologies of lignocellulosic biomass for bioethanol production: An overview. *Energy*, 199, 117457. <https://doi.org/10.1016/j.energy.2020.117457>.
- Rezende, C. A., Atta, B. W., Breitzkreitz, M. C., Simister, R., Gomez, L. D., & McQueen-Mason, S. J. (2018). Optimization of biomass pretreatments using fractional factorial experimental design. *Biotechnology for biofuels*, 11(1), 1-15.
- Rodrigues Mota, T., Matias de Oliveira, D., Marchiosi, R., Ferrarese-Filho, O., & Dantas dos Santos, W. (2018). Plant cell wall composition and enzymatic deconstruction. *Bioengineering*, 5(1), 63–77. <https://doi.org/10.3934/bioeng.2018.1.63>.
- Rodrigues, C. I. S., Jackson, J. J., & Montross, M. D. (2016). A molar basis comparison of calcium hydroxide, sodium hydroxide, and potassium hydroxide on the pretreatment of switchgrass and miscanthus under high solids conditions. *Industrial Crops and Products*, 92, 165-173. <https://doi.org/10.1016/j.indcrop.2016.08.010>.
- Roy, H., Islam, M. S., Arifin, M. T., & Firoz, S. H. (2022). Chitosan-ZnO decorated Moringa oleifera seed biochar for sequestration of methylene blue: Isotherms, kinetics, and response surface analysis. *Environmental Nanotechnology, Monitoring and Management*, 9(7), 34-67
- Sadaqat, B., Sha, C., Dar, M. A., Dhanavade, M. J., Sonawane, K. D., Mohamed, H., Shao, W., & Song, Y. (2022). Modifying thermostability and reusability of hyperthermophilic mannanase by immobilization on glutaraldehyde cross-linked chitosan beads. *Biomolecules*, 12(7), 45-89. <https://doi.org/10.3390/biom12070999>.
- Sahare, P., Singh, R., Laxman, R. S., & Rao, M. (2012). Effect of Alkali Pretreatment on the Structural Properties and Enzymatic Hydrolysis of *Corn cob*. *Applied Biochemistry and Biotechnology*, 168(7), 1806–1819. <https://doi.org/10.1007/s12010-012-9898-y>.
- Saifuddin, N., Raziah, A. Z., & Junizah, A. R. (2013). Carbon nanotubes: a review on structure and their interaction with proteins. *Journal of Chemistry*, 2(13),56-88. <https://doi.org/10.1155/2013/676815>.
- Saini, J. K., Saini, R., & Tewari, L. (2015). Lignocellulosic agriculture wastes as biomass feedstocks for second-generation bioethanol production: concepts and recent developments. *Biotechnology*, 5(4), 337-353. <https://doi.org/10.1007/s13205-014-0246-5>.
- Saini, S., & Sharma, K. K. (2021). Fungal lignocellulolytic enzymes and lignocellulose: A critical review on their contribution to multiproduct biorefinery and global biofuel research. *International Journal of Biological Macromolecules*, 193, 2304–2319. <https://doi.org/10.1016/j.ijbiomac.2021.11.063>
- Sajjadi, B., Chen, W. Y., & Egiebor, N. O. (2019). A comprehensive review on physical activation of biochar for energy and environmental applications. *Reviews in Chemical Engineering*, 35(6), 735–776. <https://doi.org/10.1515/revce-2017-0113>.
- Salihu, A., Abbas, O., Sallau, A. B., & Alam, M. Z. (2015). Agricultural residues for

cellulolytic enzyme production by *Aspergillus niger*:. *Biotechnology*, 5(6), 1101–1106. <https://doi.org/10.1007/s13205-015-0294-5>

- Sánchez-Ramírez, J., Martínez-Hernández, J. L., Segura-Ceniceros, P., López, G., Saade, H., Medina-Morales, M. A., Ramos-González, R., Aguilar, C. N., & Ilyina, A. (2017). Cellulases immobilization on chitosan-coated magnetic nanoparticles: application for *Agave Atrovirens* lignocellulosic biomass hydrolysis. *Bioprocess and Biosystems Engineering*, 40(1), 9–22. <https://doi.org/10.1007/s00449-016-1670-1>.
- Sanjivkumar, M., Brindhashini, A., Deivakumari, M., Palavesam, A., & Immanuel, G. (2018). Investigation on Saccharification and Bioethanol Production from Pretreated Agro-Residues Using a Mangrove Associated *Actinobacterium Streptomyces variabilis*. *Waste and Biomass Valorization*, 9(6), 969–984. <https://doi.org/10.1007/s12649-017-9886-0>.
- Santa-Maria, M., Ruiz-Colorado, A. A., Cruz, G., & Jeoh, T. (2013). Assessing the feasibility of biofuel production from lignocellulosic banana waste in rural agricultural communities in Peru and Colombia. *Bioenergy Research*, 6, 1000-1011. <https://doi.org/10.1007/s12155-013-9333-4>.
- Saraiva, B., Pacheco, E. B. V., Visconte, L. L. Y., Bispo, E. P., Escócio, V. A., de Sousa, A. F., ... & Brito, G. F. D. C. (2012). Potentials for utilization of post-fiber extraction waste from tropical fruit production in Brazil—the example of banana pseudo-stem. *International Journal of Environment and Bioenergy*, 4(2), 101-119. <https://doi.org/10.4314/ijeb.v19i4.11>.
- Satari, B., Karimi, K., & Kumar, R. (2019). Cellulose solvent-based pretreatment for enhanced second-generation biofuel production: A review. *Sustainable Energy and Fuels*, 3(1), 51–62. <https://doi.org/10.1039/c8se00287h>.
- Sawarkar, A. N., Kirti, N., Tagade, A., & Tekade, S. P. (2022). Bioethanol from various types of banana waste: a review. *Bioresource Technology Reports*, 2(1), 101092. <https://doi.org/10.1016/j.biteb.2022.101092>.
- Seiboth, B., Ivanova, C., & Seidl-Seiboth, V. (2011). *Trichoderma reesei*: A Fungal Enzyme Producer for Cellulosic Biofuels. *Biofuel Production-Recent Developments and Prospects*, 4(7), 88-94. <https://doi.org/10.5772/16848>.
- Seol, E., Sekar, B. S., Raj, S. M., & Park, S. (2016). Co- production of hydrogen and ethanol from glucose by modification of glycolytic pathways in *Escherichia coli*—from Embden- Meyerhof-Parnas pathway to pentose phosphate pathway. *Biotechnology Journal*, 11(2), 249-256. <https://doi.org/10.1186/s13068-017-0768-2>.
- Shaaban, A., Se, S. M., Dimin, M. F., Juoi, J. M., Mohd Husin, M. H., & Mitan, N. M. M. (2014). Influence of heating temperature and holding time on biochars derived from rubber wood sawdust via slow pyrolysis. *Journal of Analytical and Applied Pyrolysis*, 107, 31–39. <https://doi.org/10.1016/j.jaap.2014.01.021>.
- Shah, A., Patel, H., & Narra, M. (2017). Bioproduction of fungal cellulases and hemicellulases through solid state fermentation. *Fungal Metabolites*, 349, 393. http://dx.doi.org/10.1007/978-3-319-19456-1_7-1

- Shah, K., & Vishwa, A. P. (2019). Microbial Xylanase production and their Industrial application microbial xylanase production and their industrial application in industry: a review. *Applied Biochemistry and Biotechnology*, 22(35), 77- 96.
- Sharifyazd, S., & Karimi, K. (2017). Effects of fermentation conditions on valuable products of ethanolic fungus *Mucor indicus*. *Electronic Journal of Biotechnology*, 30, 77-82. <https://doi.org/10.1016/j.ejbt.2017.09.003>.
- Sharma, A., Tewari, R., Rana, S. S., Soni, R., & Soni, S. K. (2016). Cellulases: Classification, Methods of Determination and Industrial Applications. *Applied Biochemistry and Biotechnology*, 179(8), 1346–1380. <https://doi.org/10.1007/s12010-016-2070-3>.
- Shi, J., Claussen, J. C., McLamore, E. S., Haque, A., Jaroch, D., Diggs, A. R., Calvo-Marzal, P., Rickus, J. L., & Marshall Porterfield, D. (2011). A comparative study of enzyme immobilization strategies for multi-walled carbon nanotube glucose biosensors. *Nanotechnology*, 22(35), 78-90. <https://doi.org/10.1088/0957-4484/22/35/355502>.
- Shimizu, F. L., Monteiro, P. Q., Ghiraldi, P. H. C., Melati, R. B., Pagnocca, F. C., de Souza, W., ... & Brienzo, M. (2018). Acid, alkali and peroxide pretreatments increase the cellulose accessibility and glucose yield of banana pseudostem. *Industrial Crops and Products*, 115, 62-68.
- Shokravi, Z., Shokravi, H., Aziz, M. A., & Shokravi, H. (2019). The Fourth-Generation Biofuel: A Systematic Review on Nearly Two Decades of Research from 2008 to 2019. *Fossil Free Fuels*, 3(5), 213–251. <https://www.taylorfrancis.com/10.1201/9780429327773>.
- Shokrkar, H., & Ebrahimi, S. (2018). Synergism of cellulases and amylolytic enzymes in the hydrolysis of microalgal carbohydrates. *Biofuels, Bioproducts and Biorefining*, 12(5), 749–755. <https://doi.org/10.1002/bbb.1886>.
- Siaut, M., Cuine, S., Cagnon, C., Fessler, B., Nguyen, M., Carrier, P., & Peltier, G. (2011). Oil accumulation in the model green alga *Chlamydomonas reinhardtii*: characterization, variability between common laboratory strains and relationship with starch reserves. *Biotechnology*, 11(7), 23-34. <https://doi.org/10.1186/1472-6750-11-7>.
- Sierra Solache, R. E., Muro-Urista, C., Elena Ortega Aguilar, R., Arana Cuenca, A., & Téllez Jurado, A. (2016). Application of immobilized fungi on food effluent treatment using airlift reactor. *Desalination and Water Treatment*, 57(27), 12743–12754. <https://doi.org/10.1080/19443994.2015.1052565>.
- Simonyan, K. J., & Fasina, O. (2013). Biomass resources and bioenergy potentials in Nigeria. *African Journal of Agricultural Research*, 8(40), 4975-4989. <https://doi.org/10.5897/ajar2013.6726>.
- Sims, R. E., Mabee, W., Saddler, J. N., & Taylor, M. (2010). An overview of second-generation biofuel technologies. *Bioresource Technology*, 101(6), 1570-1580. <https://doi.org/10.1186/1472-6750-11-7>.
- Sindhu, R., Binod, P., & Pandey, A. (2016). Biological pretreatment of lignocellulosic biomass - An overview. *Bioresource Technology*, 199, 76–82.

<https://doi.org/10.1016/j.biortech.2015.08.030>.

- Singh, D. P., & Trivedi, R. K. (2013). Acid and alkaline pretreatment of lignocellulosic biomass to produce ethanol as biofuel. *International Journal of ChemTech Research*, 5(2), 727–734. <https://www.cabdirect.org/cabdirect/abstract/20133146836>.
- Singh, J., Boddula, R., & Digambar Jirimali, H. (2020). Utilization of secondary agricultural products for the preparation of value-added silica materials and their important applications: a review. *Journal of Sol-Gel Science and Technology*, 96, 15-33. <https://doi.org/10.1007/s10971-020-05353-5>.
- Singh, R., Kapoor, V., & Kumar, V. (2012b). Utilization of agro-industrial wastes for the simultaneous production of amylase and xylanase by thermophilic actinomycetes. *Brazilian Journal of Microbiology*, 43(4), 1545–1552. <https://doi.org/10.1590/S1517-83822012000400039>.
- Singh, S. J., Krausmann, F., Gingrich, S., Haberl, H., Erb, K. H., Lanz, P., & Temper, L. (2012a). India's biophysical economy, 1961–2008. Sustainability in a national and global context. *Ecological Economics*, 76, 60-69. <http://dx.doi.org/10.1016/j.ecolecon.2012.01.022>.
- Singla, A., Paroda, S., Dhamija, S.S., Goyal, S., Shekhawat, K., Amachi, S., & Inubushi, K. (2012). Bioethanol production from xylose: problems and possibilities. *Journal of Biofuels*, 3, 39–49. <http://dx.doi.org/10.5958/j.0976-3015.3.1.004>.
- Sluiter, a., Hames, B., Ruiz, R., Scarlata, C., Sluiter, J., Templeton, D., & Crocker, D. (2012). NREL/TP-510-42618 analytical procedure - Determination of structural carbohydrates and lignin in Biomass. *Laboratory Analytical Procedure*, 17, 510-724. <https://doi.org/NREL/TP-510-42618>.
- Smith, P. (2016). Soil carbon sequestration and biochar as negative emission technologies. *Global Change Biology*, 22(3), 1315–1324. <https://doi.org/10.1111/gcb.13178>.
- Song, H. T., Gao, Y., Yang, Y. M., Xiao, W. J., Liu, S. H., Xia, W. C., Liu, Z. L., Yi, L., & Jiang, Z. B. (2016). Synergistic effect of cellulase and xylanase during hydrolysis of natural lignocellulosic substrates. *Bioresource Technology*, 219, 710–715. <https://doi.org/10.1016/j.biortech.2016.08.035>.
- Song, J., He, W., Shen, H., Zhou, Z., Li, M., Su, P., & Yang, Y. (2020). Exquisitely designed magnetic DNA nanocompartment for enzyme immobilization with adjustable catalytic activity and improved enzymatic assay performance. *Chemical Engineering Journal*, 390, 569-734
- Sonkar, K., & Singh, D. P. (2020). Biochemical characterization and thermodynamic study of lipase from psychrotolerant *Pseudomonas punonensis*. *Biocatalysis and Agricultural Biotechnology*, 28, 77-90.
- Sripudorn, B., Laopaiboon, P., Phukoetphim, N., Polsokchuak, N., Butkun, K., & Laopaiboon, L. (2020). Enhancement of ethanol production efficiency in repeated-batch fermentation from sweet sorghum stem juice: Effect of initial sugar, nitrogen and aeration. *Electronic Journal of Biotechnology*, 46, 55–64. <https://doi.org/10.1016/j.ejbt.2020.06.001>.

- Steckel, J. C., Brecha, R. J., Jakob, M., Strefler, J., & Luderer, G. (2013). Development without energy? Assessing future scenarios of energy consumption in developing countries. *Ecological Economics*, 90, 53–67. <https://doi.org/10.1016/j.ecolecon.2013.02.006>.
- Stryer, L; Tymoczko, J; & Berg, J. (2002). Chapter 8 Enzymes: Basic Concepts and Kinetics, Table 8.5. *Biochemistry*, 5th edition. New York: Freeman and Company.
- Subtil, T., & Boles, E. (2012). Competition between pentoses and glucose during uptake and catabolism in recombinant *Saccharomyces cerevisiae*. *Biotechnology for Biofuels*, 5(1), 1-12. <https://doi.org/10.1186/1754-6834-5-14>.
- Sues, A., Millati, R., Edebo, L., & Taherzadeh, M. J. (2005). Ethanol production from hexoses, pentoses, and dilute-acid hydrolyzate by *Mucor indicus*. *FEMS Yeast Research*, 5(6–7), 669–676. <https://doi.org/10.1016/j.femsyr.2004.10.013>.
- Sukmawati, D., Dellanerra, D., & Risandi, A. (2018). Screening the capabilities of Indonesian indigenous mold in producing cellulase enzyme. *Materials Science and Engineering*, 434(1), 4578-6011. <https://doi.org/10.1088/1757-899X/434/1/012125>.
- Sun, R., Lawther, J. M., & Banks, W. B. (1995). Influence of alkaline pre-treatments on the cell wall components of wheat straw. *Industrial Crops and Products*, 4(2), 127–145. [https://doi.org/10.1016/0926-6690\(95\)00025-8](https://doi.org/10.1016/0926-6690(95)00025-8).
- Sun, S., Sun, S., Cao, X., & Sun, R. (2016). The role of pretreatment in improving the enzymatic hydrolysis of lignocellulosic materials. *Bioresource Technology*, 199, 49-58. <https://doi.org/10.1016/j.biortech.2015.08.061>
- Sun, Y., & Cheng, J. (2002). Hydrolysis of lignocellulosic materials for ethanol production: A review. *Bioresource Technology*, 83(1), 1-11. [https://doi.org/10.1016/S0960-8524\(01\)00212-7](https://doi.org/10.1016/S0960-8524(01)00212-7)
- Tabah, B., Nagvenkar, A. P., Perkas, N., & Gedanken, A. (2017). Solar-heated sustainable biodiesel production from waste cooking oil using a sonochemically deposited SrO catalyst on microporous activated carbon. *Energy and Fuels*, 31(6), 6228-6239. <https://doi.org/10.1021/acs.energyfuels.7b00932>.
- Taherzadeh, M., & Karimi, K. (2008). Pretreatment of lignocellulosic wastes to improve ethanol and biogas production: a review. *International Journal of Molecular Sciences*, 9(9), 1621-1651. <https://doi.org/10.3390%2Fijms9091621>.
- Tanimura, A., Kikukawa, M., Yamaguchi, S., Kishino, S., Ogawa, J., & Shima, J. (2015). Direct ethanol production from starch using a natural isolate, *Scheffersomyces shehatae*: Toward consolidated bioprocessing. *Scientific Reports*, 5, 665-679. <https://doi.org/10.1038/srep09593>.
- Tao, L., Tan, E. C., McCormick, R., Zhang, M., Aden, A., He, X., & Zigler, B. T. (2014). Techno- economic analysis and life- cycle assessment of cellulosic isobutanol and comparison with cellulosic ethanol and n- butanol. *Biofuels, Bioproducts and Biorefining*, 8(1), 30-48 <https://doi.org/10.1002/bbb.1431>.
- Tayel, A. A., Moussa, S., Opwis, K., Knittel, D., Schollmeyer, E., & Nickisch-Hartfiel, A. (2010). Inhibition of microbial pathogens by fungal chitosan. *International*

Journal of Biological Macromolecules, 47(1), 10–14. <https://doi.org/10.1016/j.ijbiomac.2010.04.005>.

- Tikka, C., Osuru, H. P., Atluri, N., Raghavulu, P., Yellapu, N. K., Mannur, I. S., Prasad, U. V., Aluru, S., K, N. V., & Bhaskar, M. (2013). Isolation and characterization of ethanol tolerant yeast strains. *Bioinformation*, 9(8), 421–425. <https://doi.org/10.6026/97320630009421>.
- Tock, J. Y., Lai, C. L., Lee, K. T., Tan, K. T., & Bhatia, S. (2010). Banana biomass as potential renewable energy resource: A Malaysian case study. *Renewable and Sustainable Energy Reviews*, 14(2), 798-805. <https://doi.org/10.1016/j.rser.2009.10.010>.
- Tomczyk, A., Sokołowska, Z., & Boguta, P. (2020). Biochar physicochemical properties: pyrolysis temperature and feedstock kind effects. *Reviews in Environmental Science and Biotechnology*, 19(1), 191–215). <https://doi.org/10.1007/s11157-020-09523-3>.
- Tripathi, S. K., Kaur, D., Bhardwaj, N. K., Pathak, P., & Kumar, S. (2021). Improving Biogas Production by Co-digestion of Banana Stem Juice with Agro-Based Material Washings and Digestate Along with Microbial Culture. *Waste and Biomass Valorization*, 12(3), 1385–1393. <https://doi.org/10.1007/s12649-020-01101-6>.
- Tulashie, S. K., Akpari, E. E. A., Appiah, G., Adongo, A., & Andoh, E. K. (2021). Acid hydrolysis of sawdust waste into bioethanol. *Biomass Conversion and Biorefinery*, 2(3), 1-14. <https://link.springer.com/article/10.1007%2Fs13399-021-01725-1>.
- Uday, U. S. P., Choudhury, P., Bandyopadhyay, T. K., & Bhunia, B. (2016). Classification, mode of action and production strategy of xylanase and its application for biofuel production from water hyacinth. *International Journal of Biological Macromolecules*, 82, 1041–1054. <https://doi.org/10.1016/j.ijbiomac.2015.10.086>.

- Udomkun, P., Masso, C., Swennen, R., Innawong, B., Fotso Kuate, A., Alakonya, A., & Vanlauwe, B. (2021). Consumer preferences and socioeconomic factors decided on plantain and plantain-based products in the central region of Cameroon and Oyo State, Nigeria. *Foods*, 10(8), 1955. <https://doi.org/10.3390/foods10081955>.
- Ukwuru, M., U., & Awah, J., I. (2013). Properties of Palm Wine Yeast and its Performance in Wine Making. *African Journal of Biotechnology*, 12(19): 2670-2677 <https://api.semanticscholar.org/CorpusID:56270823>.
- Umar, U. U., Ado, S. G., Aba, D. A., & Bugaje, S. M. (2015). Studies on genetic variability in maize (*Zea mays* L.) under stress and non-stress environmental conditions. *International Journal of Agronomy and Agricultural Research*, 7(1), 70–77. <http://www.innspub.net>.
- Valliammai, M. G., Gopal, N. O., & Anandham, R. (2021). Probing cellulolytic yeast from forest ecosystem for the saccharification of Napier fodder biomass. *Journal of Environmental Biology*, 42, 1152-1161. [https://doi.org/10.22438/jeb/42/4\(SI\)/MRN-1538a](https://doi.org/10.22438/jeb/42/4(SI)/MRN-1538a).
- Vane, L. M., Alvarez, F. R., Rosenblum, L., & Govindaswamy, S. (2013). Efficient ethanol recovery from yeast fermentation broth with integrated distillation-membrane process. *Industrial and Engineering Chemistry Research*, 52(3), 1033–1041. <https://doi.org/10.1021/ie2024917>.
- Vanholme, R., Demedts, B., Morreel, K., Ralph, J., & Boerjan, W. (2010). Lignin biosynthesis and structure. *Plant Physiology*, 153(3), 895-905. <https://doi.org/10.1104/pp.110.155119>.
- Varghese, N. & Joy P. P. (2014). *Microbiology Laboratory Manual*. Kerala India: *Aromatic and Medicinal plant Research Station*.
- Varma, A. K., Thakur, L. S., Shankar, R., & Mondal, P. (2019). Pyrolysis of wood sawdust: Effects of process parameters on products yield and characterization of products. *Waste Management*, 89, 224–235. <https://doi.org/10.1016/j.wasman.2019.04.016>.
- Vasilescu, C., Marc, S., Hulka, I., & Paul, C. (2022). Enhancement of the Catalytic Performance and Operational Stability of Sol-Gel-Entrapped Cellulase by Tailoring the Matrix Structure and Properties. *Gels*, 8(10),67-89. <https://doi.org/10.3390/gels8100626>.
- Verma, N., Kumar, V., & Bansal, M. C. (2018). Utility of *Luffa cylindrica* and *Litchi chinensis* peel, an agricultural waste biomass in cellulase production by *Trichoderma reesei* under solid state cultivation. *Biocatalysis and Agricultural Biotechnology*, 16, 483–492. <https://doi.org/10.1016/j.bcab.2018.09.021>.
- Vohra, M., Manwar, J., Manmode, R., Padgilwar, S., & Patil, S. (2014). Bioethanol production: feedstock and current technologies. *Journal of Environmental Chemical Engineering* 2(1), 573-584. <https://doi.org/10.1016/j.jece.2013.10.013>.
- Wang, Q., Wang, W., Tan, X., Chen, X., Guo, Y., Yu, Q., & Zhuang, X. (2019). Low-temperature sodium hydroxide pretreatment for ethanol production from sugarcane bagasse without washing process. *Bioresource Technology*, 291, 121844. <https://doi.org/10.1016/j.biortech.2019.121844>.

- Wang, W., Bai, J., Lu, Q., Zhang, G., Wang, D., Jia, J., Guan, Y., & Yu, L. (2021). Pyrolysis temperature and feedstock alter the functional groups and carbon sequestration potential of *Phragmites australis*- and *Spartina alterniflora*-derived biochars. *Bioenergy*, 13(3), 493–506. <https://doi.org/10.1111/gcbb.12795>.
- Wang, W., Wang, X., Zhang, Y., Yu, Q., Tan, X., Zhuang, X., & Yuan, Z. (2020). Effect of sodium hydroxide pretreatment on physicochemical changes and enzymatic hydrolysis of herbaceous and woody lignocelluloses. *Industrial Crops and Products*, 145, 668 - 701. <https://doi.org/10.1016/j.indcrop.2020.112145>.
- Waqas, M., Aburiazaiza, A. S., Miandad, R., Rehan, M., Barakat, M. A., & Nizami, A. S. (2018). Development of biochar as fuel and catalyst in energy recovery technologies. *Journal of cleaner production*, 188, 477-488. <https://doi.org/10.1016/j.jclepro.2018.04.017>.
- Weber, K., & Quicker, P. (2018). Properties of biochar. *Fuel*, 217, 240–261. <https://doi.org/10.1016/j.fuel.2017.12.054>.
- Wehaidy, H. R., Abdel-Naby, M. A., El-Hennawi, H. M., & Youssef, H. F. (2019). Nanoporous Zeolite-X as a new carrier for laccase immobilization and its application in dyes decolorization. *Biocatalysis and Agricultural Biotechnology*, 19, 56-77. <https://doi.org/10.1016/j.bcab.2019.101135>.
- Weng, Z.-H., Nargotra, P., Kuo, C.-H., & Liu, Y.-C. (2022). Immobilization of Recombinant Endoglucanase (CelA) from *Clostridium thermocellum* on Modified Regenerated Cellulose Membrane. *Catalysts*, 12(11), 1356. <https://doi.org/10.3390/catal12111356>.
- Whangchai, K., Inta, W., Unpaprom, Y., Bhuyar, P., Adoonsook, D., & Ramaraj, R. (2021). Comparative analysis of fresh and dry free-floating aquatic plant *Pistia stratiotes* via chemical pretreatment for second-generation (2G) bioethanol production. *Bioresource Technology Reports*, 14, 100651. <https://doi.org/10.1016/j.biteb.2021.100651>.
- Wojnarowska, Z., Knapik, J., Jacquemin, J., Berdzinski, S., Strehmel, V., Sangoro, J. R., & Paluch, M. (2015). Effect of pressure on decoupling of ionic conductivity from segmental dynamics in polymerized ionic liquids. *Macromolecules*, 48(23), 8660-8666. <https://doi.org/10.1021/acs.macromol.5b02130>.
- Wu, D., Xie, X., Zhang, Y., Zhang, D., Du, W., Zhang, X., & Wang, B. (2020). MnO₂/Carbon Composites for Supercapacitor: Synthesis and Electrochemical Performance. *Frontiers in Materials* 7, 67-90.
- Wu, G., Li, M., Luo, Z., Qi, L., Yu, L., Zhang, S., & Liu, H. (2022). Designed Synthesis of Compartmented Bi-enzyme Biocatalysts Based on Core–Shell Zeolitic Imidazole Framework Nanostructures. *Small*. 7(1), 60–71. <https://doi.org/10.1002/smll.202206606>.
- www.factfish.com/statistic-country/nigeria/bagasse,+production (retrieved 4 August 2019).
- Wyman, C. E. (2001). Twenty years of trials, tribulations, and research progress in bioethanol technology: selected key events along the way. *Applied Biochemistry and Biotechnology*, 91, 5-21. <https://doi.org/10.1385/abab:91-93:1-9:5>.

- Wyman, C. E. (2007). What is (and is not) vital to advancing cellulosic ethanol. *TRENDS in Biotechnology*, 25(4), 153-157. <https://doi.org/10.1016/j.tibtech.2007.02.009>.
- Wyman, C. E., & Yang, B. (2017). Combined severity factor for predicting sugar recovery in acid-catalyzed pretreatment followed by enzymatic hydrolysis. *Springer International Publishing*. 3(1), 161–180. https://doi.org/10.1007/978-3-319-56457-9_6.
- Wyman, C. E., Dale, B. E., Elander, R. T., Holtzapple, M., Ladisch, M. R., & Lee, Y. Y. (2005). Comparative sugar recovery data from laboratory scale application of leading pretreatment technologies to corn stover. *Bioresource Technology*, 96(18), 2026–2032. <https://doi.org/10.1016/j.biortech.2005.01.018>.
- Xie, A. J., Lee, D. J., & Lim, S. T. (2021). Characterization of resistant waxy maize dextrins prepared by simultaneous debranching and crystallization followed by acidic or enzymatic hydrolysis. *Food Hydrocolloids*, 3(12) 121. <https://doi.org/10.1016/j.foodhyd.2021.106942>.
- Xu, D., Chen, C., Xie, J., Zhang, B., Miao, L., Cai, J., & Zhang, L. (2016a). A hierarchical N/S- codoped carbon anode fabricated facilely from cellulose/polyaniline microspheres for high- performance sodium- ion batteries. *Advanced Energy Materials*, 6(6), 1501929 <https://doi.org/10.1002/aenm.201501929>.
- Xu, H., Li, B., & Mu, X. (2016b). Review of Alkali-Based Pretreatment to Enhance Enzymatic Saccharification for Lignocellulosic Biomass Conversion. 7(1), 70–77 <https://doi.org/10.1021/acs.iecr.6b01907>.
- Xu, J., Dai, L., Zhang, C., Gui, Y., Yuan, L., Lei, Y., & Fan, B. (2020). Ionic liquid-aided hydrothermal treatment of lignocellulose for the synergistic outputs of carbon dots and enhanced enzymatic hydrolysis. *Bioresource Technology*, 7(4), 305. <https://doi.org/10.1016/j.biortech.2020.123043>.
- Xu, W., Sun, Z., Meng, H., Han, Y., Wu, J., Xu, J., Xu, Y., & Zhang, X. (2018). Immobilization of cellulase proteins on zeolitic imidazolate framework (ZIF-8)/polyvinylidene fluoride hybrid membranes. *New Journal of Chemistry*, 42(21), 17429–17438. <https://doi.org/10.1039/c8nj03366h>.
- Yang, C., Wu, H., Zeng, X., Pan, Z., Tan, H., & Chen, S. (2022). Biochar derived from mild temperature carbonization of alkali-treated sugarcane bagasse for efficient adsorption to organic and metallic pollutants in water. *Biomass Conversion and Biorefinery*. 5(1), 70–79. <https://doi.org/10.1007/s13399-022-03009-8>.
- Yang, J., Shen, M., Luo, Y., Wu, T., Chen, X., Wang, Y., & Xie, J. (2021). Advanced applications of chitosan-based hydrogels: From biosensors to intelligent food packaging system. *Trends in Food Science and Technology*, 110, 822–832. <https://doi.org/10.1016/j.tifs.2021.02.032>.
- Yildirim, O., Ozkaya, B., Altinbas, M., & Demir, A. (2021). Statistical optimization of dilute acid pretreatment of lignocellulosic biomass by response surface methodology to obtain fermentable sugars for bioethanol production. *International Journal of Energy Research*, 45(6), 8882–8899. <https://doi.org/10.1002/er.6423>.

- Yu, H., Xiao, W., Han, L., & Huang, G. (2019). Characterization of mechanical pulverization/phosphoric acid pretreatment of corn stover for enzymatic hydrolysis. *Bioresource Technology*, 282, 69–74. <https://doi.org/10.1016/j.biortech.2019.02.104>.
- Zabed, H., Faruq, G., Sahu, J. N., Azirun, M. S., Hashim, R., & Nasrulhaq Boyce, A. (2014). Bioethanol production from fermentable sugar juice. *The Scientific World Journal*, 2014, 678-703. <https://doi.org/10.1155/2014/957102>.
- Zabed, H., Sahu, J. N., Suely, A., Boyce, A. N., & Faruq, G. (2017). Bioethanol production from renewable sources: Current perspectives and technological progress. *Renewable and Sustainable Energy Reviews*, 71, 475–501. <https://doi.org/10.1016/j.rser.2016.12.076>.
- Zainab, A., Amos, Y., Sani, M., Datsugwai, S., & Mathew, B. (2019). Quality Assessment of Water Melon (*Citrulus lanatus*) Wine Produced Using *Saccharomyces cerevisiae* Isolated from Palm Wine. *Journal of Biomaterials*, 2(2), 65–73. <https://doi.org/10.11648/j.jb.20180202.17>.
- Zargar, V., Asghari, M., & Dashti, A. (2015). A Review on Chitin and Chitosan Polymers: Structure, Chemistry, Solubility, Derivatives, and Applications. *ChemBioEng Reviews*, 2(3)204–226. <https://doi.org/10.1002/cben.201400025>.
- Zawawi, F. S. M., Karim, L., Omar, S. R., & Ali, A. (2020). Enzyme activity and stability of lactase immobilized on two different supports: Calcium alginate and magnetic chitosan. *Malaysian Journal of Fundamental and Applied Sciences*, 16(4), 413–417. <https://doi.org/10.11113/mjfas.v16n4.1915>.
- Zdarta, J., Meyer, A. S., Jesionowski, T., & Pinelo, M. (2018). A general overview of support materials for enzyme immobilization: Characteristics, properties, practical utility. *Catalysts*, 8(2), 92-102. <https://doi.org/10.3390/catal8020092>.
- Zentou, H., Abidin, Z. Z., Yunus, R., Biak, D. R. A., & Korelskiy, D. (2019). Overview of alternative ethanol removal techniques for enhancing bioethanol recovery from fermentation broth. *Processes*, 7(7), 88-107. <https://doi.org/10.3390/pr7070458>.
- Zhang, H., Han, L., & Dong, H. (2021). An insight to pretreatment, enzyme adsorption and enzymatic hydrolysis of lignocellulosic biomass: Experimental and modeling studies. *Renewable and Sustainable Energy Reviews*, 140, 780-811. <https://doi.org/10.1016/j.rser.2021.110758>.
- Zhang, J., Dai, Y., Jiang, B., Zhang, T., & Chen, J. (2020). Dual-enzyme co-immobilization for the one-pot production of glucose 6-phosphate from maltodextrin. *Biochemical Engineering Journal*, 6(2), 161. <https://doi.org/10.1016/j.bej.2020.107654>.
- Zhang, J., Li, J., Tang, Y., Lin, L., & Long, M. (2015). Advances in catalytic production of bio-based polyester monomer 2, 5-furandicarboxylic acid derived from lignocellulosic biomass. *Carbohydrate Polymers*, 130, 420-428. <https://doi.org/10.1016/j.carbpol.2015.05.028>.
- Zhang, N., Meng, X. G., Wu, Y. Y., Song, H. J., Huang, H., Wang, F., & Lv, J. (2019a). Highly selective isomerization of glucose into fructose catalyzed by a mimic glucose isomerase. *ChemCatChem*, 11(9), 2355-2361.

- Zhang, W., Bai, A., Chen, X., & Wei, G. (2012). Ethanol production from lignocelluloses hydrolyzates with immobilized multi-microorganisms. *Energy Sources, Part A: Recovery, Utilization, and Environmental Effects*, 34(13), 1206-1212. <https://doi.org/10.1080/15567031003681960>.
- Zhang, X., Sun, B., Tang, Q., Chen, R., & Han, S. (2019b). Molecular identification and phylogenetic analysis of nuclear rDNA sequences of *clonorchis sinensis* isolates from human fecal samples in Heilongjiang Province, China. *Frontiers in Microbiology*, 10(1), 235-256. <https://doi.org/10.3389/fmicb.2019.00026>.
- Zhang, Z., Li, X., Liu, B., Zhao, Q., & Chen, G. (2016). Hexagonal microspindle of NH₂-MIL-101(Fe) metal-organic frameworks with visible-light-induced photocatalytic activity for the degradation of toluene. *Advances*, 6(6), 4289–4295. <https://doi.org/10.1039/c5ra23154j>.
- Zhao, Y., Wang, J. Y., Zhu, A. R. and Y. Deng. (2008). Enhanced enzymatic hydrolysis of spruce by alkaline pretreatment at low temperature, *Biotechnology and Bioengineering*, 6(99), 1320–1328. <https://doi.org/10.1002/bit.21712>.
- Zhou, Y., Gao, B., Zimmerman, A. R., Fang, J., Sun, Y., & Cao, X. (2013). Sorption of heavy metals on chitosan-modified biochars and its biological effects. *Chemical Engineering Journal*, 231, 512–518. <https://doi.org/10.1016/j.cej.2013.07.036>.
- Zhou, Z., Liu, D., & Zhao, X. (2021). Conversion of lignocellulose to biofuels and chemicals via sugar platform: An updated review on chemistry and mechanisms of acid hydrolysis of lignocellulose. *Renewable and Sustainable Energy Reviews*, 12(146), 5647-5662. <https://doi.org/10.1016/j.rser.2021.111169>.
- Zhu, C. Wan, V., and Li, Y. (2010). Enhanced solid-state anaerobic digestion of corn stover by alkaline pretreatment, *Bioresourc Technology*, 19(101), 7523–7528 <https://doi.org/10.1016/j.biortech.2010.04.060>.

APPENDICES

Appendix A: Standard curves

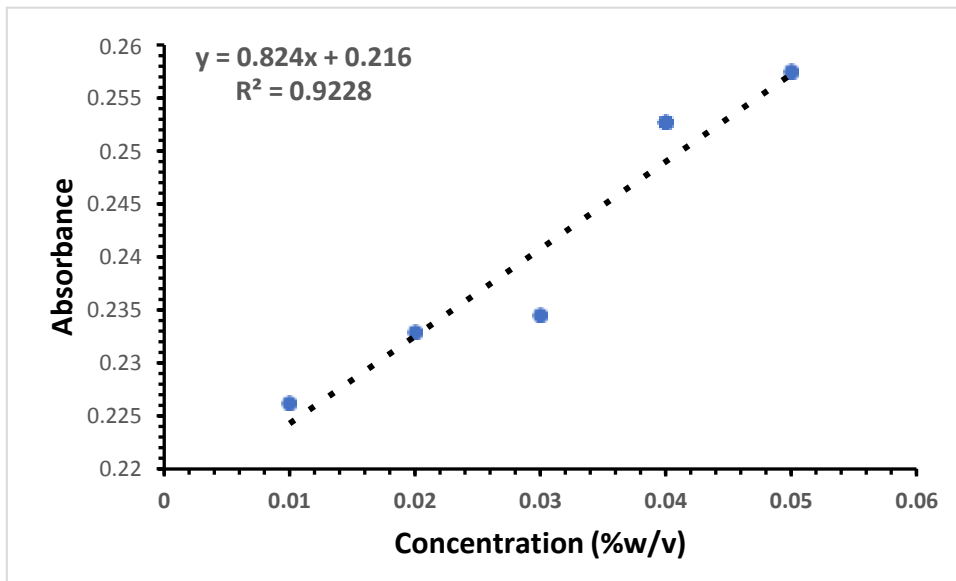


Figure 1: Bial's xylose standard curve at 671nm

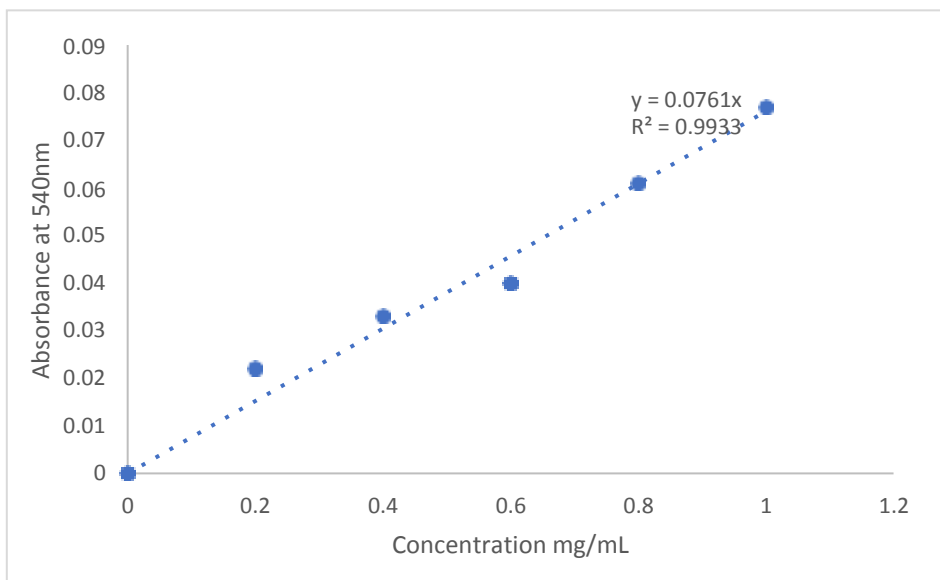


Figure 2: Xylose standard curve using DNS method

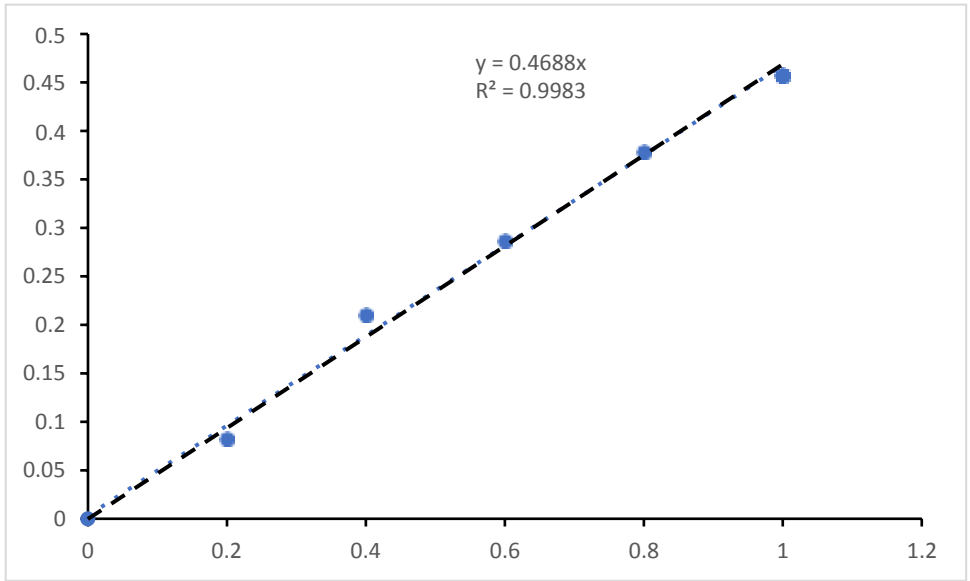


Figure 3: Glucose standard curve using DNS method

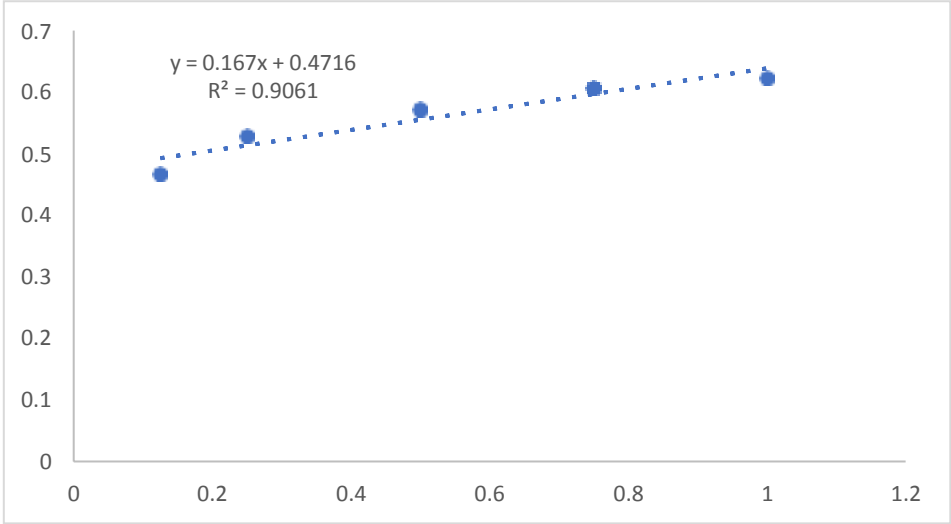


Figure 4: BSA standard curve using DNS method

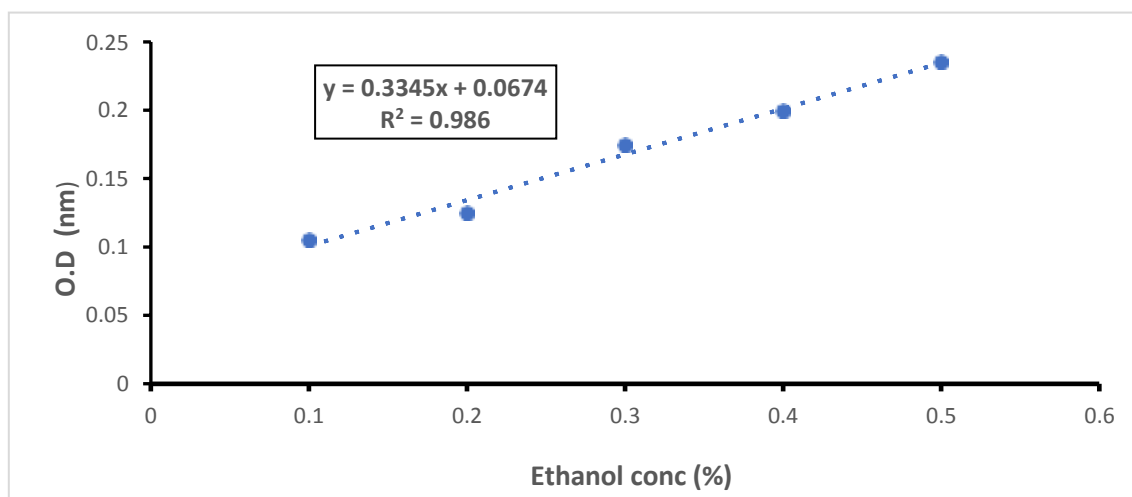


Figure 5: Ethanol standard curve using potassium dichromate method

Calculation of Enzyme activity

$$\text{activity of Enzyme (U)} = \frac{\text{reducing sugar released} \left(\frac{\text{mg}}{\text{mL}} \right) \times \text{dilution factor} \times 1000}{\text{Incubation time (min)} \times \text{volume of Enzyme} \times \text{molecular weight of product}}$$

Appendix B: Confirmation Test for microwave-alkaline pretreated agrowastes

Table 1a: Confirmation Test for plantain pseudostem biomass

Response	Predicted Mean	Predicted Median	Std Dev	n	SE Pred	95% PI low	Data Mean	95% PI high
Delignification	61.06	61.07	2.71	3	2.64	55.18	60.23	66.96
Cellulose	59.85	59.85	0.77	3	0.75	58.18	60.67	61.52
Hemicellulose	22.17	22.17	0.98	3	1.03	19.73	22.33	24.61

Table 1c: Confirmation Test for sugarcane bagasse

Response	Predicted Mean	Predicted Median	Std Dev	N	SE Pred	95% PI low	Data Mean	95% PI high
delignification	62.63	62.63	1.89	3	1.64	59.09	61.00	66.18
cellulose	73.90	73.90	1.24	3	1.48	70.60	71.67	77.20
Hemicellulose	22.00	22.00	0.57	3	0.67	20.50	20.67	23.50

Table 1b: Confirmation for corn cob biomass

Response	Predicted Mean	Predicted Median	Std Dev	N	SE Pred	95% PI low	Data Mean	95% PI high
Delignification	65.54	65.54	1.74	3	1.76	61.63	67.60	69.45
Cellulose	62.77	62.77	1.56	3	1.58	59.24	61.00	66.29
Hemicellulose	18.15	18.15	1.24	3	1.01	15.97	17.67	20.34

Appendix C: Statistical results and model equations for microwave-alkaline pre-treated agrowaste biomass

Table 2: Statistical significance of developed model for Microwave-alkaline pre-treatment of Agrowastes

	Model	R ²	Adjusted R ²	Predicted R ²	p-value
PLANTAIN PSEUDOSTEM					
Delignification	2FI	0.9601	0.9361	0.8516	< 0.0001
Cellulose content	2FI	0.9616	0.9386	0.9094	< 0.0001
Hemicellulose Content	Quadratic	0.9591	0.9065	0.8463	0.0005
SUGARCANE BAGASSE					
Delignification	2FI	0.9735	0.9576	0.9398	< 0.0001
Cellulose content	2FI	0.9653	0.9446	0.8593	< 0.0001
Hemicellulose Content	2FI	0.9643	0.9429	0.8868	< 0.0001
CORNCOB BIOMASS					
Delignification	2FI	0.9812	0.8796	0.9504	< 0.0001
Cellulose content	2FI	0.9247	0.8796	0.7518	< 0.0001
Hemicellulose Content	2FI	0.9404	0.9266	0.9124	< 0.0001

Table 3a: Model equations of percentage lignin removed, cellulose content and hemicellulose content of microwave-alkaline pre-treated plantain pseudostem biomass

Responses		Equations
Cellulose Content	Coded Factors	$Y = 60.4529 + 2.00625 * A + -0.36875 * B + 0.875 * C + 3.3375 * AB + -4 * AC + 0.25 * BC$
	Actual Factors	Cellulose content = $52.1953 + 3.92708 * \text{CONC. OF NaOH} + -0.0235516 * \text{POWER} + 4.28472 * \text{REACTION TIME} + 0.0105952 * \text{CONC. OF NaOH} * \text{POWER} + -2 * \text{CONC. OF NaOH} * \text{REACTION TIME} + 0.000396825 * \text{POWER} * \text{REACTION TIME}$
Hemicellulose Content	Coded Factors	$Y = 18.32 + -0.575 * A + -2.7675 * B + -2.1925 * C + -2.9 * AB + 1.25 * AC + 0.135 * BC + 0.1975 * A^2 + 1.5825 * B^2 + 0.7325 * C^2$
	Actual Factors	Hemicellulose = $27.852 + 0.304444 * \text{CONC. OF NaOH} + -0.0032963 * \text{POWER} + -3.5275 * \text{REACTION TIME} + -0.00920635 * \text{CONC. OF NaOH} * \text{POWER} + 0.625 * \text{CONC. OF NaOH} * \text{REACTION TIME} + 0.000214286 * \text{POWER} * \text{REACTION TIME} + 0.1975 * \text{CONC. OF NaOH}^2 + 1.59486e-05 * \text{POWER}^2 + 0.183125 * \text{REACTION TIME}^2$
Delignification	Coded Factors	$Y = 58.2382 + 6.565 * A + 9.32 * B + 7.595 * C + -8.175 * AB + 0.725 * AC + 0.085 * BC$
	Actual Factors	Delignification = $-4.67212 + 15.4692 * \text{CONC. OF NaOH} + 0.0810873 * \text{POWER} + 3.02056 * \text{REACTION TIME} + -0.0259524 * \text{CONC. OF NaOH} * \text{POWER} + 0.3625 * \text{CONC. OF NaOH} * \text{REACTION TIME} + 0.000134921 * \text{POWER} * \text{REACTION TIME}$

Where **Y**, **A**, **B** and **C** are the coded values of Responses, NaOH concentration, power and treatment time respectively

Table 3b: Model equations of percentage lignin removed, cellulose content and hemicellulose content of microwave-alkaline pre-treated sugarcane bagasse

Responses		Equations
Cellulose Content	Coded Factors	$Y = 63.8235 + 2.25 * A + 1.125 * B + 1.125 * C + -9 * AB + 2 * AC + 2.75 * BC$
	Actual Factors	Cellulose content = $45.3027 + 10.25 * \text{NaOH Conc} + 0.047619 * B + -3.11806 * C + -0.0285714 * \text{NaOH Conc} * \text{Power} + 1 * \text{NaOH Conc} * \text{Time} + 0.00436508 * \text{Power} * \text{Time}$
Hemicellulose Content	Coded Factors	$Y = 19.0765 + -1.425 * A + -2.275 * B + 1.45 * C + -0.15 * AB + 1.5 * AC + 0.9 * BC$
	Actual Factors	Hemicellulose content = $28.3154 + -3.49167 * \text{NaOH Conc} + -0.0105556 * \text{Power} + -1.325 * \text{Time} + -0.00047619 * \text{NaOH Conc} * \text{Power} + 0.75 * \text{NaOH Conc} * \text{Time} + 0.00142857 * \text{Power} * \text{Time}$
Delignification	Coded Factors	$Y = 58.9824 + 2.2625 * A + 9.1 * B + 9.7375 * C + -1.15 * AB + 0.475 * AC + 0.4 * BC$
	Actual Factors	Delignification = $28.0761 + 2.95556 * \text{NaOH Conc} + 0.0342857 * \text{Power} + 4.14931 * \text{Time} + -0.00365079 * \text{NaOH Conc} * \text{Power} + 0.2375 * \text{NaOH Conc} * \text{Time} + 0.000634921 * \text{Power} * \text{Time}$

Where **Y**, **A**, **B** and **C** are the coded values of Responses, NaOH concentration, power and treatment time respectively

Table 3c: Model equations of percentage lignin removed, cellulose content and hemicellulose content of microwave-alkaline pre-treated corncob

Responses		Equations
Cellulose Content	Coded Factors	$Y = 54.0235 + 3.55 * A + -3.3125 * B + 3.2625 * C + 0.125 * AB + 2.275 * AC + 1.25 * BC$
	Actual Factors	Cellulose content = $55.5006 + -0.0152778 * \text{NaOH conc.} + -0.0172619 * \text{Power} + -1.40764 * \text{Time} + 0.000396825 * \text{NaOH Conc} * \text{Power} + 1.1375 * \text{NaOH Conc} * \text{Time} + 0.00198413 * \text{Power} * \text{Time}$
Hemicellulose Content	Coded Factors	$Y = 25.7176 + -2.225 * A + 2.8375 * B + -5.1375 * C + 0.3 * AB + 0.75 * AC + -0.475 * BC$
	Actual Factors	Hemicellulose = $36.5183 + -3.71667 * \text{NaOH Conc} + 0.00936508 * \text{Power} + -3.02847 * \text{Time} + 0.000952381 * \text{NaOH Conc} * \text{Power} + 0.375 * \text{NaOH Conc} * \text{Time} + -0.000753968 * \text{Power} * \text{Time}$
Delignification	Coded Factors	$Y = 48.4961 + 7.36054 * A + 5.34996 * B + 8.16991 * C + -9.09326 * AB + 3.21934 * AC + -1.58074 * BC$
	Actual Factors	Delignification = $-0.486673 + 13.6455 * \text{NaOH Conc} + 0.0822463 * \text{Power} + 1.83162 * \text{Time} + -0.0288675 * \text{NaOH Conc} * \text{Power} + 1.60967 * \text{NaOH Conc} * \text{Time} + -0.00250912 * \text{Power} * \text{Time}$

Where **Y**, **A**, **B** and **C** are the coded values of Responses, NaOH concentration, power and treatment time respectively

Appendix D: Characteristics of treated and untreated Agrowaste

Table 4: Eliminated lignin waveband observed in FTIR from microwave-assisted alkaline pretreated agrowaste

Biomass	Wave length (cm ⁻¹)	Residual Lignin
Plantain pseudostem biomass	711.5 – 1571	Lowest
Sugar Cane bagasse	626.2 - 1119.5	Medium
Corn Cob biomass	626.2 - 994.5	Highest

Calculation of crystallinity index of pretreated and untreated agrowaste

Calculation of crystallinity index for Unpretreated sugarcane bagasse (US)

$$\text{At } 2\theta = 15.7^{\circ}$$

$$I_{\text{Min}} = 5645$$

$$\text{At } 2\theta = 22.08^{\circ}$$

$$I_{\text{Max}} = 8813$$

$$C. I (\%) = \frac{(I_{\text{Max}} - I_{\text{am}}) \times 100}{I_{\text{Max}}} \quad (1)$$

$$C. I (\%) = \frac{(8813 - 5645) \times 100}{8813} = 35.94\%$$

Calculation of crystallinity index for Pretreated sugarcane bagasse (PS)

$$\text{At } 2\theta = 16.25^{\circ}$$

$$I_{\text{Min}} = 5860$$

$$\text{At } 2\theta = 22.15^{\circ}$$

$$I_{\text{Max}} = 10337$$

$$C.I (\%) = \frac{(10337 - 5860) \times 100}{10337} = 43.31\%$$

Calculation of crystallinity index for Untreated plantain pseudostem biomass (PP)

$$\text{At } 2\theta = 18.62^{\circ}$$

$$I_{\text{Min}} = 3987$$

$$\text{At } 2\theta = 22.29^{\circ}$$

$$I_{\text{Max}} = 6197$$

$$C.I (\%) = \frac{(6197 - 3987) \times 100}{6197} = 35.66\%$$

Calculation of crystallinity index for Pretreated plantain pseudostem biomass (UP)

$$\text{At } 2\theta = 18.87^{\circ}$$

$$I_{\text{Min}} = 4238$$

$$\text{At } 2\theta = 22.5^{\circ}$$

$$I_{\text{Max}} = 10175$$

$$\text{C.I (\%)} = \frac{(10175 - 4238) \times 100}{10175} = 58.36\%$$

Calculation of crystallinity index for unpretreated corncob biomass (UC)

$$\text{At } 2\theta = 16.11^{\circ}$$

$$I_{\text{Min}} = 5351$$

$$\text{At } 2\theta = 21.68^{\circ}$$

$$I_{\text{Max}} = 8025$$

$$\text{C.I (\%)} = \frac{(8025 - 5351) \times 100}{8025} = 33.32\%$$

Calculation of crystallinity index for Pretreated corncob biomass (PC)

$$\text{At } 2\theta = 196^{\circ}$$

$$I_{\text{Min}} = 5149$$

$$\text{At } 2\theta = 21.85^{\circ}$$

$$I_{\text{Max}} = 6213$$

$$\text{C.I (\%)} = \frac{(6213 - 5149) \times 100}{6213} = 17.13\%$$

APPENDIX E: Organisms Isolated from for the Production of Enzyme and for Fermentation Process

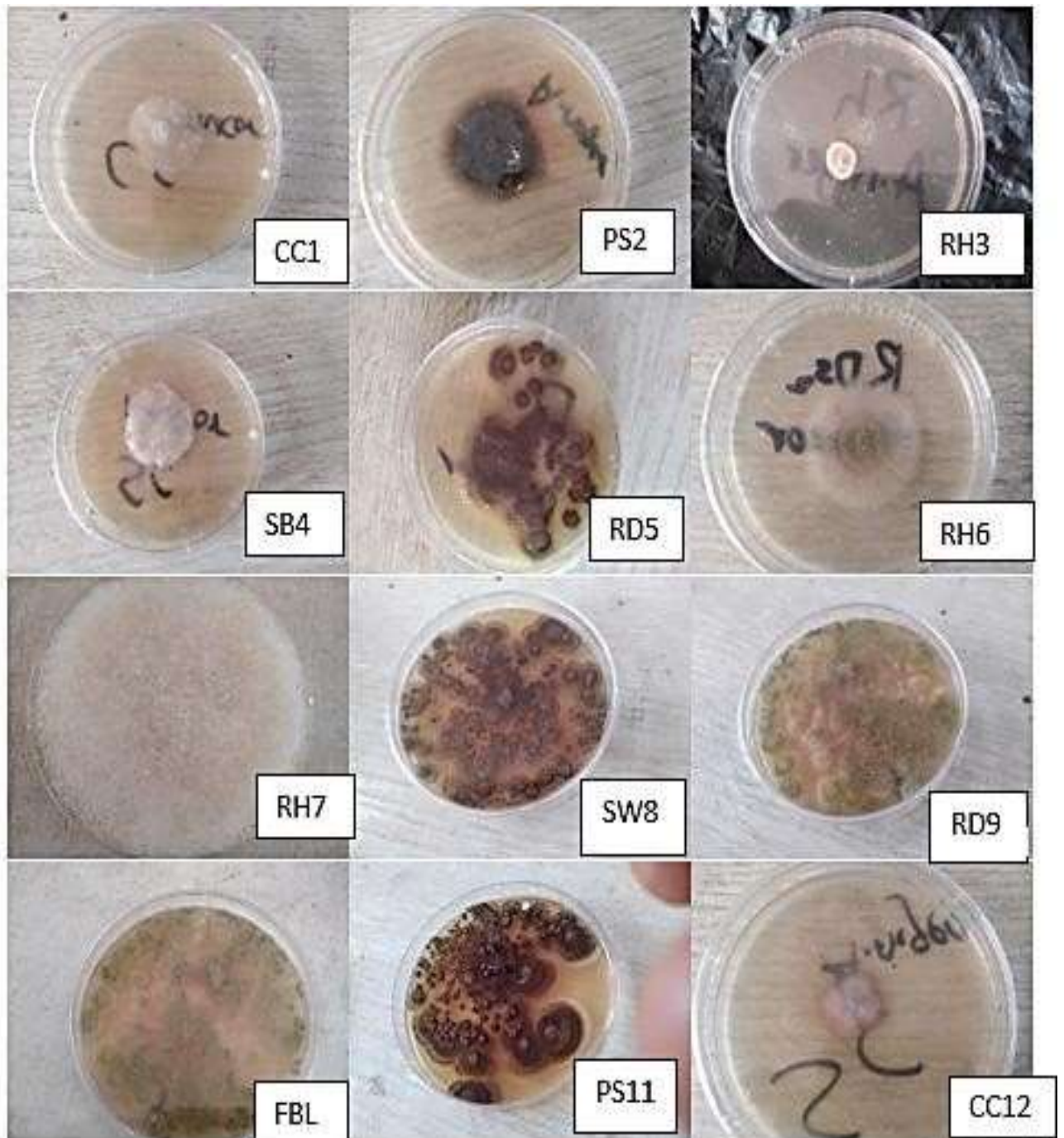


Plate 4: Pure Fungi Isolates From Different Soil Samples for the Production of Cellulase and Xylanase

CC1, CC12-from corncob dump site ; **PS2, PS11**- from plantain stem dump site; **RH3, RH6, RH7**- from rice husk dump site; **SB4**- from sugarcane waste dumpsite; **RD5, RD9**- from refuse dump site; **SW8, FBL**: from sewage sludge

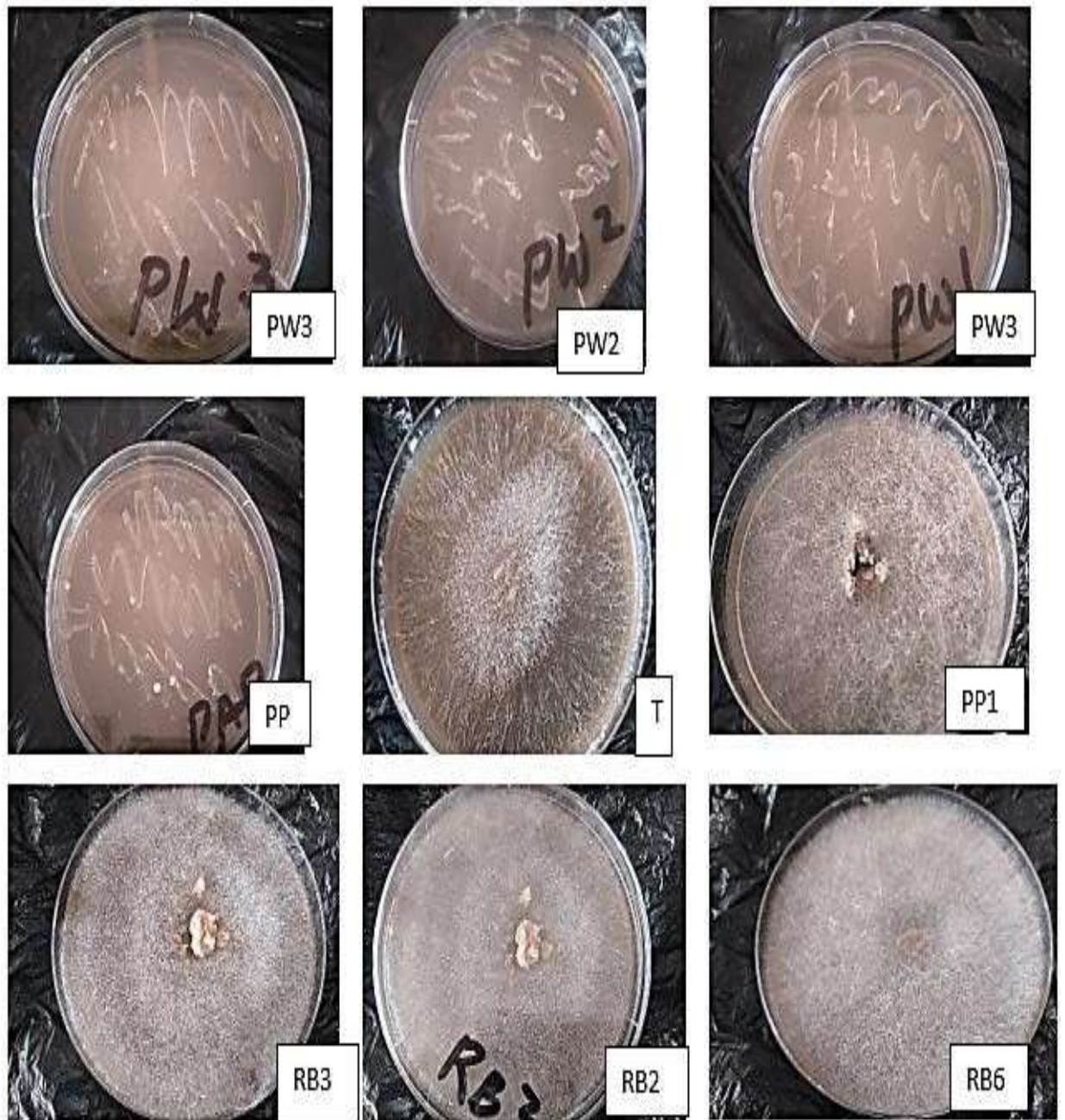
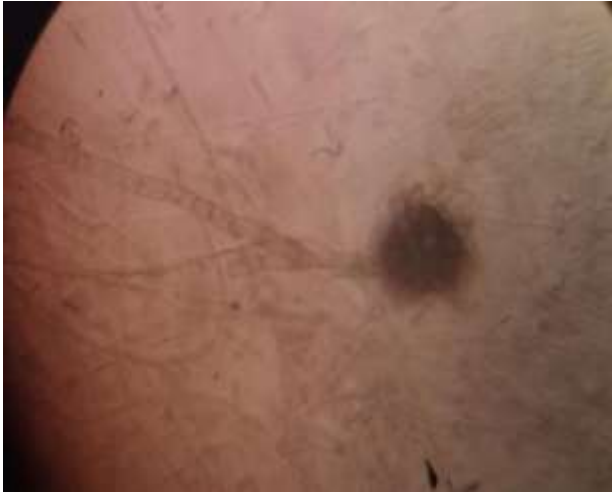


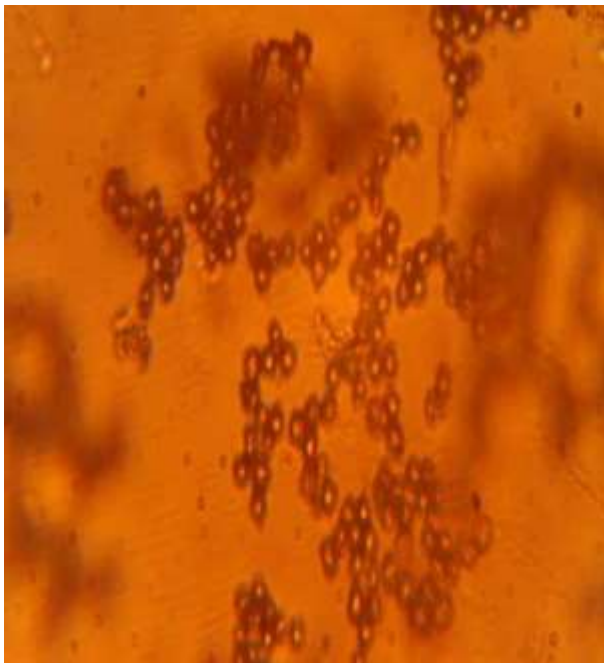
Plate 5: Pure Fungi Isolates from Different Sources for Fermentation Process
PW1, PW2, PW3 -from palmwine; **PP, PP1**- fermented food; **T**- from termite hill; **RB3, RB2, RB6**- from rice bran dump site



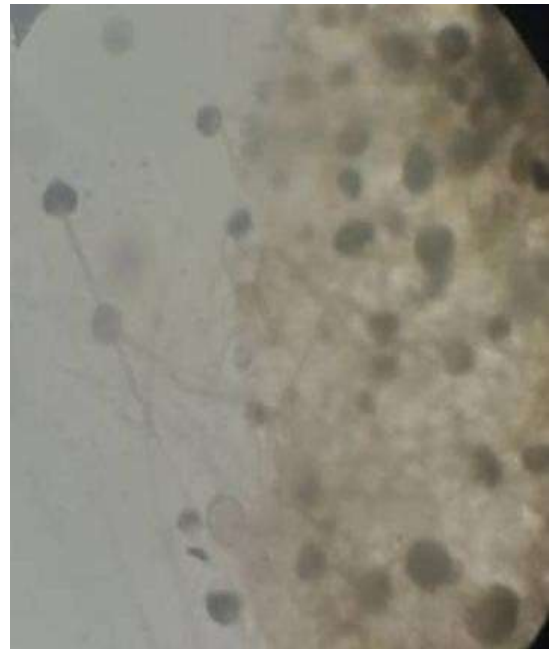
RD5: *A. niger* from refuse dump site



FLB: *A. flavus* from sewage sludge



PP: *S. cerevisiae* from fermented food



M. indicus from rice husk dump site

Plate 6: Microscopic view of selected organisms for enzyme production and fermentation process

Appendix F: Production and Characterization of Enzyme Support



Plate 7: Porous Biochar Produced with Sugarcane Bagasse

i. Table 11: BET Results for Biochar-chitosan Composites

	BIOCHAR (m²/g)	FRESH BEADS	FREEZE DRIED	AIR DRIED	OVEN DRIED
Surface area	3.758e ⁰² m ² /g	1.786e ⁰² m ² /g	2.763e ⁰² m ² /g	1.771e ⁰² m ² /g	1.708e ⁰² m ² /g
pore volume	1.839e ⁻⁰¹ cc/g	8.804e ⁻⁰² cc/g	1.361e ⁻⁰¹ cc/g	8.666e ⁻⁰² cc/g	8.445e ⁻⁰² cc/g
pore size	2.138e ⁰⁰ nm	2.128e ⁰⁰ nm	2.105e ⁰⁰ nm	2.132e ⁰⁰ nm	2.100e ⁰⁰ nm

Appendix G: Production and Characterization of Bioethanol



Plate 8: Fermentation Process using Free Enzyme and Free fungi

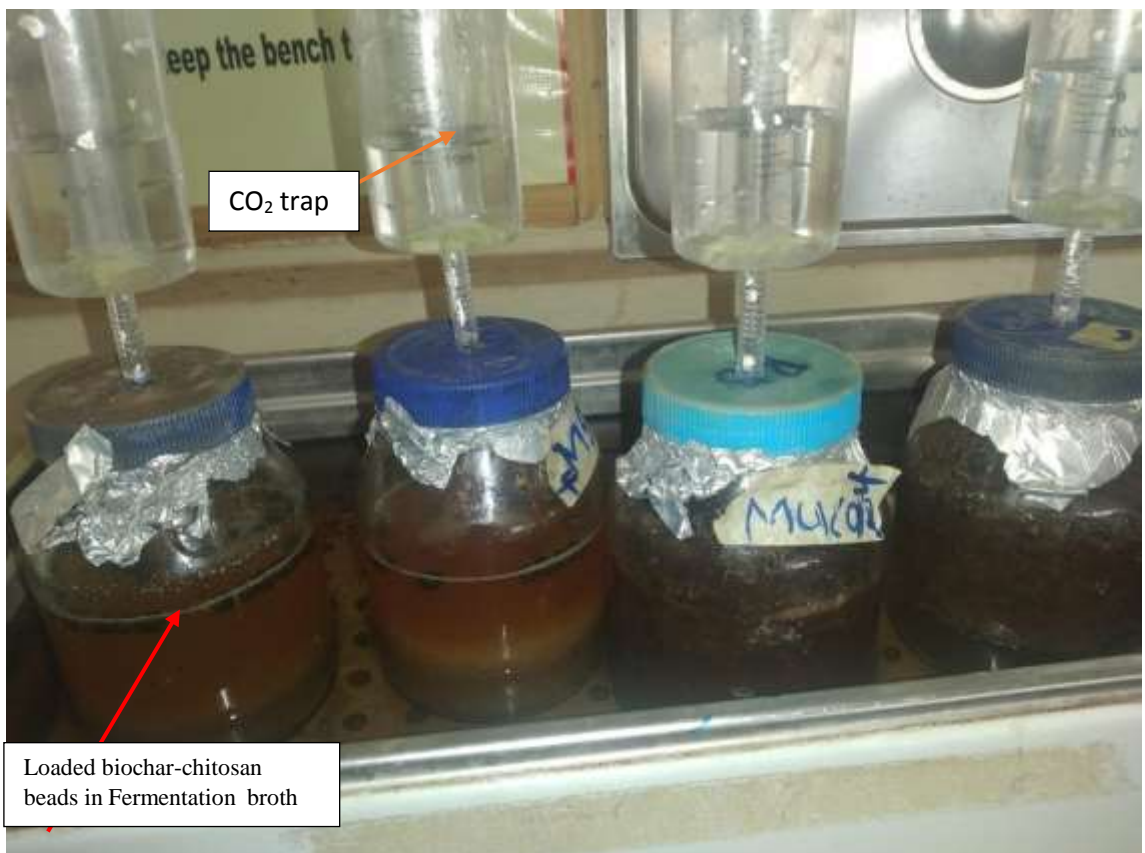


Plate 9: Fermentation Process Using Co-immobilized Enzymes and Co-immobilized Fungi

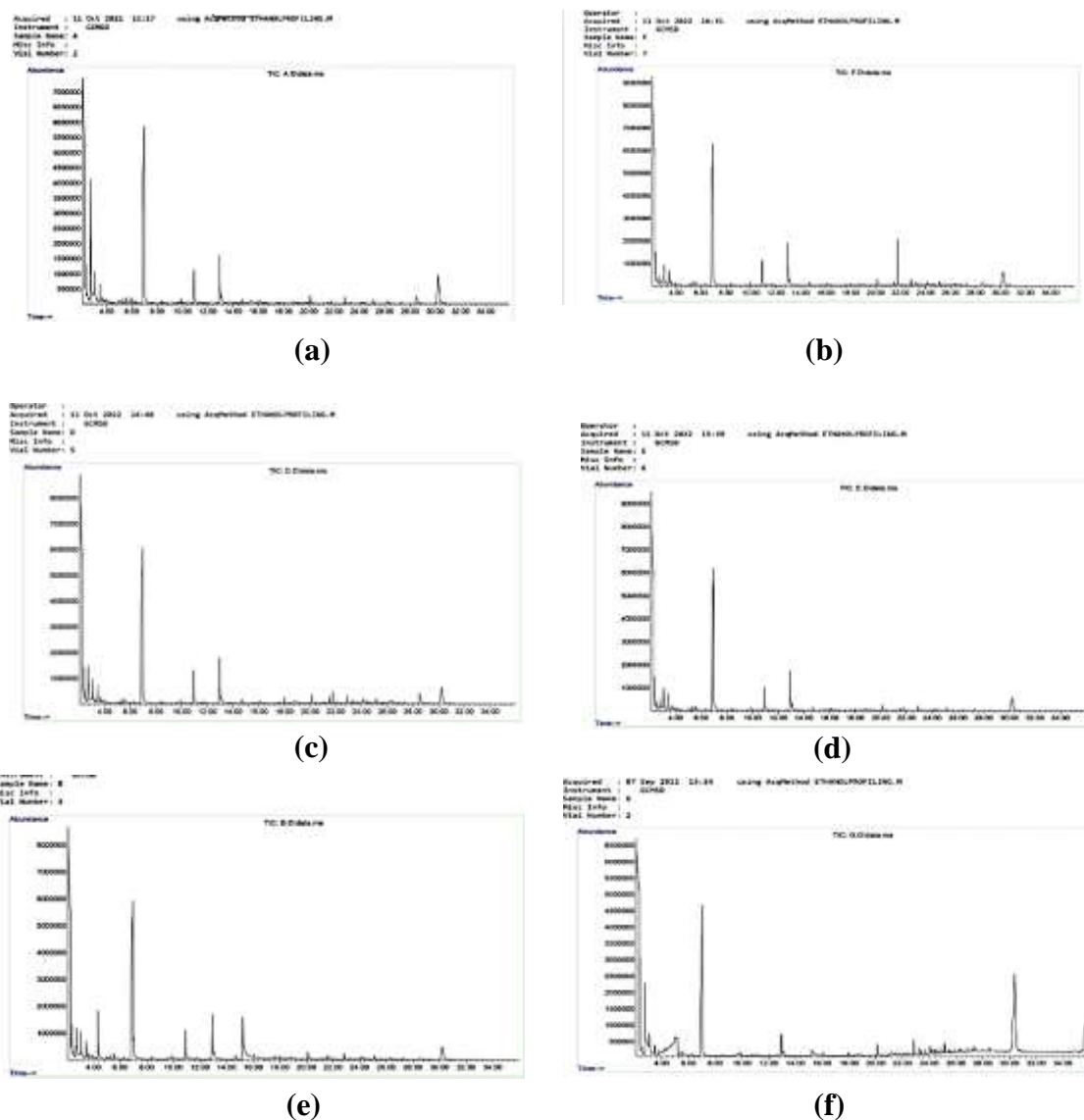


Figure 6: Chromatogram of Fermentation Distillate for Bioethanol Produced from Agrowastes using Enzymes and Fungi. Plantain pseudostem biomass as substrate for free cellulase, free xylanase and free mucor (a); Sugarcane bagasse as substrate for free cellulase, free xylanase and free yeast (b); Plantain pseudostem biomass as substrate for free cellulase, free xylanase and free mucor (c); Sugarcane bagasse as substrate for Free cellulase, free xylanase, and free yeast (d); Plantain pseudostem biomass as substrate for co-immobilized mucor and yeast plus co-immobilized cellulase and xylanase (e); Sugarcane bagasse as substrate for co-immobilized mucor and yeast plus co-immobilized cellulase and xylanase (f).

Appendix H: Molecular Identification and Characterization of Organisms

i. Identification of organisms for enzyme production and fermentation process

>SAMPLE FBL *Aspergillus flavus*

CCATAGGTGAACCTGCGGAAGGATCATTACCGAGTGTAGGGTTCCTAGCGA
GCCCAACCTCCCACCCGTGTTTACTGTACCTTAGTTGCTTCGGCGGGCCCGC
CATTTCATGGCCGCCGGGGGCTCTCAGCCCCGGGCCCGCGCCCCGCCGGAGAC
ACCACGAACTCTGTCTGATCTAGTGAAGTCTGAGTTGATTGTATCGCAATCA
GTTAAAACCTTCAACAATGGATCTCTTGGTTCCGGCATCGATGAAGAACGCA
GCGAAATGCGATAACTAGTGTGAATTGCAGAATTCGGTGAATCATCGAGTC
TTTGAACGCACATTGCGCCCCCTGGTATTCCGGGGGGGCATGCCTGTCCGAGC
GTCATTGCTGCCCATCAAGCACGGCTTGTGTGTTGGGTCGTCGTCCCCTCTC
CGGGGGGGACGGGCCCAAAGGCAGCGGGCGGCACCGCGTCCGATCCTCGA
GCGTATGGGGCTTTGTCACCCGCTCTGTAGGCCCGGCCGGCGCTTGCCGAAC
GCAAATCAATCTTTTTCCAGTTGACCTCGGATCAGGTAGGGATACCCGCTG
AACTTAAGCATATCAATAAGGGCGGAGGAA

>SAMPLE RDS *Aspergillus niger*

AGGAAGGATCATTACCGAGTGCGGGTCTTTGGGCCCAACCTCCCATCCGT
GTCTATTGTACCCTGTTGCTTCGGCGGGCCCGCCGCTTGTTCGGCCGCCGGGG
GGGCGCCTCTCCCCCGGGCCCGTGCCCGCCGGAGACCCCAACACGAACAC
TGTCTGAAAGCGTGCAGTCTGAGTTGATTGAATGCAATCAGTTAAAACCTTC
AACAATGGATCTCTTGGTTCCGGCATCGATGAAGAACGCAGCGAAATGCGA
TAACTAATGTGAATTGCAGAATTCAGTGAATCATCGAGTCTTTGAACGCACA
TTGCGCCCCCTGGTATTCCGGGGGGGCATGCCTGTCCGAGCGTCATTGCTGCC
CTCAAGCCCGGCTTGTGTGTTGGGTCGCCGTCCCCCTCTCCGGGGGGACGGG
CCCGAAAGGCAGCGGGCGGCACCGCGTCCGATCCTCGAGCGTATGGGGCTTT
GTCACATGCTCTGTAGGATTGGCCGGCGCCTGCCGACGTTTTCCAACCATTC
TTTTCCAGTTGACCTCGGATCAGGTAGGGATACCCGCTGAACTTAAC

>SAMPLE RB *Mucor indicus*

GATAATTAATAAAATTATCTTATTTACTGTGAACTGTTTTTATTTATGACGTAT
AAGGGGATGTCTTTAGGCTATAAGGGTAGGCCTATGGAATGCTAACCTAGT
CATAGTCAAGCTTGATGCTTGGTACCCGATTATTACTTACCAAAAAGAATTCA
GTTTAAAATATTGTAACATAGACCTAAAAAATCTATAAAACAACCTTTTAACA
ATGGATCTCTTGGTTCTCGCATCGATGAAGAACGTAGCAAAGTGCGATAAC
TAGTGTGAATTGCATATTCAGTGAATCATCGAGTCTTTGAACGCATCTTGCA
CTCAATGGTATTCCATTGAGTACGCCTGTTTCAGTATCAAAAACAACCCTTA
TTCAAAAATTTTTTTTGGAGTAGATATGAGTGTAGCAACCTTACAAGTTGAGA
CATTTTAAATAAAGTCAGGCCATATCGTGGATTGAGTGCCGATACTTTTAAT
TTTGAAAAGGTAAAGCATGTTGATGTCCGCTTTTTGGGCCTCCCAAATAACT
TTTTAAACTTGATCTGAAATCAGGTGGGATTACCCGCTGAACTTAAGCATAT
CAATAAGCGGAGGAA

>SAMPLE PP *Saccharomyces cerevisiae*

AAAGAAATTTAATAATTTTGAAAATGGATTTTTTTGTTTTGGCAAGAGCATG
AGAGCTTTTACTGGGCAAGAAGACAAGAGATGGAGAGTCCAGCCGGGCCTG
CGCTTAAGTGCGCGGTCTTGCTAGGCTTGTAAGTTTCTTTCTTGCTATTCCAA
ACGGTGAGAGATTTCTGTGCTTTTGTTATAGGACAATTA AAAACCGTTTCAAT
ACAACACACTGTGGAGTTTTTCATATCTTTGCAACTTTTTCTTTGGGCATTCTGA
GCAATCGGGGCCAGAGGTAACAAACACAAACAATTTTATCTATTTCATTAA
ATTTTTGTCAAAAACAAGAATTTTCGTAACCTGGAAATTTTAAAAATATTAAA
AACTTTCAACAACGGATCTCTTGGTTCTCGCATCGATGAGAACGCAGCGAA
ATGCGATACGTAATGTGAATTGCAGAATTCCTGTAATCATCGAATCTTTGAA
CGCATTGCCCCCTTGGTATTCCAGGGGGCATGCCTGTTTGAGCGTCATTTC
TTCTCAAACATTCTGTTTGGAGTGAGTGATACTCTTTGGAGTAACTTGAAA
TTGCTGGCCTTTTCATTGGATGTTTTTTTTTCCAAAGAGAGGTTTCTCTGCGTG
CTTGAGGTATAATGCAAGTACGGTCGTTTTAGGTTTTACCAACTGCGGCTAA
TCTTTTTTATACTGAGCGTATTGGAACGTTATCGATAAGAAGAGAGCGTCTA
GGCAACAATGTTCTTAAAGGT

ii. Sequence of enzyme producing gene in selected microorganisms

Sequencing for endo-beta-1,4-glucanase B gene *Aspergillus flavus* strain RBL

CCCAGGTAAGTTGCTCATCTGCCAAAAAAAATATCTTGGGTTTGACGAGG
CTTGCAGGTGGTCAATGCCGTCCTGATGCGGGTGTCCATGCTATCTTGGAC
CCCATAACTATGGCAGATTGTGAGTATCTCGAAGGCCTCGAAGTAGTGTAT
TACGGGCATTTAAACATGAGGATGTCTGCTAACTTGAACATGGCAGCAATG
GCGAGATCATGTCCACTCCATCTGATTTCCAAACATTCTGGAAGAACTTGGC
AGGACAGTTCCAGAGCAACTCTTTGGTTATCTTCGATACCAGTGAGTCGGCC
CAATCCGTTTCTTCCCCAGTATCCCATCGAGTTGGGTATCCTCGATCCTAAC
GCCAATTCACAGACAATGAATACCATGACATGGACCAAGAGCTGGTCCTGA
ACCTCAACCAAGCCGCCATTGACGGGATCCGAGAGGCTGGCGCCACGGAGC
AATATATCTTCGTTGAAGGTAACCTCGTACACCGGGCCTGGACCTGGACCG
ATGTGAACGACAACATGAAGAACTTGGAGGATCCCCAGGACAAGATCGTCT
ATCAGATGCACCAGTATTTGGACTCGGATGGGTCTGGTACTTCCGAGACCTG
CGTGTCTGGTACCATTGGCCAGGAGCGTGTACCAGCGCTACTCAATGGCTC
AAGGACAACAAGAAGGACT

Sequence of endo-1,4-beta-xylanase (xyn11B) gene amplified from *Aspergillus Niger* strain RDS

CCATATCACGTCACCCGATAAAAAGCTTAGCTTTGGTATCTTTTGACTACTA
AGGCACTTATCTCTTAAGAAGATATCGTGACACTGGCACTGCCAGCACCGTT
CCATGCCTCCACCGCCATGACCTGATAATTGAAGTTGCTATTGCCGAACCCA
TGCTGCGCCCAGAAATTGAAATGGTTGGCGATAGTCACTGTTCCGGATGTGC
GTGTACTTTACGAACGGAGAAGTACTGCGTGAACGTGCTTGTTCCTGTGAT
AGATGGCGCGTTTCGTCCGAGTGTCCGGTGCAGACTTGGTAGGTGCTTCCATCA
GAGTACACGGTACCAAGGCTCGTGGCCGAGCTGCAAGGGTTGTAATCACCG
TAATCCTCGACGATGTAGTATTCGGCCTGAGGAAT

iii. Pairwise alignment of the sample organisms with their most identical organisms

Aspergillus sp. isolate Rubia plants small subunit ribosomal RNA gene, partial sequence; internal transcribed spacer 1, 5.8S ribosomal RNA gene, and internal transcribed spacer 2, complete sequence; and large subunit ribosomal RNA gene, partial sequence
 Sequence ID: [MN844036.1](#) Length: 600 Number of Matches: 1

Range 1: 4 to 600 [GenBank](#) [Graphics](#) ▼ Next Match ▲ Previous Match

Score	Expect	Identities	Gaps	Strand
1098 bits(594)	0.0	596/597(99%)	0/597(0%)	Plus/Plus
Query 1	CCATAGGTGAACCTGCCGAAGGATCATTACCGAGTG TAGGGTTCTAGCGAGCCCAACCT	60		
Sbjct 4	CCGTAGGTGAACCTGCCGAAGGATCATTACCGAGTG TAGGGTTCTAGCGAGCCCAACCT	63		
Query 61	CCCACCCGTGTTACTGTACCTTAGTTGCTTCGGCGGGCCCGCCATTATGGCCGCCGGG	120		
Sbjct 64	CCCACCCGTGTTACTGTACCTTAGTTGCTTCGGCGGGCCCGCCATTATGGCCGCCGGG	123		
Query 121	GGCTCTCAGCCCCGGGCCCGCGCCCGCGGAGACACCACGAACTCTGTCTGATCTAGTGA	180		
Sbjct 124	GGCTCTCAGCCCCGGGCCCGCGCCCGCGGAGACACCACGAACTCTGTCTGATCTAGTGA	183		
Query 181	AGTCTGAGTTGATTGTATCGCAATCAGTAAAAAC TTTCAACAATGGATCTCTTGGTTCCG	240		
Sbjct 184	AGTCTGAGTTGATTGTATCGCAATCAGTAAAAAC TTTCAACAATGGATCTCTTGGTTCCG	243		
Query 241	GCATCGATGAAGAACGCAGCGAAATGCGATAACTAGTGTGAATTGCAGAATTCGGTGAAT	300		
Sbjct 244	GCATCGATGAAGAACGCAGCGAAATGCGATAACTAGTGTGAATTGCAGAATTCGGTGAAT	303		
Query 301	CATCGAGTCTTTGAACGCACATTGCGCCCCCTGGTATTCCGGGGGGCATGCCGTCCGAG	360		
Sbjct 304	CATCGAGTCTTTGAACGCACATTGCGCCCCCTGGTATTCCGGGGGGCATGCCGTCCGAG	363		
Query 361	CGTCATTGCTGCCCATCAAGCACGGCTTGTGTGTTGGGTCGTCGCCCTCTCC g 420			
Sbjct 364	CGTCATTGCTGCCCATCAAGCACGGCTTGTGTGTTGGGTCGTCGCCCTCTCCGGGGGG	423		
Query 421	g ACGGGCCCCAAAGGCAGCGGCGGCACCGCGTCCGATCCTCGAGCGTATGGGGCTTTGTC	480		
Sbjct 424	GACGGGCCCCAAAGGCAGCGGCGGCACCGCGTCCGATCCTCGAGCGTATGGGGCTTTGTC	483		
Query 481	ACCCGCTCTGTAGGCCCGGCCGGCGCTTGCCGAACGCAATCAATCTTTTCCAGGTTGA	540		
Sbjct 484	ACCCGCTCTGTAGGCCCGGCCGGCGCTTGCCGAACGCAATCAATCTTTTCCAGGTTGA	543		
Query 541	CCTCGGATCAGGTAGGGATACCCGCTGAACTTAAGCATATCAATAAGGGCGGAGGAA	597		
Sbjct 544	CCTCGGATCAGGTAGGGATACCCGCTGAACTTAAGCATATCAATAAGGGCGGAGGAA	600		

Aspergillus niger isolate AOE19 small subunit ribosomal RNA gene, partial sequence; internal transcribed spacer 1, 5.8S ribosomal RNA gene, and internal transcribed spacer 2, complete sequence; and large subunit ribosomal RNA gene, partial sequence
 Sequence ID: [MW548412.1](#) Length: 577 Number of Matches: 1

Range 1: 14 to 576 [GenBankGraphics](#)

Score	Expect	Identities	Gaps	Strand
1033 bits(559)	0.0	562/563(99%)	1/563(0%)	Plus/Plus
Query 2	GGAAGGATCATTACCGAGTGC	GGTCCCTTTGGGCCAACCTCC	CATCCGTGTCTATTGTA	61
Sbjct 14	GGAAGGATCATTACCGAGTGC	GGTCCCTTTGGGCCAACCTCC	CATCCGTGTCTATTGTA	73
Query 62	CCCTGTTGCTTCGGCGGGCC	CGCGCTTGTGCGCCGCC	ggggggCGCCTCT-CCCCCG	120
Sbjct 74	CCCTGTTGCTTCGGCGGGCC	CGCGCTTGTGCGCCGCC	GGGGGGCGCCTCTGCCCCCG	133
Query 121	GGCCCGTGCCCGCCGAGAC	CCCAACACGAACACTGTCT	GAAAGCGTCAGTCTGAGTTG	180
Sbjct 134	GGCCCGTGCCCGCCGAGAC	CCCAACACGAACACTGTCT	GAAAGCGTCAGTCTGAGTTG	193
Query 181	ATTGAATGCAATCAGTTAAA	ACTTTCAACAATGGATCTCT	TGGTCCGGCATCGATGAAG	240
Sbjct 194	ATTGAATGCAATCAGTTAAA	ACTTTCAACAATGGATCTCT	TGGTCCGGCATCGATGAAG	253
Query 241	AACGCAGCGAAATGCGATA	ACTAATGTGAATTGCAGAAT	TTCAGTGAATCATCGAGTCTT	300
Sbjct 254	AACGCAGCGAAATGCGATA	ACTAATGTGAATTGCAGAAT	TTCAGTGAATCATCGAGTCTT	313
Query 301	GAACGCACATTGCGCCCTG	GTTCCGGGGGCATGCCTGT	CCGAGCGTCATTGCTGC	360
Sbjct 314	GAACGCACATTGCGCCCTG	GTTCCGGGGGCATGCCTGT	CCGAGCGTCATTGCTGC	373
Query 361	CCTCAAGCCCGGCTTGTGT	TGGTTCGCCGTCCCCTCTC	CGGGGGACGGGCCGAAA	420
Sbjct 374	CCTCAAGCCCGGCTTGTGT	TGGTTCGCCGTCCCCTCTC	CGGGGGACGGGCCGAAA	433
Query 421	GGCAGCGGGCACC	CGGTCGATCCTCGAGCGT	ATGGGGCTTTGTCACATG	CTGTAG 480
Sbjct 434	GGCAGCGGGCACC	CGGTCGATCCTCGAGCGT	ATGGGGCTTTGTCACATG	CTGTAG 493
Query 481	GATTGCGCGCGCTG	CCGACGTTTTTCAACCAT	TCTTTCCAGTTGACCTC	GGATCAGG 540
Sbjct 494	GATTGCGCGCGCTG	CCGACGTTTTTCAACCAT	TCTTTCCAGTTGACCTC	GGATCAGG 553
Query 541	TAGGGATACCCGCTGA	ACTTAAC		563
Sbjct 554	TAGGGATACCCGCTGA	ACTTAAC		576

Mucor indicus isolate AU-CB-AS-04 small subunit ribosomal RNA gene, partial sequence; internal transcribed spacer 1, 5.8S ribosomal RNA gene, and internal transcribed spacer 2, complete sequence; and large subunit ribosomal RNA gene, partial sequence

Sequence ID: [OQ660484.1](#) Length: 664 Number of Matches: 1

Range 1: 77 to 664 [GenBankGraphics](#)

Score	Expect	Identities	Gaps	Strand
1068 bits(578)	0.0	585/588(99%)	2/588(0%)	Plus/Plus
Query 1	GATAATTAATAAAATATTCTTATTTACTGTGAAGTGTCTTTATTTATGACGTATAAGGGGA	60		
Sbjct 77	GATAATTCAAAAATTATCTTATTTACTGTGAAGTGTCTTTATTTATGACGTATAAGGGGA	136		
Query 61	TGCTTTAGGCTATAAGGGTAGGCCATGGAATGCTAACCTAGTCATAGTCAAGCTTGAT	120		
Sbjct 137	TGCTTTAGGCTATAAGGGTAGGCCATGGAATGCTAACCTAGTCATAGTCAAGCTTGAT	196		
Query 121	GCTTGGTACCCGATTATTACTTACCAAAAAGAATTCAGTTAAAAATATTGTAACATAGACC	180		
Sbjct 197	GCTTGGTACCCGATTATTACTTACCAAAAAGAATTCAGTTAAAAATATTGTAACATAGACC	256		
Query 181	TAAAAATCTATAAAAACAATTTTAAACAATGGATCTCTTGGTTCTCGCATCGATGAAGAA	240		
Sbjct 257	TAAAAATCTATAAAAACAATTTTAAACAATGGATCTCTTGGTTCTCGCATCGATGAAGAA	316		
Query 241	CGTAGCAAAGTGCATAACTAGTGTGAATTGCATATTCAGTGAATCATCGAGTCTTTGAA	300		
Sbjct 317	CGTAGCAAAGTGCATAACTAGTGTGAATTGCATATTCAGTGAATCATCGAGTCTTTGAA	376		
Query 301	CGCATCTTGCACTCAATGGTATTCCATTGAGTACGCCTGTTTCAGTATCAAAAACAACCC	360		
Sbjct 377	CGCATCTTGCACTCAATGGTATTCCATTGAGTACGCCTGTTTCAGTATCAAAAACAACCC	436		
Query 361	TTATTCAAAAAtttttttGAGTAGATATGAGTGTAGCAACCTTACAAGTTGAGACATTT	420		
Sbjct 437	TTATTCAAAAATTTTTTGGAGTAGATATGAGTGTAGCAACCTTACAAGTTGAGACATTT	496		
Query 421	TAAATAAAGTCAGGCCATATCGTGGATTGAGTGCCGATAC--TTTAAATTTGAAAAGGT	478		
Sbjct 497	TAAATAAAGTCAGGCCATATCGTGGATTGAGTGCCGATACTTTTTAAATTTGAAAAGGT	556		
Query 479	AAAGCATGTTGATGTCCGCTTTTTGGGCCTCCCAAATAACTTTTTAAACTTGATCTGAAA	538		
Sbjct 557	AAAGCATGTTGATGTCCGCTTTTTGGGCCTCCCAAATAACTTTTTAAACTTGATCTGAAA	616		
Query 539	TCAGGTGGGATTACCCGCTGAACCTAAGCATATCAATAAGCGGAGGAA	586		
Sbjct 617	TCAGGTGGGATTACCCGCTGAACCTAAGCATATCAATAAGCGGAGGAA	664		

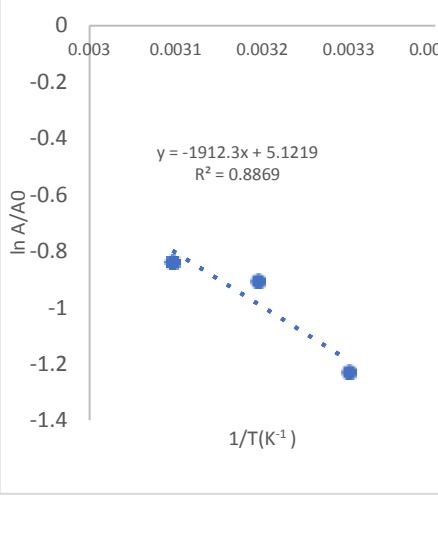
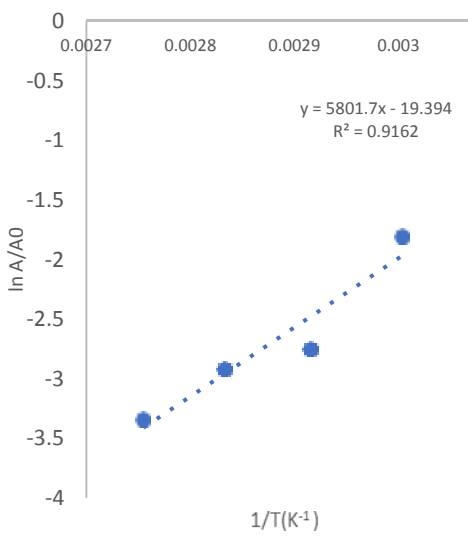
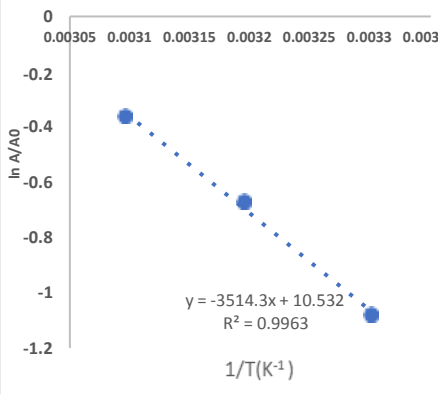
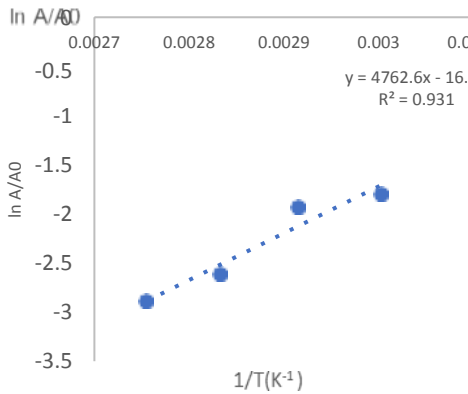
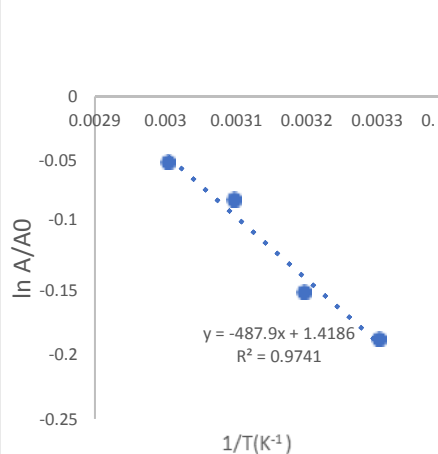
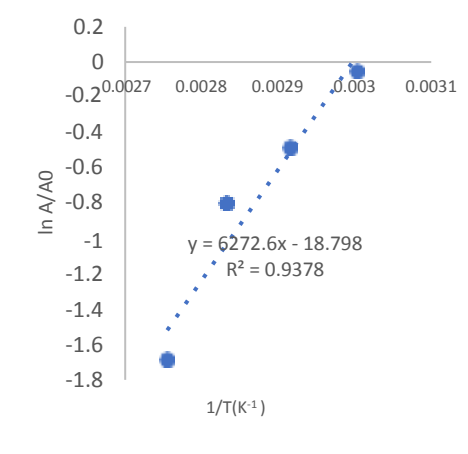
Saccharomyces cerevisiae isolate 10-1356 internal transcribed spacer 1, partial sequence;
 5.8S ribosomal RNA gene and internal transcribed spacer 2, complete sequence; and large
 subunit ribosomal RNA gene, partial sequence

Sequence ID: [MF276989.1](#) Length: 814 Number of Matches: 1

Range 1: 12 to 765 [GenBankGraphics](#)

Score	Expect	Identities	Gaps	Strand
1347 bits(729)	0.0	747/754(99%)	7/754(0%)	Plus/Plus
Query 1	AAAGAAATTTAATAATTTTGAAAATGGAttttttGTTTTGGCAAGAGCATGAGAGCTTT	60		
Sbjct 12	AAAGAAATTTAATAATTTTGAAAATGGATTTTTTGTGTTTGGCAAGAGCATGAGAGCTTT	71		
Query 61	TACTGGGCAAGAAGACAAGAGATGGAGAGTCCAGCCGGGCTGCGCTTAAGTGC GCGGTC	120		
Sbjct 72	TACTGGGCAAGAAGACAAGAGATGGAGAGTCCAGCCGGGCTGCGCTTAAGTGC GCGGTC	131		
Query 121	TTGCTAGGCTTGTAAAGTTTCTTTCTTGCTATTCCAACCGGTGAGAGATTCTGTGCTTTT	180		
Sbjct 132	TTGCTAGGCTTGTAAAGTTTCTTTCTTGCTATTCCAACCGGTGAGAGATTCTGTGCTTTT	191		
Query 181	GTTATAGGACAATTAACCGTTTCAATACAACACACTGTGGAGTTTTTCATATCTTTGCA	240		
Sbjct 192	GTTATAGGACAATTAACCGTTTCAATACAACACACTGTGGAGTTTTTCATATCTTTGCA	251		
Query 241	ACTTTTCTTTGGGCATTCGAGCAATCGGGGCCAGAGGTAACAAACACAAACAATTTTA	300		
Sbjct 252	ACTTTTCTTTGGGCATTCGAGCAATCGGGGCCAGAGGTAACAAACACAAACAATTTTA	311		
Query 301	TCTATTCAATAAATTTTGTCAAAAACAAGAAATTTTCGTAACGGAAATTTTAAAAATAT	360		
Sbjct 312	TCTATTCAATAAATTTTGTCAAAAACAAGAAATTTTCGTAACGGAAATTTTAAAAATAT	371		
Query 361	TAAAAACTTTCAACAACGGATCTCTTGGTTCTCGCATCGATG-AGAACGCAGCGAAATGC	419		
Sbjct 372	TAAAAACTTTCAACAACGGATCTCTTGGTTCTCGCATCGATGAAGAACGCAGCGAAATGC	431		
Query 420	GATACGTAATGTGAATTGCAGAATCCGTGAATCATCGAATCTTTGAACGCA--TTGC-C	476		
Sbjct 432	GATACGTAATGTGAATTGCAGAATCCGTGAATCATCGAATCTTTGAACGCAATTGCGC	491		
Query 477	CCCTTGGTATTCCAGGGGGCATGCCGTTTGGAGCGTCAATTCCTTCTCAAACATTCGT	536		
Sbjct 492	CCCTTGGTATTCCAGGGGGCATGCCGTTTGGAGCGTCAATTCCTTCTCAAACATTCGT	551		
Query 537	TGG-AGTGAGTGATACTCTTTGGAGTTAACTTGAAATGCTGGCCTTTTCATTGGATGtt	595		
Sbjct 552	TGGTAGTGAGTGATACTCTTTGGAGTTAACTTGAAATGCTGGCCTTTTCATTGGATGTT	611		
Query 596	ttttttCCAAAGAGAGGTTTCTGCGTGTCTGAGGTATAATGCAAGTACGGTCGTTTTTA	655		
Sbjct 612	TTTTTCCAAAGAGAGGTTTCTGCGTGTCTGAGGTATAATGCAAGTACGGTCGTTTTTA	671		
Query 656	GGTTTTACCAACTGCGGCTAATC-TTTTTTATACTGAGCGTATTGGAACGTTATCGATAA	714		
Sbjct 672	GGTTTTACCAACTGCGGCTAATCTTTTTTATACTGAGCGTATTGGAACGTTATCGATAA	731		
Query 715	GAAGAGAGCGTCTAGGC-AACAATGTTCTTAAAG 747			
Sbjct 732	GAAGAGAGCGTCTAGGCCAACAATGTTCTTAAAG 765			

Appendix I: Arrhenius plot for the determination of activation and deactivation energy of free and co-immobilized enzymes

ENZYME	ACTIVATION ENERGY	DEACTIVATION ENERGY
Free cellulose	 <p> $y = -1912.3x + 5.1219$ $R^2 = 0.8869$ </p>	 <p> $y = 5801.7x - 19.394$ $R^2 = 0.9162$ </p>
Free xylanase	 <p> $y = -3514.3x + 10.532$ $R^2 = 0.9963$ </p>	 <p> $y = 4762.6x - 16.01$ $R^2 = 0.931$ </p>
Co-immobilized cellulase and xylanase	 <p> $y = -487.9x + 1.4186$ $R^2 = 0.9741$ </p>	 <p> $y = 6272.6x - 18.798$ $R^2 = 0.9378$ </p>

Appendix J: Infrared Spectra of Free Biochar Chitosan Bead (F) and Biochar-Chitosan Ceads and Biochar-chitosan Beads Loaded with Co-immobilized Enzyme (CIE) and co-immobilized fungi (CMY)

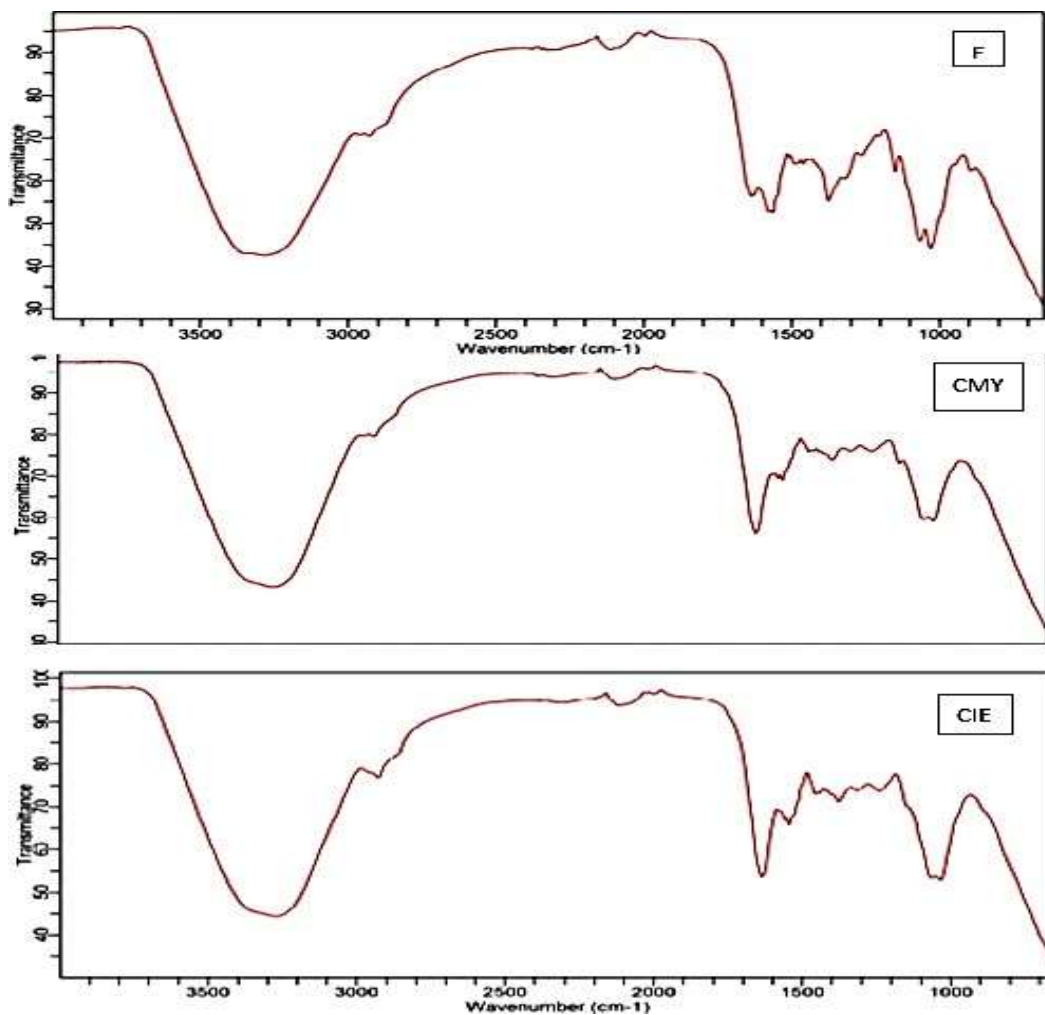
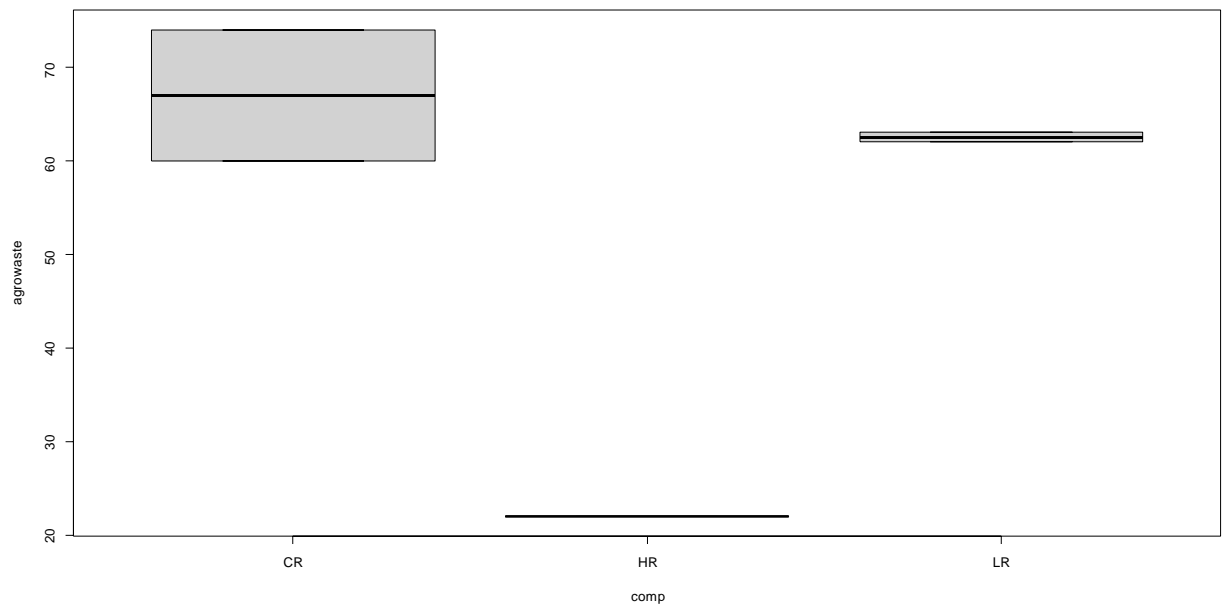


Figure 7: Infrared Spectra of free biochar-chitosan bead (**F**); biochar-chitosan bead loaded with co-immobilized cellulase and xylanase (**CIE**); and biochar-chitosan bead loaded with co-immobilized *Mucor* and Yeast (**CMY**)

Appendix K: Statistical result for the comparison of plantain pseudostem biomass (PS) and sugarcane bagasse (SB) using R statistical package.

Analysis (Pretreatment of plantain pseudostem biomass and sugarcane bagasse)



```
> summary(D1)
      Df Sum Sq Mean Sq F value Pr(>F)
waste  1   37.5    37.5     1.23  0.3830
comp   2 2457.0  1228.5    40.28  0.0242 *
Residuals  2   61.0    30.5
---
```

Signif. codes: 0 '***' 0.001 '**' 0.01 '*' 0.05 '.' 0.1 ' ' 1
>

Post ANOVA test

> TukeyHSD(D1)

Tukey multiple comparisons of means

95% family-wise confidence level

Fit: aov(formula = agrowaste ~ waste + comp)

\$waste

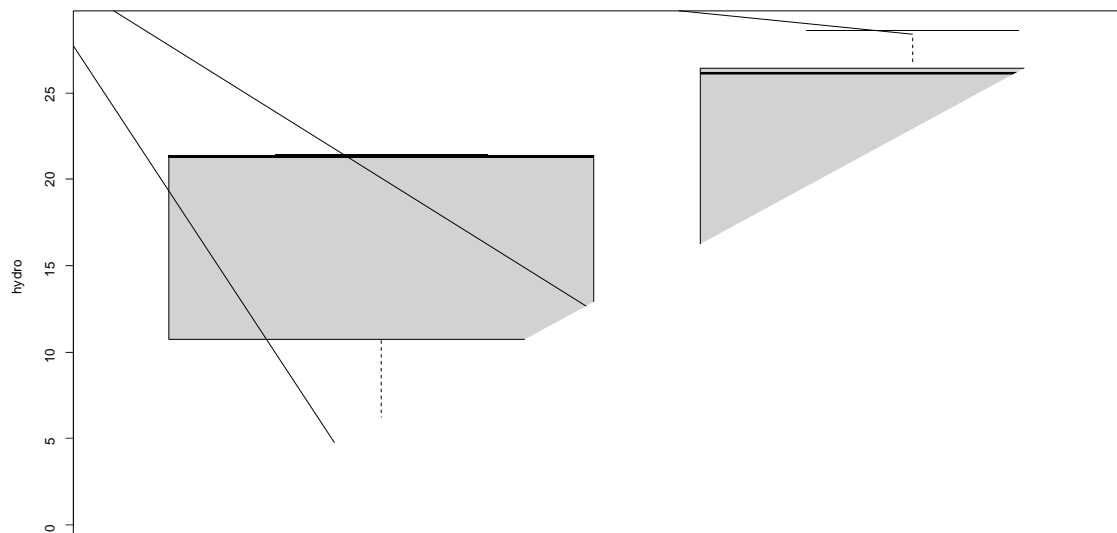
	diff	lwr	upr	p adj
SB-PS	5	-14.38505	24.38505	0.3829621

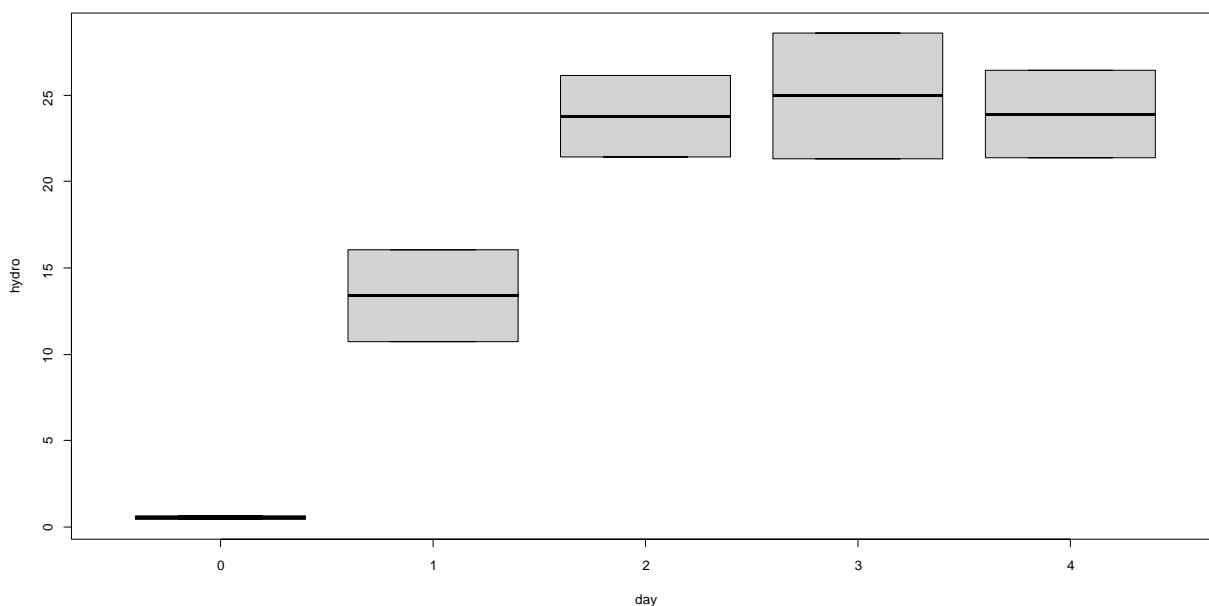
\$comp

	diff	lwr	upr	p adj
HR-CR	-45.0	-77.532746	-12.46725	0.0267760
LR-CR	-4.5	-37.032746	28.03275	0.7324359
LR-HR	40.5	7.967254	73.03275	0.0328491

Note: HR-Hemicellulose retained; CR- cellulose retained; LR-lignin retained

Hydrolysis of plantain pseudostem biomass and sugarcane bagasse for four days using co-immobilized enzyme.





```
> summary(D2)
```

	Df	Sum Sq	Mean Sq	F value	Pr(>F)
sample	1	62.2	62.2	14.22	0.019598 *
day	4	1700.4	425.1	97.23	0.000309 ***
Residuals	4	17.5	4.4		

```
---
```

Signif. codes: 0 '***' 0.001 '**' 0.01 '*' 0.05 '.' 0.1 ' ' 1

```
Post ANOVA Test
```

```
> TukeyHSD(D2)
```

Tukey multiple comparisons of means
95% family-wise confidence level

```
Fit: aov(formula = hydro ~ sample + day)
```

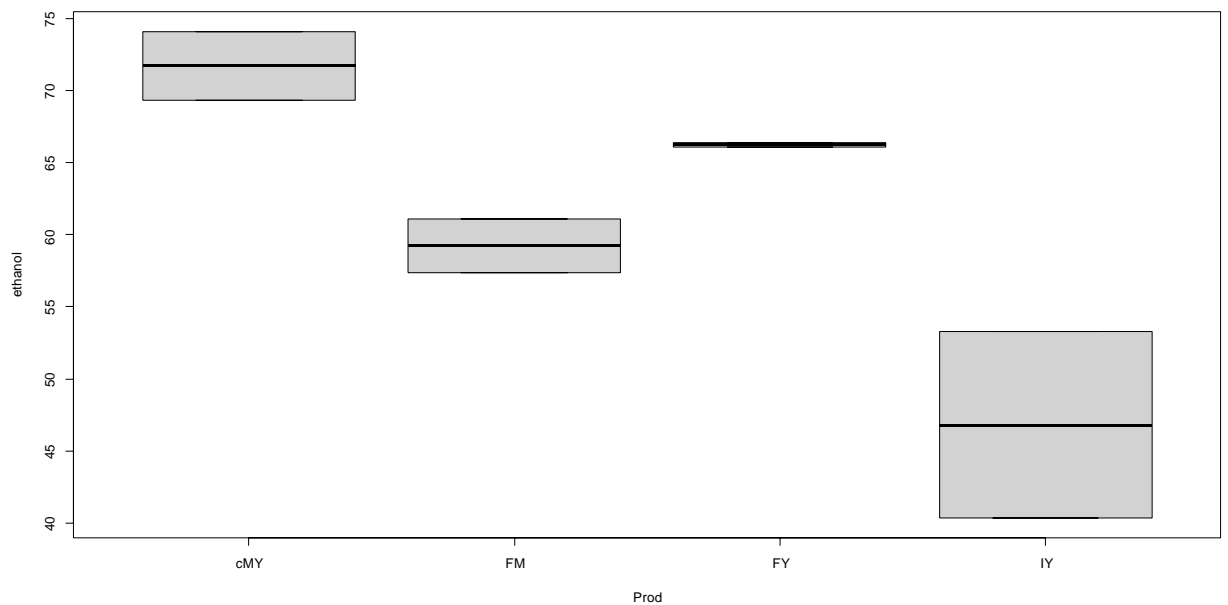
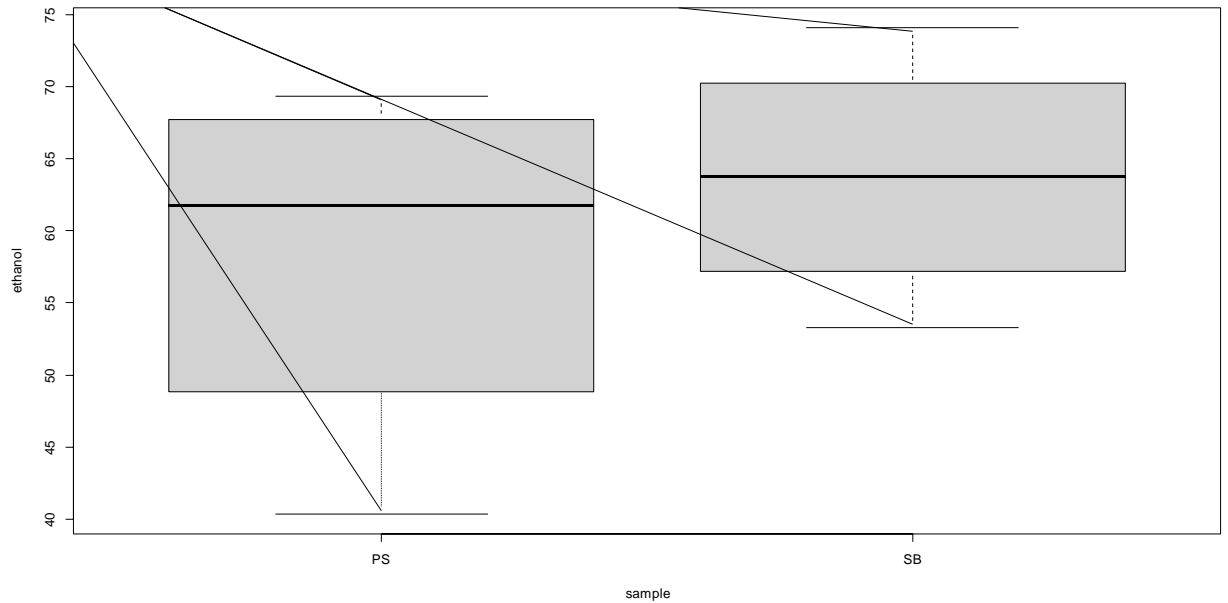
```
$sample
```

	diff	lwr	upr	p adj
SB-PS	4.986	1.314388	8.657612	0.0195987

```
$day
```

	diff	lwr	upr	p adj
1-0	15.210	5.914641	24.505359	0.0088696
2-0	29.270	19.974641	38.565359	0.0007124
3-0	33.685	24.389641	42.980359	0.0004065
4-0	33.455	24.159641	42.750359	0.0004175
2-1	14.060	4.764641	23.355359	0.0118406
3-1	18.475	9.179641	27.770359	0.0042798
4-1	18.245	8.949641	27.540359	0.0044879
3-2	4.415	-4.880359	13.710359	0.3618602
4-2	4.185	-5.110359	13.480359	0.3995165
4-3	-0.230	-9.525359	9.065359	0.9999508

Ethanol produced from plantain pseudostem biomass and sugarcane bagasse using co-immobilized enzyme and co-immobilized fungi.



```
> summary(D3)
      Df Sum Sq Mean Sq  F value    Pr(>F)
sample  1   58.9    58.92     4.108    0.1358
Prod    3  694.2   231.38    16.134    0.0235 *
Residuals 3   43.0    14.34
```

Signif. codes: 0 '***' 0.001 '**' 0.01 '*' 0.05 '.' 0.1 ' ' 1

```
> TukeyHSD(D3)
Tukey multiple comparisons of means
```

95% family-wise confidence level

Fit: aov(formula = ethanol ~ sample + Prod)

\$sample

	diff	lwr	upr	p adj
SB-PS	5.4275	-3.094609	13.94961	0.1357605

\$Prod

	diff	lwr	upr	p adj
FM-cMY	-12.495	-30.77005	5.780048	0.1293860
FY-cMY	-5.475	-23.75005	12.800048	0.5548395
IY-cMY	-24.915	-43.19005	-6.639952	0.0214545
FY-FM	7.020	-11.25505	25.295048	0.3990345
IY-FM	-12.420	-30.69505	5.855048	0.1312086
IY-FY	-19.440	-37.71505	-1.164952	0.0424066